THE FOSSIL *LAGERSTÄTTE* AT VALLECILLO, NORTH-EASTERN MEXICO: PELAGIC *PLATTENKALKS* RELATED TO CENOMANIAN-TURONIAN BOUNDARY ANOXIA

Zur Erlangung des akademischen Grades eines

Doktors der Naturwissenschaften

der Fakultät für Bauingenieur-, Geo- und Umweltwissenschaften der

Universität Fridericiana Karlsruhe (TH)

vorgelegte

DISSERTATION

von

Christina Ifrim

aus

Ilmenau

2006

Hiermit erkläre ich, dass ich die vorgelegte Dissertation selbst verfasst und mich keiner anderen als der von mir ausdrücklich bezeichneten Quellen und Hilfen bedient habe. Alle verwendeten Zitate sind gekennzeichnet und im Literaturverzeichnis angegeben.

Karlsruhe, den 12. April 2006   Christina Ifrim

ACKNOWLEDGEMENTS

ABSTRACT

The early Turonian Vallecillo *Plattenkalk,* famous for its fossil fishes*,* is interpreted regarding petrography, sedimentology, geochemistry, invertebrate taxonomy, biostratigraphy, palaeobiogeography, taphonomy and statistical distribution of fossils. The *Plattenkalk* is part of the Vallecillo Member, which forms a distinct unit of the Agua Nueva Formation, a monotonous limestone-marl alternation that was deposited in the outer shelf environment of the ancient western Gulf of Mexico. SEM, XRD and geochemical analyses show that the *Plattenkalk* petrography was controlled by three different processes: biogenic precipitation of calcite and aragonite, probably aeolian sedimentation of quartz, feldspars and clay minerals, and precipitation of sulphides under anoxic conditions. The anoxic conditions at the Vallecillo sea floor extended from the late Cenomanian to the early Turonian and are linked to the global Oceanic Anoxic Event 2 (OAE 2).

The *Plattenkalk* yields a diverse fossil assemblage. Ammonites are preserved with fine details of ornamentation and occasionally even with stomach contents. Long, loosely jointed spines are documented for *Pseudaspidoceras flexuosum* for the first time. Inoceramid bivalves represent the only benthic organisms found at Vallecillo. Vallecillo fossil fishes and reptiles are preserved flattened. The palaeobiogeographic analysis of the Vallecillo assemblage shows that a mixture of Tethyan taxa and Western Interior endemic species is present. This reflects the palaeogeographic position of the Vallecillo area at the southern end of the Western Interior Seaway, overlapping with the western Tethyan faunal province.

The invertebrate fossils and planktic foraminifers assign a latest Cenomanian to early Turonian age and allow for a detailed biostratigraphic subdivision of the Vallecillo section. The following biozones are distinguished: Ammonites: the late Cenomanian *Nigericeras scotti* zone, the early Turonian *Watinoceras, P. flexuosum, Vascoceras birchbyi* and *Mammites nodosoides* zones; Inoceramids: the late Cenomanian *Inoceramus pictus* and *Mytiloides hattini* zones, and the early Turonian *M. puebloensis* and *M. kossmati* zones; planktic foraminifers: the *Whiteinella archaeocretacea* and the *Helvetoglobotruncana helvetica* zones. The Vallecillo *Plattenkalk* is compared to the GSSP of the Cenomanian-Turonian boundary, which is the Pueblo section in Colorado, and to the Eastbourne section in UK, leeading to the conlcusion that the Vallecillo section is stratigraphically the most complete. The correlation also indicated that several early Turonian marker species show a diachronous first and/or last appearance between the three faunal provinces.

Statistical data from scientific excavations and the random surface collection revealed the absolute composition of the Vallecillo fossil assemblage. The abundance of fossils allows the taphonomic interpretation of the three most abundant Vallecillo fishes: *Rhynchodercetis* sp., *Tselfatia formosa* and *Nursallia* cf. *N. gutturosum* differed in locomotion, feeding habits and preferred water depths. The even distribution of fishes over the Vallecillo section contrasts the highly variable distribution of invertebrates. Ammonites show three phases of empoverished faunas and recovery, indicated by

increase in abundance and/or diversity. The distribution of inoceramids covaries with foraminifers during the early Turonian, but not with ammonites. This is remarkable, because both ammonites and inoceramids possibly depended on the distribution of larvae by oceanic currents.

A new outcrop of the Vallecillo Member was recognized at Las Mitras near Monterrey, 100 km to the south of Vallecillo, thus indicating a wide regional occurrence of the *Plattenkalk*. In this section, the Vallecillo Member overlies the Indidura Formation. The member consists in its lower part of black shales related to OAE 2, which upsection gradually pass into *Plattenkalk*. The Las Mitras section is biostratigraphically complete from the late Cenomanian to the early Turonian, as shown by planktic foraminifers. Petrography depended on the same three processes known from Vallecillo, but the distribution is more heterogeneous in the Las Mitras section. The anchimetamorphous overprint of the Las Mitras section did not allow for detailed comparison of the clay mineralogy to Vallecillo. The expansion of the low oxygen zone during the late Cenomanian and re-oxygenation of the upper water column in the early Turonian is reflected by a decerase and subsequent increase in abundance, diversity and size of the foraminiferal assemblages.

The Vallecillo *Plattenkalks* formed on the open shelf, outside a restricted basin, with a wide regional occurrence. This is remarkable for *Plattenkalk* deposits, but suggests, that a global OAE can cause conditions, which allow for the formation of *Plattenkalk* in the open sea. These conditions include oxygenated surface waters for the carbonate production, stagnant conditions in large parts of the water column and a hostile environment at the sea floor.

KURZFASSUNG

Der frühturone Vallecillo-Plattenkalk, bekannt für seine fossilen Fische, wird hinsichtlich seiner Petrographie, Sedimentologie, Geochemie, Invertebraten-Taxonomie, Biostratigraphie, Paläobiogeographie, Taphonomie und der statistischen Verteilung der Fossilien untersucht. Der Plattenkalk ist Teil des Vallecillo-Members, das seinerseits eine ausgeprägte Einheit der Agua-Nueva-Formation ist, einer monotonen Kalk-Mergel-Wechselfolge, die auf dem äußeren Schelf des alten Golfes von Mexiko abgelagert wurde. REM-, XRD- und geochemische Analysen zeigen, dass die Petrographie des Plattenkalkes von drei verschiedenen Prozessen gesteuert wurde: biogene Fällung von Kalzit und Aragonit, wahrscheinlich äolische Sedimentation von Quarz, Feldspäten und Tonmineralen, und Fällung von Sulfiden unter anoxischen Bedingungen. Die anoxischen Bedingungen am Meeresboden reichten vom späten Cenomanium bis in das frühe Turonium und kennzeichnen das globale Ozeanische Anoxische Event 2 (OAE 2).

Der Plattenkalke enthält eine diverse Fossilgemeinschaft. Ammoniten sind mit feinen Details und gelegentlich sogar Mageninhalten erhalten. Lange, bewegliche Stacheln werden erstmals für *Pseudaspidoceras flexuosum* dokumentiert. Inoceramide Muscheln verkörpern die einzigen benthonischen Organismen, die in Vallecillo gefunden wurden. Fossile Fische und Reptilien aus Vallecillo sind abgeflacht erhalten. Die paläobiogeographische Analyse zeigt, das die Vallecillo-Gemeinschaft eine Mischung aus tethyalen Taxa und endemischen Arten des Western Interior Seaway ist. Diese Mischung spiegelt die paläogeographische Position von Vallecillo am südlichen Ende des Western Interior Seaway wider, mit Überlappung der westlichen Tethys-Faunenprovinz.

Die Wirbellosen und planktonischen Foraminiferen ordnen dem Vallecillo-Profil ein spätcenomanes bis frühturones Alter zu und erlauben dessen detaillierte biostratigraphische Unterteilung. Folgende Biozonen werden unterschieden: Ammoniten: die spätcenomane *Nigericeras-scotti*-Zone, die unter-turone *Watinoceras*-Zone, die *P.-flexuosum-*, *Vascoceras-birchbyi-* und *Mammites-nodosoides*-Zone; Inoceramiden: die spätcenomanen *Inoceramus-pictus-* und *Mytiloides-hattini*-Zonen, und die frühturonen *M.-puebloensis-* und *M.-kossmati*-Zonen; planktonische Foraminiferen: die *Whiteinella-archaeocretacea-* und *Helvetoglobotruncana-helvetica*-Zonen. Der Vallecillo *Plattenkalk* wird mit der GSSP der Cenomanium-Turonium-Grenze, dem Rock-Canyon-Profil in Colorado, verglichen, und mit dem Eastbourne-Profil in Großbritannien, was zu der Schlußfolgerung führt, dass das Vallecillo-Profil das stratigraphisch vollständigste ist. Die Korrelation zeigt auf, dass mehrere wichtige stratigraphische Markierer-Arten des frühen Turoniums ein diachrones Einsetzen zwischen den drei Faunenprovinzen zeigen.

Statistische Daten aus wissenschaftlichen Grabungen und der Haldensammlung zeigen die absolute Zusammensetzung der fossilen Gemeinschaft aus Vallecillo auf. Die Häufigkeit der Fossilien ermöglicht die taphonomische Interpretation der drei häufigsten Vallecillo-Fische: *Rhynchodercetis* sp., *Tselfatia formosa* und *Nursallia* cf. *N. gutturosum* unterschieden sich in Lokomotion,

Ernährungsbeschaffenheit und bevorzugten Wassertiefen. Die gleichmäßige Verteilung der Fische über das Vallecillo-Profil unterscheidet sich deutlich von der stark variierenden Verteilung der Invertebraten. Ammoniten zeigen drei Phasen von verarmten Faunen und Erholung, angezeigt durch Größen-, Häufigkeits- und/oder Diversitätszunahme. Die Variationen in der Verteilung von Inoceramiden während des frühen Turoniums entsprechen denen von Foraminiferen, aber nicht von Ammoniten. Das ist bemerkenswert, weil sowohl Ammoniten als auch Inoceramiden vermutlich Larven besaßen, deren Vertielung von Ozeanströmungen abhängig war.

Ein neuer Aufschluss des Vallecillo-Members wurde bei Las Mitras nahe Monterrey erkannt, 100 km südlich von Vallecillo, der ein weites regionales Vorkommen des Plattenkalks anzeigt. In dieseem Aufschluss überlagert das Vallecillo-Member die Indidura-Formation. Das Member besteht im unteren Teil aus Schwarzschiefern mit Bezug zu OAE 2, die nach oben graduell in Plattenkalke übergehen. Das Las-Mitras-Profil ist stratigraphisch vollständig, vom späten Cenomanium bis zum frühen Turonium, belegt durch planktonische Foraminiferen. Die Petrographie hing von den gleichen drei Prozessen ab wie in Vallecillo, aber die Verteilung ist variabler im Las-Mitras-Profil. Die anchimetamorphe Überprägung des Las-Mitras-Profils machte den detaillierten Vergleich der Tonmineralogie mit Vallecillo unmöglich. Die Expansion der Niedrig-Sauerstoff-Zone während des späten Cenomaniums und die Wiederversorgung der oberen Wasserschichten mit Sauerstoff im frühen Turonium wird durch eine Verringerung und eine darauf folgende Zunahme in der Häufigkeit, Diversität und Größe der Foraminiferen-Gemeinschaften widergespiegelt.

The Vallecillo *Plattenkalks* formed on the open shelf, outside a restricted basin, with a wide regional occurrence. This is remarkable for *Plattenkalk* deposits, but suggests, that a global OAE can cause conditions which allow for the formation of *Plattenkalk* in the open sea. These conditions include oxygenated surface waters for the carbonate production, stagnant conditions in large parts of the water column and a hostile environment at the sea floor.

Die Vallecillo-Plattenkalke bildeten sich auf dem offenen Schelf, außerhalb eines abgeschnittenen Beckens, mit einer weiten regionalen Verbreitung. Das ist bemerkenswert für Plattenkalke, deutet aber an, dass ein globales OAE die notwendigen Bedingungen für die Bildung von Plattenkalken im offenen Meer verursachen kann. Diese Bedingungen schließen sauerstoffreiche Oberflächenwässer für die Karbonatproduktion, Stagnation in weiten Teilen der Wassersäule und eine lebensfeindliche Umgebung am Meeresboden ein.

RESUMEN

Los depósitos tipo *Plattenkalk* del Turoniano temprano en Vallecillo, son famosos por sus peces fósiles, y son interpretados con respecto a su petrología, sedimentología, geoquímica, taxonomía, bioestratigrafía, paleobiogeografía, tafonomía y a la distribución estadística de los fósiles. El *Plattenkalk* es parte del Miembro Vallecillo, el cual es una unidad distintiva de la Formación Agua Nueva, que consiste de una monótona alternancia de caliza-margosa depositada en un ambiente de plataforma externa en la parte occidental del antiguo Golfo de México. SEM, XRD y análisis geoquímicos, muestran que la petrogénesis del *Plattenkalk* estuvo controlada por tres diferentes procesos: precipitación biogénica de la calcita y aragonita, probable sedimentación eólica del cuarzo, feldespato y minerales de arcilla, y precipitación de sulfatos bajo condiciones anóxicas. Las condiciones anóxicas en el piso marino se extienden desde el Cenomaniano tardío hasta el Turoniano temprano y marcan el Evento Oceánico Anóxico 2 (OAE 2), ocurrido a nivel global.

El *Plattenkalk* propició una asociación fósil diversa. Los amonites son preservados mostrando a gran detalle su ornamentación y ocasionalmente sus contenidos estomacales. Espinas largas y ligeramente articuladas de *Pseudaspidoceras flexuosum* son reportadas por primera vez. Bivalvos inocerámidos representan el único organismo bentónico encontrado en Vallecillo. Los peces y reptiles de Vallecillo son preservados de manera aplanada. El análisis paleogeográfico del conjunto fósil de Vallecillo, muestra que existe una mezcla de taxa Tethysianos y especies endémicas del Corredor Marino Occidental Interior, las cuales reflejan la posición paleogeográfica del área de Vallecillo, hacia la parte más al sur de dicho corredor, traslapándose con la provincia faunística Tethysiana.

Los fósiles de invertebrados y los foraminíferos planctónicos, asignan una edad del Cenomaniano tardío al Turoniano temprano, y permiten la subdivisión bioestratigráfica detallada de la sección Vallecillo. Las siguientes biozonas pueden ser distinguidas: Amonites: la zona de *Nigericeras scotti* del Cenomaniano tardío, la zona de *Watinoceras* del Turoniano temprano, de *Pseudaspidoceras flexuosum*, *Vascoceras birchby* y *Mammites nodosoides*; Inocerámidos: las zonas de *Inoceramus pictus* y *Mytiloides hattini* del Cenomaniano tardío, y las zonas de *M. puebloensis* y *M. kossmati* del Turoniano temprano; Foraminíferos planctónicos: las zonas de *Whiteinella archaeocretacea* y *Helvetoglobotruncana helvetica*. Una comparación de la sección Vallecillo con el GSSP del límite Cenomaniano-Turoniano, la sección de Rock Canyon en Colorado, y la sección Eastbourne en UK, reveló que la sección Vallecillo es la más completa. Sin embargo algunos marcadores estratigráficos importantes muestran una aparente diacronía durante el Turoniano temprano.

Datos estadísticos de excavaciones científicas y la colecta aleatoria en superficie, revelan la composición absoluta del conjunto fósil de Vallecillo. La abundancia de fósiles permite la interpretación tafonómica de los tres tipos de peces más abundantes en Vallecillo, interpretando que: *Rhynchodercetis* sp., *Tselfatia formosa* y *Nursallia* cf. *N. gutturosum* difieren en su locomoción, hábitat alimenticio y preferencia en la profundidad del agua. La regular distribución de peces en

Vallecillo, contrasta con la altamente variable distribución de invertebrados. Los amonites muestran tres fases de empobrecimiento y recuperación de faunas, indicadas por el incremento en su abundancia y/o diversidad. La distribución de los inocerámidos covaría con los foraminíferos durante el Turoniano temprano, pero no con los amonites. Esto es notable debido a que tanto los amonites como los inocerámidos, pueden tener dependencias en la distribución de sus larvas por las corrientes oceánicas.

Un nuevo afloramiento se reconoció en Las Mitras, cerca de Monterrey 100km al sur de Vallecillo, indicando así una amplia distribución regional. En esta sección el Miembro Vallecillo sobreyace a la Formación Indidura. El Miembro Vallecillo consiste en su parte inferior de lutita negra relacionado al OAE 2, el cual hacia la cima de la sección pasa gradualmente a *Plattenkalk*. La sección Las Mitras es bioestratigráficamente completa, abarcando desde el Cenomaniano tardío al Turoniano temprano, como lo demuestran los foraminíferos planctónicos. Petrogénicamente depende de los tres mismos procesos conocidos para Vallecillo, pero la distribución es más heterogénea en la sección Las Mitras. La característica de una incipiente foliación en la sección Las Mitras, no permite una comparación detallada de la mineralogía de arcillas con esa de Vallecillo. La expansión de la zona empobrecida en oxígeno durante el Cenomaniano tardío y la re-oxigenación de la parte superior de la columna de agua en el Turoniano temprano, está reflejada en abundancia, diversidad y tamaño de los conjuntos de foraminíferos.

El *Plattenkalk* de Vallecillo se formó en una plataforma abierta, fuera de cuencas restringidas y con una amplia distribución regional. Eso es notable para un *Plattenkalk* pero indica que un evento global OAE puede causar condiciones para permitir la formación de *Plattenkak* en zonas de mar abierto. Esas condiciones incluyen aguas superficiales oxigenadas para la producción de carbonato, condiciones estancamiento en gran parte de la columna de agua, y un ambiente hostil en el piso marino.

CONTENT

1 OBJECTIVES

The Vallecillo fossil *Lagerstätte* is particularly known for the excellent preservation and abundance of its fossils fishes. However, the precise age of the locality remains unknown to date, and nothing is known about the regional extent of the sediments. Knowledge about the sediment is restricted to a small part of the column as quarries were smaller in the past than they are today. The aim of this thesis is to clarify the above points of this important Mexican fossil locality, and to investigate the taphonomy, sedimentology, petrography, and geochemistry.

The first field campaign at Vallecillo was carried out in spring 2002. The largest section of the Vallecillo quarries was registered and sampled. All other quarries were subsequently visited and correlated to this section, or additional layers were added to the composite section if possible. The survey also included the investigation of coeval sediments outside the Vallecillo area. The Las Mitras section west of Monterrey was recorded and sampled, which spans sediments coeval to the Vallecillo lithologies, as well as older layers. Invertebrate fossils were revised, which already existed in the Facultad de Ciencias de la Tierra of the Universidad Autónoma de Nuevo León (FCT-UANL) in Linares. First conclusions could be reached, for instance on the early Turonian age of the sediments.

In autumn 2002, first taphonomic interpretations could be reached, after the collection of Vallecillo fossils in the FCT-UANL was registered and documented, resulting in a first statistical database. The major part of the invertebrate collection, but also unprepared vertebrates from Vallecillo, were sent to Germany for taxonomical determination.

In autumn 2003, a pilot excavation was held in Vallecillo, with the objective to evaluate the abundance of fossils in the sediment and gain quantitative data regarding the composition of the assemblage, as well as changes of the assemblages in the excavated column. Subsequent excavations in autumn 2004 and spring 2005 used the same method, covering other parts of the sedimentary column. The most important specimens were sent to Karlsruhe for further investigation.

All field campaigns were used to collect additional fossils in random surface survey, but also to collect additional fossils in stratigraphic context. This latter approach considerably increased our knowledge of the stratigraphic distribution of Vallecillo taxa over the section, apart from excavated material. In addition, short visits to Vallecillo in spring 2003 and 2004 were used to expand the random surface collection.

The samples collected were investigated regarding microfossils, stable isotopes (δ^{13}C and δ^{18}O), micro- and ultrafacies, as well as major and minor elements. The excavation data are summarized in a series of databases for statistical interpretations. All fossils recovered in the random survey, as well as fossils collected in stratigraphic context, are registered in an additional database.

The present set of data allows a multidisciplinary interpretation of the Vallecillo locality. Sedimentology, invertebrate stratigraphy, geochemistry, taphonomy and statistics are included here into the examination of the Vallecillo sediments and fossils. The absolute, but also the

palaeobiogeographical composition of the fossil assemblage and the precise age could be determined. These data allow an interpretation of the palaeoenviroment, as well as an evaluation of changes of the assemblages throughout the section, taphonomy, or the composition and the origin of the sediment, and the genesis of the fossil deposit. Preliminary data are published (Ifrim *et al.* 2005, in press). The Vallecillo fossil *Lagerstätte* may now be compared to other *Plattenkalk* localities, for instance the famous Solnhofen Lithographic Limestone. There are remarkable differences in the genesis of *Plattenkalk* fossil deposits, even though the lithologies and the type of fossil preservation are similar.

2   INTRODUCTION TO THE VALLECILLO LOCALITY

2.1   SIGNIFICANCE OF THE VALLECILLO FOSSIL *LAGERSTÄTTE*

Many lucky circumstances are necessary to fossilize a dead animal, and fossil *Lagerstätten* with detailed preservation are rare. Some of the best preserved fossils come from the late Jurassic Solnhofen *Plattenkalk* (Barthel *et al.* 1990). The fine grained limestones and fortunate embedding circumstances preserved dead organisms in this locality, including very fine details such as intestine contents, skin imprints, or animals complete to the most distal extremities. Over the last 50 years, many other *Plattenkalk* localities became known, such as the Tlayúa quarry in east-central Mexico (Albian, Espinosa-Arrubarrena and Applegate 1996) or the Hjoula and Haquel limestones in Lebanon (Cenomanian, Hückel 1970). Fossils of these sites are equally well preserved and even allow a palaeobiological interpretation of individual species and entire assemblages.

The sediments in Vallecillo mostly consist of marly limestone which forms platy slabs when opened. This platy cleavage refers the marly limestone to *Plattenkalk* although it is not as pure as the lithographic limestone of Solnhofen. Many fishes known from this Vallecillo *Plattenkalk* are very well preserved, with fins complete and every fin ray present, with soft part imprints or scales. Prior to this dissertation, more than 400 fossils were collected. They included well-preserved, articulated fishes and reptiles, as well as disarticulated specimens and primary fragments, but also ammonites, inoceramid bivalves, few coproliths and pellets. These fossils gave an idea about the potential of the Vallecillo quarries. No *Plattenkalk* deposit with comparable quality of vertebrate fossils is known from the early Turonian of North America. The Múzquiz *Plattenkalk*, late Turonian to early Coniacian in age, was recently described by Stinnesbeck *et al.*(2005). It formed on an open shelf, similar to the Vallecillo deposit. At a global scale, the Cenomanian-Turonian Komen Pelagic Limestone in Slovenia (Cavin *et al.* 2000; Jurkovsek *et al.* 2001) is the only other *Plattenkalk* similar to the Vallecillo deposit in genesis and age, although little investigated.

2.2   THE HISTORY OF THE VALLECILLO *LAGERSTÄTTE*

Vallecillo is situated 100 km to the north of Monterrey in the north-eastern Mexican state of Nuevo León, along Mexican Highway 85 which connects Monterrey with Laredo, Texas (Figure 2.1). West of the village, platy marly limestone is quarried for commercial purposes.

The Vallecillo *Plattenkalks* were discovered during building of the highway 85 in the 1960s. They were little exploited as flagstones until the late 1980s when rock trading intensified.
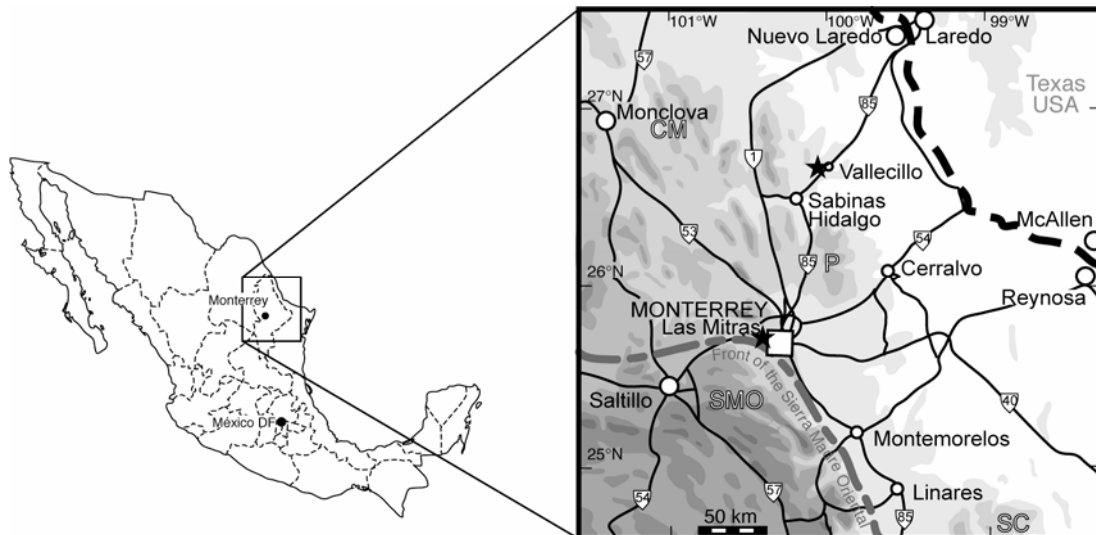
Figure 2.1: Geographic location of Vallecillo within Mexico and Nuevo León. Important mountain chains are CM: Sierra de Candela-Monclova; P: Sierra de Picachos; SC: Sierra de San Carlos; SMO: Sierra Madre Oriental. Localities of the Vallecillo Member described herein are marked with an asterisk.

Since then several small quarries were opened along a dirt road of 1 km length (Figure 2.2). Extraction and preparation of the slabs is entirely manual. Large bars are used to extract suitable blocks, which are then split with axe and hammer to thicknesses between two and five centimetres, with the shape and size of the resulting slabs left casual. About three quarters of the rocks extracted in the Vallecillo quarries is suitable as flagstones for floors and walls.
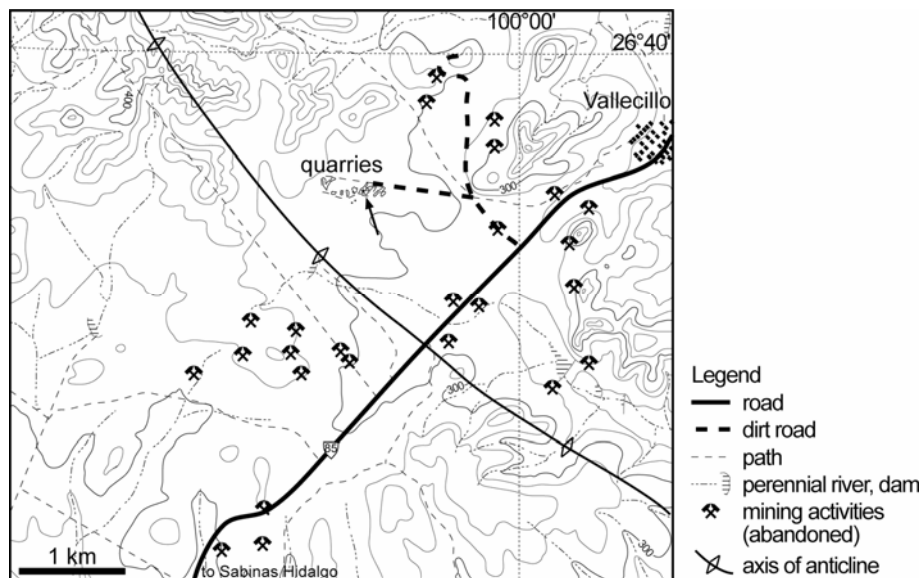
Figure 2.2. Map of the vicinity of Vallecillo with quarries and old mines.

The importance of the Vallecillo sediments as a fossil deposit were first recognized in 1995, when a private collector from Monterrey, Mauricio Fernandez, called the attention of Prof. Dr W. Stinnesbeck, the advisor of this thesis, who was a palaeontologist at the FCT-UANL at that time. In the following years investigations, financed by the Volkswagen-Stiftung and the Mexican Instituto

Nacional de Antropología y Historia (INAH), were directed by W. Stinnesbeck (UKRG) and Dr J.-G. López Oliva (FCT-UANL). They focused on the vertebrates, particularly the abundant fishes (Blanco *et al.* 2001; Blanco-Piñon *et al.* 2002; Blanco and Cavin 2003; Blanco Piñon 2003; Blanco-Piñon and Alvarado-Ortega 2005). In 2002 a project supported by the Deutsche Forschungsgemeinschaft (DFG, German Science Foundation) was initiated, directed by W. Stinnesbeck (UKRG), and Dr J.-G. López Oliva (FCT-UANL), with the objective to investigate the geological context and the age of the Vallecillo *Plattenkalks*. The results of this project are presented herein.

Preliminary data of this project are published on the taphonomy of the fishes (Ifrim *et al.* 2005, in press), the taxonomy of an aigialosaur (Buchy *et al.* 2005) and on the taxonomy of the ammonite assemblage from Vallecillo (Ifrim and Stinnesbeck submitted).

3   GEOLOGICAL SURVEY

3.1   GEOLOGICAL HISTORY OF NORTH-EASTERN MEXICO

The geology of north-eastern Mexico is characterized by the predominant presence of folded Mesozoic sediments that rest upon a Palaeozoic and Precambrian basement. During the late Jurassic, the opening of the Gulf of Mexico led to a transgression which covered the basement in north-eastern Mexico (Morán-Zenteno 1994, p. 38ff). A passive continental margin started to develop, which is reflected by the facies succession in north-eastern Mexico: Redbeds of late Triassic to early late Jurassic age underlie shallow water evaporates, carbonates and shales of late Jurassic and earliest Cretaceous age, followed by uniform, open marine, carbonaceous-pelitic sediments and platform carbonates which reflect steady subsidence rates (Götte 1990, p. 5).

During the early Cretaceous, the pre-Mesozoic basement is still recognized by changes of facies and submarine topography, but this topography is gradually smoothened out, and only the regional increase in the thickness of formations indicates the development of a foredeep in this region (Götte 1990, p. 7). During the early late Cretaceous, when the Vallecillo *Plattenkalks* formed, the opening of the Gulf of Mexico and the related extension had ceased. In consequence, the north-eastern Mexican shelf was tectonically inactive (Gray and Johnson 1995).

The Cupido and Aurora carbonate platform, which extend from central Coahuila into New Mexico (Figure 3.1), developed during the early Cretaceous, but stepped back due to the increasing sea level during the Cenomanian. Locally, small carbonate build-ups overlie formerly larger carbonate platforms and kept up with the overall transgression in the early Cenomanian. Locally they extended into the upper Cenomanian until they also vanished. The monotonous series of the Indidura and Agua Nueva formations and the Eagle Ford shale blanketed the entire north-eastern Mexican region during Cenomanian-Turonian times and reached as far as the Western Interior and Gulf of Mexico Basin (Goldhammer and Johnson 2001).

The global sea level was at a major highstand in the early Turonian, the second highest sea level recorded in Earth history, and the highest since the beginning of the Mesozoic era (Hallam 1992, p. 158). This major super-imposed first and second order eustatic flooding event inundated the Gulf of Mexico province, and connected the Western Interior Seaway to the Gulf of Mexico (Goldhammer and Johnson 2001). The warm Tethyan waters penetrated the epicontinental Western Interior Seaway as far north as the prairie provinces of southern Canada (Kauffman and Caldwell 1993), and the sea expanded to nearly 2000 km width (Hay *et al.* 1993).

The subduction of the Farallon plate at the western margin of the North American plate induced magmatic activities and crustal shortening in the western North American continent (Windley 1995, p. 103). This tectonic activity formed the Sevier orogenic belt to the north and is associated with active magmatism which reached its highest activity at about 90 to 95 Ma, roughly coincident with the peak

of Cretaceous sea level (Armstrong and Ward 1993). Magmatism continued south into western Mexico, where the Alisitos magmatic arc was active and formed a continuous barrier towards the Pacific (Figure 3.1). It is composed of volcanic and volcaniclastic rocks of dacite-andesitic composition (Morán-Zenteno 1994, p. 7). East of the Alisitos arc, a back-arc basin existed with a variety of volcaniclastic-related facies.
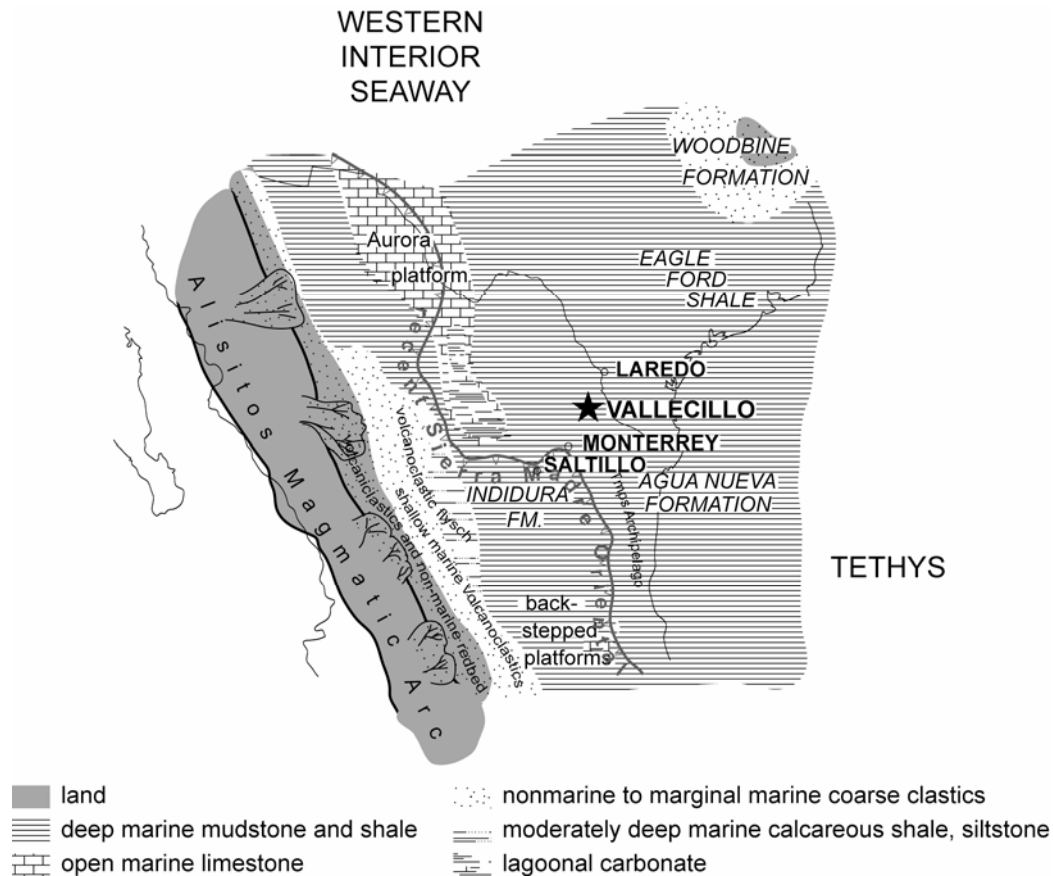
Figure 3.1. Palaeogeographic map of southern North America during Cenomanian-Turonian times (modified after Seibertz 1998; Goldhammer and Johnson 2001).

During late Cretaceous times, gradual uplift from west to east led to a regional regression which is expressed in a decrease in carbonaceous content and an increase of detrital content. The Mesozoic sediment sequence was folded in the Laramide orogenesis during the latest Cretaceous and the earliest Palaeogene. Deformation continues until today in the folded and thrusted Mesozoic sediments of the Sierra Madre Oriental (Figure 2.1), but east of its thrust front, the deformation is expressed in large anticlines in the recent Gulf Coastal Plain (Götte 1990, p. 7).

Parallel to the Sierra Madre Oriental, the east-Mexican Alkaline Province is characterized by alkaline magmatites of Tertiary age. Seven magmatic centres lie on or near the Gulf coastal Plain, among them the Candela-Monclova volcanic belt, the Sierra de Picachos, and the Sierra de San Carlos (Figure 2.1). This magmatism appears to be caused by a change in subduction style at the western active continental margin (Byerly 1991).

3.2   THE AGUA NUEVA AND INDIDURA FORMATIONS

During Cenomanian-Turonian times, the monotonous series of the Indidura and Agua Nueva formations blanketed the entire shelf of today's north-eastern Mexican Gulf Coast (Goldhammer and Johnson 2001). The Vallecillo marly *Plattenkalks* form a distinct member within the Agua Nueva Formation. They are absent in the coeval Indidura Formation which is characterized by more clastic lithology. Both formation names are variably applied by different authors.

3.2.1   Definitions of the Agua Nueva, the Indidura and the San Felipe Formations

The **Agua Nueva Formation** was first recognized as a separate unit by Stephenson (1921, in Muir 1936, p. 382) in an unpublished report. It was formally introduced by Muir (1934), with the type locality in the Cañon de la Borrega in the south-eastern Sierra de Tamaulipas (Figure 3.2).

Figure 3.2. Map of localities of the Agua Nueva, Indidura and San Felipe Formations mentioned in the text. Distribution of the Agua Nueva and Indidura formations after Schoenherr (1988) and Seibertz (1998).

The Agua Nueva Formation is there described as a series of black microcrystalline limestones interlayered with black marls (Figure 3.3). Occasionally it contains chert nodules or interlayers of carbonaceous black shale, bentonite, bentonitic marls or marly shales (Sohl *et al.* 1991). Where the Agua Nueva Formation overlies former carbonate platforms, e.g. the Aurora platform, it contains abundant ichnofauna, whereas trace fossils are rare in the more distal, basinal facies. The thickness of the Agua Nueva Formation ranges from a few metres above former carbonate platforms (Schoenherr 1988, p. 12) to 350 m in basinal facies (Padilla y Sanchez 1982). The contact to the underlying Cuesta

del Cura Formation is mostly conformable, although occasional disconformities occur (Schoenherr 1988, p. 12). In places where the Agua Nueva Formation overlies El Abra or Aurora platform limestones, the contact is always disconformable (Padilla y Sanchez 1982; Schoenherr 1988, p. 12).

Figure 3.3. The monotonous limestone-marls alternation of the Agua Nueva Formation in a road cut 20 km south of Sabinas Hidalgo.

The **Indidura Formation** is often discussed along with the Agua Nueva Formation. It is similar in lithology, but contains a certain amount of siliciclastic detritus. The Indidura Formation was first described by Böse (1906). It is composed of thin to intermediately layered calcareous and sandy shales with thin intercalations of dark grey, sometimes sandy limestones (Humphrey 1949).
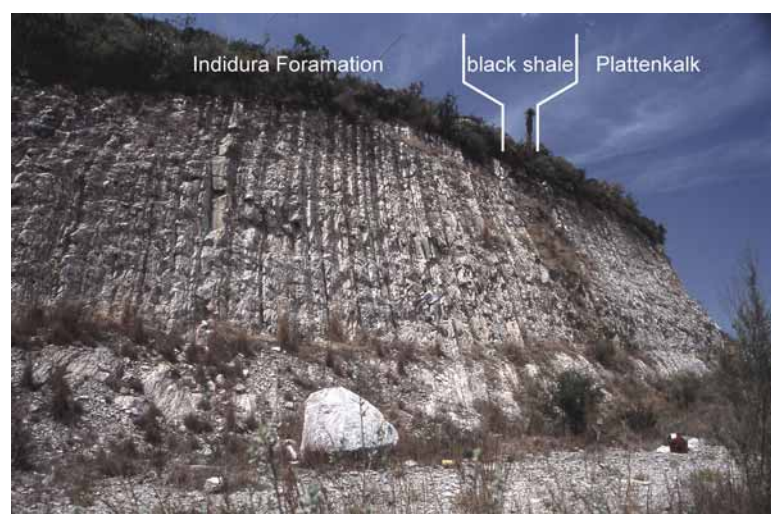
Figure 3.4. The Indidura Formation at Las Mitras is exposed in the lower (left) part of the section. It underlies black shale (dark), which is overlain by the *Plattenkalks* of the Vallecillo Member (right). The latter two lithologies are here included in the Vallecillo Member of the Agua Nueva Formation.

Kelly (1936, p. 1028) defined the type locality of the Indidura Formation 19 km to the south-west of Las Delicias, Coahuila, where 33 m of shale and limestone conformably overlie the Cuesta del Cura Formation. Imlay (1936, p. 1127) re-defined the formation, choosing the type locality in the western Sierra de Parras. In this region, the Indidura Formation is 641 m thick; it conformably overlies the Cuesta del Cura Formation and underlies the siliciclastic Caracol Formation. The formation ranges from 33 m (Kelly 1936) to 858 m (Imlay 1936) in thickness.

The term "**San Felipe Formation**" was introduced in 1910 in an unpublished report by Jeffreys for strata between the El Abra formation and the Méndez Shale (Muir 1936, p. 58). The first reference to the formation was published by White (1913, p. 255). Muir (1936) formally defined the formation, that conformably overlies either the Indidura or the Agua Nueva Formation. The type locality is situated 4 km east of Ciudad Valles, in the State of San Luis Potosí (Figure 3.2), along the railway to Tampíco. The section includes a complex and incomplete succession of limestone and olive-grey shale. It is present throughout north-eastern Mexico (Schoenherr 1988).

The above formations are often introduced in different senses. Goldhammer und Lehmann (in Goldhammer *et al.* 1993) and Goldhammer (2001) regard the Agua Nueva and overlying San Felipe formations as a single unit which they name Indidura Formation. Bishop (1970) includes the sediments here assigned to the Agua Nueva Formation into the San Felipe Formation. The present research follows the view of Schoenherr (1988) and Seibertz (1998) who consider the Agua Nueva Formation as distinct from the coeval Indidura Formation. The monotonous limestones and marls of the Agua Nueva Formation lack coarse siliciclastic detritus. The Indidura and Agua Nueva formations show gradual transition between each other and are then difficult to differentiate (Schoenherr 1988). The San Felipe Formation that conformably overlies both the Agua Nueva and Indidura formations, is less monotonous in lithology. The amount of clastic components is higher, and its rocks are brighter and weather to yellow-brown and green colours. This unit contains glauconitic sand- and siltstone, marls of different colours and sandy limestone (Seibertz 1985).

3.2.2 The Vallecillo Member

The Vallecillo *Plattenkalk* member was defined by Blanco Piñon (2003, p. 39 ff.) in the quarries near Vallecillo (Figure 2.2) as a locally developed monotonous series of finely laminated, pink marls with interlayered brown mudstones and "goethite lenses" (p. 48) of tentatively early to middle Turonian age. He assigned it "Lower Unit" (p. 49) of the Agua Nueva Formation.

However, this definition that does not consider the fact that the outcrops of the Agua Nueva Formation *sensu stricto* to the north and south of the Vallecillo quarries place the member within the Agua Nueva Formation, not at the base. This description also dismisses the Cenomanian-Turonian age of the rocks (see Chapter 8). The Cenomanian-Turonian boundary is usually found in the lower fourth or third of the Agua Nueva Formation (Goldhammer and Johnson 2001), not at the base. The

Vallecillo *Plattenkalk* consists of thin-bedded micritic marly limestones, interbedded with white to grey mudstones that contain goethitic crusts. The thicker goethitic layers contain concretions. These rocks weather to bright pink and grey or yellow colours (Figure 3.5).

At Las Mitras, in the western part of Monterrey, it overlies the Indidura Formation with a sudden change in lithology, indicating a hiatus. Black shales of latest Cenomanian age (the Bonarelli event of Schlanger *et al.* 1987) overlie the hiatus and gradually transist into the *Plattenkalks* of the Vallecillo Member. The Las Mitras section is described in detail in Chapter 10.1. The Vallecillo Member also appears to occur in sections near Ciudad Victoria, Tamaulipas (Schoenherr 1988, p. 63ff). These outcrops remain to be evaluated.

Figure 3.5. The *Plattenkalks* of the Vallecillo Member at the type quarries. Note the goethite concretions in two of the intercalated mudstone beds.

The present data suggest a re-definition of the Vallecillo Member: It has a wide regional occurrence in the lower fourth or third of the Agua Nueva Formation and is distinguished from the monotonous limestone-marl alternation of this lithostratigraphic unit by black shale lithologies, followed by finely laminated, marly *Plattenkalk* with Fe-oxide concretions. These thin bedded marls and limestones are interlayered with goethitic mudstones that contain concretions.

3.2.3   Occurrence, facies and age of the Agua Nueva and Indidura Formations

Outcrops of the Agua-Nueva-Formation are widely distributed in north-eastern Mexico and particularly abundant in the Sierra Madre Oriental. Below surface it is known to exist in the eastern part of the Burgos Basin, the Tampíco-Misantla Basin, and the Macuspana Basin (Sohl *et al.* 1991). The Agua Nueva Formation is restricted to deeper basinal areas without input of coarse siliciclastic

material (Seibertz 1998). To the north it grades into the Eagle Ford Formation which is less calcareous (Sohl *et al.* 1991).

The Indidura Formation crops out to the west of the Agua Nueva Formation, closer to the ancient coast lines where the influx of coarse siliciclastic material gradually increases. The two formations are transitional to each other (Seibertz 1998).

A Cenomanian-Turonian age is generally assigned to both the Agua Nueva and Indidura Formations (Sohl *et al.* 1991; Seibertz 1998). Both formations show diachronous lower and upper transitions (Ice and McNulty 1980; Goldhammer and Johnson 2001). The Cenomanian-Turonian boundary was recognized in different levels within the two formations. For instance, it was identified in the lower fourth of the Agua Nueva Formation to the north-west of Ciudad Victoria (Schoenherr 1988, p.61), but in the middle Agua Nueva Formation to the south of Ciudad Victoria (Soto-Jaramillo 1981). These differences reflect local tectonic activity in shallow sedimentation areas.

3.2.4   Geology in the Vallecillo area

Near Vallecillo, the Agua Nueva Formation *sensu stricto* crops out in a mountain chain to the north-west and south-east of the village. In the centre of the anticline, the lithology of the Agua Nueva Formation includes to marly *Plattenkalks*, which are weathered to pink and yellow colours and are interbedded with Fe-oxide layers, the Vallecillo Member. These lithologies are exposed in a series of quarries which are aligned over a distance of 1 km (Figure 2.2). The oldest sediments in the core of the anticline are mostly overgrown by the vegetation, but few small outcrops to the north and south of the Vallecillo quarries display weathered layers of the Agua Nueva Formation *sensu stricto*.

Pb-Zn-Ag ore minerals were mined in the area around Vallecillo, with ubiquitous mine shafts and small spoil heaps (Figure 2.2). In the Vallecillo quarries, a 10 cm thick vein is present that cuts through the Cretaceous sediments along a vertical joint. Three layers of mineralization are visible, but they were not further studied. No reaction zone is observed between the ore and the host rock. The type and age of the Vallecillo ore deposit is unknown until today; despite a long tradition of mining in Vallecillo, the ore deposits were not investigated scientifically, with the only study published 120 years ago (Chism 1885). The ore formation was likely related to the formation of Tertiary Alkaline Magmatic province (Byerly 1991), because the Vallecillo area is situated between the volcanic centres of the Candela-Monclova Magmatic belt and the Sierra de Picachos (Figure 2.1).

4 **METHODS**

4.1 SECTIONS AND SAMPLING

A sediment sequence of 6·5 m layers is exposed in the largest of the Vallecillo quarries. An additional 1·5 m are present in the quarry adjacent to the east (Figure 2.2). The sediment layers of all other quarries correspond to the middle part of the registered section. In 2002, the Vallecillo section was sampled, starting with the bottom of the quarry as 0·00 m level of the section. This section was enlarged downwards since then, because the quarry grew and cut into older strata. The lowermost layers were reached by excavation in spring 2005, and the 0·00 m level is actually 0·65 m above today's base.. The original 0·00 level was kept to avoid confusion related to re-numbering, and to allow correlation with former publications.

The Las Mitras Section (see Chapter 10.1) was sampled from base to top in 1 m distances, enhanced to 0·1 m distances in the black shale and lower *Plattenkalk*.

4.2 MICRO- AND ULTRAFACIES ANALYSES

Classification of carbonate rocks follows Dunham (1962), classification of siliciclastic rocks follows Folk (1974; in Tucker 1991, p. 92). Using these definitions, the term "mudstone" becomes ambiguous. It describes either a micritic limestone low in bioclasts (Dunham 1962) or a claystone with a siltstone component (Folk 1974). The term mudstone is used herein for carbonates exclusively in the discussion of microfacies analysis. These carbonates are described as *Plattenkalks* in every other context, whereas the fine-grained fine-silty claystones intercalated in the *Plattenkalks* are generally classified as mudstones.

Three samples from a lower, middle and upper level of the section were chosen for SEM analysis. Small chips of rock were dried at 50°C for several days and analysed, while an additional specimen was etched in 1%HCl for 1 minute, washed under running water for another minute, and finally washed with deionised water. This procedure eases identification of non-carbonaceous components (see Tucker 1996, p. 288 for details). All samples were stained with platinum and analysed in a Noran Gemini scanning electron microscope at the Laboratory for Electron Microscopy (LEM) of the University of Karlsruhe, kindly supported by V. Zibat. Element composition of grains larger than 1 μm was measured by X-ray reflection in each mineral documented in Figure 5.4.

4.3 X-RAY DIFFRACTOMETRY (XRD)

Sample preparation for X-ray diffractometry of clay minerals followed Kübler (1987). Samples were dried at 60°C, then ground 3 minutes in an automatic agate mill. Carbonate was extracted by

treatment with chloric acid for 10 minutes. Ultrasonic disaggregation was accomplished during 3 minute intervals. Then samples were washed and centrifuged in an automatic centrifuge for 10 minutes. This procedure was repeated at least three times or until a suspension with neutral pH-value was obtained. Separation of different grain size fractions (>2µm and 2 to 16µm) was obtained by the timed settling method based on Stoke's law. The selected fraction was then pipetted onto a glass plate and air-dried at room temperature. XRD analysis of oriented clay samples was made after air drying at room temperature and ethylene-glycol solvated conditions or on random powder samples. The samples were measured by T. Adatte at the Geological Institute of the University of Neuchâtel, Switzerland, in a SCINTAG XRD 2000 diffractometre under Cu-kα-radiation. Scanning rate was 0·03 °2θ s^{-1}.

The diffractograms were interpreted with the free software MacDiff (Petschick 2001). Data were corrected at the 003-Peak of Illite/Quartz at 20,85 2θ. The baseline was subtracted with a simple algorithm and, where necessary, by hand. Then basal reflections were analyzed with the amplitude registered as counts per second (cps).

Whole rock composition is based on methods for semi-quantitative analysis of the bulk rock mineralogy, with XRD patterns obtained from random powder samples. Identification of the 060 peak of clay minerals in the random powder sample was not possible as the chlorite 060 peak interferes with the quartz 211 peak at 59,95 °2θ, whereas the calcite 214, 208 and 119 peaks at 60,7 °2θ 61,0 °2θ and 61,3 °2θ may hide the 060 reflections of other clay minerals (Moore and Reynolds 1997, p. 245). The illite 060 peak at 61,90 °2θ is clearly identifiable in all samples containing this clay mineral. Quantification of random powder raw data was kindly done by T. Adatte, Neuchâtel.

In the 2 to 16 µm fraction, clastic minerals such as quartz, plagioclase and alkali feldspar were quantified relative to each other. They cannot be correlated with the clay minerals in the same diffractogram due to different mass absorption coefficients. The intensities of 001 peaks characterizing each clay mineral (e.g. chlorite, illite, kaolinite, and expandable clay minerals) were measured for a semi-quantitative estimate of the proportion of clay minerals present in the size fractions <2µm and 2 to 16 µm (error 5 wt%). Clay mineral contents were calculated without correction factors and are given in percentage. Determination of chlorite and kaolinite was obtained by separation of their 002 and 004 peaks respectively, at 24,9°2θ (kaolinite) and 25,2°2θ (chlorite). Chlorite seems to contain a small amount of expandable smectite, but it is difficult to quantify in small contents of chlorite (Moore and Reynolds 1997, p. 280).

The Kübler index is used for the analysis of illite crystallinity in the glycolated samples, as discussed by Kisch (1990), Krumm (1992) and Merriman and Peacor (1999). The peak width of the illite 001 peak is measured as °Δ2θ at half height. The limit between diagenesis and the anchizone is at 0·42 °Δ2θ, the transition to the metazone at 0·25 °Δ2θ. As no standardization was used here, results are to be understood qualitatively. The chlorite crystallinity could not be used here because of the presence of expandable 14Å clay minerals at the Chl001 peak and kaolinite at the Chl002 peak.

The samples do not represent uniform lithologies. In fact, it was intended to cover the entire spectrum of rock composition in both sections, and results vary respectively.

The primary data and four sets of unfiltered diffractograms are given in Appendix A.

4.4 COMPACTION RATES OF THE SEDIMENT

Compaction rates of the sediment are estimated by uncompacted fossils such as vertebrae or early mineralized coproliths. The distance of laminae in the surrounding sediment is measured at the largest displayed diameter of the fossil and next to it, where the sediment is compacted. The distances were measured with the transformation tool of the Adobe Illustrator software and then scaled. The resulting ratio is the percentage of the uncompacted sediment. Lower percentage indicates higher compaction of the sediment. This imprecise method can only provide results for a subquantitative estimation. The sediment may have been dispersed, when fossils touched the ground, particularly in rounded or pointed fossils such as coproliths or isolated vertebrae. Fine sets of lamination are not always well enough defined in the sediment. Sets of lamination, which are interrupted by tips of fossils, were not used, as these tips fossils may have penetrated the layers during sediment compaction.

Each thin section used for the determination of compaction rates is displayed with and without measures and interpretation to enable an objective view.

4.5 X-RAY FLUORESCENCE SPECTROMETRY (EDX)

The air dried samples were ground for 3 min in an automatic agate mill. The bulk powder samples were analyzed by energy-dispersive X-ray fluorescence spectrometry (EDX) with a SPECTRACE 5000 X-ray analyzer at the Institute for Mineralogy and Geochemistry at the University of Karlsruhe. Quantification was kindly carried out by U. Kramar and B. Oetzel. Analytical procedures, detection limits and standards used are described by Kramar (1997). A list of the analysed samples and detected amounts of elements is attached as Appendix B. Main elements are detected with a precision of ± 5%. The standard deviation of others is 10 to 20 %.

Main elements considered here are Ca, Ti, Mn and Fe. Trace elements are Ni, Cu, Zn, Ga, As, Rb, Sr, Y, Zr, Cd, Nb, Ba, La, Ce and Pb. The content of Mo, Ag, Br, Sn and Sb is at or below detection limit and left out of interpretation. Interferences of the signals of Ni with Ca, and As with Pb are problematic, as they produce sum peaks which grow quadratic to the concentration of the contributing elements (Kramar, pers. comm.). This is not the case for Ni and Ca, as Ca occurs at much higher contents than Ni in the samples studied here. However, As and Pb were detected at similar concentrations, and results and interpretations regarding these elements must be taken with caution.

The geochemical data were interpreted with the software Statistica™. Cluster analysis included detection limits.

Two sets of data are considered for each section analysed. The first set of data includes all samples measured, the second excludes goethite rich layers. Samples rich in Fe-oxides are quite different in composition, which distorts the elemental distribution of the *Plattenkalks*. Conclusions regarding the origin of the goethite layers can be drawn by distinguishing them from the "normal" carbonaceous sedimentation. But the results should be taken with caution. Only few samples with high Fe-content were analysed for a first overview, so the correlation is either very good or very bad.

4.6   TAXONOMY AND PALAEOBIOGEOGRAPHICAL INTERPRETATION

Taxonomic citations are only used in the faunal lists. The palaeobiogeographical interpretations are based on citations in the current literature, with the sources given as citations. Taxa described in open nomenclature are assumed to represent indeed the species in the palaeobiogeographical interpretation.

4.7   BIOSTRATIGRAPHY

Foraminifers could not be separated from the surrounding sediment and were identified from the thin sections used for microfacies analysis. Identification from thin section is bound to certain biases. Some taxa, e.g. the biserial species of *Heterohelix*, are more easily identified than trochospiral species. Others can only be identified when cut in particular directions and therefore appear to be rare, e.g. *Hedbergella simplex*. In addition, the amount of microfossils present in thin sections depends on the amount of microfossils in the water column and the sedimentation rate. Little information can be drawn from sediments that formed when the water column was depleted in foraminifers.

These biases lead to the conclusion that quantitative interpretation of the assemblages is impossible. They also affect the biostratigraphic zonation, as rare marker species are possibly identified prior to their real LA (last appearance) or after their real FA (first appearance).

Identification of planktic foraminifers is based on Robaszynski and Caron (1979), Caron (1985) and Keller and Pardo (2004), with initial kind guidance by Dr. Caron, Fribourg. Biozonation is from Keller and Pardo (2004).

4.8   SEDIMENTATION RATES

The absolute age for many late Cenomanian and early Turonian stratigraphic marker fossils is known. An estimation of sedimentation rates is therefore possible by plotting the stratigraphic datum in the lithologic column against a time scale (Keller and Pardo 2004).

Biases bound to this method result from the identification of the index fossils from thin sections. Biozonal markers of the late Cenomanian are generally defined by LA. This is problematic, because these fossils may be rare prior to their extinction, and the LA may be recorded too early, particularly when samples with a low density of microfossils are analysed. In contrast, early Turonian biozones are

defined by the FA. If the marker species is rare, this is also problematic. Calculated sedimentation rates between zonal boundaries defined by LAs and FAs are then exaggerated.

The absolute ages are from Kirkland (1991, *fide* Kennedy *et al.* 2000), Hardenbol *et al.* (1998, *fide* Keller and Pardo 2004) and Keller and Pardo (2004). These data relate to the Rock Canyon section near Pueblo, Colorado, which is the GSSP of the Cenomanian-Turonian boundary. They are all based on the data published by Kirkland (1991), but the absolute ages given by the authors mentioned above are calculated using different methods. In addition, Obradovich (1993), who uses the same data, noted that the data around the Cenomanian-Turonian boundary are not without problems, as only some samples of Kirkland (1991) yield results consistent with other of her data, whereas others yielded anomalously old ages, which may also be problematic for the calculation of sedimentation rates.

4.9   STABLE ISOTOPES

In diagenetically altered sections bulk rock samples provide a more reliable isotopic signal than foraminiferal tests, because diagenetic cement preferentially concentrates in pores of foraminifera and calcispheres, leaving the surrounding sediments largely lacking in cement (Mitchell *et al.* 1997). Diagenetic cement preferentially concentrates in limestones (Paul *et al.* 1999); the differential concentration of cement would affect the $\delta^{18}O$ signal, but not the $\delta^{13}C$ signal, as pore waters have low concentration of carbon (Magaritz 1975; Brand and Veizer 1980; Schrag *et al.* 1995).

Air dried whole rock samples were ground for 3 min in an automatic agate mill. The bulk powder samples were analyzed with a Micromass Optima Isotope Ratio Mass Spectrometer at the Institute for Mineralogy and Geochemistry at the University of Karlsruhe, in MultiCarb mode. Details of the analytical procedure are described by Norra (2001, p. 39-41).

4.10   EXCAVATION AND STATISTICS

Five scientific excavations (VC I to VC V) were carried out in defined areas of the Vallecillo quarries. These areas differed from each other in size and shape. The extracted rocks were split as thin as possible, with the thickness varying between 0·5 and 3 cm. Data registered for each finding include size, orientation, position in the excavation area and stratigraphic layer. Drawing and photographic documentation of each specimen were also included. The stratigraphic layer was measured with a precision of ± 1 cm.

All data from this statistical data collection were included in a series of Microsoft Access™ databases. Stratigraphic data of fossil-containing layers were summarized to 5-cm-thick sediment layers for statistical calculations. A species-area plot (Figure 4.1) reveals an approximately linear relation between the number of species found per area and area size, which allows a standardization of excavation data to 10 m^2 area size.
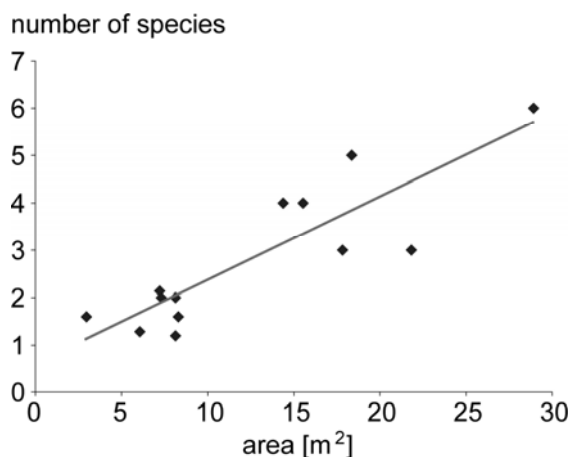
number of species

Figure 4.1. Species-area graph with extrapolated regression line, which shows an approximately linear relation between the number of species and area size. This relation is linear because the number of taxa identified per area size is much smaller than the maximum number of taxa that could be found per layer. If these numbers approximate each other, the species-area-relation are not linear (see Etter 1999 for details).

Abundances of fossils in the sediment are given as number per $10m^2$ standardized excavation area in a 5 cm thick bed ($10m^2 \times 5cm$).

4.11   VALLECILLO FOSSIL COLLECTIONS

The first fossils were collected by quarrymen in the 1980ies and 1990ies. Their families sold them at first along the highway that crosses the village. The trade of fossils, even though forbidden by law, continues in secret. Many pieces are owned by private persons in Vallecillo and the nearby town of Sabinas Hidalgo. For instance, a large private collection is owned by Mauricio Fernández, the first collector of Vallecillo fossils.

The largest number of Vallecillo fossils used for science is housed in the UANL-FCT in Linares. Their registration is UANL-FCT-VC (VC for Vallecillo), with the exception of the reptiles, which are registered as UANL-FCT-R (R for reptile collection). Fossils from the random surface collection are registered with this abbreviation and a number (e.g. UANL-FCT-VC500), whereas fossils found by statistical data collection include the registration number of the excavation (e.g. UANL-FCT-VCI/150). At present, the UANL-FCT collection comprises about 400 specimens from Vallecillo. The material under investigation in Karlsruhe will be returned to Linares and further increase this collection, as all fossils published belong to this collection.

Additional material is available in the Coahuila State Collection (Collección Estatal de Paleontología, CEP), housed in the Museo del Desierto de Coahuila in Saltillo (MUDE). Some replicas are also housed in the Institute of Regional Geology at the University of Karlsruhe (UKRG) and the State Museum of Natural History Karlsruhe (SMNK), where most of the fossils and the replicas were prepared.

5   PETROGRAPHY AND SEDIMENTOLOGY

5.1   LITHOLOGY OF THE COMPOSITE VALLECILLO SECTION

The Vallecillo *Plattenkalk* consists of marly limestone beds between eight and forty cm thick (Figure 3.5). Layers are tabular and can be traced over several tens of metres without changing their particular properties, such as colour, internal lamination, and thickness. The thickness hardly varies between the quarries, although the colours may change from pink (hematite) to yellow (goethite).

The main site studied here is the largest of the quarries, which also exposes the longest section. It is about 80×200 m in extend and up to 3 m deep, with beds inclined 5°N. It is situated at 26°39,32'N and 100°00,82'W (Figure 2.2). Only the upper 1·5 metres of section were recorded in the quarry adjacent to the east.
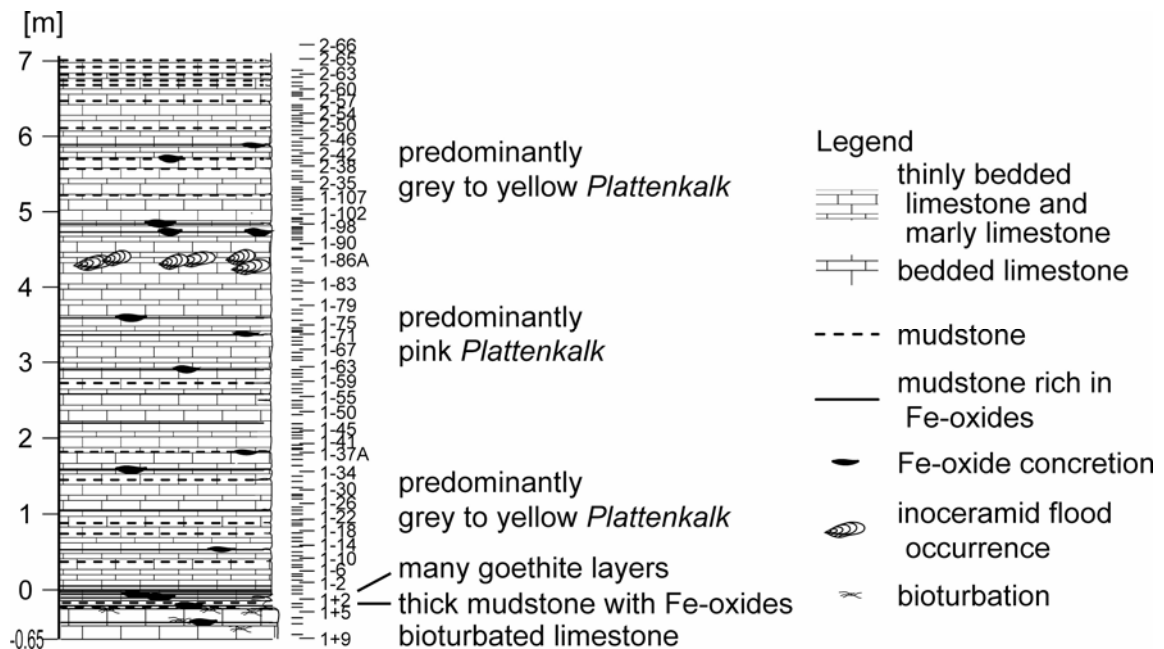
Figure 5.1. The Vallecillo composite section with all samples and explanation of lithology.

The lowest layers of the Vallecillo section consist of grey, bedded and bioturbated limestone, which does not split to slabs. The beds are up to 17 cm thick. This limestone is overlain by a 10 cm thick clay bed which contains layers of goethite and goethite concretions at the -0·25 m level of the section. Above this bed there is a 10 cm thick interval with thin-bedded marly limestone and many intercalated, partially crinkled goethite layers, but without concretions. These rocks form slabs of less than 5 mm thickness.

The typical Vallecillo *Plattenkalk* lithologies of platy marly limestone and mudstone begins at the 0·05 m level of the section, and continues for approximately 7·0 m until the upper end of the registered section. Limestone beds are up to 30 cm thick and intercalated by mudstones up to 10 cm thick. The

Plattenkalks are millimetrically laminated, resulting from changes in the contents of carbonate, clay minerals, or Fe-oxides. They split perfectly parallel to lamination when dry, and preferably through fossils contained in the sediment. The splitting surfaces form slightly rough surfaces. The colour of the rock varies from grey to yellow in the lower and upper part of the section, but is pink in the middle part. These colours do not persist laterally; the same layers are bright yellow in the westernmost quarry. In some beds, black traces of extant organic matter are preserved. Weathering structures such as Liesegang patterns or dendrites are rare and little developed. The intercalated mudstones are white, grey, or coloured ochre or red by goethite and/or hematite (Figure 5.2a-b), with occasional traces of lepidocrosite. Some of these mudstones include thin but massive layers of goethite, sometimes hematite. The thickest goethite layers contain concretions of goethite. Some of them include cubic pseudomorphs, probably after pyrite (Figure 5.2b). These mudstones with Fe-oxide concretions are unevenly distributed over the lithologic section.

Two marker layers within the *Plattenkalk* are used for correlation between the quarries. There is a conspicuous layer at the 2·19 m level, composed of 3 cm mudstone and 3 cm clear calcite crystals, probably representing a cement. This mudstone does not contain Fe-oxides. The layer with calcite crystals is unique in the section. It presents striation on the upper surface, which is normal to the axis of the Vallecillo anticline and may be an accommodation surface for folding. The other interval used for correlation is a set of two goethite layers with concretions at the 4·73 and 4·84 m levels of the section. These two layers are closer to each other than any other Fe-oxide layers with concretions in the section.
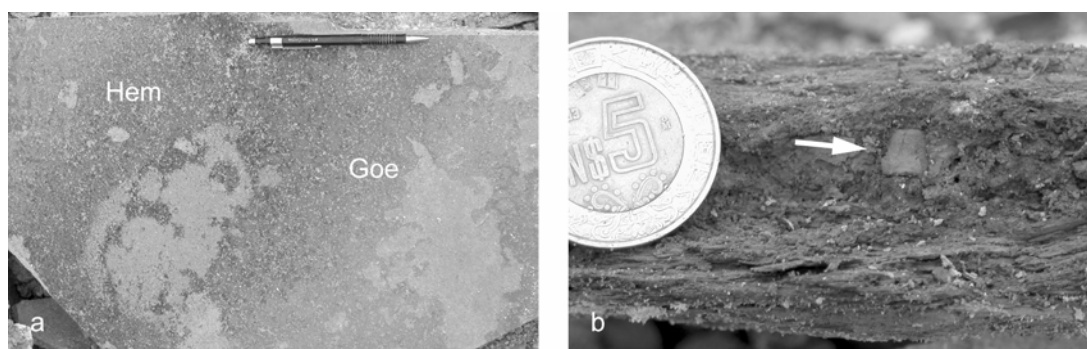
Figure 5.2. Fe-oxide layers in the Vallecillo section. a: change from hematite (Hem) to goethite (Goe) within a slab. b: Goethite concretion with a cubic pseudomorph (arrow) in the centre. The goethite-rich mudstone below and above the concretion is laminated.

5.2 MICRO- AND ULTRAFACIES ANALYSES OF THE VALLECILLO ROCKS

5.2.1 Microfacies

Vallecillo marls and limestones, including the basal limestone, are best described as recrystallized mud- to wackestones. The matrix of the marl and limestone is microcrystalline and recrystallized.

Bioclasts include abundant planktic foraminifers (Figure 5.3b), and to lesser amount calcispheres and recrystallized radiolarians. They all indicate a pelagic environment.
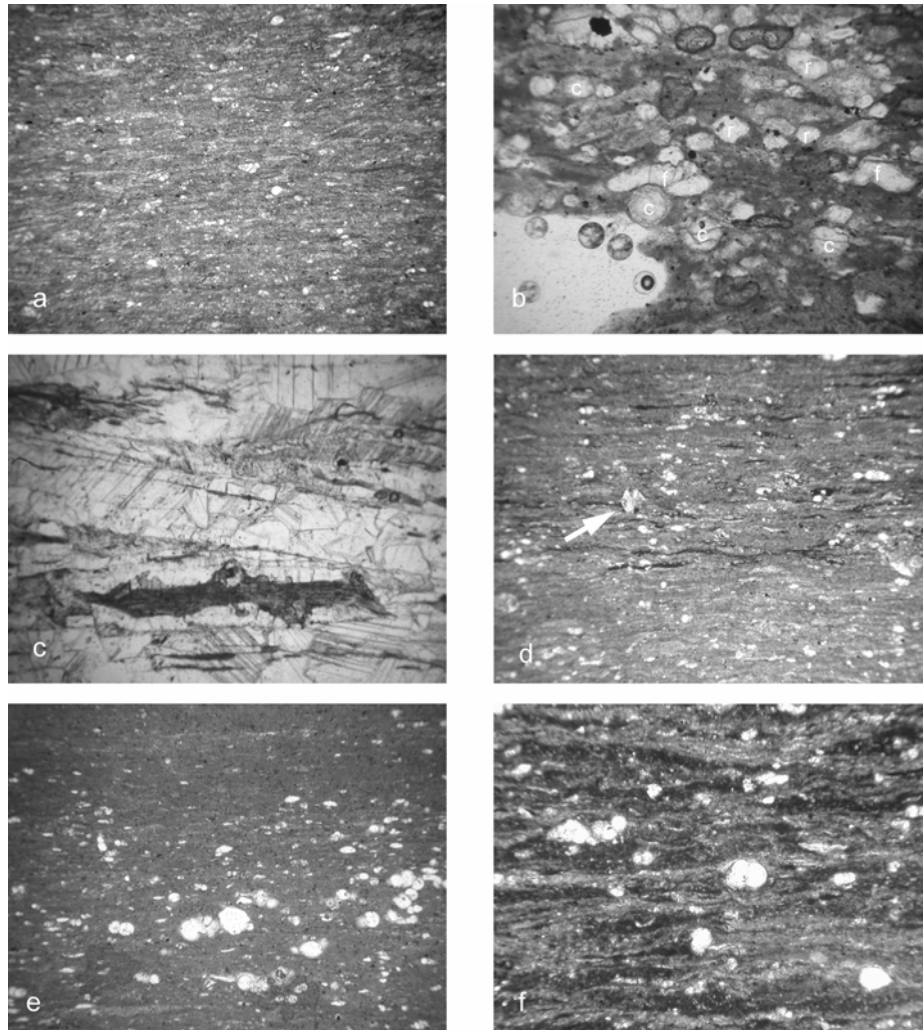
Figure 5.3. Microfacies of the Vallecillo section. a: mudstone. VC1-16. b: wackestone with abundant calcispheres (c), recrystallized radiolarians (r) and large, but badly preserved foraminifers (f). VC1-40. c: layer composed of calcite cement. VC1-48. d: mudstone with hematite (dark) causing millimetric lamination. Note the dedolomite (arrow). VC1-80. e: mudstone overlying wackestone. VC1-109. Dark spots in Figures a-b and d-e are Fe-oxides (hematite or goethite). f: wackestone with organic matter bound to clay minerals (dark) with small fine-grained lenses in between (brighter). UANL-FCT-VC182. All are ×25.

Thin sections reveal lamination in and below mm-scales (Figure 5.3a, d). This lamination is caused by sharp changes in the content of bioclasts, thin layers of goethite or hematite, but particularly by oriented phyllosilicates. Phyllosilicates are subparallel to the bedding planes, visibly best in samples with organic matter preserved (Figure 5.3e). The presence of organic matter, which is bound to the clay minerals, also uncovers the presence of tiny clastic grains in the fine-silt to clay size, forming microlenses between the phyllosilicates. These grains cannot be further identified from thin sections. Single grains of rounded quartz and feldspar are present in few layers, but their content is always below 1 %.

The layer at the 2·19 m level of the section is composed of oriented, clear calcite crystals (Figure 5.3c).

5.2.2   Ultrafacies

The fine-grained structure of the Vallecillo rocks cannot be determined by thin section, only. Questions remain, for instance regarding the composition of the fine-grained lenses or the origin of the carbonate.

SEM analysis revealed that the matrix is composed of micrite grains <1 µm and microspar (3 to 5 µm; e.g. Figure 5.4a, h). This indicates partial diagenetic alteration of the matrix by dissolution of metastable aragonite and high-Mg-calcite, and precipitation of the available carbonate as microspar (Munnecke and Samtleben 1996). This process transformed the once soft sediment into a compact rock.

Organisms that contributed to carbonate sedimentation include abundant coccoliths in the basal limestone and in the *Plattenkalk* samples. In sample VC1-30, abundant tubular structures with diameters of around 1 µm were identified (Figure 5.4h), but the producing organism is unknown.

Quartz grains are preserved in the calcitic matrix. They are subidiomorph (Figure 5.4a), some with traces of etching (Figure 5.4b). All quartz grains identified are at diameters of around 4 µm. This grain size is close to the limit between the fine silt and clay fraction and explains, why quartz was previously detected as accessory mineral, not as a major component of the sediment. The grains do not show signs of mechanical abrasion, but of exposure to corrosional conditions, such as present on beaches or in deserts (Tucker 1996, p. 238). This silicic component originated from a sedimentary source with a well-working sorting mechanism and corrosional conditions, but without abrasion. They may have been quickly eroded in a dry climate and immediately transported by wind, which may have caused the good sorting. An origin from the secondary recrystallization of radiolarians is unlikely as no overgrowth of quartz of other minerals is noticed, nor are chert layers present.

Another fine clastic component is flaky illite (Figure 5.4b, d), with diameters of <1µm to 10µm. This c lay mineral can only be identified clearly in the etched samples. In unetched carbonate rocks, the recrystallized calcite matrix obscures small particles. Illite is the only clay mineral found in the SEM analysis of Vallecillo rocks.

Framboids of Fe-oxide were found in a thin Fe-oxide layer in the etched sample. They have sizes of around 2 µm (Figure 5.4c-e) and represent microframboids in the sense of Sawlowicz (2000). Sulphide framboids are especially common in anoxic sediments, where bacterial sulphate reduction is active, and sufficient metals, mainly iron are available. This is the case in Vallecillo, where the sediment is coloured by Fe-oxides throughout the column, and extant organic matter indicates original organic-rich sediments.
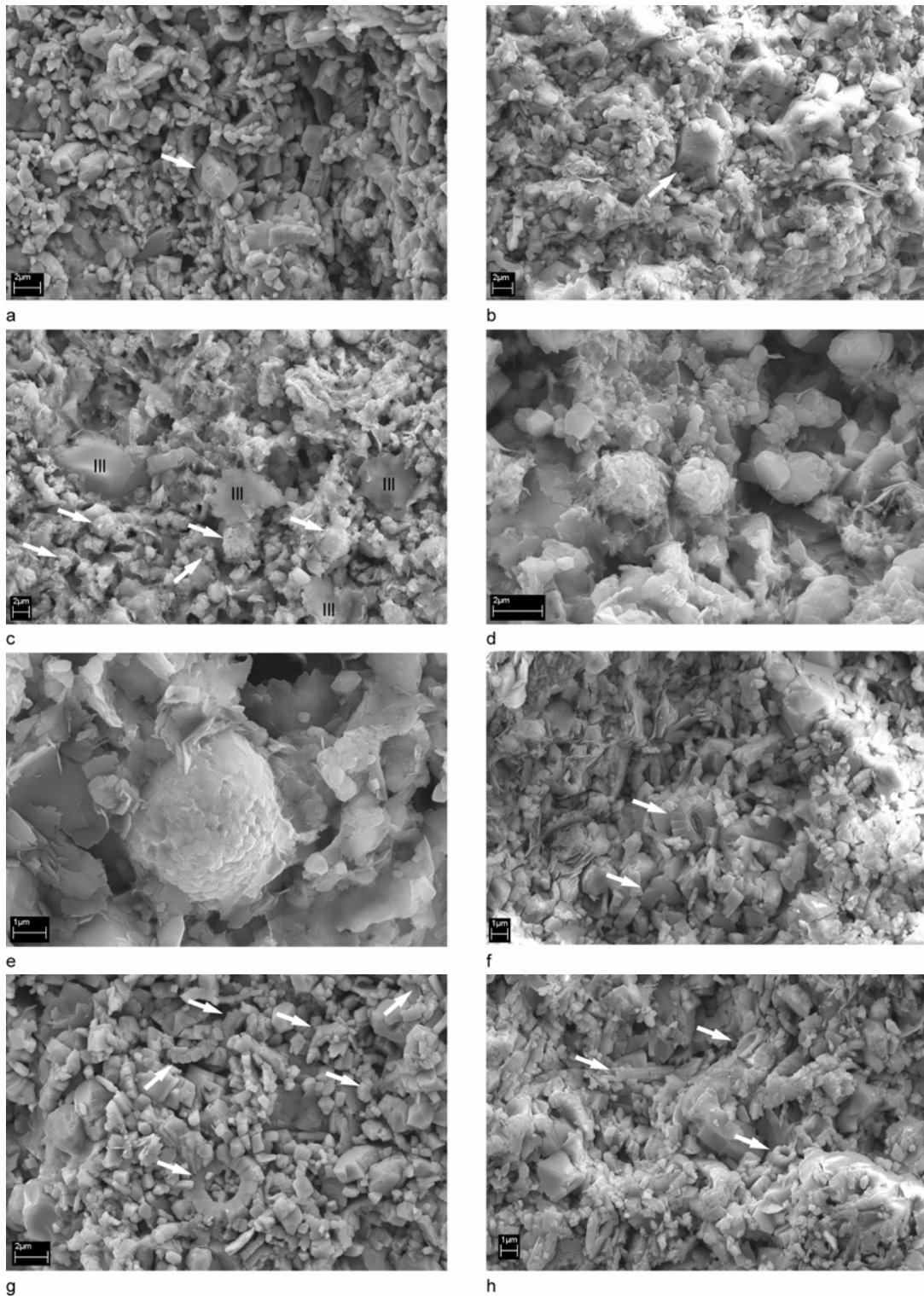
Figure 5.4. SEM photographs of Vallecillo rocks. a: Carbonate matrix composed of micrite (mc) and Microspar (ms), with an angular quartz grain (arrow) in the centre. VC1+7, basal limestone. b: angular quartz grain (arrow) with traces of corrosion. VC1-102, *Plattenkalk*. a-b unetched, normal to bedding plane. c: Flaky illite crystals (Ill) and small framboids of Fe-oxide (arrows). d: Two framboids of Fe-oxide on calcite, surrounded by flaky illite (Ill). e: Close-up of a framboid reveals its honeycomb structure in fine details. c-e VC1-30, *Plattenkalk*, etched, parallel to bedding plane. f: Coccolith in calcite matrix. Note the ultralamination, determined by clay minerals, in the upper left corner. g: Several coccoliths or fragments (arrows) in calcitic matrix. VC1+7. h: Tubular biogenous structures (arrows) composed of geometrically arranged calcite prisms. The matrix consists of micrite (mc) and microspar (ms). VC1-30. f-h unetched, normal to bedding plane. Scales see bars.

23

Framboidal texture is typical of pyrite, but it is also found among other minerals, such as Fe-, Cu or Zn-sulphides, spinels, hematite, goethite, garnet, and dolomite. The non-pyrite framboids can be both primary and/or form through the replacement of Fe-sulphides; the oxidation of Fe-sulphide framboids is a common phenomenon (Sawlowicz 2000). In laboratory experiments, goethite is only an accessory phase in the precipitation of Fe-sulphides in organic-rich sediments, and present in traces (Benning *et al.* 2000). In consequence, it is more likely that the framboids in the Vallecillo samples were originally Fe-sulphide. All microframboids identified in the Vallecillo sample have the same morphology, indicating a common source and composition (Wilkin *et al.* 1996). The uniform size (around 2 µm) and globular shape of the framboids suggest constant forming conditions (Sawlowicz 2000).

Pyrite framboids can form syngenetically or diagenetically, although framboid growth is restricted to earliest diagenesis, and it does not vary with burial depth (Wilkin *et al.* 1996). Direct precipitation of sulphide framboids from the water column is known from the Black Sea (Lyons 1997). The small diameters of the microframboids in the Vallecillo samples and their constant shape and dimensions are indicative of euxinic conditions at the sea floor (Wilkin *et al.* 1996; 1997). This is supported by the fact that framboids in the Vallecillo sediment occur in the sedimentary matrix and are rarely found within microfossil tests or other fossils. In consequence, they likely formed in an anoxic and sulphidic water column.

5.3   X-RAY DIFFRACTOMETRY (XRD)

X-ray diffractometry was used to analyse the whole rock composition in the fine-grained sediments, but also the composition of clay minerals. The Vallecillo *Plattenkalk* is mainly composed of calcite, but contents between 50 wt% and 83 wt% show it to be marl or marly limestone. Other components are phyllosilicates (18 wt% to 5 wt%), Quartz (15 wt% to 5 wt%), and feldspars (alkali feldspar <1 wt% to 5 wt% and plagioclase, which is a calcian albite, <1 to 2 wt%). The abundances of these siliciclastic minerals correlate (Figure 5.5). Goethite, hematite and pyrite are summarized here as Fe-minerals, due to their common origin concluded from the SEM analysis (see Chapter 5.2.2). No sample rich in Fe-oxides was included in the analysis, so these minerals were detected in few samples, and their content is as high as 6 wt%. Their distribution seems to be independent from the distribution of siliciclastic minerals or calcite.

Samples from two mudstone interlayers, also poor in Fe-oxides, were included in the analysis. They are composed of phyllosilicates (26 wt% to 38 wt%), quartz (6 wt% to 53 wt%), calcite (1 wt% to 20 wt%), and alkali feldspar (4 wt% to 19 wt%). In both the marly *Plattenkalk* and the mudstone, the high content of quartz and feldspar is remarkable, as these silicates cannot be identified from thin sections. They may even form the fine-silt lenses which are interlayered with the clay minerals (Figure 5.3e).

Phyllosilicates were further identified in the 2 to 16µm fraction. Abundances are quite uniform, partially because the 14Å expandable clay minerals cannot be separated from chlorite, and illite not from mixed-layer-illite. They are therefore summarized as ChloriteSmectite and IlliteSmectite. The latter is the most abundant clay mineral with contents between 41 wt% and 1 wt% in the clay minerals. Kaolinite is present in almost all samples, with quantities of up to 32 wt%. ChloriteSmectite reaches 27 wt%. Silicic detritus was quantified separate from clay minerals. Quartz is the most abundant silicate with quantities of 64 wt% to 98 wt%, whereas plagioclase is present in quantities of up to 36 wt%, and alkali feldspar with up to 24 wt%. The two feldspars do not correlate with each other or with any other mineral.
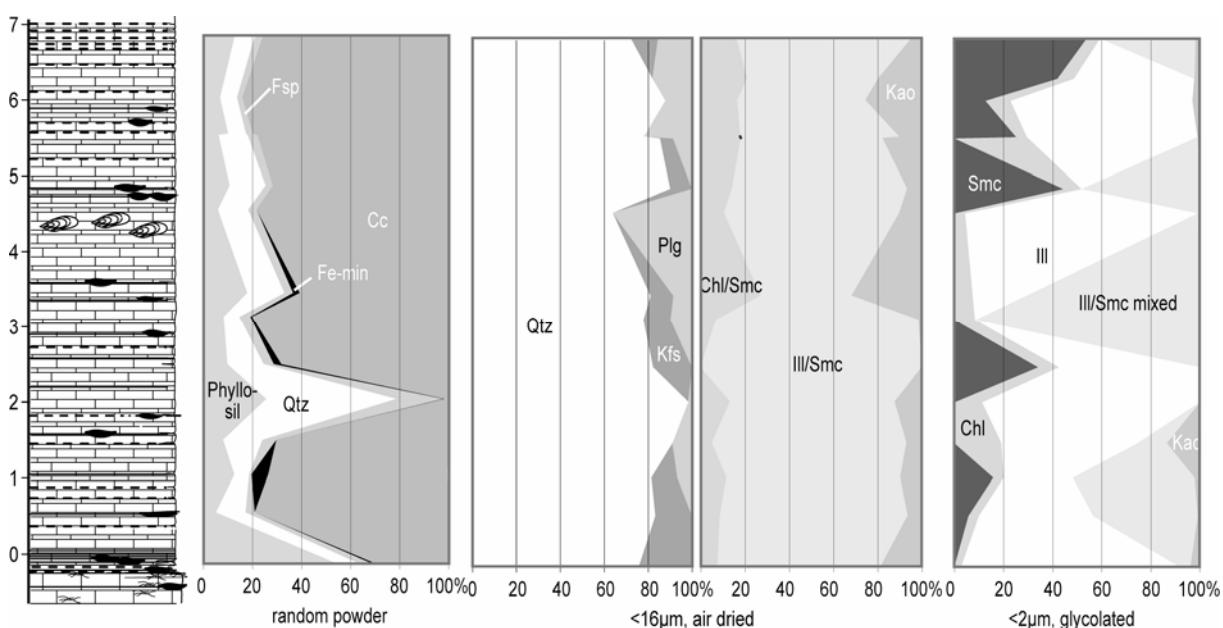
Figure 5.5. Mineralogy of the Vallecillo section from XRD analysis. Abbreviations: exp: expandable clay mineral, Chl: chlorite, Ill: illite; Ill/exp mixed: mixed-layer-illite, Kao: kaolinite, Qtz: quartz, Kfs: alkali feldspar, Plg: plagioclase, Phyllosil: phyllosilicates, Fsp: sum of plagioclase and alkali feldspar, Fe-min: Fe-minerals, sum of pyrite, hematite and goethite; Cc: calcite.

Quartz is also present throughout the section in the <2µm fraction, but it is not quantified and cannot be correlated with the clay minerals. The clay minerals, on the other hand, can be identified in detail. The most common clay mineral is illite, with contents of up to 95 wt%. In some cases, it has an expandable component, indicated by a peak shift in the glycolated slides. Separation of the two peaks is hard to identify in diffractograms from glycolated slides, as the illite is not well crystallized, and the peak is broad, overlapping with the mixed-layer-Illite peak. It is not further characterized by the method described by Moore and Reynolds (1997, p. 273) which allows quantification and type of ordering of expandable layers in an Illite/Smectite. According to this method, illites identified do not include expandable layers. A less abundant 14Å expandable clay mineral was found (up to 54 wt%),

as well as chlorite (3 to 19 wt%). The clay mineral identified with lowest quantities in this fraction is kaolinite, with contents of up to 13 wt%.

The distribution of minerals in the whole rock composition throughout the Vallecillo section reveals three sources of sediment, based on qualitative correlation of mineral abundances. Calcite, which is of biogenous origin, is independent in distribution from other minerals. Siliciclastic minerals such as feldspars, quartz and phyllosilicates correlate well, indicating a common source. The Fe-minerals do not correlate with the others and come from a third source.

The illite crystallinity averages 1·28 °Δ2θ. This suggests low ordering in illite and deepest burial in the "early diagenetic zone" in terms of metamorphism (Merriman and Peacor 1999). The clay minerals in Vallecillo are not recrystallized.

5.4   SEDIMENTARY SOURCES AND PALAEOCLIMATIC INTERPRETATION

In most regions of the world ocean, clay detrital assemblages reflect the combined influences of land petrography and continental climate (Chamley 1989, p. 176). Illite and chlorite are interpreted to be unweathered "primary minerals", whereas petrographic input from pedogenic blankets is mostly marked by irregular mixed-layers, kaolinite or halloysite, and smectite (Chamley 1989, p. 177). The relative abundance of illite tends to increase toward high latitudes parallel to chlorite, which reflects the decrease of hydrolytic processes and the increase of mechanical rock erosion under cold climatic conditions (Chamley 1989, p. 167).

Cold or temperate climatic conditions can be excluded for the Vallecillo sea. In the land area to the west and north-east, subtropical to arid conditions existed (Balukhovsky *et al.* 2004), whereas humid conditions prevailed further to the north and south (Figure 5.6).

The volcanism of the Alisitos Magmatic arc (Figure 3.1) and the related uplift may have caused strong mechanical weathering and erosion. However, volcanic rocks preferably weather to smectite, regardless of the climate conditions (Chamley 1989, p. 174). In addition, palaeoclimatic models proposed by Glancy and Arthur (1993) for Cenomanian-Turonian times suggest only minor transport by surface currents or wind from western sediment sources. Transport of clay minerals from the northern continent through the Western Interior Seaway by southward surface currents can also not be verified from the palaeoclimatic models proposed by Glancy and Arthur (1993). Their models do not support long-term ingression of boreal surface or deeper waters into the Vallecillo area.

Abundant detrital illite also characterizes the oceanic areas supplied by desertic regions such as eastern continental Asia (Chamley 1989, p. 169), or the Arabian continent and adjacent land masses (Chamley 1989, p. 187). Similar arid conditions may have prevailed on the continents north and west of the Vallecillo area (Balukhovsky *et al.* 2004, and Figure 5.6).

The low content of kaolinite can be explained by the distance from the coast line as this mineral is first deposited near the coast (Chamley 1989, p. 478). Part of the kaolinite could have been transported

by wind, another part could be of diagenetic origin: The weathering of pyrite and other sulphide minerals produces acidic solutions that can hydrolyze clay minerals into Al-rich varieties (Pollastro 1985). This may have been the case in samples rich in Fe-minerals. However, Kaolinite and Fe-minerals do not correlate in the Vallecillo sediment, and are likely not related.
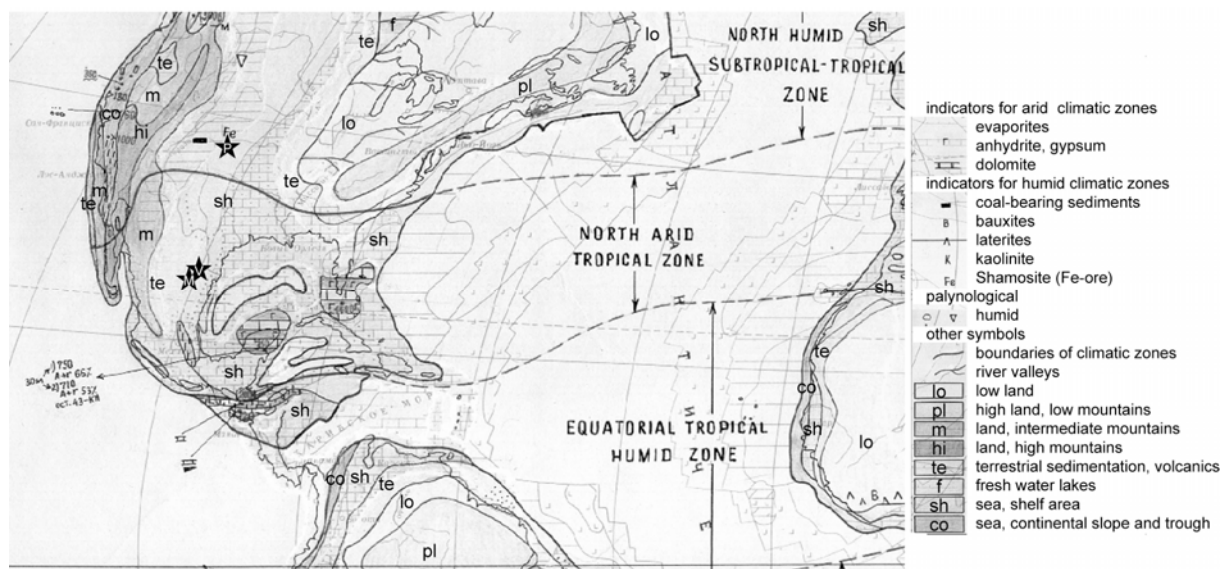
Figure 5.6. Palaeogeographic map of North America with palaeoclimatic zones assumed from geological markers (Balukhovsky *et al.* 2004). The localities of Vallecillo (V), Las Mitras (M) (see Chapter 10.1) and Pueblo (P), the GSSP of the Cenomanian-Turonian boundary, are marked by asterisks.

The phyllosilicate composition and presence of comparable amounts of fine quartz and feldspar in the sediment suggest a predominantly aeolian origin for the detrital component. A probable source was the Woodbine Peninsula to the north-east of Vallecillo (Figure 3.1), or the northern Gulf of Mexico coast. This is concluded from the climatic model of Balukhovsky *et al.* (2004, and Figure 5.6) for Cenomanian-Turonian times, combined with the climatic reconstructions of wind and marine currents of Glancy and Arthur (1993). The calcite component is biogenic in origin. The origin of the Fe-minerals will be discussed under the aspect of its geochemical composition (Chapter 6.2).

5.5   PRESERVATION OF FOSSILS

Fossils are found throughout the section. They are not restricted to limestone lithologies, but also occur in the mudstone. In this latter lithology, however, fossils cannot be recovered due to the softness of the host rock. Most fossils are preserved as dark grey calcite or as imprints; exceptions are treated below. When *Plattenkalk* slabs are opened, the fossils are split, with a slab and a counterslab for each fossil. In some specimens, one side provides more information than the other, so only one slab is recovered.

Five groups of fossils can be distinguished in Vallecillo: Cephalopods, inoceramids, crustaceans, vertebrates, and trace fossils such as pellets and coproliths.

Cephalopods are represented by ammonites, with the exception of a single coleoid. They are preserved as unilateral flat imprints in the sediment, but rare traces of black, recrystallized shells occur in at least three levels of the section. Some living chambers are filled with sediment and preserved as flat internal moulds, while others are flattened with the upper flank pressed onto the lower flank. The living chamber is present in many specimens, sometimes as flattened internal mould. Most ammonite shells were laterally embedded, but some were deposited in a vertical or oblique position (e.g. Figure 5.7). Fine details of sculpture and growth lines are particularly preserved in large ammonites. The last suture is partially visible in some specimens. The phragmocones are less well preserved, because empty shells collapsed under lithologic overburden, and the septae crushed irregularly. The unilateral preservation of the aragonitic ammonite shells indicates a sensitive equilibrium between aragonite dissolution and preservation before burial. Only thick shells survived the dissolving environment of the Vallecillo sea floor.

Aptychi are preserved in some specimens as thin crusts of iron-rich oxides, mostly goethite (e.g. Figure 5.9). Remains of the stomach content (Figure 5.8) are present inside living chambers, but they contain no identifiable matter. Structures of similar shape and position are known from the Solnhofen lithographic limestone, where they occasionally contain ostracods, small aptychi (Keupp 2000, p. 118, and pers. comm.) or crinoid remains (Westermann 1996). The preservation regime inside living chambers was apparently different than outside. This is also indicated by small shells preserved in the tests of large ammonites (see Chapter 5.6.2), while outside, two shells >100 mm have been found, while most shells >100 mm were dissolved prior to embedding, leaving only the sipho.

Some large ammonites are surrounded by a low pedestal socket in the sediment (e.g. Figure 5.11 and Figure 7.7). This "*Sockel-Erhaltung*" is comparable to the preservation of ammonites in the Tithonian lithographic limestones of Solnhofen (Barthel *et al.* 1990, p. 97). It prevented preservation of the ventral outline but provides a geopetal structure.

A white calcitic, isolated hard part of a coleoid was found during excavation. Its white colour suggests that the original skeletal matter is preserved in this flattened fossil, which it is not recrystallized to grey calcite. This fossil is further described in Chapter 7.1.

The most abundant **bivalves** in Vallecillo are inoceramids. Inoceramids are composed of an inner aragonitic layer and an outer, thick prismatic layer. The inoceramids from Vallecillo are preserved as compressed valves with the aragonitic layer completely dissolved, and the prismatic layer preserved (Figure 5.10a). Two overlying valves often dissolved each other through pressure solution. In some specimens, even the prismatic layer is dissolved, and a thin layer of dissolution residues of undetermined composition is left. Despite the compressed preservation, delicate details of sculpture such as microrugae or rugae are visible in most specimens.
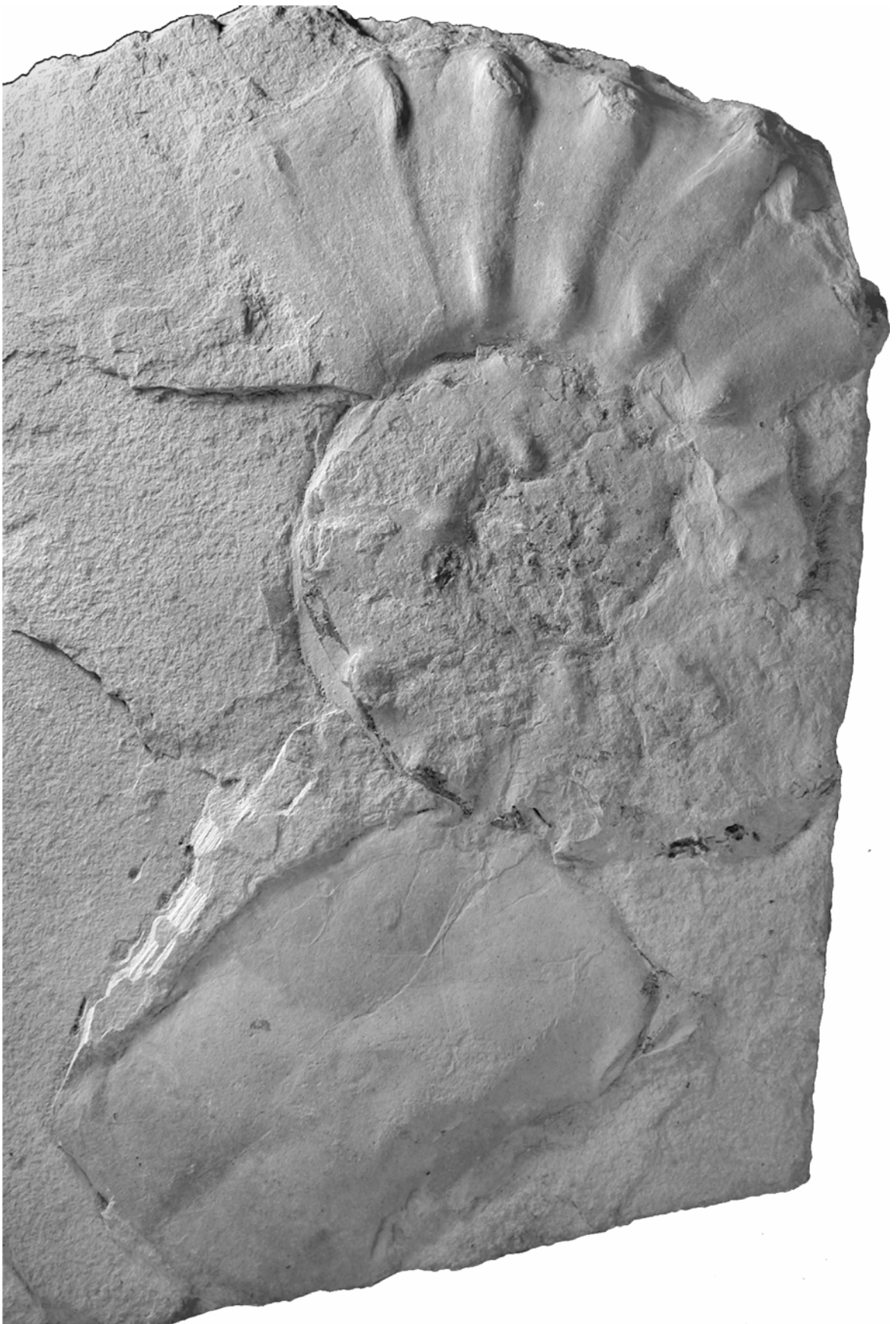
Figure 5.7. Laterally embedded *Pseudaspidoceras pseudonodosoides* next to a vertically embedded *P. flexuosum*. UANL-FCT-VC104A. ×0·75.
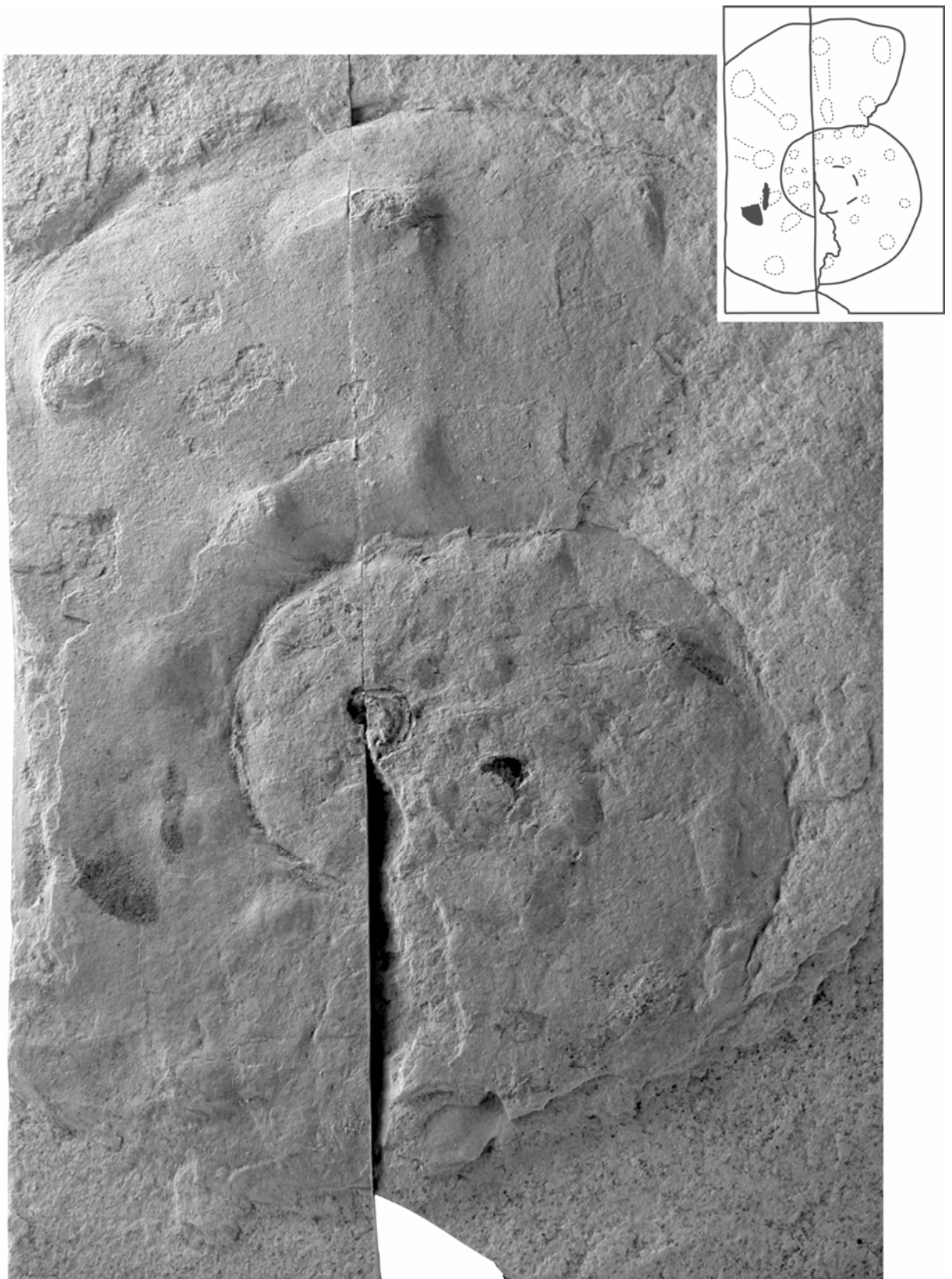
Figure 5.8. *Pseudaspidoceras flexuosum* with remains of the stomach content preserved as goethitic material (dark). UANL-FCT-VCI/114. ×1.
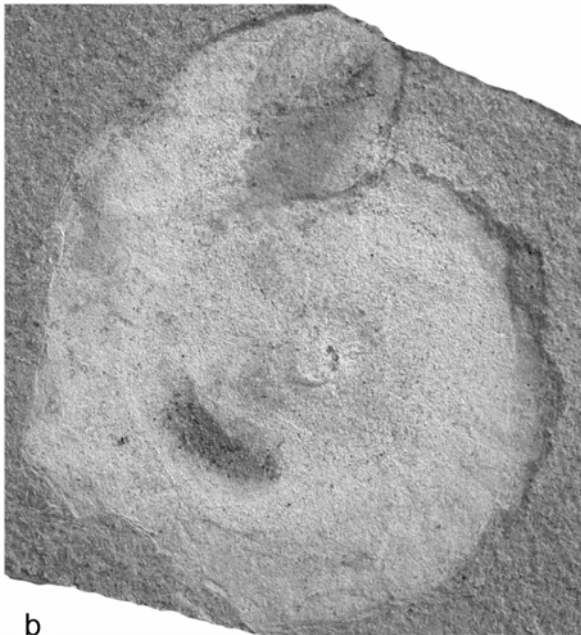
Figure 5.9. a-b: *incertae familiae*. **Specimens have remains of the stomach content preserved. a: UANL-FCT-VCI/30, with a possible aptychus near the aperture. b: UANL-FCT-VC1096. All ×1.**
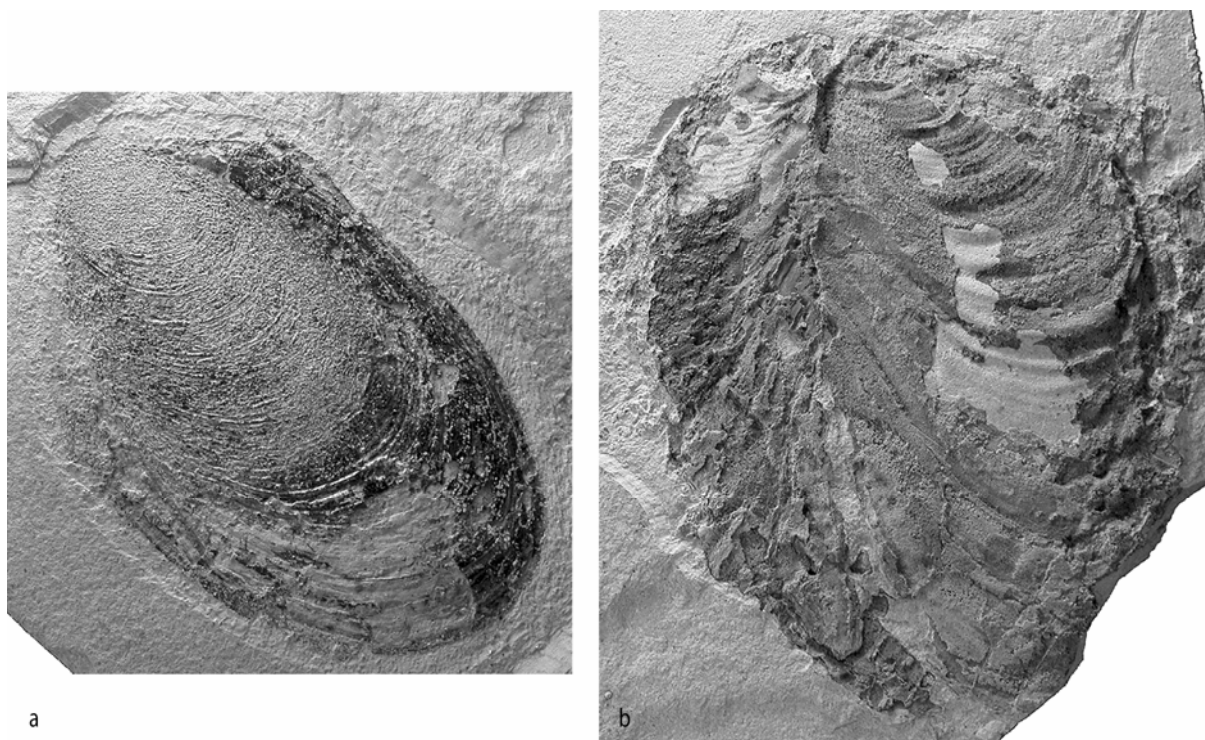
Figure 5.10. a-b *Mytiloides puebloensis* **from Vallecillo. a: Specimen preserved with goethite shell. UANL-FCT-VC112. b: The shell is flattened, only a thin layer of the prismatic layer is preserved. UANL-FCT-VC554. All ×0·75.**

Ostreids are found only as epizoans on ammonites. They are small (around 10 mm) and attached to the outer shell or the umbilicus of the ammonite (Figure 5.11). Specimens are badly preserved as coatings of dissolution residues, comparable to inoceramids. No hinge or resilium is recognized.

Crustaceans are represented in Vallecillo by the sessile cirripedian *Stramentum*. All specimens were attached to large ammonites (e.g. Figure 5.11). While the nacreous shell of the ammonites was dissolved during early diagenesis, the calcite of the epizoans is preserved. In cases when the carapaces fell out during collection or preparation of the samples, they left detailed imprints.

The bodies of **vertebrates** are usually compressed to a thickness of less than 15 mm (e.g. Figure 5.12). The sculls of the larger fishes (more than 1 m axial length) are preserved three-dimensionally, but compressed. Many complete to subcomplete articulated specimens were recovered over the years, others are in different stages of disarticulation (e.g. Figure 5.12). Bones are preserved as dark, grey calcite, in contrast to teeth. These are white with the original and unrecrystallized enamel. Intestine contents are usually preserved as dark calcite. In some specimens they have a foamy texture. Scales, fins, isolated gills and other soft parts are preserved as imprints, with only the fine rays being mineralized.
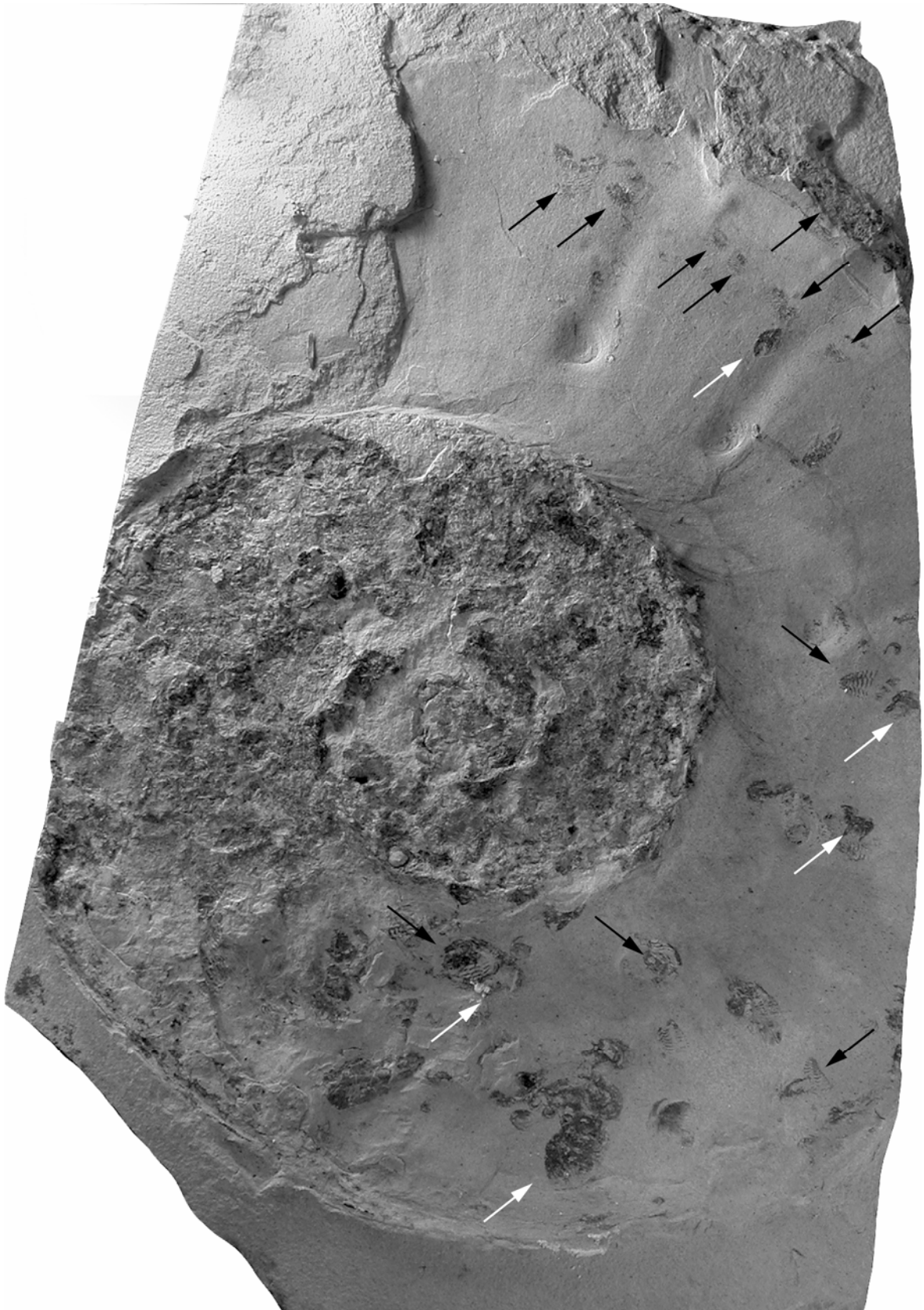
Figure 5.11. Large sized *Pseudaspidoceras flexuosum*. The specimen is covered with epizoic *Stramentum*, a sessile cirripedian (black arrows). Few ostreid shells are also preserved as coatings (white arrows). The ammonite is surrounded by a low pedestrial socket. UANL-FCT-VC104. ×0·75.
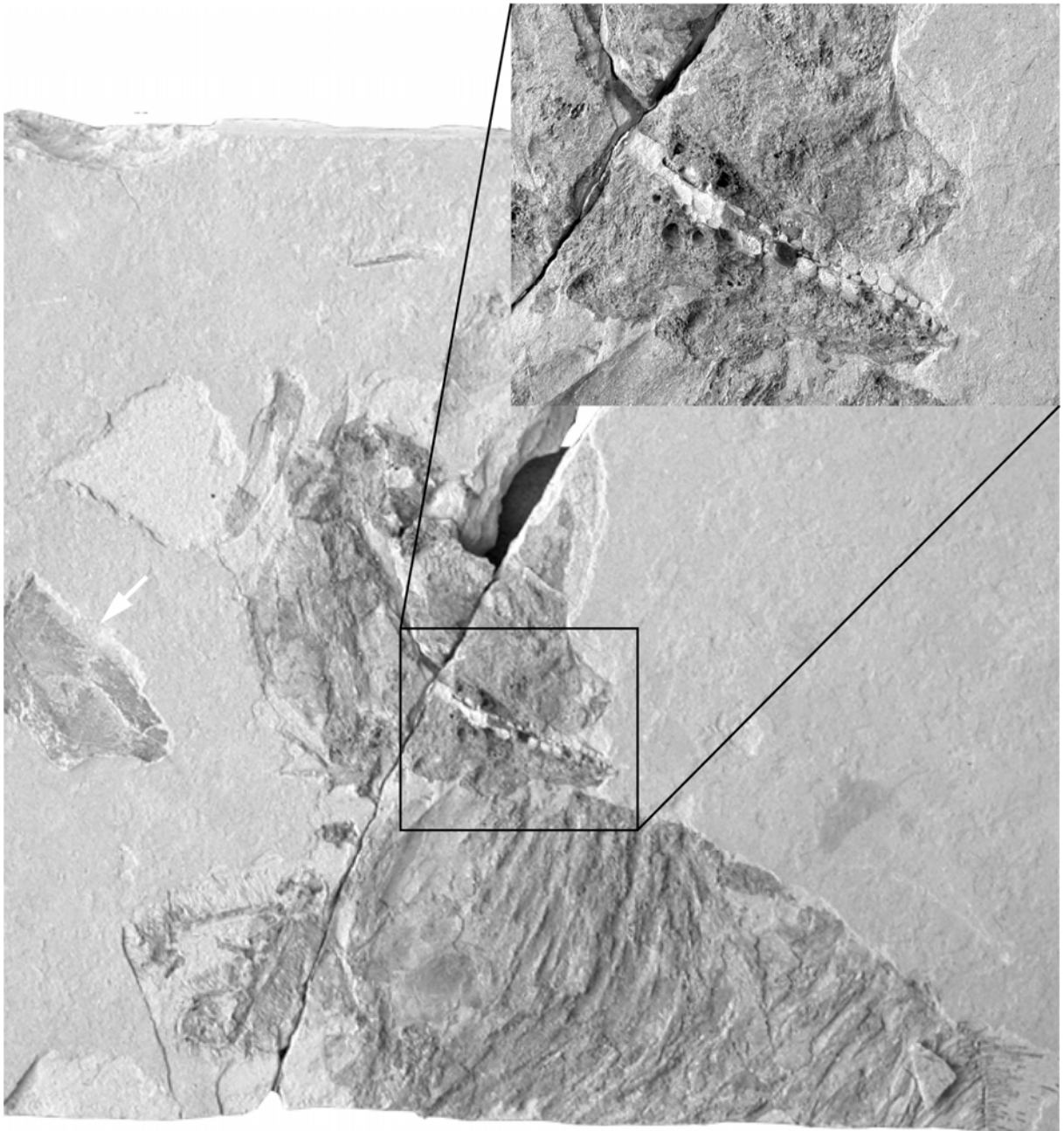
Figure 5.12. Disarticulated *Nursallia* cf. *N. gutturosum* from Vallecillo with pycnodont teeth preserved. UANL-FCT-VC 084. ×1.

The preservation of **pellets** is comparable to that of small fishes (Figure 5.13a-b). Most pellets are composed of mineralized small bones, in some cases surrounded by imprints of a soft material or Fe-oxide.

Coproliths are preserved in different ways and described according to their structure. Usually they are flattened, but three-dimensional, and composed of dark grey calcite, whereas other specimens are uncompressed and three-dimensional (Figure 5.13c-g).
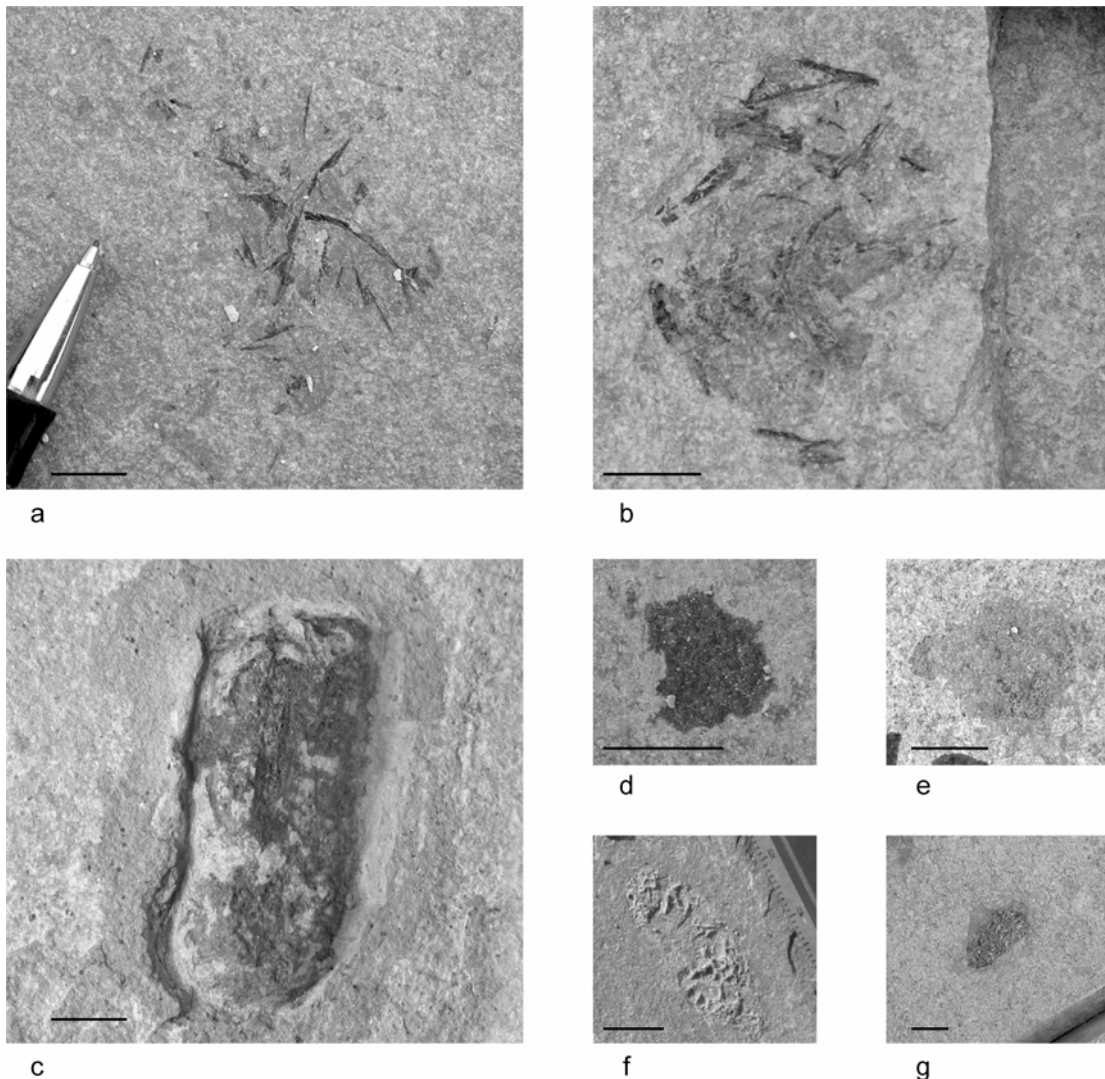
Figure 5.13. Pellets and coproliths. a-b: Isolated pellets, composed of broken bones, with imprints of soft matter (darker zones around bones). a: VCI/431. b: VCI/241. c: uncompressed coprolith with "amorphous" texture. VCII/79B. d: shapeless coprolith with fine-grained texture. VCI/413. e: strongly flattened coprolith with a fine foamy texture (lower right) and impression (upper left). VCI/247. f-g: coproliths with foamy textures. They are comparable to intestine content of some fishes and were formed by a cement surrounding rounded particles of a now dissolved substance. f: VCI/82. g: VCI/46. Scale bar 10 mm.

The Vallecillo vertebrate and coprolith fossils are commonly preserved as recrystallized calcite. This is a remarkable preservation for bones, soft tissues and ammonite siphos in a pelagic environment, because they usually are phosphatized (Prévôt and Lucas 1990)

The calcite crystals are up to 5 mm long, unoriented, and poikilotopic to opaque and unoriented needle-shaped grey crystals (Figure 5.14c, e-f). The shape, grey interference colours and sandglass structure of the latter indicate alkali feldspars (e.g. Figure 5.14g), but they are too small for a precise determination from thin section. These authigenic feldspars were not only found in coproliths, but are also present in fossil bone material.

Early mineralization, prior to compaction, is indicated by a once soft coprolith that was pressed upon an inoceramid shell and deformed it (Figure 5.14b). The poikilotopic nature of the calcite indicates that this mineral formed later than the included minerals and overgrew them. The calcite crystals thus resemble secondary cement that replaced the mineral which primary fossilized tissues or skeletal elements of the macrofossils. Even though, minute tissue structures are preserved. Larger vertebrae, for instance, show laminae of cell structures in thin section (e.g. Figure 5.14d).
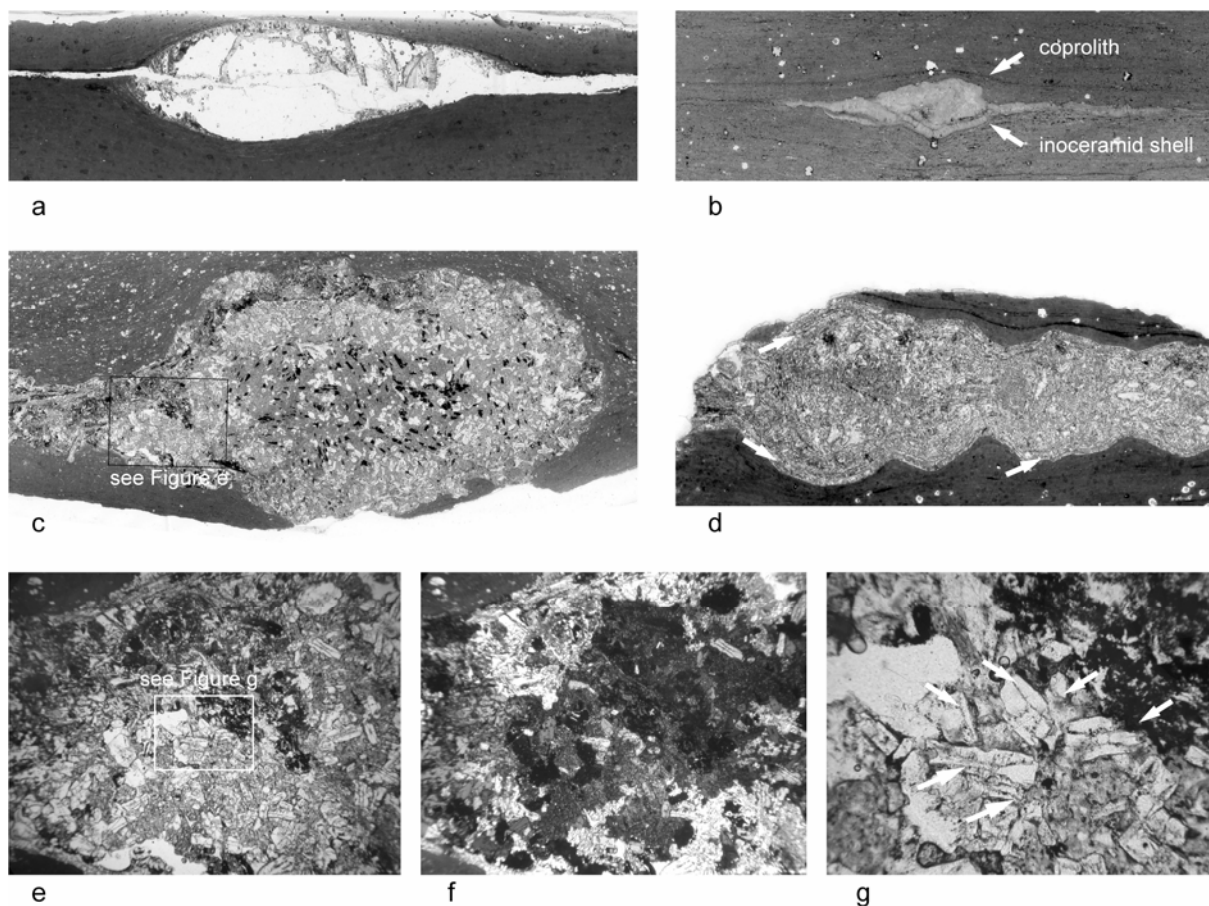
Figure 5.14. Thin sections of Vallecillo fossils. a: This coprolith with "foamy" texture is composed of calcite cement, whereas the original substance is dissolved. VCI/148. b: This coprolith was pressed upon an inoceramid shell during sediment compaction and deformed the shell, indicating very early diagenetic mineralization of a once soft substance. VC1-97. c: coprolith with fine-grained texture. Note zonation: the "grained" texture concentrates on the outer areas, whereas opaque minerals occur mostly in the central area. d: vertebra with cellular soft tissue (arrows) preserved. unregistered. Scanned, ×3. e: the zoom on Figure c reveals that "grains" are authigenic feldspar. f: same detail as before, but with crossed polars. Each extinguishing or non-extinguishing domain beyond feldspars corresponds to a calcite crystal. Feldspars and opaque grains are unoriented and overgrown by calcite crystals, indicating that the non-carbonaceous minerals formed prior to the calcite. ×10. g: Feldspar crystals with sandglass structure (arrows). Parallel polars. Unregistered. ×40.

5.6   DIAGENESIS OF THE VALLECILLO *PLATTENKALKS*

5.6.1   Sediment compaction

Compression of sediments can be estimated from uncompressed fossils, mainly bones. The strong compression, particularly of small fossils, can be explained by the high content of clay minerals. When clay minerals settle in sea water, they form card-house structures with water contents of up to 90%. These loose structures are destroyed under lithologic overburden, leading to parallel settling of the platy minerals and the release of pore waters. Carbonate and silicate particles remain mostly unaffected in these stages of burial (Merriman and Peacor 1999).

Vallecillo sediments are composed of 40 to 70 % carbonate. The rest includes fine-grained quartz, feldspars, and various types of clay minerals, particularly unordered, partially expandable illite (Chapter 5.3). All fossils embedded in this sediment are compacted unless mineralization was early enough and complete to resist compaction. This was not the case for ammonites or inoceramids. Ammonites are preserved as unilateral imprints, with the upper side dissolved. It is impossible to estimate the ratio of thickness between dissolved and preserved shell. Inoceramids are preserved as closed valves that were pressed onto each other, leading to pressure dissolution of the inner aragonite layer, but also of the calcitic prisms of the outer shells (e.g. Figure 5.14b). No sediment is preserved between the valves. Inoceramids and ammonites can thus not be used to determine compaction.

Large vertebrae, teeth, or quickly mineralized coproliths are fossils suitable to provide quantitative estimations of the compaction rate. Thin sections analyzed are presented in Figure 5.15, the results are listed in Table 5.1.

The resulting compaction rates differ much from each other. This may in part be related to the method, but can also be explained by the different lithologies of the Vallecillo section. Rocks rich in clay minerals compact much stronger than almost pure limestones.

The average compaction to 30 per cent of original thickness is remarkably high, considering the high carbonate content of the sediment, but it corresponds well to the observed flattening of macrofossils from Vallecillo. Much of the decreased thickness is due to the compaction and related loss of pore waters of illite and other clay minerals. SEM analysis showed the carbonate to be recrystallized, and this process may have caused further loss in porosity and thickness.

The organic matter was completely oxidized and disappeared out of the rock, but oxygenation also affected the Fe-sulphides such as pyrites. This oxidation is associated with a loss of 20 to 36 per cent of volume (see discussion in Sawlowicz 2000). In addition, sulphur-containing mineral such as gypsum were not found in the XRD analysis, but this may be biased by sampling.

Even though sediment compaction was high, no evidence for major pressure solution (e.g. styloliths) was found in Vallecillo. Pressure solution is only observed within inoceramid shells.
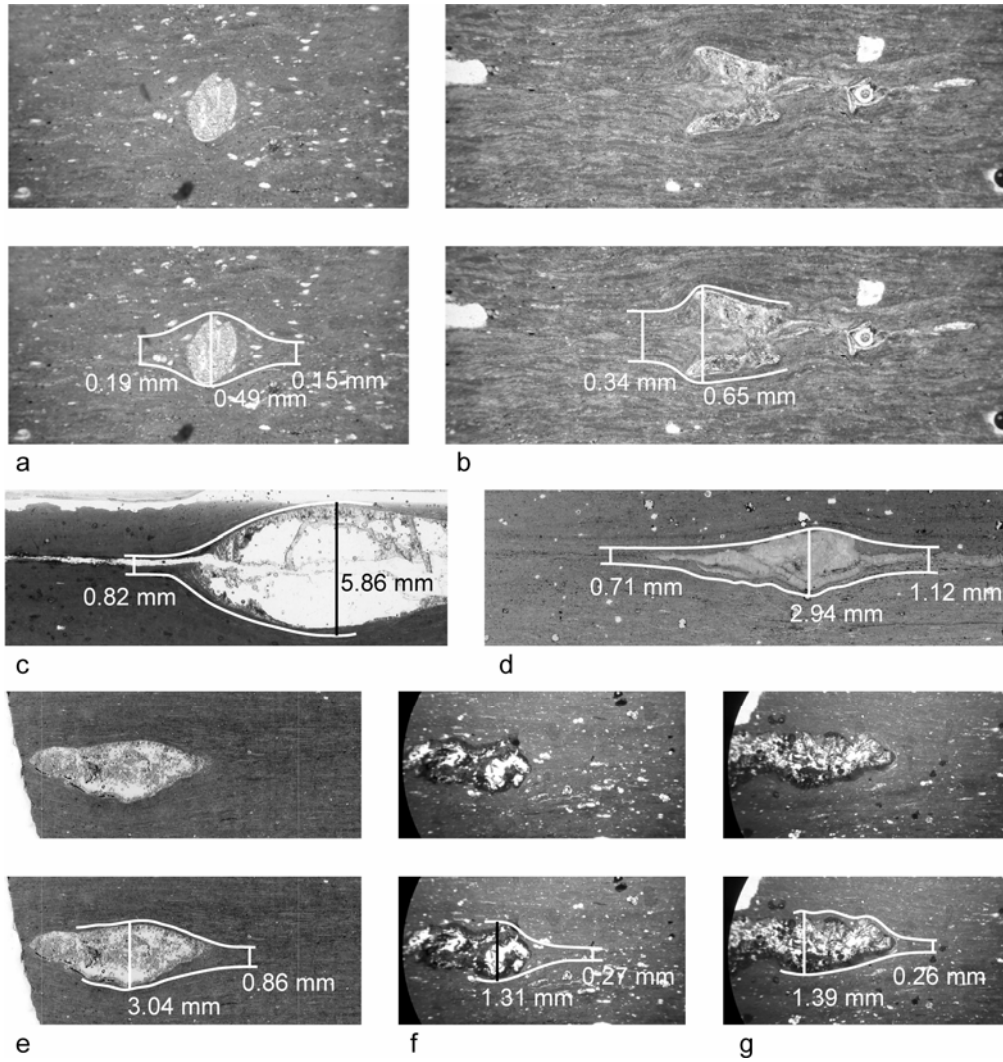
Figure 5.15. Estimation of the compaction rate from thin sections. The original image and its graphic interpretation are presented. a: Cross-cut fish bone. VC1-88. b: Small vertebra. VC1-42. parallel polars, ×20. c: Coprolith with foamy texture. The uninterpreted image is the left part of Figure 5.14a. VCI/148. d: Coprolith with dense texture. The uninterpreted image is Figure 5.14b. VC1-97. e: Coprolith. VC1-68. Scanned, ×3. f-g: Two small coproliths preserved in the same thin section.VC2-21. ×6.

sample	compaction rate		
VC1-88	left: 40%	right: 31%	
VC1-42	52%		
VCI/148	14%		total average:
VC1-97	left 24%	right: 38%	30%
VC1-68	28%		
VC2-21	21%		
VC2-21	19%		

Table 5.1. Thin sections analyzed in Figure 5.15. Compaction rates correspond to percent of original thickness. The lower the percentage, the more compacted is the sediment. The average compaction rate is used for further interpretation.

5.6.2   Aragonite dissolution

In ammonite shells smaller than 100 mm, only the sipho is preserved, while large shells occur as unilateral imprints. This preservation indicates early diagenetic aragonite dissolution heavily affecting smaller, thinner shells. The lower side of larger, thicker shells was pressed into the sediment and protected from dissolution, whereas small shells lying on the surface were dissolved completely. Small ammonite shells are only preserved in the living chambers of two *P. flexuosum* (e.g. Figure 5.16). When large ammonite shells touched the ground, they may have caused turbulence of the fine-grained sediment. Sediments with major pore waters contents (more than 80%) filled the living chamber and prevented migration of pore waters and thus the dissolution of the lower shell and included small ammonites.

The preserved halves of large tests were pressed into the sediment. Overburden lead to breaking of the shell while the surrounding sediment was still soft. These fractures are visible in many, although not all ammonites. The organic periostracum was possibly present at this early stage of burial.

Ultrafacies analysis supports the idea of early aragonite dissolution. Carbonate was dissolved and subsequently precipitated as microspar. The available Mg of dissolved high-Mg-calcite and aragonite was included in idiomorphic dolomite crystals, which are occasionally preserved (e.g. Figure 5.3d), but have frequently been dissolved in a later diagenetic phase. They are today recognized by rhombohedral cavities or pseudomorphs of calcite.

Aragonite may play an important role in differential diagenesis of limestone-marl alternations (Munnecke and Samtleben 1996; Munnecke *et al.* 1997; Munnecke *et al.* 2001), such as the Agua Nueva Formation. The observations of these authors are mostly based on SEM analysis of a diagenetically little altered limestone-marl-alternation in Gotland. There, the carbonate sediment was interpreted to have been primarily homogenous. During early diagenesis, vertical changes in pore water chemistry, mainly produced by microbial decomposition of organic material, resulted in vertical geochemical gradients. Decrease in carbonate saturation within the sediment column caused aragonite to be unstable and to be dissolved at a certain depth, producing a dissolution zone roughly parallel to the sea floor. Within this zone, aragonite was dissolved, transported by diffusion, and precipitated as microspar. The diffusional transport of carbonate ions was interpreted to have been active in upward and in downward direction. This is supported by the observation, that precipitation took partially place in sediment levels where aragonite was still stable, indicated by the pitted structure of one type of microspar type. The sedimentary levels depleted in aragonite became marls, the level with carbonate precipitation became limestones (Munnecke and Samtleben 1996).

The limestone-marl alternation of the Agua Nueva Formation likely formed by this process. The Vallecillo Member, situated within this formation, is composed of marly limestones, limestones and mud- to claystones, with an average rock composition similar to that of the Agua Nueva Formation, even regarding the content of organic matter (see below). However, differential diagenesis did not

develop in the Vallecillo Member, even though strong evidence exists that aragonite dissolution and calcite precipitation occurred.
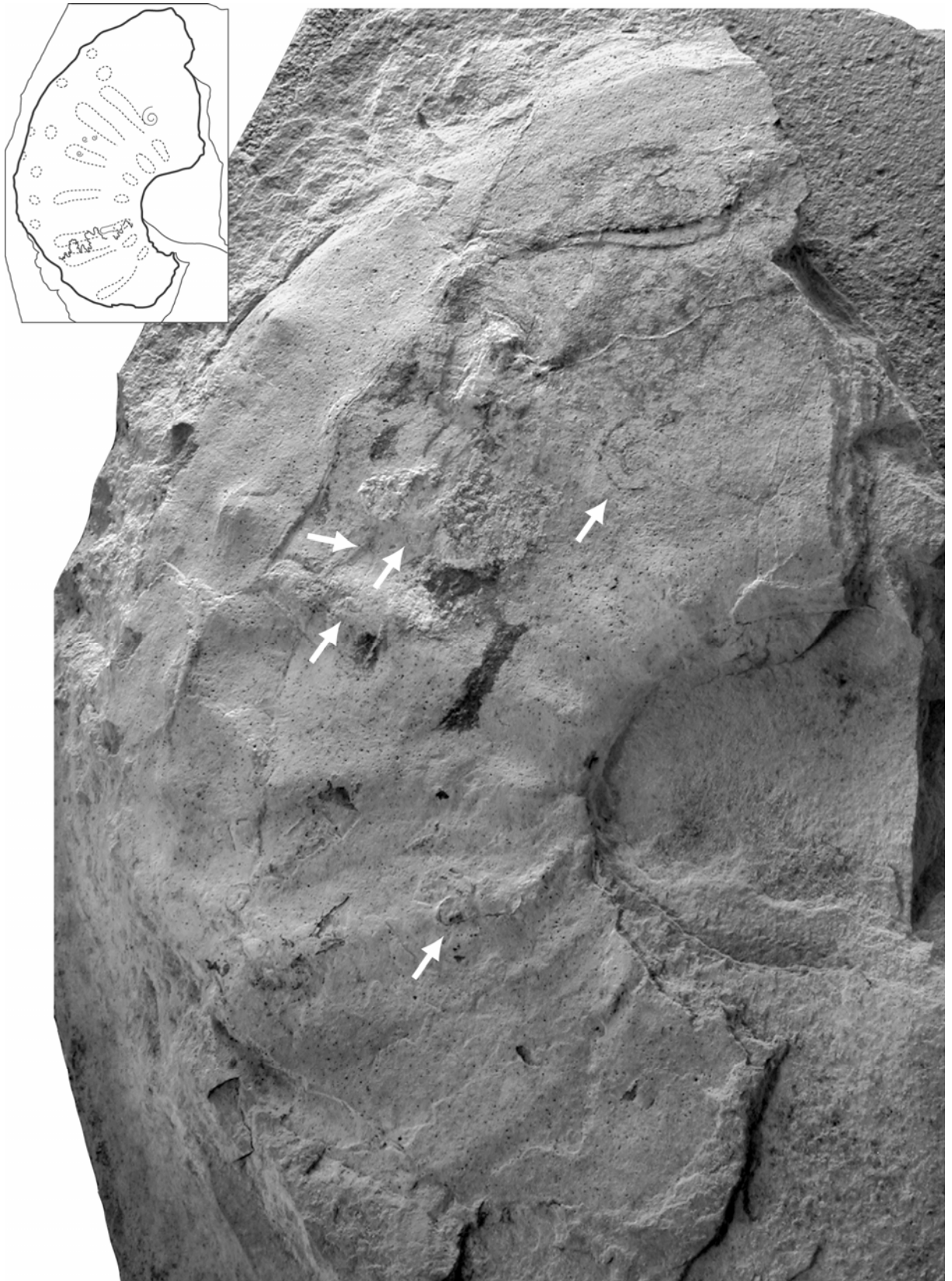
Figure 5.16. Obliquely embedded *Pseudaspidoceras flexuosum* with small ammonite shells preserved in the living chamber (arrows). UANL-FCT-VCI/482B. ×1.

Aragonite became unstable at the sea floor, as indicated by the preservation of cephalopods. It is likely that a chemical gradient did not develop within the sediment to allow migration of carbonate ions, which may be explained by low microbial activity within the sediment regarding decomposition of the abundant organic material. The carbonate was thus precipitated uniformly in the sediment as microspar. Indeed, no indicator for early diagenetic re-distribution of ions in the sediment exist, with the exception of dedolomites and Fe-oxide concretions in mudstone layers rich in Fe-oxide. The latter contrast the presence of synsedimentary framboids in the *Plattenkalk*. Dedolomites are explained by early diagenetic dissolution of metastable hi-Mg-calcite and reprecipitation as microspar and idiomorphic dolomite; they were thus independent from the presence of a geochemical gradient. Carbonaceous or silicic concretions are absent in Vallecillo.

Aragonitic shells dissolved prior to and shortly after burial, synsedimentary framboids (Chapter 5.2.2) and the absence of concretions in the organic rich sediment despite the availability of carbonate ions indicate that the composition of the water at the Vallecillo sea floor was similar to pore water composition, which prevented differential diagenesis in the Vallecillo member. In conclusion, truly anaerobic conditions must have been present above the sea floor.

5.6.3   Deepest Burial

Burial depth is usually estimated by illite crystallinity. This averages $1\cdot28$ °$\Delta2\theta$ in the Vallecillo samples, corresponding to a maximum burial depth of $3\cdot5$ km, at temperatures below 100°C. The organic matter in the sediment reached a maximum maturity to heavy oil. This indicates that most of the organic matter was preserved in the sediment until weathering (Merriman and Frey 1999).

The ore formation around Vallecillo (see Chapter 3.2.4) did not visibly change the sediments exposed in the Vallecillo quarries.

5.6.4   Weathering and Soil Formation

The Vallecillo sediments were originally rich in organic matter and black in colour, comparable to the Agua Nueva Formation *sensu stricto*. In some beds extant organic matter is preserved. This dark colour was bleached out, changing the rocks to bright colours. Weathering has reached depths of tens of meters in north-eastern Mexico as the result of semi-desertic climatic conditions.

Rocks 1 m below the surface are also altered by the formation of soil (Figure 5.17a). Weathering enhances the ability of the rock to split. Water also enters through vertical joints, which are usually coated by caliche. Water migrates through and widens the mudstone layers, leading to slight flexing of the more resistant *Plattenkalk* layers. Fossils in this zone are heavily weathered and badly preserved.

Roots of desert plants are present in mudstones, goethite layers or splitting surfaces within the marly limestone, even at the base of the quarry. They enter the rock through vertical joints and then follow subhorizontal mudstone layers. Roots dissolve the adjacent carbonate rock and leave a pattern

that is similar to some fossil algae, e.g. from the Messel Pit *Lagerstätte* (Frey, pers. comm.), but must not be confused with them. This mineralization is actually an example for a recent process which forms a plant trace fossil, as the organic material leaves permanent mineral traces in the sediment.
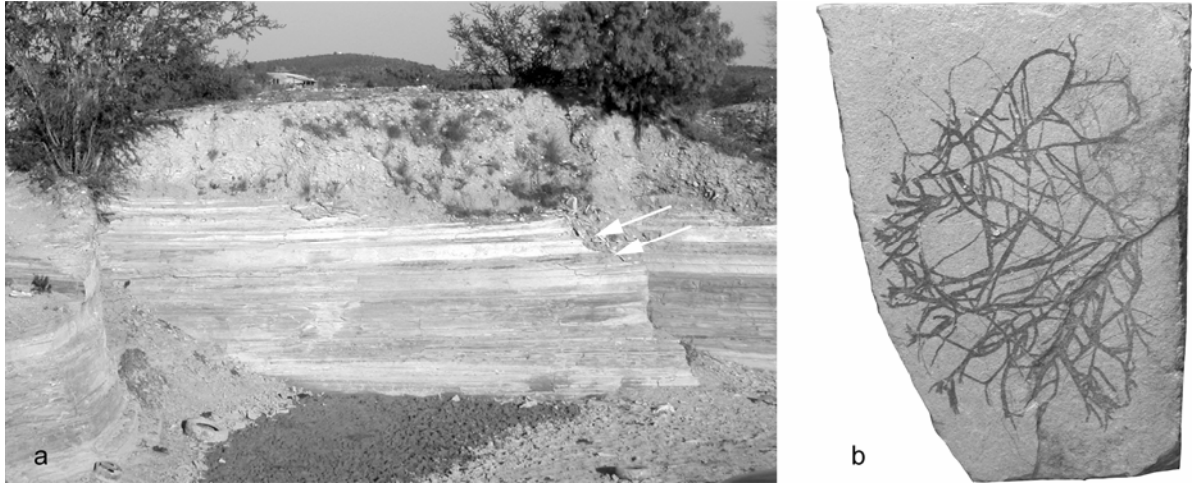
Figure 5.17. Weathering in the Vallecillo quarries. a: Layers exposed directly below the surface. White coating is caliche deposited along a vertical joint. Note the thickening of the layers marked by arrows. They are approximately 15 cm thick to the right, but only 2 to 3 cm to the left. This leads to a slight upward bending of the resistant limestone layers. The section presented here is about 3 m thick, only the upper meter is affected by soil formation. b: Recent roots cause coatings of darker colour than the surrounding sediment, resembling algae. ×0·8.

.

6   GEOCHEMICAL ANALYSIS

The distribution of selected major and trace elements is presented in Figure 6.1. Values are approximately uniform in the marly *Plattenkalks*, with the exception of the samples from mudstones rich in Fe-oxides.
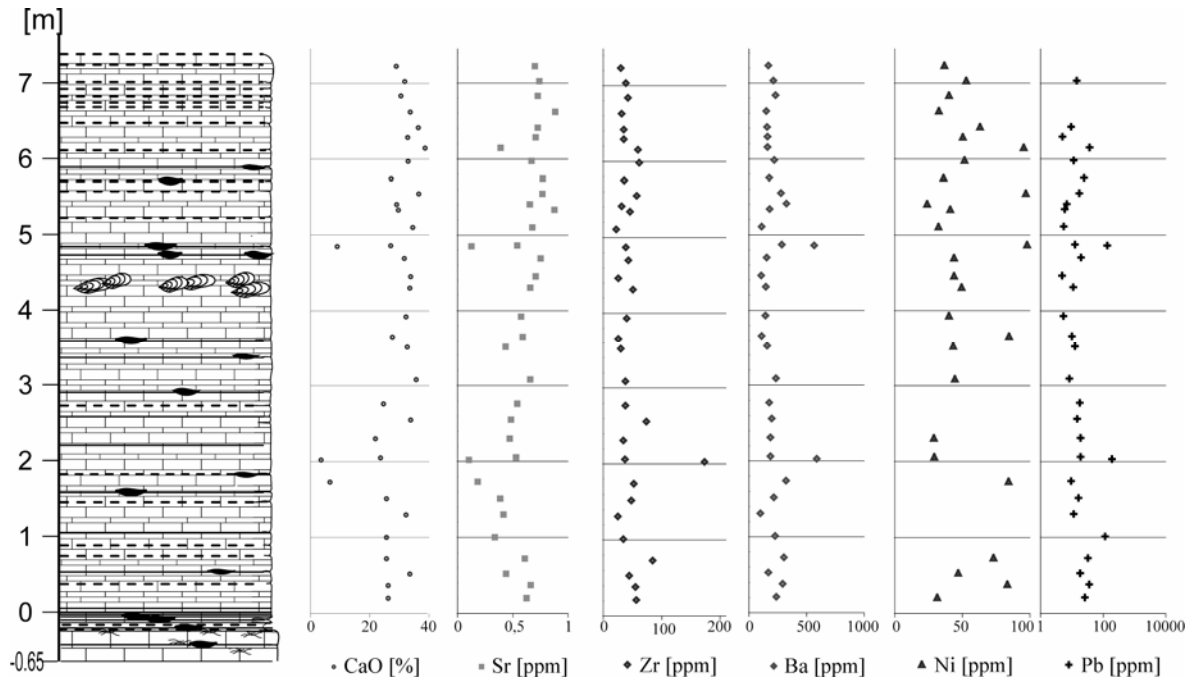
Figure 6.1. Distribution of selected elements over the Vallecillo section. The biogenic Ca and Sr behave similar, whereas detritals such as Zr and Ba oppose the behaviour of Ca. The chalcophile Ni and Pb differ in their behaviour from the other four elements presented here. Note that scales are linear with the exception of Pb, which is illustrated on a logarithmic scale

Ca is mainly bound to calcite of biogenous origin. The concentrations of CaO are between 6% and 39%. Elements related to biogenous activity correlate with Ca. The concentrations of Sr covary with those of Ca (Figure 6.1). In contrast, Zr and Ba oppose the behaviour of Ca. These elements are mostly bound to minerals of detrital origin.

A third group includes chalcophile elements, e.g. Ni and Pb, and does not correlate with the former elements. They are most probably related to sulphides precipitated in the organic-rich environment.

6.1   THE *PLATTENKALK*

Inter-elemental relationships are investigated by means of cluster analysis. A close interdependency among these elements, i.e., a good correlation between Sr and Ca, is indicated by a low linkage distance in the dendrogram (Figure 6.2). It indicates a biogenous origin for Sr. Zn and, to lesser

amount, Cd also correlate well with these elements. Both are known to be involved in the biogenous cycle as nutrients (Knauer and Martin 1982).

Ti (rutile, ilmenite), Rb (feldspars or clay minerals), Zr (zircon) and Ba (feldspars or clay minerals) are elements of mostly clastic origin and correlate very well in the Vallecillo sediments (Figure 6.2a). Their variation approximately parallels that of the rare earth elements (REE) such as Ce and Y, which are interpreted to be bound to clay minerals.

There is a general upward increasing trend over the Vallecillo section in the content of biogenic elements, whereas detrital elements show an opposite trend (Figure 6.1).

Mn can be associated with both clay minerals and carbonates. This element is generally enriched in marine waters low in oxygen. In carbonate rocks, it may be precipitated as Mn-carbonate (Brumsack in press). However, carbonate rocks which formed under these conditions are often low in Mn, in contrast to sediments formed under oxic conditions which are frequently enriched in Mn-oxides (Jarvis *et al.* 2001). Vallecillo rocks are strongly depleted in Mn, with values at or slightly above detection limits (see Appendix B), suggesting at least suboxic conditions in large parts of the water column (Brumsack in press)
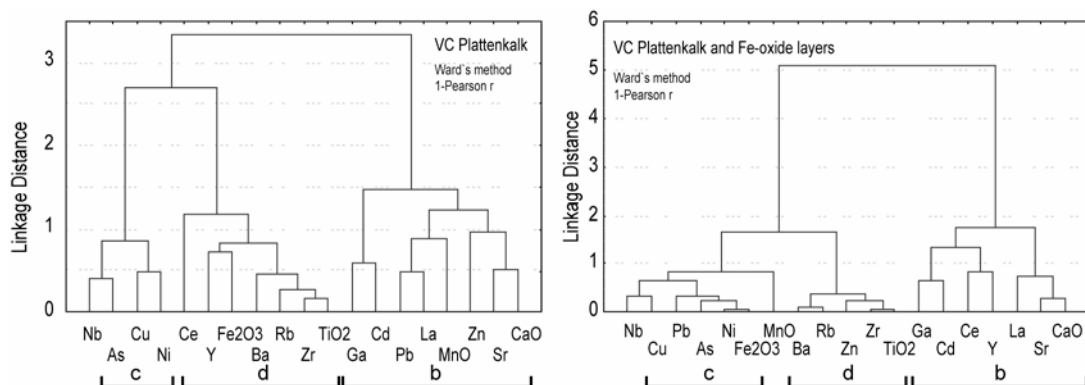
Figure 6.2. Cluster analysis of main and trace elements in the Vallecillo *Plattenkalks*. Linkage distance below 1 indicates a good correlation. c: chalcophile elements. d: elements of detrital origin. b: elements accumulated by biogenic processes. Left: only samples with *Plattenkalk* lithology were included. Samples rich in Fe-oxides are omitted from this analysis. Right: Cluster analysis of main and trace elements including the Fe-oxide layers shows a much stronger grouping of the elements. Chalcophile elements behave different from the elements of detrital or biogenic origin. Note that the scale for linkage distance is different in the two charts.

The content of Ni in the Vallecillo *Plattenkalk* is close to an average marine shale (Brumsack in press), and in many samples much higher. This high content of Ni is remarkable, as the Vallecillo sediments are diluted by the high carbonate content in the marl and limestone, compared to shales investigated by Brumsack (in press). This high Ni content is common in Cenomanian-Turonian boundary sediments around the world (Brumsack in press) and indicates deposition under sulphidic black shale conditions for the Vallecillo *Plattenkalks*. The enrichment potential for Ni is highest when

decaying microbial matter encounters anaerobic conditions shortly after or during deposition (Lewan and Maynard 1982; in Brumsack in press), which apparently existed in Vallecillo.

Cu and As correlate well with Ni, and correlate neither with the detrital group of elements nor with the biogenic group. Although Cu and Ni may be enriched as micronutrients (Brumsack in press), their opposition to elements of biogenic origin and their strong association with As rather indicates precipitation as sulphides.

6.2   LAYERS ENRICHED IN FE-OXIDES

When layers rich in Fe-oxide are included into the cluster analysis, the interpretation changes in part. Elements of the detrital group (Ti, Zn, Rb, Zr and Ba) behave similar as in the *Plattenkalks*, with the exception of Pb and the REE. Ce and Y now correlate moderately to well with Ca and Sr, in contrast to their distribution in the *Plattenkalks*. Their association with the carbonate phase suggests an origin from biogenic precipitation, although they are more enriched in phosphates. These were not found in Vallecillo, but fossil preservation suggests primary mineralization by another phase than calcite (Chapter 5.5). The correlation of REE with elements of biogenic origin may be evidence for primary mineralization of fossils by phosphate.

Pb correlates best with Fe, but also with As, Ni, and Cu in the goethite layers. This distribution points to a hydrothermal overprint or primary sulphide precipitation (Kramar, pers. comm.; Berner, pers. comm.). A Pb-Zn-Ag ore deposit of unknown type is known to exist in Vallecillo, which formed post-depositionally (Chapter 3.2.4). The goethite layers are parallel to lamination, or even cause the lamination in the sediment. In consequence they must have formed synsedimentarily as sulphides. Observations in field lead to the conclusion that there was hardly any overprint of the ore deposit on the Vallecillo sediments (Chapter 3.2.4). The low concentrations of Zn and Ag support this view. These elements were mined in the Vallecillo area, and their content and correlation would indicate a genetic link with the Vallecillo sediments.

Pyrite acts as an important sink for Cu, Mn and Ni, (Huerta-Diaz and Morse 1992). Pb and Zn tend to form their own sulphides, which may form microinclusions in pyrite (Berner, pers. comm.). Zn correlates with the elements of detrital origin and was therefore not solely involved in the biogenic cycle, as interpreted before from its distribution in the *Plattenkalks*. It was most probably bound as sulphide, although it may also have been absorbed by clay minerals. Correlation with the detrital elements may result from its opposition with elements of biogenic origin.

The geochemical analysis indicates three components from the Vallecillo section. Elements that correlate with Ca are accumulated by biogenic processes, whereas elements correlating with Zr, Ti and Rb reflect a detrital component. A third group represents chalcophile elements. This differentiation is particularly evident when samples rich in Fe-oxides are included in the analysis. The chalcophile elements covary closer with the detrital fraction, because both detritals and chalcophiles are stronger

enriched in sediment during periods of less intensive biogenic sedimentation. The chalcophile elements were accumulated in the Vallecillo sediments by precipitation as sulphides, and kept their initial trace element spectrum, though they were later transformed to Fe-oxides. This reflects a sea water chemistry that is remarkably different from normal marine sea water composition, particularly regarding the degree of oxygenation.

The geochemical analysis thus provided further evidences to constrain the depositional regime of the Vallecillo *Plattenkalks*. The low Mn and the high contents of chalcophile elements, notably Ni, are strong arguments for low oxygenated bottom waters (Jarvis *et al.* 2001; Brumsack in press) during deposition of the *Plattenkalks*.

The enrichment in Cu, Ni and Zn requires additional metal sources, possibly hydrothermal input (Brumsack in press). The Cretaceous, the mid- to late Cretaceous period in particular, was characterised by high plate tectonic activity, including elevated rates of seafloor spreading, convergent margin volcanism, and intraplate volcanism (Leckie *et al.* 1998). This agrees with a high generation rate of oceanic crust and a marked increase in hydrothermal activity (Schlanger *et al.* 1981; Arthur *et al.* 1988). The latter could be a source for chalcophile elements in the Vallecillo sediments.

The geochemical analysis did not include light elements such as S. In the XRD analysis (Chapter 5.3), no S-bearing minerals were identified. This is not significant because of bad detection limits of XRD and biased sampling, as no Fe-rich mudstone was included. On the other hand, petrography and sedimentology suggest that the sulphides initially present in the sediment were later oxidized. Further investigation would be necessary to clear this point.

7   **THE FOSSIL ASSEMBLAGE OF VALLECILLO**

This chapter provides an overview over the Vallecillo fossil assemblage. A taxonomic description of ammonites and inoceramids is included in Appendix C. The systematic description of most fishes was carried out by Blanco Piñon (2003) in an unpublished PhD thesis, part of which is published (Blanco and Cavin 2003; Blanco-Piñon and Alvarado-Ortega 2005; Blanco-Piñon *et al.* 2005).

7.1   CEPHALOPODS

Cephalopods are mainly represented through ammonites, but a phragmocone of a coleoid, probably *Palaeoctopus* (D. Fuchs, pers. comm.), was also found during excavation (Figure 7.1). Nautilids have not yet been recognized.
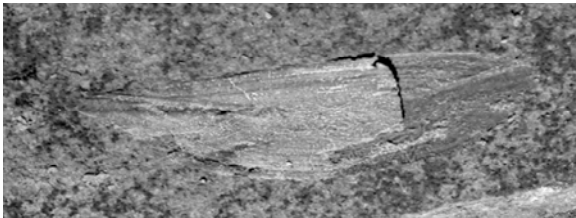
Figure 7.1. Phragmocone of a probable *Palaeoctopus*. The bright colour of this fossil indicates preservation of primary material, in contrast to the dark grey preservation of many other Vallecillo fossils. UANL-FCT-VCI/150. ×1.

7.1.1   The Ammonite Assemblage

The preservation of the Vallecillo ammonites makes determination of species difficult, and strong attention must be paid to the exact matching of ornament with the type material of other collections. Shell dimensions are usually distorted because the shells are crushed due to lithologic overburden and early diagenetic sediment compaction. The following taxa have been recognized:

Fagesia catinus (Mantell, 1822) (Figure 7.2b-c, Figure 7.3a),

Fagesia superstes (Kossmat, 1897) (Figure 7.2a),

Mammites nodosoides (Schlüter, 1871) (Figure 7.4),

Quitmaniceras reaseri Powell, 1963 (Figure 7.5d-e),

Pseudaspidoceras flexuosum Powell, 1963 (Figures 5.8, 5.11 and Figure 7.6),

Pseudaspidoceras pseudonodosoides (Choffat, 1898) (Figure 5.7),

Tragodesmoceras bassi Morrow, 1935 (Figure 7.7),

Vascoceras birchbyi Cobban and Scott, 1972 (Figure 7.3b-c),

cf. *Vascoceras* sp. (Figure 7.8),

Watinoceras coloradoense (Henderson, 1908) (Figure 7.5a-c).

Several smooth specimens are indeterminable and considered here as *incertae familiae* (Figure 5.9,

Figure 7.5e).
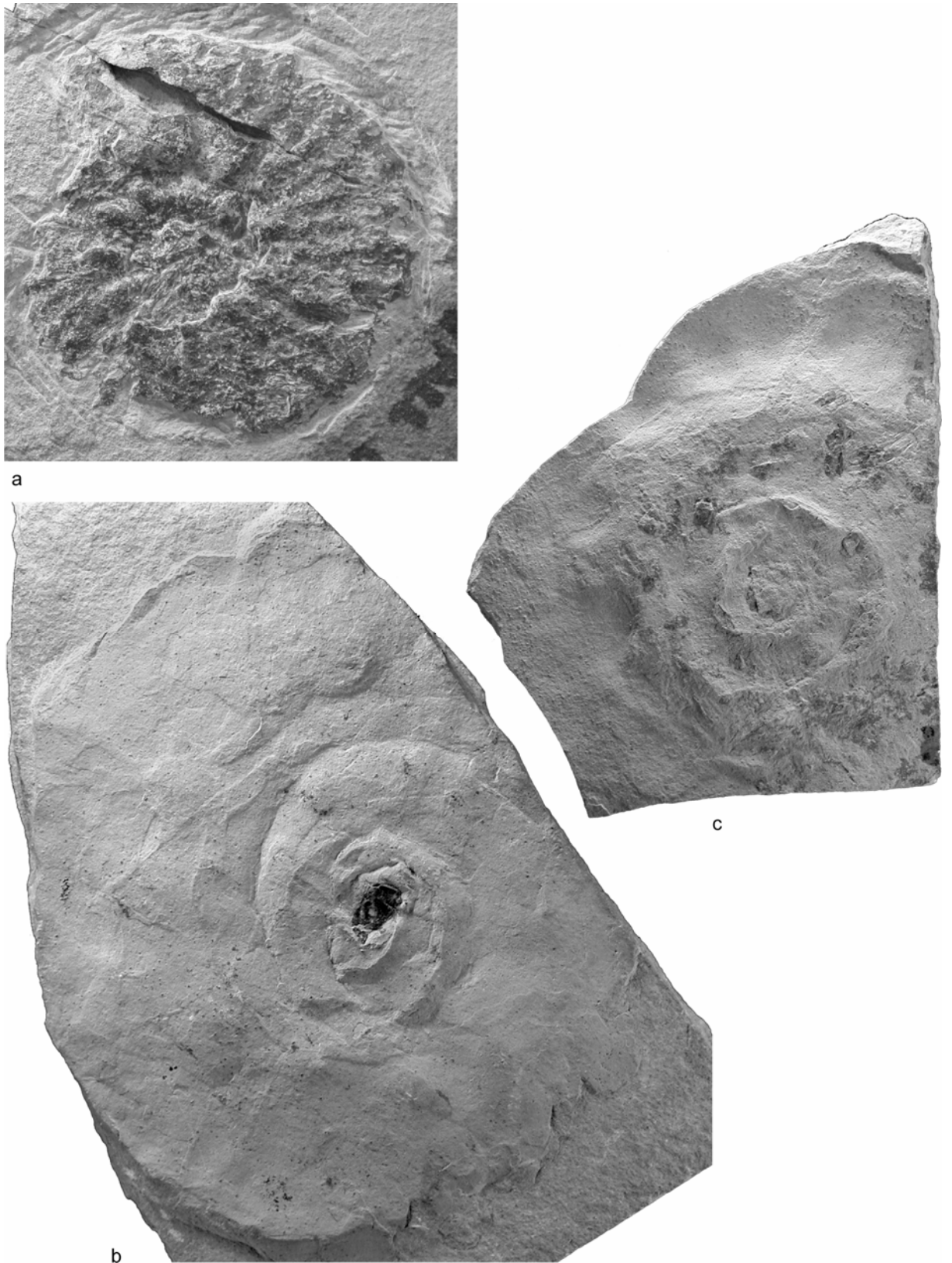
Figure 7.2. a: *Fagesia superstes*. **UANL-FCT-VC021. b-c:** *F. catinus.* **b: UANL-FCT-ASC250. c: UANL-FCT-VC838. All ×1.**
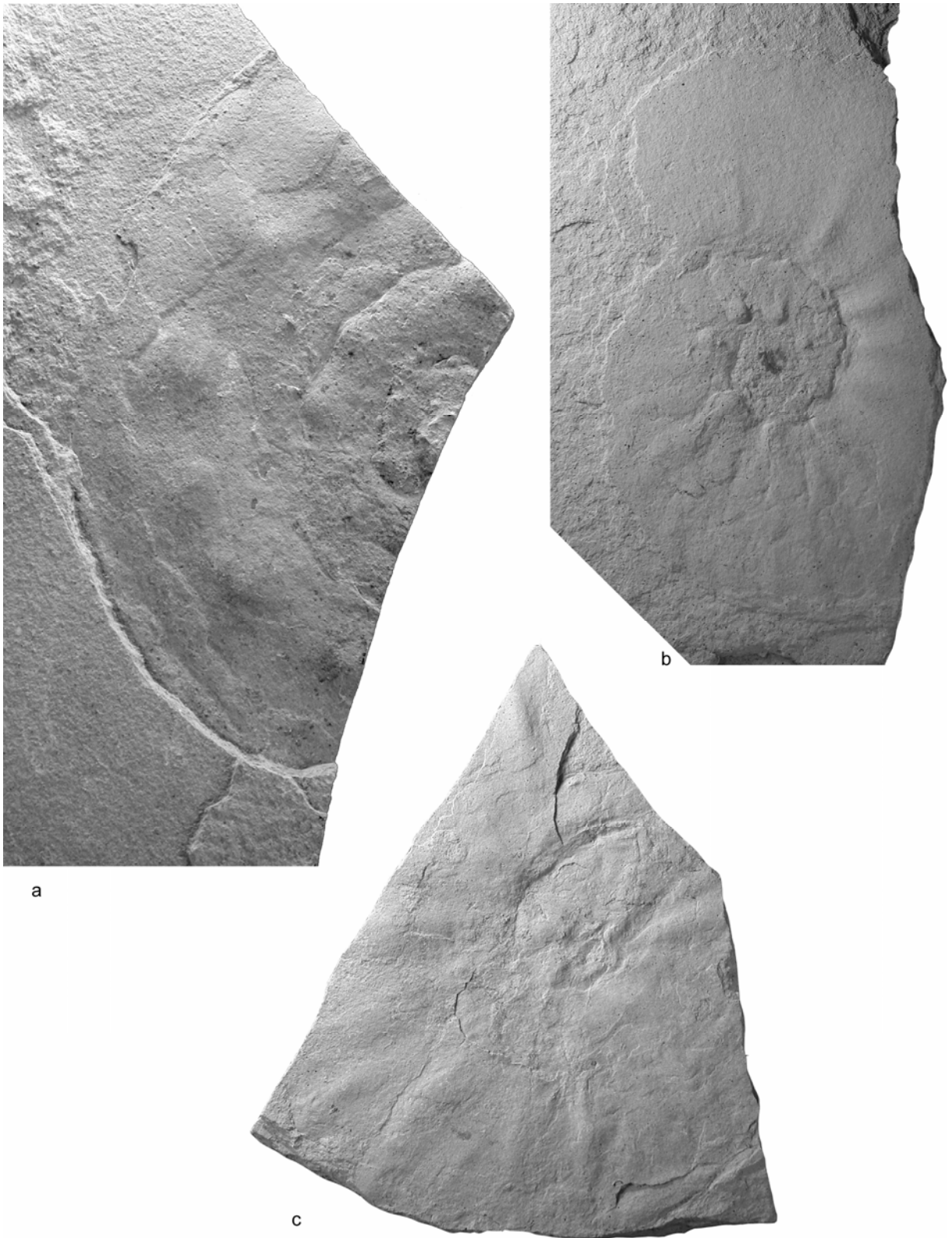
Figure 7.3. a: *Fagesia catinus*. **UANL-FCT-VC572B. b-c:** *Vascoceras birchbyi.* **b: UANL-FCT-VC038A. c: UANL-FCT-VC968. All ×1.**

Figure 7.4. *Mammites nodosoides*. **UANL-FCT-VC502. ×1.**

7.1.2   Palaeobiogeographical interpretation

Tragodesmoceras bassi was recorded solely from to the southern part of North America, excluding the Pacific coast (Cobban and Scott 1972). *Vascoceras birchbyi* was hitherto considered to be endemic to the US Western Interior (Cobban *et al.* 1989) but now extends to its southern opening. *Quitmaniceras reaseri* was previously reported from the US Western Interior and north-eastern Mexico (Kennedy *et al.* 1999), but is also known to exist in Venezuela and Spain.
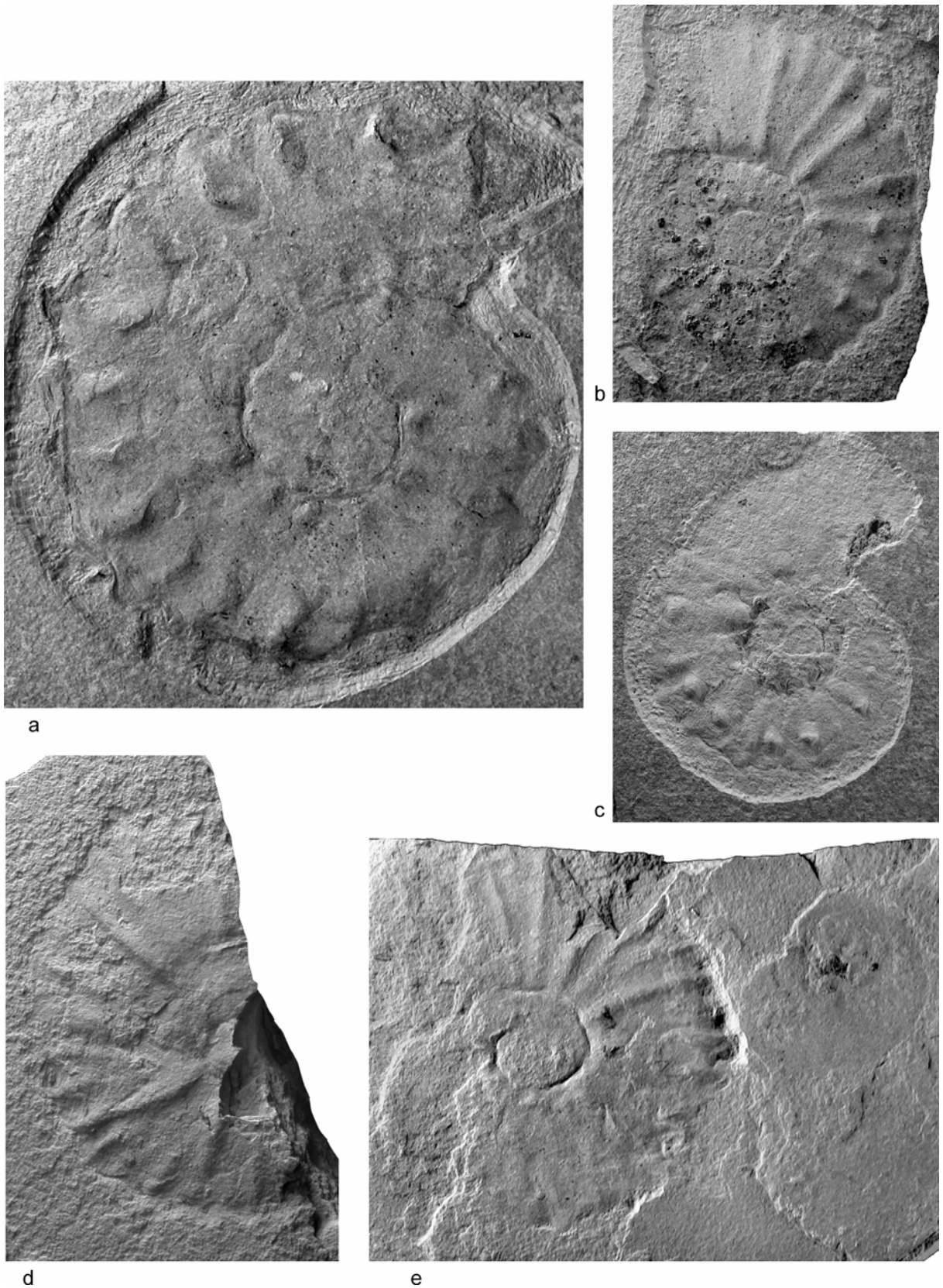
Figure 7.5. a-c: *Watinoceras coloradoense*. **a: UANL-FCT-VC075. ×0·5. b: UANL-FCT-VC555. c: UANL-FCT-VC563B. d-e:** *Quitmaniceras reaseri*. **d: UANL-FCT-VC585. e: UANL-FCT-VC583, with a small, undeterminable specimen (***incertae familiae***). ×1.**
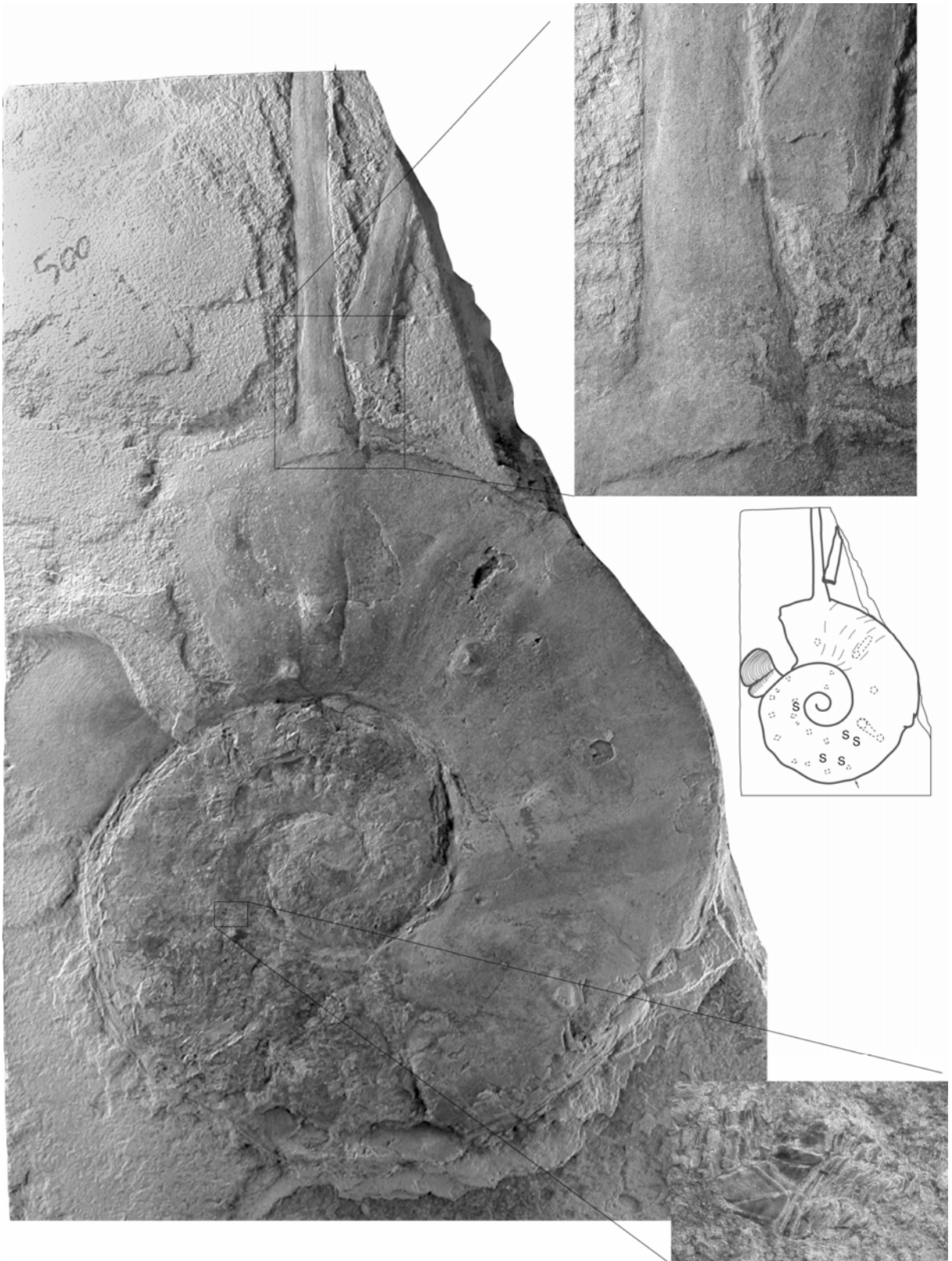
Figure 7.6. *Pseudaspidoceras flexuosum* **with spines and the aptychus preserved in front of the aperture. UANL-FCT-VC500. ×0·75. base of spines ×1·5,** *Stramentum* **sp. ×4.**

Figure 7.7. *Tragodesmoceras bassi.* **The specimen is surrounded by a low pedestrial socket UANL-FCT-VC027A. ×0·67.**

Pseudaspidoceras pseudonodosoides is present in the Western Interior Seaway and throughout the Tethys. This species seems to be restricted to low latitudes and is therefore interpreted to be a warm water species. *Pseudaspidoceras flexuosum*, *Mammites nodosoides*, *Fagesia catinus*, and *F. superstes* occur worldwide throughout low and middle latitudes, including the European boreal, and/or the eastern and southern Pacific realm.
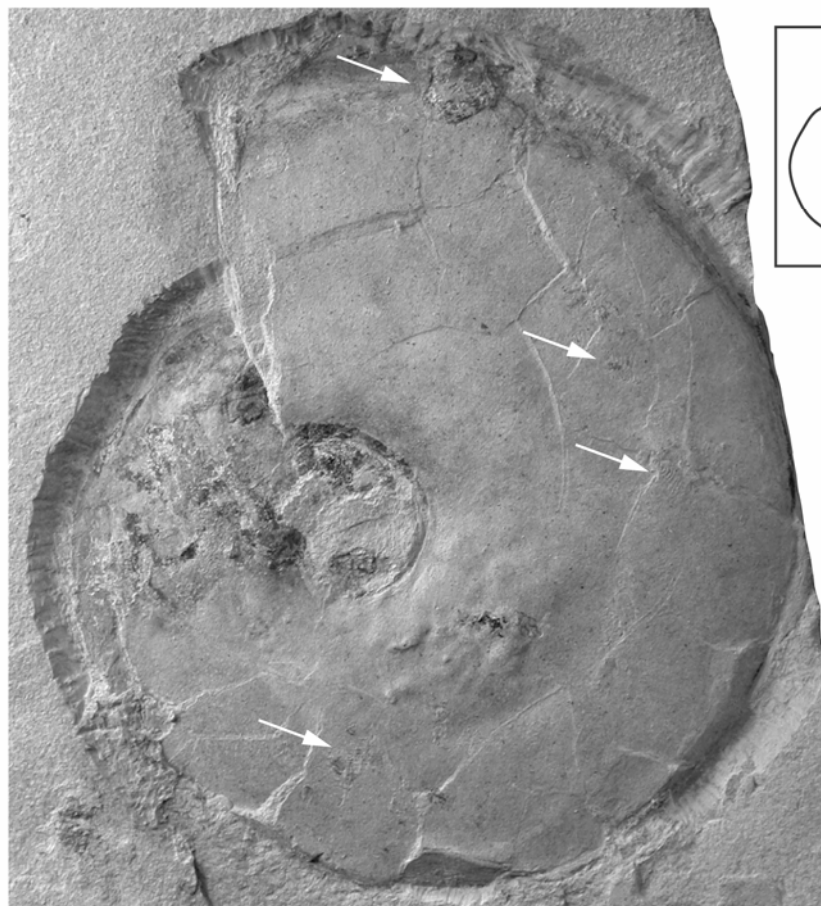
Figure 7.8. a: cf. *Vascoceras*. UANL-FCT-VCIII/72B. b: specimen with the epizoic *Stramentum* (arrows). UANL-FCT-VC837. ×1.

Figure 7.9. Map of the Turonian world with ammonite localities (Blakey 2002).

Watinoceras coloradoense is rare in the southern hemisphere and Tethys, but was recorded in abundance from England (Wright and Kennedy 1981) and the middle and northern Western Interior (Cobban 1988), including northern Alaska and the Canadian Sverdrup Islands (Stelck *et al.* 2002).

All ammonite species of the Vallecillo assemblage were previously reported from the North American continent, at least from the southern Western Interior Seaway. Two species are endemic to this region (*Tragodesmoceras bassi* and *Vascoceras birchbyi*), but others are widespread throughout the warm water belt of the Tethys and/or middle latitudes (e.g. *Pseudaspidoceras flexuosum*, *Mammites nodosoides*, *Fagesia catinus* and *F. superstes*), or the northern hemisphere (*Watinoceras coloradoense*). The Vallecillo fauna is thus largely a mixture of Tethyan and Western Interior species. This mixture may result from the palaeogeographic position of the Vallecillo sea near the southern end of the Western Interior Seaway and close to the western end of the Tethys (Figures 3.1, 7.9).

7.2   BIVALVES

The most abundant bivalves in the Vallecillo assemblage are inoceramids. The genus *Inoceramus* is present in the lowest 1·26 m of exposed layers, whereas *Mytiloides* is present from the 0·05 m level until the upper end of the section. Ostreids are only known as epizoans on intermediate- to large-sized ammonites.

7.2.1   Vallecillo Inoceramids

Inoceramids are the only benthic organisms preserved in Vallecillo. No other benthic macrofossils, benthic microfossils or trace fossils have been identified until now.

The following species have been recognized:

Inoceramus pictus pictus Sowerby, 1829 (Figure 7.10a-b)

Mytiloides hattini Elder, 1991 (Figure 7.10c)

Mytiloides puebloensis Walaszczyk and Cobban, in Kennedy *et al.*, 2000 (Figure 7.10d)

Mytiloides goppelnensis Badillet and Sornay, 1980 (Figure 7.11a)

Mytiloides kossmati (Heinz, 1930) (Figure 7.11b-c)

7.2.2   Palaeobiogeographical Interpretation

Inoceramus pictus pictus is a late Cenomanian species and was described from boreal Europe, northern South America and Brazil. The latest Cenomanian to earliest Turonian *Mytiloides hattini* is more restricted in appearance, with records from the Western Interior Seaway, south-western and boreal Europe and south-western Asia. The early Turonian *M. puebloensis* is similar in distribution. *M. goppelnensis* occurs in the Western Interior Seaway, boreal and south-western Europe. *M. kossmati* has the widest occurrence, with worldwide records in low and middle latitudes.

The inoceramids known from Vallecillo are restricted to low and middle latitudes. All of them were recorded before from the Western Interior Seaway (Walaszczyk and Cobban, in Kennedy *et al.* 2000). The late Cenomanian *Inoceramus pictus pictus* and the middle early Turonian *M. goppelnensis* and *M. kossmati* are widely distributed throughout low and middle latitudes, whereas inoceramids of the Cenomanian-Turonian transition and early Turonian species, namely *Mytiloides hattini* and *M. puebloensis*, are much more restricted in appearance, with occurrences only in North America and Europe. After the Cenomanian-Turonian global marine crisis, inoceramids became more widespread, as indicated by wider distribution of *M. goppelnensis* and *M. kossmati*.

7.2.3   Epizoic oysters on ammonites

Oysters colonized intermediate to large-sized ammonites from Vallecillo. The hypothesis developed by Kauffman (1978), that ammonites lying on the sea floor formed "benthic islands", cannot be applied for the Vallecillo specimens, because the conditions at the sea bottom are interpreted as very low in oxygen (Ifrim *et al.* 2005a; Ifrim *et al.* 2005b), and overgrowth exists on both flanks of the shell. Epizoans which grew on living ammonites are known to exist throughout the Jurassic and the Cretaceous, for instance from the Toarcian (lower Jurassic) Posidonia shale (Seilacher 1982).
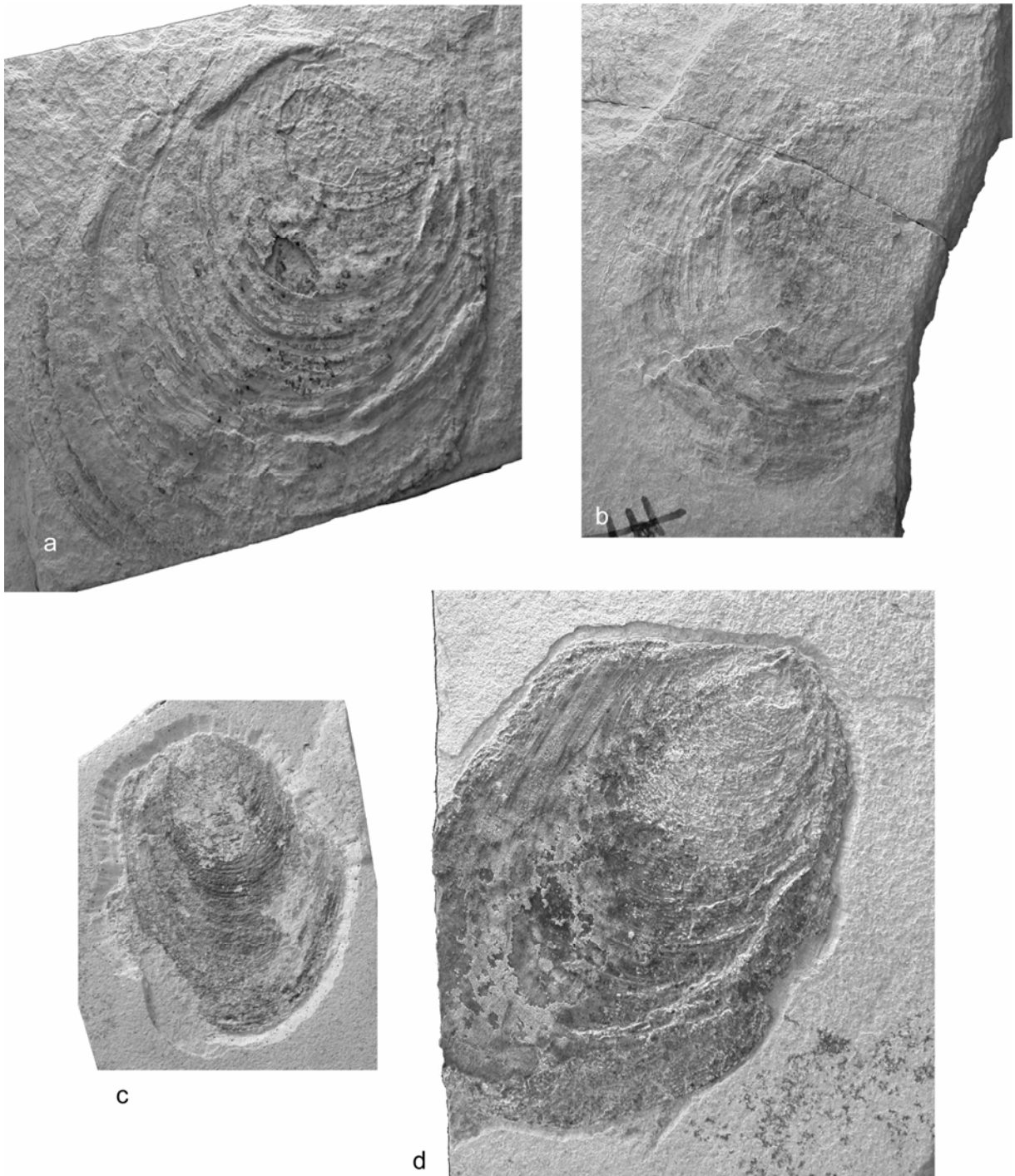
Figure 7.10. a-b: *Inoceramus pictus pictus*. **a: UANL-FCT-VC521. b: UANL-FCT-VC562. c:** *Mytiloides hattini* **UANL-FCT-VC934. d:** *Mytiloides puebloensis*. **UANL-FCT-VC182. All ×0·75.**
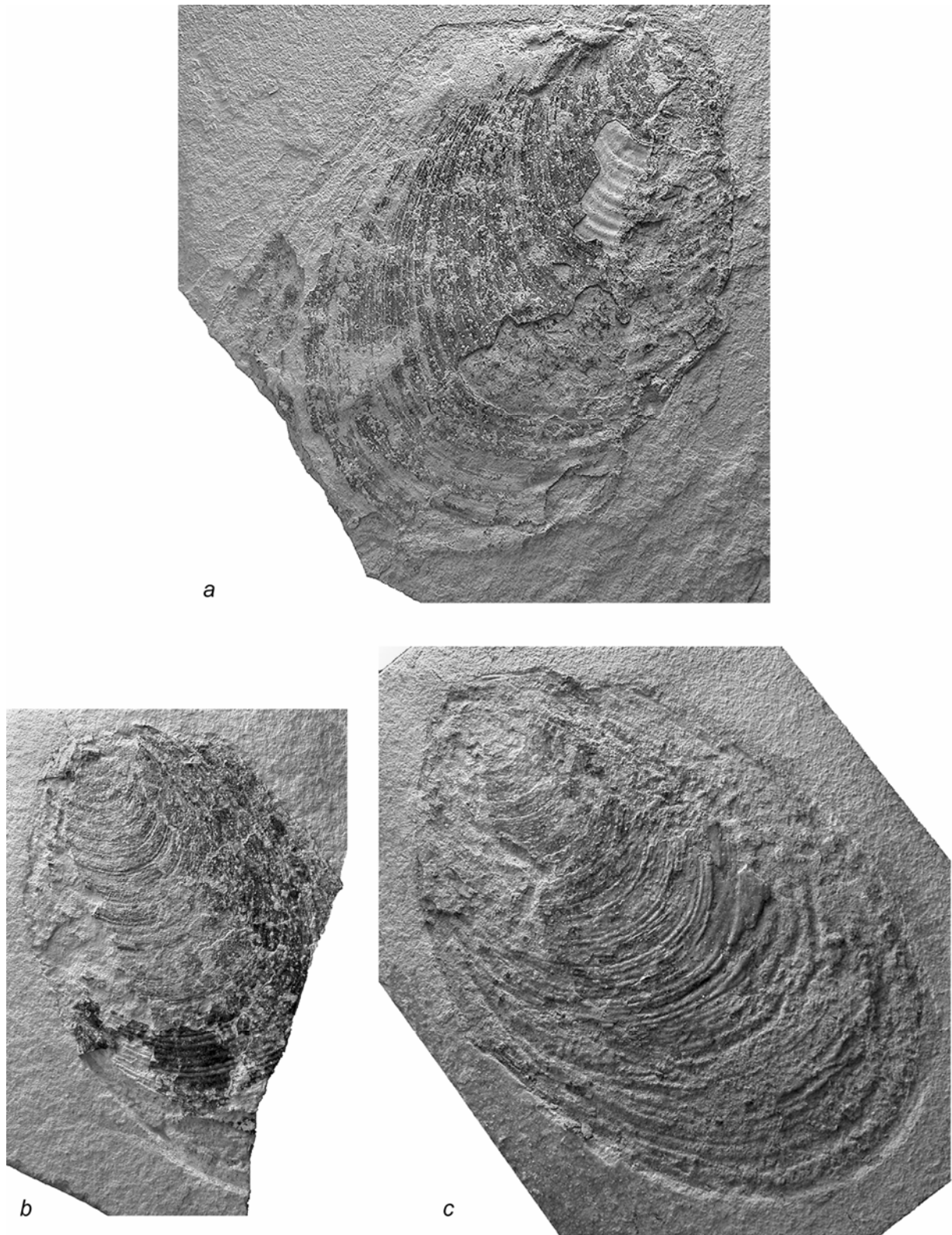
Figure 7.11. a: *Mytiloides goppelnensis***. UANL-FCT-VC592. b-c:** *M. kossmati***. b: UANL-FCT-VC245. c: UANL-FCT-VC525. All ×1.**

Figure 7.12. *P. flexuosum* **with epizoic oysters on the umbilicus and venter of the last whorl. UANL-FCT-VCI/296B, upper slab. ×1. The shells of the calcitic oysters are preserved similar to shells of inoceramids.**

Vallecillo specimen VCI/296 is an obliquely embedded *P. flexuosum* which is colonized by oysters. Figure 7.12 displays the upper slab of this fossil, showing the part that sunk into the sediment. The oysters on the umbilicus and venter of this ammonite were deposited below the test. The colonization pattern of this test is similar to that described by Seilacher (1982): Toarcian byssate

bivalves attached preferably to the venter and around the umbilicus on both flanks, but avoid the aperture. In the Vallecillo specimen a similar pattern is seen on the exposed flank, and particularly the venter. Due to unilateral preservation, the other flank cannot be observed, so it is unclear whether it was colonized.

According to Seilacher (1982), the preference for the ventral side of the shell indicates a pendant position of the swimming or floating shell. This means, that the shell was colonized before it sank down to the sea bottom. The Vallecillo specimen agrees well with this interpretation.

7.3   CRUSTACEANS

The only crustacean known from Vallecillo is *Stramentum* Sowerby, 1843. It is a sessile cirripedian which grew on ammonite shells. The specimens were kindly identified by F. Wittler, UKRG.

Stramentum is only documented in specimens from the random surface survey, so their stratigraphic occurrence in unknown. 24 specimens are attached to the flanks of a large-sized *Pseudaspidoceras flexuosum* (UANL-FCT-VC109, Figure 5.11), several others are preserved next to its venter. Six individuals of *Stramentum* are visible on another large *P. flexuosum* (UANL-FCT-VC500, Figure 7.6), but they were also found on a well preserved, although undeterminable specimen (UANL-FCT-VC837, Figure 7.8).

7.4   VERTEBRATES

Fishes and their primary fragments from the Vallecillo section are abundant and diverse. Fifteen species of chondrichthyes, holosteids and teleosteids were recorded. Twelve taxa were described by Blanco Piñon (2003) in an unpublished PhD thesis, but only five were hitherto published (Blanco and Cavin 2003; Blanco-Piñon and Alvarado-Ortega 2005; Blanco-Piñon *et al.* 2005). The fossil reptiles are under study by M.-C. Buchy and K. Smith, with preliminary results published by Buchy *et al.* (Buchy *et al.* 2003, 2005).

7.4.1   The fish assemblage

The list of species hitherto recorded includes the following taxa:

Sharks:	Fam. Lamniformes, genus and species undetermined
	Fam. Elasmobranchii, genus and species undetermined
	Ptychodus mortoni (Agassiz, 1843)
Holostei:	*Nursallia* cf. *N. gutturosum* (Arambourg 1954) (Figures 5.12, 7.15)
	Fam. Pachycormidae, genus and species undetermined
Teleostei:	*Vallecillichthys multivertebratum* Blanco and Cavin, 2003
	Rhynchodercetis sp. (Figure 7.16)

Robertichthys riograndensis Blanco-Piñon and Alvarado-Ortega, 2005

Fam. Pachyrhizodontidae, genus and species undetermined

Goulmimichthys roberti Blanco and Cavin, 2003

Tselfatia formosa Arambourg, 1954 (Figure 7.14)

Araripichthys sp.

Fam. Nothacanthidae, genus and species undetermined

teleosteid, gen. et sp. indet; this small taxon may be a previously unrecorded species.

Selected specimens are figured in Figure 7.13 to Figure 7.16.

7.4.2   Palaeobiogeographical interpretation of the fish assemblage

Ptychodus is a cosmopolitan Albian to Maastrichtian selachian (Johnson *et al.* 2002). *Ptychodus mortoni* was reported before from the ?Turonian (Shimada 1996) and Coniacian to Maastrichtian of the Western Interior Seaway (Johnson *et al.* 2002), but it is also known from the Upper Cretaceous of Mexico and Italy (*fide* Applegate 1970). *Nursallia gutturosum* was described from the Cenomanian of Morocco (Arambourg 1954) and Italy (*fide* Blanco Piñon, 2003, p. 247). *Tselfatia formosa* is known from the Cenomanian of Morocco (Arambourg 1943), the late Cenomanian (Bonarelli event) of Italy (Avanzini and Luciani 1999), the Cenomanian-Turonian of Croatia and the ?Turonian Austin Chalk of Texas (Bardack and Teller Marshall 1980). *Vallecillichthys multivertebratum*, *Goulmimichthys roberti* and *Robertichthys riograndensis* are species only known from Vallecillo (Blanco and Cavin 2003; Blanco-Piñon and Alvarado-Ortega 2005)

In *Araripichthys* and *Rhynchodercetis*, only the distribution of the genus is considered, as the Vallecillo specimens are not determined to species level. The genus *Araripichthys* was reported from the Aptian of Venezuela (*A. axelrodi* Maisey and Moody, 2001) and the Albian Santana Formation of Brazil (*A. castilhoi* da Silva Santos, 1985). *Rhynchodercetis* occurs only in the Tethyan province: Morocco (Arambourg 1954), Italy (d'Erasmo 1946), Slovenia (Jurkovsek *et al.* 2001), Greece (Koch and Nicolaus 1969), Lebanon (Forey *et al.* 2003) and Israel (Chalifa 1989). A doubtful record exists from the Canadian Western Interior Seaway (Wilson and Chalifa 1989).

Figure 7.13 (subsequent page). Fishes from Vallecillo. a: Undetermined shark. UANL-FCT-VC059. ×0·1 b: *Ptychodus mortoni* (Agassiz 1833-1844). UANL-FCT-VC722. ×0·25 c: Undetermined pachycormid. UANL-FCT-VC087. ×0·1. d: Pachyrhizodontidae indet. UANL-FCT-VC689. ×0·25. e: *Araripichthys* sp. UANL-FCT-VC863. ×0·5. f: *Robertichthys riograndensis* Blanco-Piñon and Alvarado-Ortega, 2005. UANL-FCT-VC720. ×0·25 g: Undetermined taxon. ×2. h: *Goulmimichthys roberti* Blanco and Cavin, 2003. UANL-FCT-VC706. ×0·25. i: *Vallecillichthys multivertebratum* Blanco and Cavin, 2003. UANL-FCT-VC701. ×0·1.
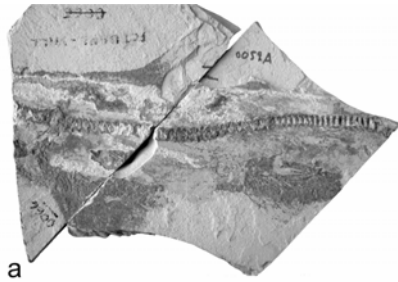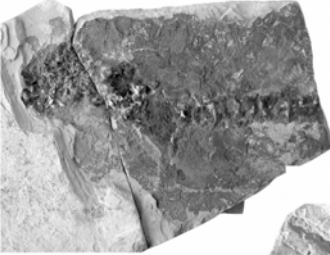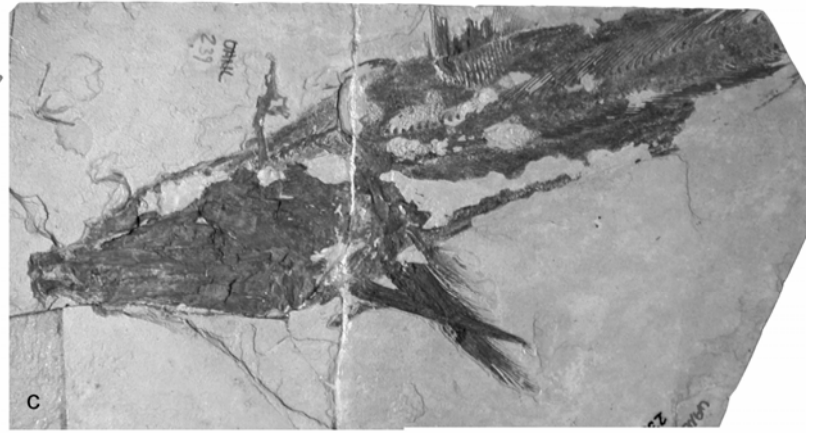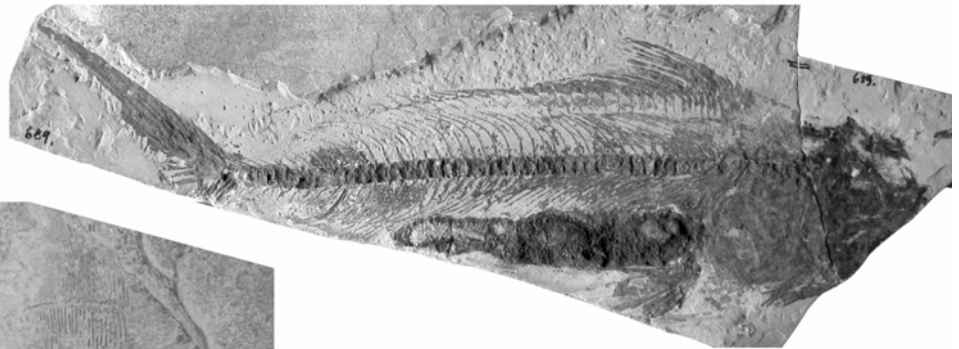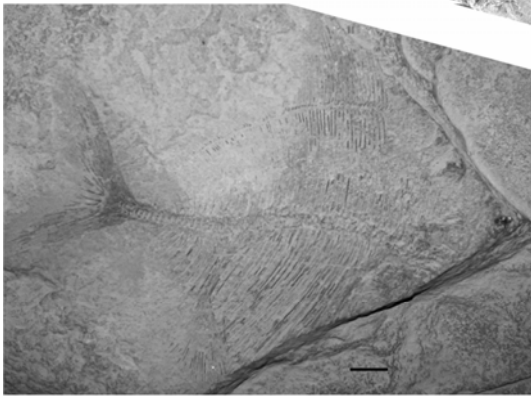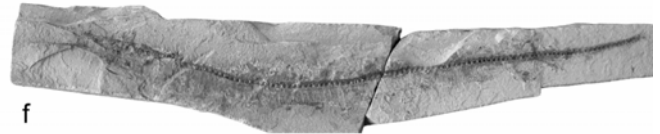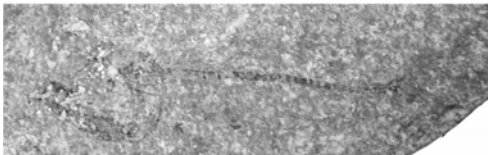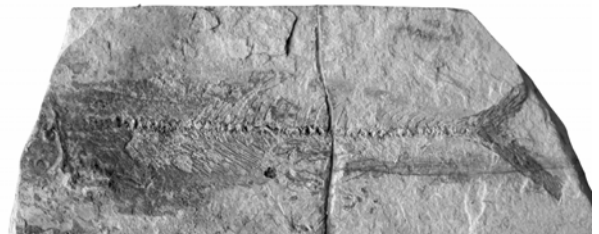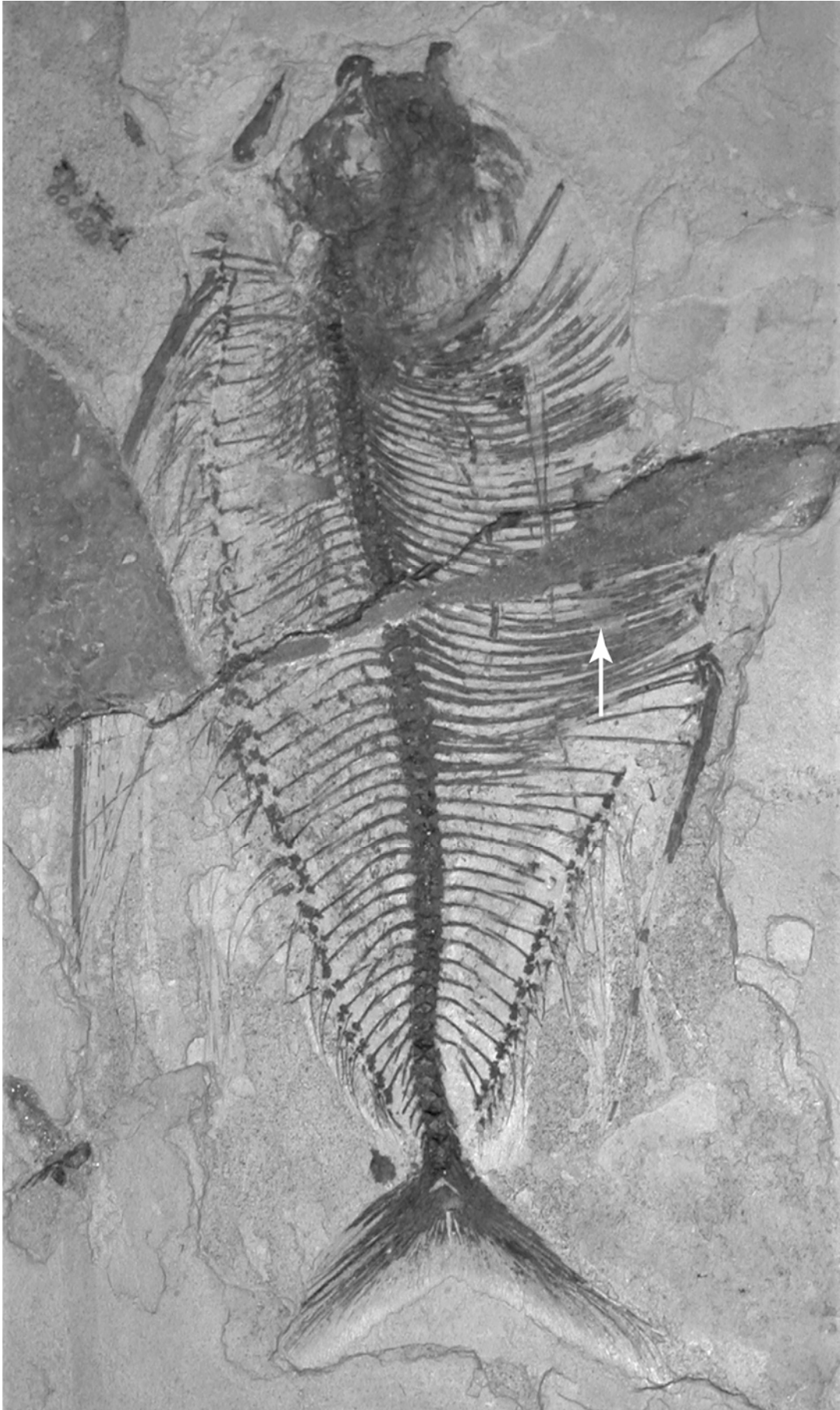
Figure 7.14. *Tselfatia formosa* from Vallecillo. UANL-FCT-VC068A. ×0·33.
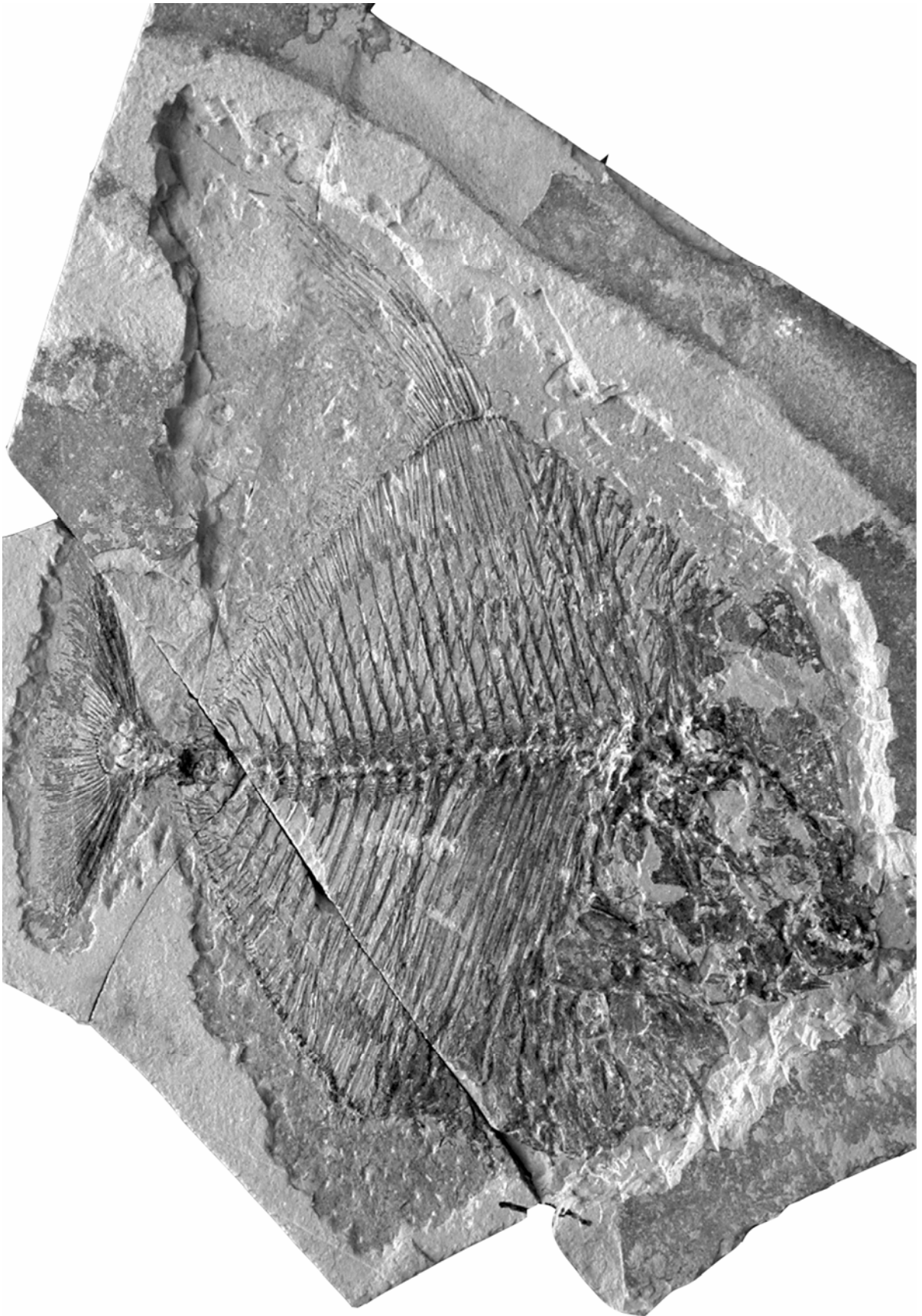
Figure 7.15. : *Nursallia* **cf.** *N. gutturosum***. UANL FCT VC 669. ×0·9.**
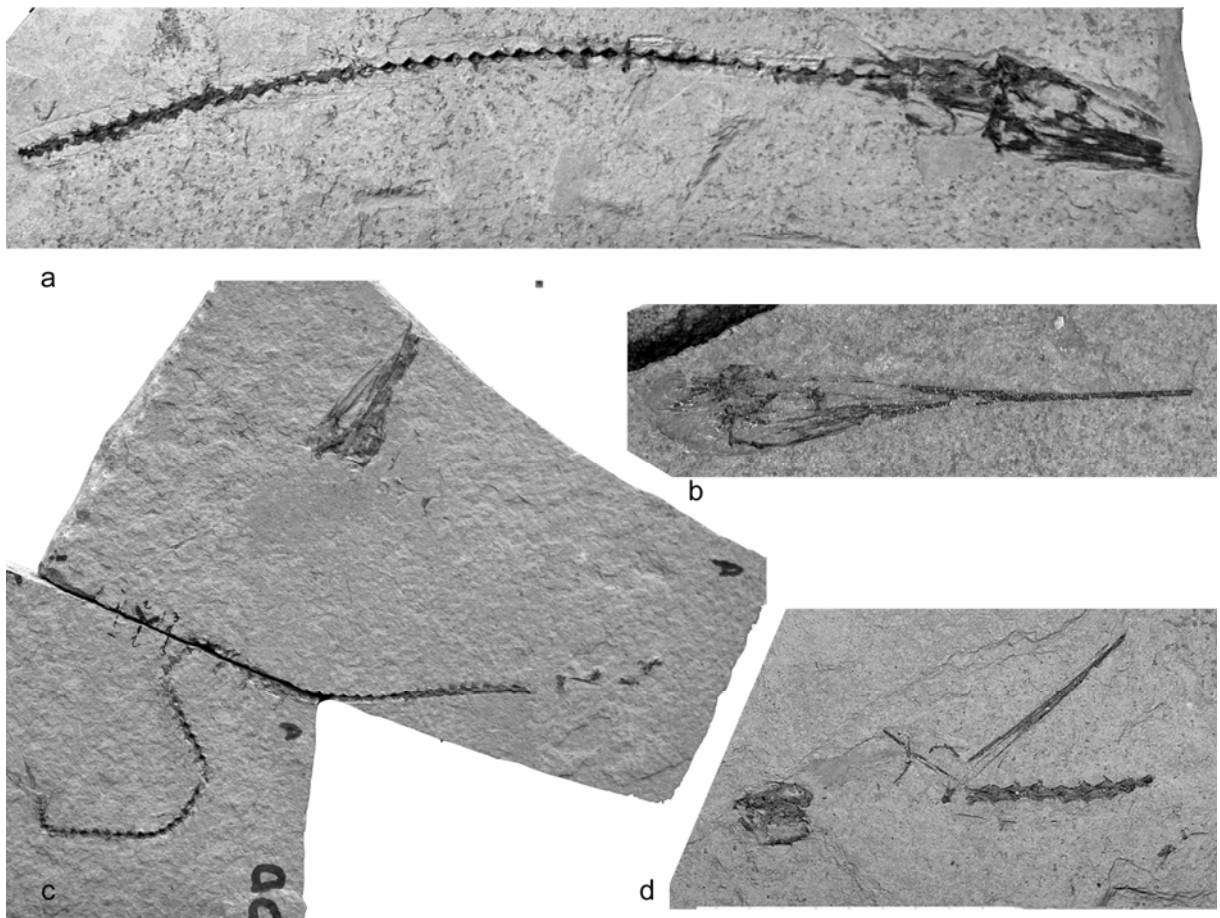
Figure 7.16. : *Rhynchodercetis* **sp. a: UANL FCT VC 858. ×0·75. b: isolated head. VCI/163. c:** *in situ* **disarticulated, subcomplete specimen. UANL FCT VC 049A. d: primary fragment,** *in situ* **further disarticulated. UANL FCT VC1/212A. ×1.**

The above taxa are restricted to the Tethyan realm, with the exception of *P. mortoni*, *T. formosa*, possibly *Rhynchodercetis*, which also occur in the Western Interior Seaway, and *Araripichthys*, which was not reported outside northern South America. The above taxa are restricted to low latitudes and represent warm water species. Their distribution is more restricted to low latitudes than that of the invertebrates (with the possible exception of *Rhynchodercetis*), but similar to them forms a mixture of Tethyan, South American and Western Interior taxa.

7.4.3   Reptiles

Reptiles are rare in Vallecillo. All specimens are from the random surface survey. They comprise three specimens of turtles, which represent at least two species, a pliosaur tooth which is possibly referable to cf. *Polyptychodon*, and the well preserved caudal part of an aigialosaur (Figure 7.17). The reader is referred to the publications by Buchy *et al.* (Buchy *et al.* 2003, 2005) for further reading.
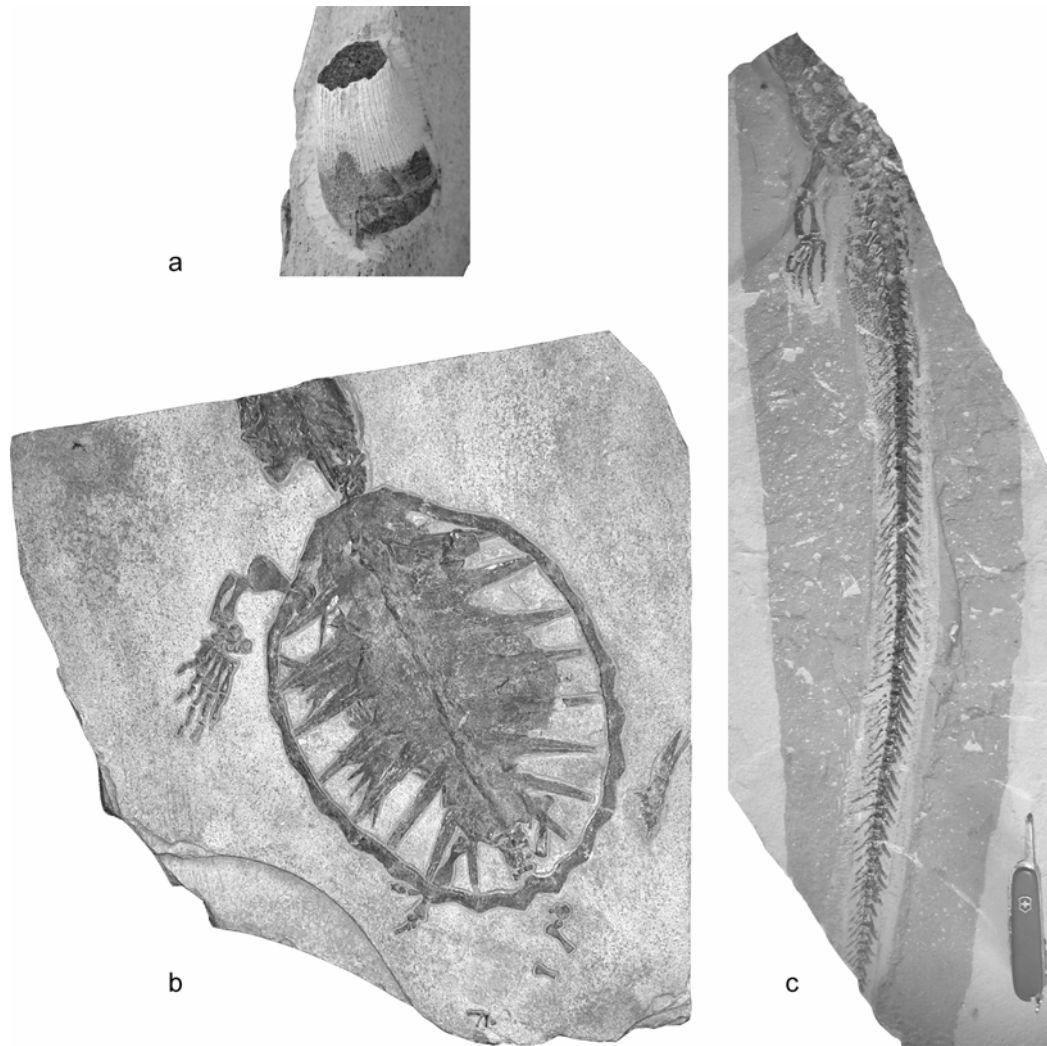
Figure 7.17. Vallecillo reptiles. a: isolated tooth of cf. *Polyptychodon* UANL-FCT-R26. ×1. b: undetermined turtle. UANL-FCT-R 09. ×0·5. c: caudal part of an aigialosaurid. UANL-FCT-R 27. ×0·1.

8   STRATIGRAPHY

8.1   THE CENOMANIAN-TURONIAN BOUNDARY

The Cenomanian-Turonian transition in the Western Interior is stratigraphically well defined by ammonites and inoceramids. These fossils provide reliable regional correlation and were discussed in various publications (e.g. Cobban 1983; Cobban and Hook 1983; Cobban 1984, 1988; Cobban *et al.* 1989; Kennedy and Cobban 1991; Kennedy *et al.* 2000).

The GSSP of the Cenomanian-Turonian transition was elected in a section in the Western Interior Seaway near Pueblo, Colorado (Kennedy *et al.* 2000). The boundary level is defined by the first appearance (FA) of the ammonite genus *Watinoceras*, notably *Watinoceras devonense*. A series of secondary stratigraphic markers was chosen for additional correlation, some with absolute ages (Hardenbol *et al.* 1998, *, fide* Keller and Pardo 2004, and Keller and Pardo 2004, from oldest to youngest):

> The last appearance datum (LA) of the planktonic foraminifer *Rotalipora*, namely *R. cushmani* (93·90 ± 0·02 Ma*),
>
> The full range of the ammonite species *Neocardioceras juddii* (FA 93·73 ± 0·2 Ma*, LA 93·59 Ma* or 93·49 ± 0·2 Ma**),
>
> The LA of the inoceramid *Inoceramus pictus,*
>
> The FA of the inoceramid *Mytiloides hattini,*
>
> The FA of *Watinoceras devonense*. This species co-appears with other species of *Watinoceras* and marks the base of the Turonian (93·49 ± 0·2 Ma*),
>
> The FA of the inoceramid *Mytiloides puebloensis*, in the same bed as *Watinoceras,*
>
> The FA of the planktonic foraminifer *Helvetoglobotruncana helvetica* (93·29 ± 0·2 Ma*),
>
> The FA of *Mytiloides kossmati* at approximately the same level as *H. helvetica*
>
> The FA of the ammonite *Mammites nodosoides* indicates a late early Turonian age,
>
> The FA of *Mytiloides mytiloides* (youngest).

The first and last appearances of index species provide the base for detailed zonal subdivisions of the upper Cenomanian and lower Turonian sediment sequence of the GSSP based on ammonites, inoceramids and planktic foraminifers. These results are summarized in Figure 8.1.
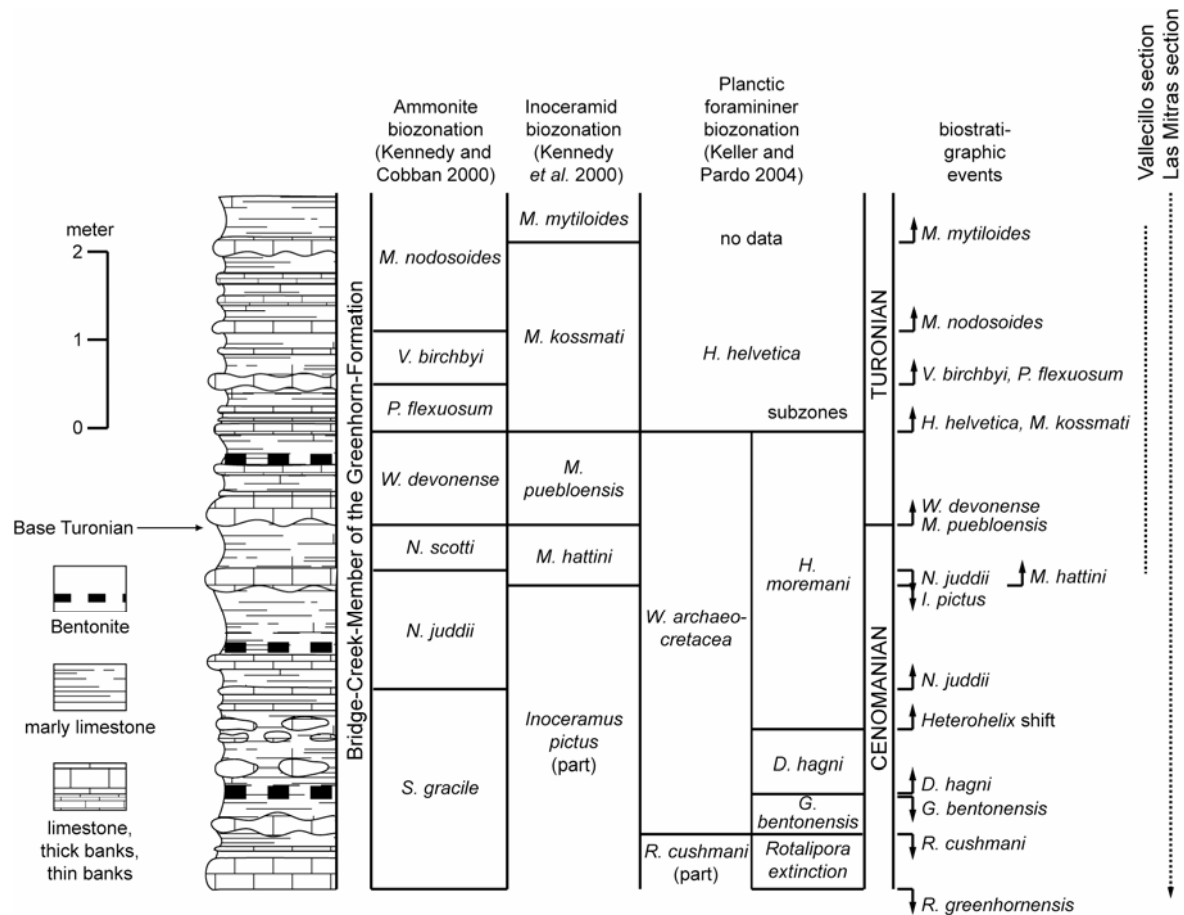
Figure 8.1: The GSSP of the Cenomanian-Turonian boundary and biostratigraphic subdivisions by ammonites, inoceramids and foraminifera, with FA and LA of zonal marker species.

The following ammonite zones were proposed for the Cenomanian-Turonian boundary interval (Kennedy and Cobban 1991):

Nigericeras scotti (latest Cenomanian; the base of this zone is defined by the LA of *Neocardioceras juddii*),

Watinoceras devonense (the FA of *Watinoceras* spp. defines the base of the Turonian),

Pseudaspidoceras flexuosum; at the GSSP this is a rare species. The base of this zone therefore placed at the FAs of *Mytiloides kossmati* and *Vascoceras proprium*. The latter is a synonym of *Vascoceras globosum proprium* according to Zaborski, 1996),

Vascoceras birchbyi, with the FA of this species at the base of the zone,

Mammites nodosoides; the base of this zone is defined by the FA of the index species, the top is marked by the FA of *Collignoniceras woollgari*.

Inoceramids also allow for a biostratigraphic subdivision of the Cenomanian-Turonian transition (Kennedy *et al.* 2000):

Inoceramus pictus pictus (oldest; base defined by the LA of *Neocardioceras juddii*),

Mytiloides hattini (FA of this species at the base of the zone),

Mytiloides puebloensis (FA at the base of the zone, in the same bed as *Watinoceras*; consequently, the FA of *M. puebloensis* also marks the base of the Turonian),

Mytiloides kossmati (youngest zone, with the base defined by the FA of the index species; the top is defined by the FA of *Mytiloides mytiloides*).

A biostratigraphic subdivision based on planktic foraminifers was recently proposed by Keller and Pardo (2004):

Rotalipora cushmani zone (oldest, the base of this upper Cenomanian zone is defined by FA of the index species). This zone is subdivided into three subzones in its upper part is: *Praeglobotruncana praehelvetica* (base defined by the FA of the index species), *Anaticinella multiloculata* (base defined by the FA of the index species), and the *Rotalipora* extinction zone (base defined by the LA of *R. greenhornensis*)

Whiteinella archaeocretacea zone (the base is defined by the LA of *Rotalipora*, notably *R. cushmani*). This zone is subdivided into three subzones: *Globigerinelloides bentonensis* (the base is defined by the LA *R. cushmani*), *Dicarinella hagni* (LA of *G. bentonensis* or FA of *D. hagni* defines the base of this subzone), and *Heterohelix moremani* (shift from *Hedbergella* dominated assemblages to *Heterohelix* dominated assemblages); this latter subzone spans the Cenomanian-Turonian boundary as defined by ammonites (Figure 8.1).

Helvetoglobotruncana helvetica in the early Turonian. The base is defined by the FA of the index species; the top is marked by the FA of *Marginotruncana*. *H. helvetica* is a rare species with a diachronous FA. Identification of this species and unambiguous separation from its evolutionary ancestor *Praeglobotruncana praehelvetica* may be difficult due to transitional forms between both species

8.2   PLANKTIC FORAMINIFERS FROM THE VALLECILLO SECTION

8.2.1   Biostratigraphy

Foraminifers identified in the Vallecillo sediments are shown in Figure 8.2. Only two foraminiferal biozones are present (Figure 8.3): The upper *W. archaeocretacea* zone is identified in the lower part of the Vallecillo section, from –0·65 m to 3·60 m. The *H. helvetica* zone spans the upper part of the Vallecillo section, with the FA of this species at 3·60 m section.

Foraminifers are rare in the lower part of the section frequently, < 10 identifiable individuals are present per thin section. Consequently, the registered diversity is low. *H. helvetica* appears abruptly; its ancestor *Praeglobotruncana praehelvetica* or transitional forms between the two species were not found.

The opportunist *Guembelitria* is rare at Vallecillo and only present as isolated specimens in few

thin sections. this is a clear difference with regard to coeval sections in the Western Interior Seaway where *Guembelitria* is abundant in the Cenomanian-Turonian boundary transition (Leckie *et al.* 1998; Keller and Pardo 2004).
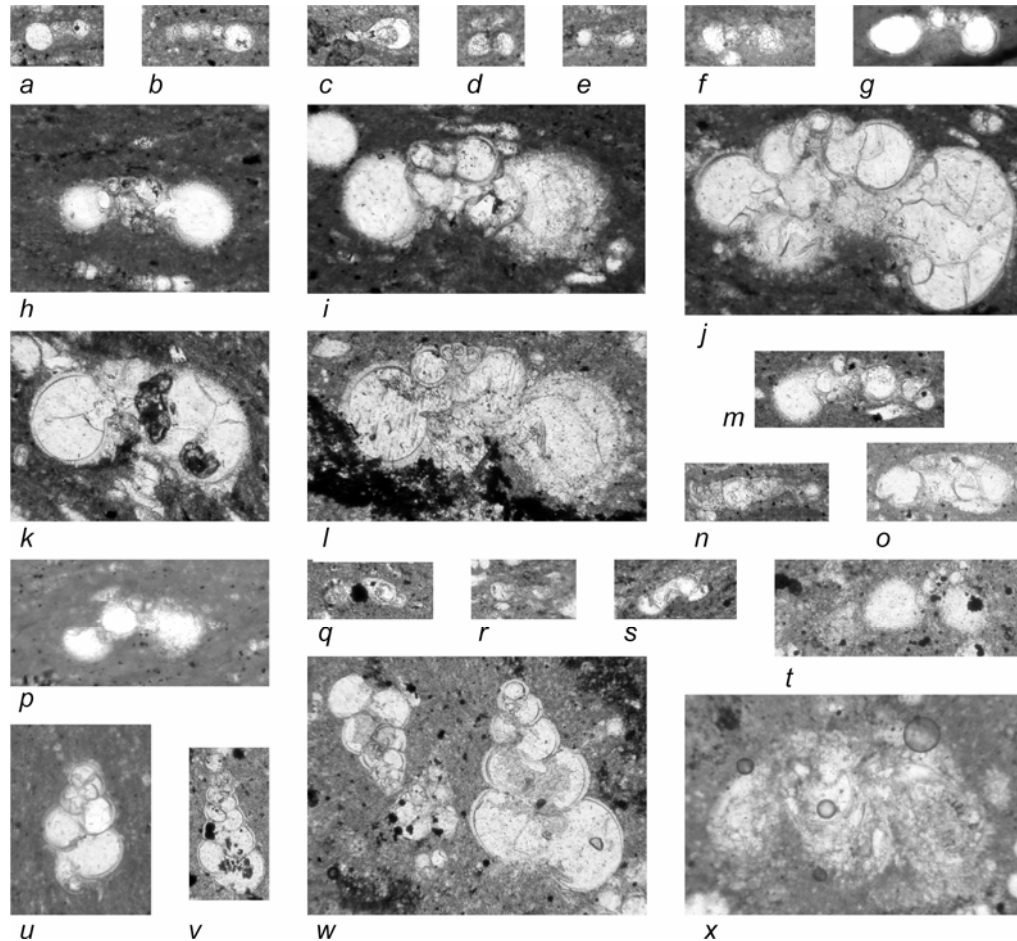
Figure 8.2. Foraminifers identified from the Vallecillo section. a: *Hedbergella delrioensis***. VC1-115. b:** *Hed. planispira***. VC2-65. c:** *Hed. hoelzli***. VC1-3. d:** *Hed. simplex***. VC1-12. e:** *Globigerinelloides ultramicra***. VC1-56. f-g:** *Whiteinella archaeocretacea***. f: VC1-16. g: VC2-21. h:** *W. baltica***. VC2-54. i:** *W. aprica***. VC2-58A. j:** *W. paradubia***. VC2-58A. k:** *Whiteinella sp.* **VC2-58A. l:** *W. brittonensis***. VC2-58A. m-n:** *Helvetoglobotruncana helvetica***. m: VC2-54. n: VC1-77. o:** *D. hagni.* **VC1-109. p:** *Praeglobotruncana inornata***. VC1-94. q:** *P. stephani.* **VC2-65. r:** *P. aumalensis***. VC1-16. s:** *P. gibba***. VC1-16. t:** *Dicarinella algeriana***. VC2-44. u:** *Heterohelix reussi***. VC1-88. v:** *Het. moremani***. VC2-44. w:** *Het. reussi* **(left),** *Het. globulosa* **(right) and** *Guembelitria cenomana* **(middle). VC2-44. x:** *D. imbricata***. VC2-54. All are ×70.**

8.2.2   Planktic foraminifer palaeoecology

Most species of modern planktic foraminifera are adapted to narrow ranges of temperature and salinity (Be 1977), comparable to most marine organisms, and probably to Cretaceous foraminifera. Some foraminifer morphotypes, such as the planispiral *Globigerinelloides* and the trochospiral *Hedbergella*, were more tolerant to a range of living conditions; they were abundant and widespread surface-dwelling during the Cenomanian-Turonian, with records from the open ocean to epicontinental seas, and from low latitudes to the northern slope of Alaska. Keeled morphotypes such as *Rotalipora*,

Dicarinella, *Praeglobotruncana* and *Marginotruncana* were more restricted in appearance to lower latitudes. They are interpreted to be deep-water dwellers, indicating water depths >200 m in a distal "blue water" settings, with warm, normal marine water masses (Leckie *et al.* 1998). The planktic foraminiferal assemblages of Vallecillo include two of the above genera and indicate open marine "blue water" conditions.

The foraminiferal assemblages were strongly affected by the environmental perturbation caused by OAE 2. The faunal turnover is marked by increased surface productivity (dominance of *Hedbergella* and *Whiteinella*), followed by the temporary decrease in diversity and size of the assemblages. This may reflect early sexual maturation resulting from the unfavourable environment and an expanded oxygen minimum zone (Keller *et al.* 2001). This phase is followed by a *Heterohelix* dominance and general dwarfism, likely a consequence of the expansion of the oxygen minimum zone, warmer temperatures and a marine transgression (Keller and Pardo 2004). Biserial *Heterohelix* and triserial *Guembelitria* proliferated with the low-oxygen environments of the Cenomanian-Turonian transition. Recent homeomorphs are sparse in the present-day oceans but fairly abundant in the Red Sea and upwelling areas of the Indian Ocean (Leckie *et al.* 1998). *Heterohelix* species are low-oxygen tolerant, and their increased abundance in the Cenomanian-Turonian boundary level of several sections reflects an enhanced oxygen minimum zone. The *Heterohelix* dominance is weakly developed in Vallecillo; in fact, foraminifers are generally rare in the lower half of the section, and they are all dwarfed. This may indicate a very thick oxygen minimum zone in the Vallecillo area. A proximal facies could also be the cause of a weakly expressed *Heterohelix* shift (Leckie *et al.* 1998), but this can be excluded from the palaeobiogeographical situation of Vallecillo.

The foraminiferal assemblages of the Vallecillo sections are dominated by planktic foraminifers, similar to the deep basinal GSSP at Pueblo (Leckie *et al.* 1998; Keller and Pardo 2004). In contrast to this locality, no benthic foraminifera could be identified. Some benthic foraminifera are adapted to low oxygen conditions at the sea bottom through symbiotic associations with chemoautotrophic bacteria (West 1993; in Leckie *et al.* 1998), whereas others may be microaerophiles or facultative anaerobes (Bernard 1996). Their general absence throughout the Vallecillo Member is best explained by constant anoxic conditions.

8.3   INOCERAMID BIOSTRATIGRAPHY OF THE VALLECILLO SECTION

Inoceramus pictus is documented from the lower 1·30 m section (-0·65 m to 0·65 m section; Figure 8.3). At 0·05 m of the section, small specimens of *Mytiloides hattini* appear and mark the base of this uppermost Cenomanian inoceramid biozone. The FA of *M. puebloensis* defines the base of the Turonian at the 0·17 m level of the section. *Inoceramus pictus* is still present above this level. The FA of *M. kossmati* is at the 3·48 m level, marking the beginning of this zone.
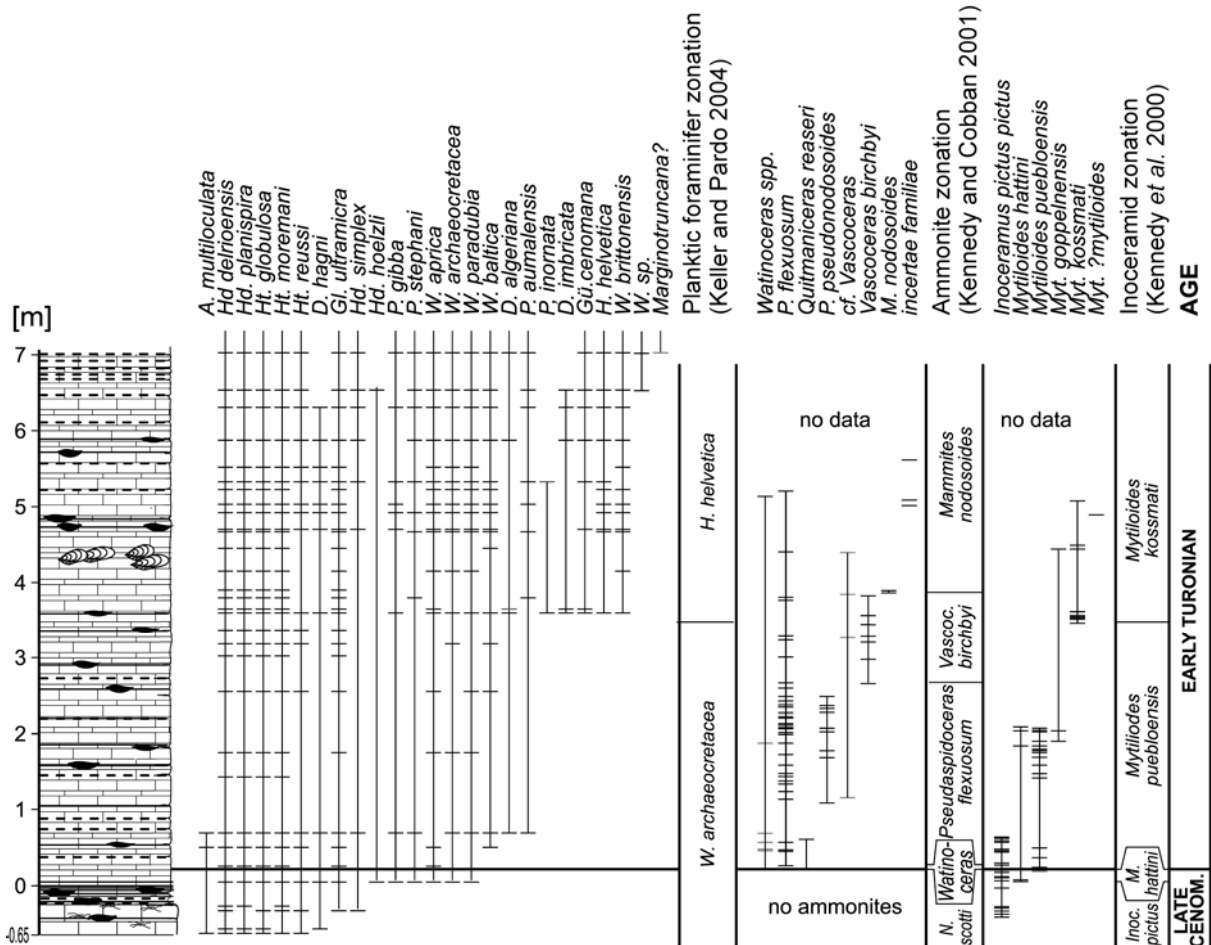
Figure 8.3. Stratigraphic ranges of foraminifers, ammonites and inoceramids and biozonation of the Vallecillo section. Excavated molluscs and all other specimens with known stratigraphic position are included.

An inoceramid abundance event of *M. kossmati* co-occurring with rare *M. goppelnensis* was identified at approximately 4·4 m section, in the lower *Mammites nodosoides* ammonite zone. The increase in abundance of *M. kossmati* is not a result of sediment condensation; this is indicated by ammonites and fish fossils co-occurring with the inoceramids. Their abundance remains similar to the strata below and above (see Chapter 9). Similar flood occurrences of *Mytiloides* are known to exist in the basal *M. nodosoides* zone of Germany. However, the German sections are incomplete, with a hiatus that spans the early Turonian *M. hattini* to *M. kossmati* zones. The inoceramids identified from the German *Mytiloides* flood occurrence events include *M. labiatus* and *M. mytiloides* (Walaszczyk, in Niebuhr *et al.* 1999),m which both indicate a late early Turonian age. They are thus younger than the sediments present at Vallecillo. consequently, the *Mytiloides* flood occurrence in the Vallecillo section represents an earlier event of local or regional extension which cannot be correlated to Europe.

8.4   AMMONITE BIOSTRATIGRAPHY OF THE VALLECILLO SECTION

No ammonites are present in the lowermost 0·86 m of the sediments exposed at Vallecillo (Figure 8.3). This absence of ammonites characterizes the uppermost Cenomanian *Nigericeras scotti* biozone

at the GSSP (Kennedy and Cobban 1991). At Vallecillo, this zone is defined as the interval between the LA of *Neocardioceras juddii* and the FA of *Watinoceras*. At 0·21 m of the section, the FA of *Watinoceras coloradoense* defines the Cenomanian-Turonian boundary. This is a rare species in Vallecillo, and no other species of *Watinoceras* (e.g. *W. devonense*) have been identified. At 0·27 m section, only 6 cm above the base of the Turonian, the first *Pseudaspidoceras flexuosum* appears in the section and defines the base of the early Turonian *P. flexuosum* zone. This ammonite is abundant at Vallecillo and ranges well into the *Mammites nodosoides* zone. The FA of *Vascoceras birchbyi* is at 2·67 m section. The latest early Turonian *Mammites nodosoides* zone is indicated by the FA of this species at the 3·84 m level.

P. pseudonodosoides is present from 1·09 m to 2·50 m of the Vallecillo section, in the middle and upper *P. flexuosum* zone. The presence of *P. pseudonodosoides* in the early Turonian sediments of Vallecillo is remarkable, because the species was considered a late Cenomanian index fossil in the southern Western Interior Seaway (e.g. Cobban and Hook 1983). However, *P. pseudonodosoides* was also recorded from early Turonian strata in Portugal (Lauverjat and Berthou 1974).

8.5 STRATIGRAPHIC DISTRIBUTION OF FISHES

Fishes are present throughout the excavated Vallecillo section (Figure 8.4).
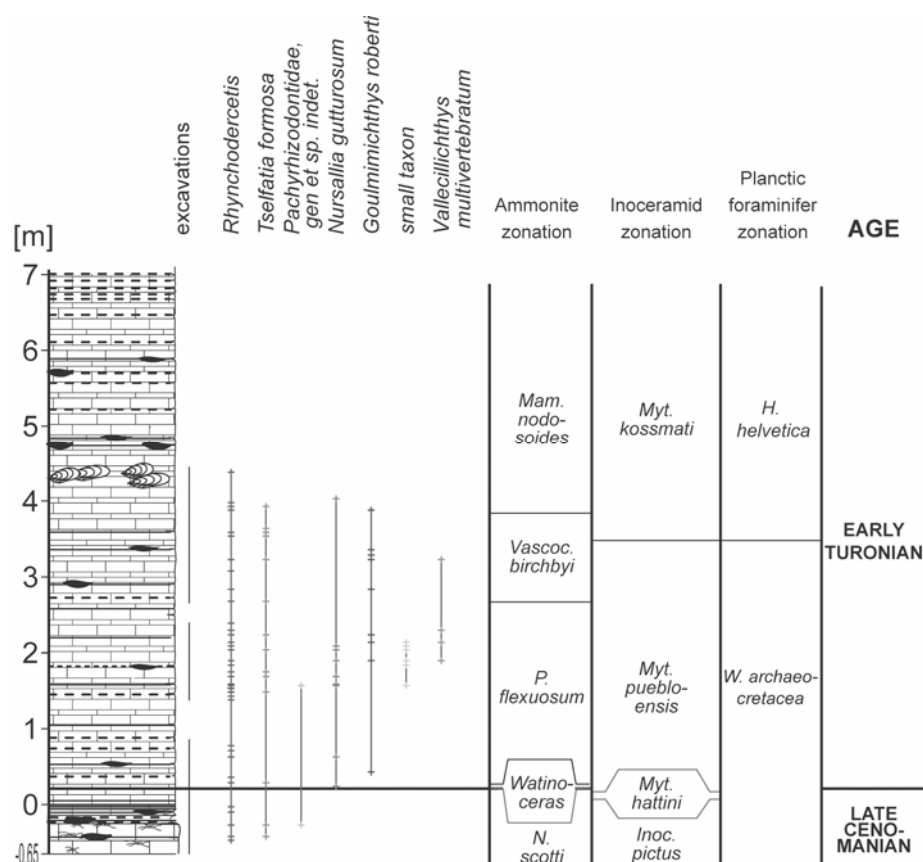
Figure 8.4. Stratigraphic distribution of the most abundant Vallecillo fishes with stratigraphic biozonation. This distribution is preliminary, as many of the excavated primary fragments are not yet examined taxonomically.

Tselfatia formosa and *Rhynchodercetis* occur from the lowest to highest layers of the excavated Vallecillo section (Figure 8.4). *Nursallia* is occurs frequently in the lower part of the section; above the 2·2 m level, it was recorded only in a primary fragment at 4·03 m. The distribution of *Goulmimichthys roberti* points to a continuous occurrence of this species throughout the excavated part of the column. Specimens referred to as "small taxon" seem to be restricted to the short interval from the 1·57 to 2·14 m level. The Pachyrhizodontidae (*gen. et sp. indet.*) and *Vallecillichthys roberti* are too rare to be interpreted.

8.6 THE VALLECILLO SECTION COMPARED TO OTHER CENOMANIAN-TURONIAN BOUNDARY SECTIONS

8.6.1 Biostratigraphic correlation between Vallecillo and the GSSP of the Cenomanian-Turonian boundary

All biostratigraphic markers recognized in the GSSP are also present at Vallecillo (Figure 8.5). Good correlation is reached between the two sections by the FAs of *Mytiloides puebloensis* and *Watinoceras*, which define the base of the Turonian. *Watinoceras* is abundant in the GSSP at Pueblo, and three species (*W. depressum*, *W. devonense* and *W. praecursor*) have been recognized. At Vallecillo, in contrast, the species is rare, and only *W. coloradoense* appears to be present. Other good correlation levels are defined by the FAs of *Vascoceras birchbyi* and *Mammites nodosoides*. The latter ammonite is also characterized by a wide geographic occurrence. The FAs of the ammonites *Watinoceras* spp., *V. birchbyi* and *M. nodosoides* as well as the inoceramid *M. puebloensis* are suggested to be approximately isochronous in the sections. The FAs and LAs of other stratigraphic marker species differ considerably (Figure 8.5). At the GSSP, for instance, the LA of *Inoceramus pictus* is in the late Cenomanian *Neocardioceras juddii* zone (Kennedy *et al.* 2000). At Vallecillo, in contrast, *I. pictus* ranges into the early Turonian where it co-occurs with *M. hattini* and *M. puebloensis*.

P. flexuosum is extremely rare in the GSSP, with only a single specimen identified so far (*Ampakabites collignoni* of Cobban and Scott, 1972, see Kennedy and Cobban, 1991). The base of the *P. flexuosum,* zone was therefore defined by the FA of *M. kossmati*. At Vallecillo, *P. flexuosum* is abundant and appears much earlier, only 6 cm above the FA of *Watinoceras*, which defines the base of the Turonian. Upsection, *P. flexuosum* ranges well into the *M. nodosoides* zone. This long stratigraphic range of *P. flexuosum* and its abundance at Vallecillo clearly contrasts the scarce occurrence of this species at the GSSP. *P. flexuosum* can thus not be used for long-distance correlation beyond the Western Interior Seaway.

Figure 8.5. Comparison of the ranges of stratigraphic relevant foraminifers, ammonites and inoceramids at Vallecillo, at the GSSP of the Cenomanian-Turonian boundary, and at the Eastbourne section in southern England. Stratigraphic data are from Kennedy and Cobban (1991), Kennedy et al. (2000), Keller and Pardo (2004), Keller et al. (2001) and Gale et al. (2005). Note that the Vallecillo section is more expanded than the GSSP, but less expanded than the Eastbourne section.

The planktic foraminifer *Helvetoglobotruncana helvetica* also shows a diachronous FA. In the GSSP, it first appears at the base of the *P. flexuosum* zone and thus much earlier than at Vallecillo, where its FA is in the upper *V. birchbyi* zone. The FA of *H. helvetica*, on the other hand, coincides with the FA of *M. kossmati* in both sections.

The present data indicate that the Cenomanian-Turonian boundary interval at Vallecillo is more expanded than the GSSP, and that the Vallecillo section provides a higher stratigraphic resolution. Even though, several stratigraphic markers (FAs of *M. kossmati*, *H. helvetica* and LAs of *I. pictus*, *P. flexuosum*) occur at higher stratigraphic levels at Vallecillo. *P. flexuosum*, on the other hand, appears much earlier at Vallecillo. These differences clearly indicate diachrony, and caution is required for the use of these biostratigraphic markers in long-distance correlation.

8.6.2 Biostratigraphic correlation with the Eastbourne section in Europe

The Cenomanian-Turonian boundary section at Eastbourne, southern England, has received considerable attention for its expanded and stratigraphically complete sediment sequence (Gale *et al.* 2005) and was proposed as a European reference type section for the Cenomanian-Turonian boundary (Paul *et al.* 1999). The Eastbourne sediments contain abundant well-preserved planktic foraminifers (Keller *et al.* 2001) as well as ammonites and inoceramids (Gale *et al.* 2005). The ranges of selected fossils from the Eastbourne section are presented in Figure 8.5 and there compared to their ranges in at Vallecillo and the GSSP.

Similar to Vallecillo and contrary to the GSSP, *I. pictus* ranges into the early Turonian at Eastbourne. As outlined before, the LA of this species is not indicative of the latest Cenomanian.

The FA of *M. puebloensis* is coeval to the FA of *Watinoceras* in the tree sections. *P. flexuosum* is widely distributed in the western Tethyan faunal province and abundant in Vallecillo, but very rare in the Western Interior Seaway (e.g. the GSSP) and absent (e.g. Eastbourne) or rare (e.g. Germany) in boreal Europe.

The FA of *H. helvetica* is clearly diachronous in the three sections with the earliest appearance at Eastbourne, followed by its appearance at the vase of the *V. birchbyi* zone of the GSSP. At Vallecillo, the species appears even later, in the upper *V. birchbyi* zone.

A similar pattern of diachronous FA likely exists in *Fagesia catinus*, although less expressed than that of *H. helvetica*. *F. catinus* is a potential index species because of its widespread occurrence in the Early Turonian, for instance in France (Kennedy 1994), England (e.g. Mantell 1822; Wright and Kennedy 1981), Venezuela (Renz 1982), northern Mexico (Böse 1920), Texas (Kennedy *et al.* 1987), California (Matsumoto 1959), New Mexico (*fide* Kennedy 1994), Montana (Reeside 1923), and the Oman (Kennedy and Simmons 1991). However, biostratigraphic data for this species are rare at present, except for the three sections correlated here.

Mytiloides kossmati was introduced by Kennedy et al. (2000) as a stratigraphic marker based on its occurrence in the GSSP. At Vallecillo, its FA is at a higher level than in the GSSP, in the upper *V.*

birchbyi zone. In all other locations, the range of this species is not known with precision and no calibration exists with other taxa or with the stable isotopic record. For instance, *M. kossmati* has been described from England, although it was not yet found at Eastbourne. However, the species is widely distributed, with occurrences in the early Turonian of the U.S. Western Interior, Colombia, France, Germany, Spain, Poland, Czech Republic, Ukraine, Kazakhstan, Japan and Madagascar (Walaszczyk and Cobban, in Kennedy *et al.* 2000) and Brazil (Andrade 2005). This almost cosmopolitan occurrence suggests that *M. kossmati* potentially is an excellent stratigraphic marker for long-distance correlation.

Stratigraphic ranges of early Turonian ammonites, inoceramids and planktic foraminifers differ considerably between faunal provinces. This diachrony indicates that large-distance biostratigraphic correlation of early Turonian sediments must be used with care. The GSSP located in the central Western Interior Seaway appears to be intermediate in position between boreal Europe and Vallecillo, which is characterized by a mixed Western Interior Seaway-Tethyan assemblage. *Watinoceras* spp. and *Mammites nodosoides* seem to be reliable biostratigraphic markers with widespread and approximately isochronous FAs. Additional species (e.g. *Mytiloides puebloensis, Vascoceras birchbyi*) may also be used but are more restricted in geographical distribution.

8.7   DEPOSITIONAL RATES

Absolute ages are based on publications by Kirkland (1991, *fide* Kennedy *et al.* 2000) and Hardenbol *et al.* (1998, *fide* Keller and Pardo 2004). They could only be assigned to three stratigraphic marker levels of the Vallecillo section (Figure 8.6). These levels allow the calculation of sedimentation rates to 27·3 mm/ka and 8·4 mm/ka, with an average rate of 16·8 mm/ka. Differences in the calculated rates may result from the fact that the absolute ages used here are from different sources. They are based on the ages of bentonite layers in the GSSP of the Cenomanian-Turonian boundary, the Rock Canyon section in Colorado. Kennedy *et al.* (2000) cited the data published by Kirkland (1991), whereas Keller and Pardo (2004) apparently interpolated the absolute ages from the charts of Hardenbol *et al.* (1998).

In addition, different zonal thicknesses and diachronous FAs of several zonal marker species (Chapter 8.6) are recognized, also distorting sedimentation rates, as interpolated absolute ages are based on the sedimentation rates of the Rock Canyon section. In the further discussion, only the average sedimentation rate of 16·8 mm/ka is considered for the Vallecillo section.

The compaction rate was calculated to roughly 30% of original thickness (Table 5.1). In consequence, pre-diagenetic sedimentation rate would average 56 mm/ka. This primary sedimentation rate is surprisingly high as the Vallecillo sediments are very fine-grained.
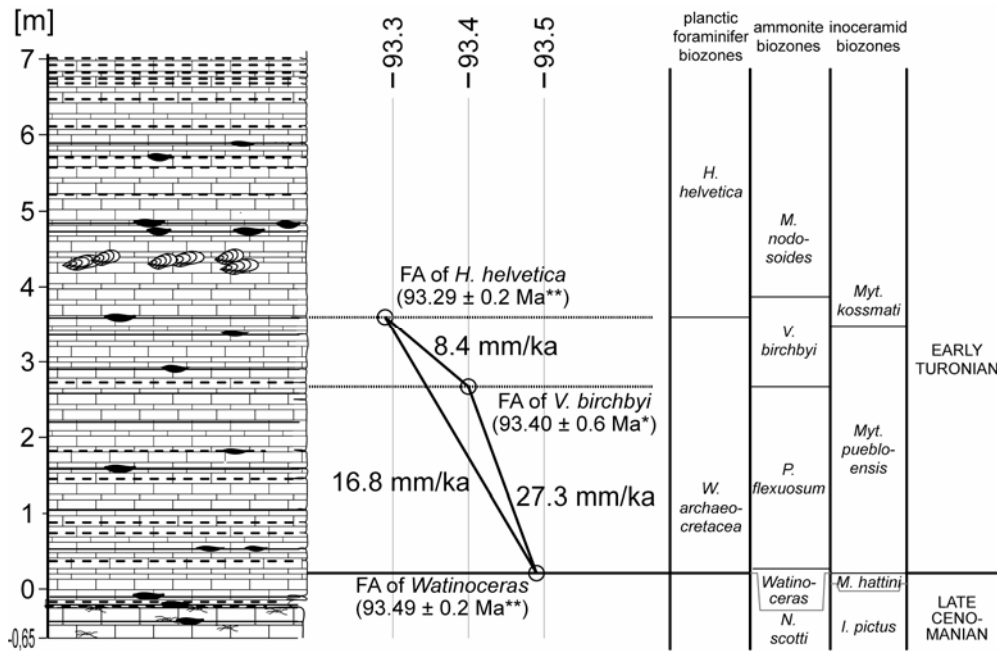
Figure 8.6. Age-depth plot of the Vallecillo section, based on FA data of Kirkland (1991, *, *fide* **Kennedy** *et al.* **2000) and Hardenbol** *et al.* **(1998, **,** *fide* **Keller and Pardo 2004).**

The average sedimentation rate for the early Turonian sediments of GSSP was calculated to 8·7 mm/ka (Keller and Pardo 2004). This value is considerably lower than the sedimentation rate at Vallecillo, thus indicating the higher stratigraphic resolution of the Vallecillo section.

8.8   STABLE ISOTOPES

A large positive δ^{13}C-excursion is known from the Cenomanian-Turonian transition, caused by the OAE 2 (see e.g. Schlanger and Jenkyns 1976; Arthur *et al.* 1988; Tsikos *et al.* 2004). This registered globally in the sediment record, and the detailed isotope curve usually provides an excellent tool for correlation. At Vallecillo, however, δ^{13}C values alter between –5·7‰ and 2·1‰, and there is no general trend visible in the signal. The δ^{18}O values are very negative; they vary between –6·3‰ to –8·7‰. The general trend of the δ^{18}O signal shows a decrease of values from about –7‰ to –8‰ upsection. This strong variation of isotopic signal does not correspond to isotopic data from the GSSP or the Eastbourne section (e.g. Keller *et al.* 2001; Keller and Pardo 2004). Isotopic data from Vallecillo carbonates are thus not suited for long-distance correlation to other Cenomanian-Turonian boundary sections.
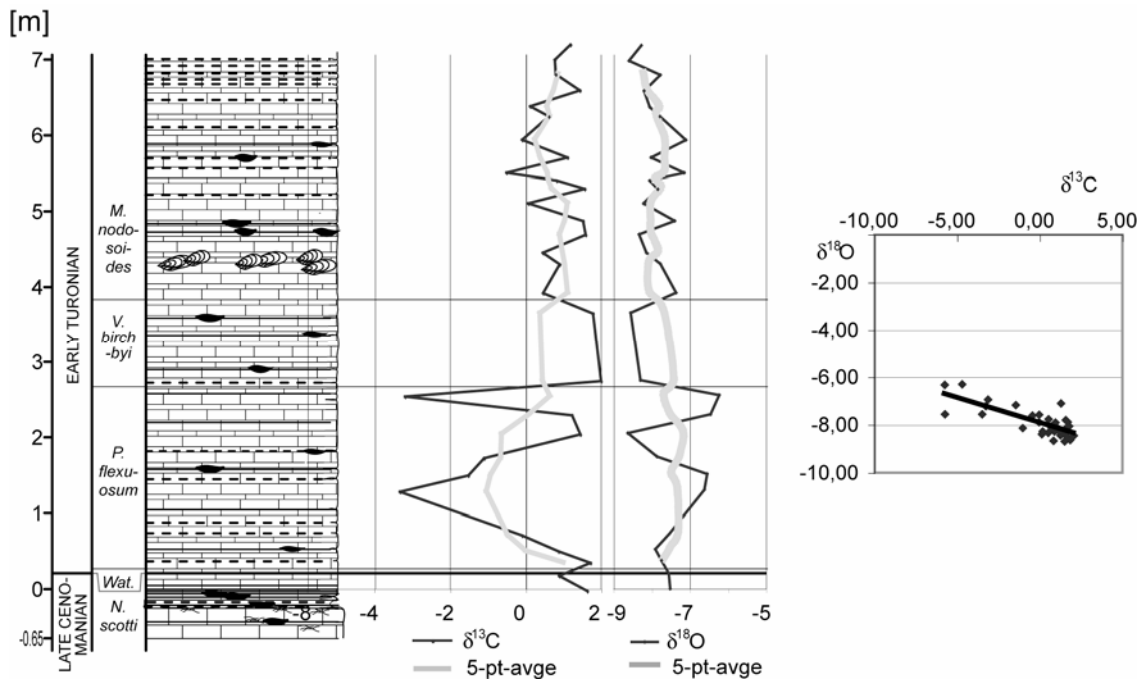
Figure 8.7. Left: Stable isotope data and biozonation of the Vallecillo section. Right: The cross-plot of δ¹³C and δ¹⁸O values shows a correlation between the values, indicating at least one overprint on the primary isotope signal.

The variation of $\delta^{13}C$ values of Vallecillo rocks is higher than in the $\delta^{18}O$ values, although the oxygen isotopes are usually more affected by diagenesis than the carbon isotopes. The $\delta^{13}C$ and the $\delta^{18}O$ curves mirror each other in some peaks, e.g. at the 1·00 and 6·10 m levels of the section. These peaks, marked by strongly negative $\delta^{13}C$ values, cannot be related to low carbonate values and are interpreted to reflect diagenetic signals.

The influence of diagenesis on isotopy can be estimated by cross-plotting $\delta^{13}C$ and $\delta^{18}O$ values. At Vallecillo, this cross-plot shows a clear correlation, thus indicating that the isotopic signal is not pristine. This interpretation is supported by recrystallization noted in the sediment (Chapters 5.2.2 and 5.5) and by oxidation of the organic matter by meteoric waters (Chapter 5.1).

The end members of this correlation (i.e. the lowest and highest values) are compared to stable isotope data of other early Turonian sections. In the GSSP, salinity variations in the epicontinental Western Interior Seaway influenced the isotopy of the rocks, thus providing a regional signal (Keller *et al.* 2004). The isotopic signal of the marine sediments in the Eastbourne section is thus more suitable for correlation. There, $\delta^{13}C$ values vary between 4 and 6 ‰ for the early Turonian, and the variation is considerably lower than the Vallecillo values. $\delta^{18}O$ values are between –2 and –4 ‰ at Eastbourne, and thus higher than in Vallecillo (Keller *et al.* 2001). None of the end members of the correlation of the Vallecillo data corresponds to these values, indicating a diagenetic shift of the isotopy at Vallecillo. In addition, the stable isotope signals of both sections differ significantly in their trends. The Vallecillo rocks are not suitable for by stable isotope stratigraphy.

9 STATISTICAL INTERPRETATION OF THE FOSSIL ASSEMBLAGE

9.1 THE COMPOSITION OF THE VALLECILLO ASSEMBLAGE

9.1.1 The databases

As pointed out in the Chapters 4.10 and 4.11, there are two types of fossil collections for Vallecillo: the statistical data collection and a random surface collection. The random surface collection was used for a first overview over the fossil assemblage, particularly ammonites, inoceramids and fishes. Its composition is shown in Figure 9.1, together with the absolute composition of the Vallecillo fossil assemblage, which is the result of the statistical data collection from the scientific excavations.
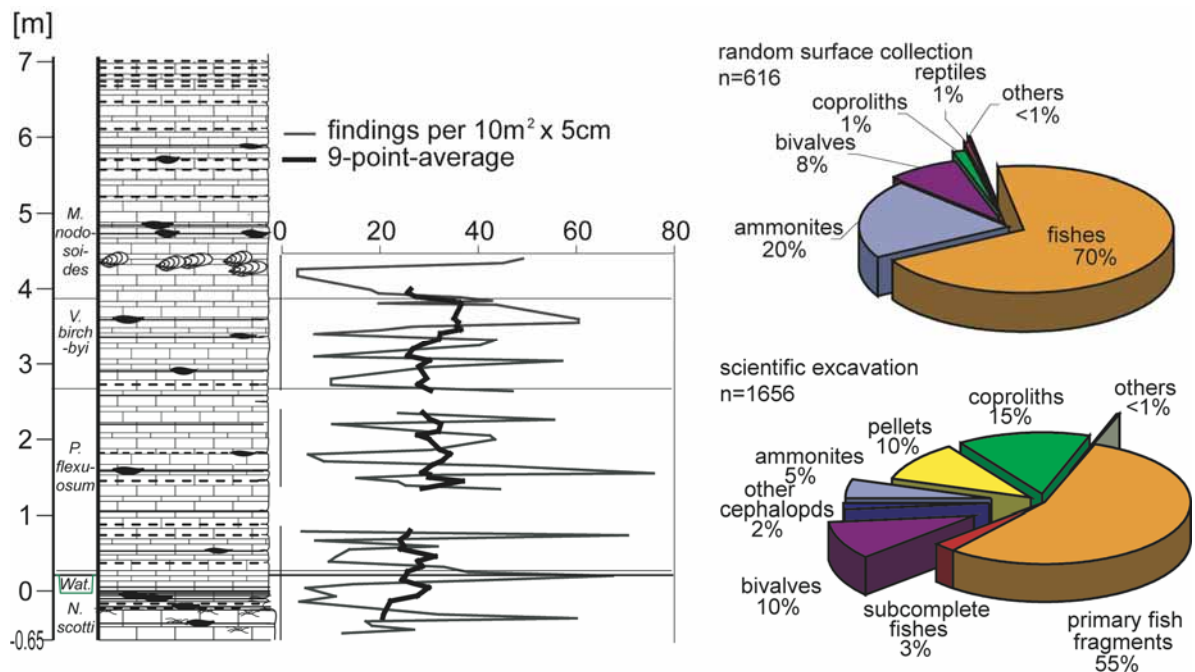
Figure 9.1. Left: Quantified distribution of fossils over the section excavated. Right: Statistical composition of the random surface collection (above), and composition of the excavated assemblage (below). In both charts, the same colours are used for the fossil groups.

Comparison of random surface collection and statistical data collection reveals a biased composition of the random surface collection. The abundances are overrepresented by factor 1·3 for vertebrates and by factor 4 for ammonites. Bivalves, on the other hand, are represented by approximately the same amount in both types of collections. Coproliths were scarcely recovered in the random surface collection, and pellets were missing completely.

The statistical data collection allows the monitoring of the stratigraphic distribution of fossils, but also their abundance throughout the section (Figure 9.1). The fossils are evenly distributed throughout

the section, with an average of 29·0 findings per 10m^2×5cm. A slight shift towards a lower number of findings per 10m^2×5cm is noted in the excavated basal limestone. This shift should not be over-interpreted, because few data exist from this part of the section.

The resulting finding rate in the Vallecillo *Plattenkalk* includes all kinds of fossils, e.g. single bones. This fossil abundance of the Vallecillo locality cannot be compared to other localities, because similar quantitative analyses were never published before for other *Plattenkalks*.

9.1.2   Random surface collection versus scientific excavation

The systematic collection of Vallecillo fossils is biased by the selective search of local workers for fishes, reptiles, or large ammonites. The stratigraphic context of these fossils is mostly lost. Only statistical data collections provide unambiguous data on abundance and distribution of fossils in the lithologic column.

The random surface collection yields many well-preserved fossils, but without stratigraphic data. On the other hand, the enormous surface surveyed by the local quarrymen brought to light rare taxa such as *Robertichthys riograndensis*, sharks or reptiles, as well as complete and well preserved fish and invertebrate specimens. These well-preserved fossils are essential for anatomical studies. It is highly unlikely that such taxa or specimens are discovered during a statistical data collection, which is always aligned with a limited turnover of rock. In conclusion, both types of collection are necessary for the interpretation of the Vallecillo fossil *Lagerstätte*, but statistical data collection by several teams over a long period of time would yield a maximum of scientific information.

9.2   DISTRIBUTION OF INOCERAMIDS OVER THE VALLECILLO SECTION

Inoceramids are rare in the basal 0·8 m of the section (Figure 9.2). There is a minor increase in abundance around the Cenomanian-Turonian boundary level (0·21 m) from three to ten specimens per 10m^2×5cm, paralleled by the increase from one (*I. pictus*) to three species (*I. pictus*, *M. hattini*, *M. puebloensis*) in these beds. The abundance declines again above the 0·6 m level, and a monospecific *M. puebloensis* assemblage is present throughout the *P. flexuosum* zone, with few exceptions around the 2·0 m level.

The FA of *M. kossmati* at the 3·46 m level of the Vallecillo section is followed by a maximum in abundance of this species in the upper *V. birchbyi* zone. In this level, the abundance of inoceramids increases from virtually zero to 34 specimens per 10m^2×5cm. This first maximum in abundance coincides with a considerable increase in size and diversity in the foraminiferal assemblage and the FA of *H. helvetica* (Figure 8.3).

The highest 0·1 m of layers excavated (around the 4·45 m level) include the lowest level of an inoceramid flood occurrence, with a maximum abundance of 34 specimens per 10m^2×5cm registered in the highest excavated layers. Inoceramids are more abundant above this level, to almost rock-

forming quantities, and their cross sections are frequently recognized along the vertical joints in the quarries, allowing for correlation. The maximum abundance of this flood occurrence was not yet quantified during the excavation, because the sediment containing so many inoceramids cannot be split fine enough to register all individuals. The estimated abundance of the maximum is >1000 specimens per $10m^2 \times 5cm$.
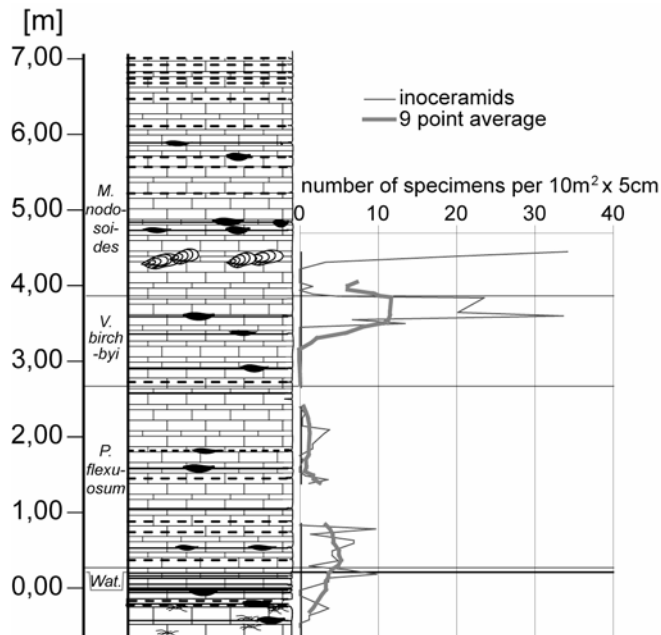
Figure 9.2. Abundance of inoceramids plotted from the statistical data collection.

The taphonomic interpretation of the vertebrate assemblage (Chapter 9.4) and petrographic and geochemical evidence indicate the existence of permanent anoxic conditions at the Vallecillo sea floor (see Chapters 5.1, 5.2.2, 5.6.2, 6.2, and Ifrim *et al.* 2005a; Ifrim *et al.* 2005b). Inoceramids were apparently capable to live under these permanently anoxic conditions. A H_2S-based metabolism was assumed for these bivalves by MacLeod and Hoppe (1992) and Fisher and Bottjer (1995), consistent with the interpretation of the inoceramids from the Vallecillo section and the surrounding sediments.

The Vallecillo faunal assemblage consists of 10% inoceramids. This rate results from the two *Mytiloides* abundance maxima in the upper part of the section; it is 5 % in the sediments outside the two abundance maxima. The abundance of inoceramids appears to be independent from the substrate they lived on, because no lithological changes were recognized in the surrounding sediment in layers with increased abundance of *Mytiloides*, so it may have depended on the ecology of their small, planktotrophic larvae (see Chapter 9.5).

9.3   CEPHALOPODS

Findings during the Vallecillo excavations include a coleoid (Figure 7.1) and indeterminable isolated siphos. Both are summarized as undeterminable cephalopods in the following discussion.

9.3.1 Cephalopods in the statistical data collection from Vallecillo

The abundance of ammonites and other cephalopods is variable over the Vallecillo section (Figure 9.3). There is a first increase in abundance from zero to four specimens per $10m^2 \times 5cm$ at the Cenomanian-Turonian boundary and the lower *P. flexuosum* zone of the excavated Vallecillo section. This minor increase coincides with the FA of three basal Turonian index species (*Watinoceras coloradoense, P. flexuosum and Quitmaniceras reaseri*). The abundance of ammonites and undeterminable cephalopods declines to an average of one specimen per $10m^2 \times 5cm$ in the middle *P. flexuosum* biozone.
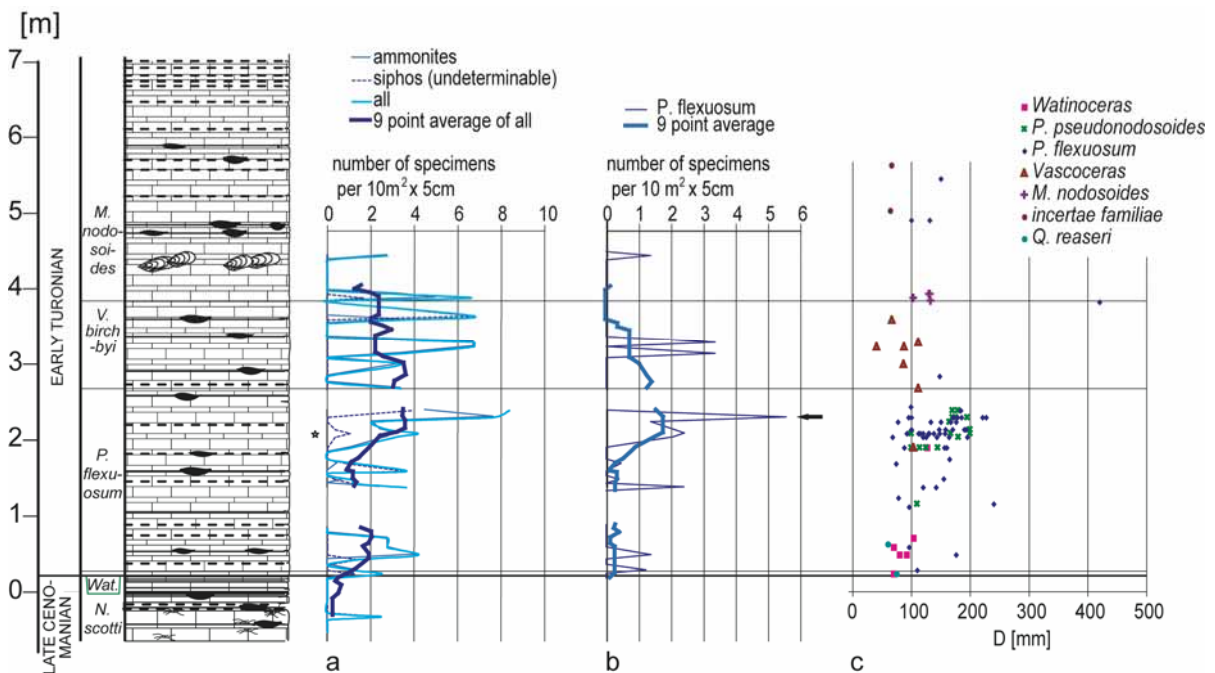
Figure 9.3. Distribution of ammonites in the Vallecillo section. a: abundance of cephalopods excavated in the statistical data collection. *: *Palaeoctopus***. b: abundance of** *P. flexuosum* **only. The peak in abundance of this ammonite (arrow) is clearly noted in the distribution of all cephalopods. c: diameters of the ammonite taxa in the lithological column. Specimens collected outside the statistical data collection from with known stratigraphic provenance are also included.**

The second increase is related to a maximum in abundance of *P. flexuosum* at the 2·2 m level of the section (compare Figure 9.3a and b). There, 8·5 cephalopods were registered per $10m^2 \times 5cm$, of which 5·6 are *P. flexuosum*. Up to this 2·2 m level, the ammonite assemblage is low in diversity, with only the two *Pseudaspidoceras* species present. Above, *P. pseudonodosoides* disappears at the 2·5 m level, and *P. flexuosum* becomes rare, although specimens identified increase further in size, leading to maximum diameters during the *Vascoceras birchbyi* biozone (Figure 9.3c). The assemblage is then dominated by vascoceratids.

The database above the FA of *Mammites nodosoides* at 3·84 m section is poor. This part of the column was excavated with a small excavation area up to the 4·7 m level, whereas the section above is

not yet covered by statistical data collection. Indeterminable ammonites ("*incertae familiae*") and *Fagesia* appear in the uppermost beds of the section. These taxa indicate another change in the ammonite assemblage, but this cannot, yet, be quantified.

9.3.2 Taphonomic Interpretation of the Vallecillo Ammonites

Shells of dead *Nautilus*, *Spirula* and some sepiids are known to float at the water surface over a period of time and are frequently dispersed over hundreds or even thousands of kilometres (Chamberlain *et al.* 1981), which was consequently also assumed for ammonoids (Westermann 1996). Post-mortem drift may thus influence the composition of fossil ammonite taphocoenoses (e.g. Maeda and Seilacher 1996). Only the presence of aptychi in the living chamber or the preservation of soft tissue would indicate autochthonous ammonite assemblages; aptychi are assumed to fall out of the phragmocone within a day or two after death of the animal (Westermann 1996). The statistical data collection provided 82 ammonites and 27 other cephalopod remains (mostly siphos with the shell dissolved, but also the rostrum of a possible *Palaeoctopus*; D. Fuchs, pers. comm.). Among these excavated specimens, no unequivocal aptychus was found. Only a faint stain next to the aperture of an undeterminable ammonite may represent remains of an aptychus (Figure 5.9a). Goethitic remains of the stomach content (Chapter 5.5) are present in two specimens of *Vascoceras* sp., a juvenile *Mammites nodosoides*, and *P. flexuosum* (e.g. Figure 5.8). All other ammonite shells hitherto excavated at Vallecillo lack aptychi and stomach contents and may thus be allochthonous. In consequence, only six percent of the 82 ammonites can be interpreted as autochtonous faunal elements (Ifrim and Stinnesbeck submitted).

The idea of long-lasting post-mortem drift of ammonite shells contrasts with the excellent state of preservation of many shells. Undamaged apertures and living chambers, and the preservation of delicate details of the ornamentation such as striation or long spines in *P. flexuosum* (Figure 7.6) suggest that these shells did not drift for a long time. Long time post-mortem drift is considered a rare phenomenon in epeiric seas such as the Vallecillo sea, less common than in the open ocean; it was even considered the exception, not the rule, in ammonite taphonomy by Page (1996).

Maeda & Seilacher (1996) concluded that below an unquantified critical water depth, ammonite shells did likely not rise to the surface. They were quickly waterlogged and buried, as observed for shells of *Nautilus* that died below 300 m (Chamberlain *et al.* 1981).

The previous hypotheses were recently challenged by Wani *et al.* (2005), who carried out taphonomic experiments with freshly dead *Nautilus* of sizes from 72 to 195 mm in diameter, which they let decay up to 14 days in water depths of 50 m and 320 m. These authors concluded, that the phragmocone is only waterlogged after the posterior mantle detached. This happened much faster in the shallow water due to a faster decay at high water temperatures. Large specimens became waterlogged faster than small ones, because a much greater volume of decay gases developed in the larger bodies, leading to a faster detachment of the critical part of the mantle. This supports the

observation at Vallecillo, that large shells are well preserved. The longer drift of small ammonite shells assumed by Wani *et al.* (2005) may in part explain the different preservation of large and small shells, but early diagenetic aragonite solution contributed largely to a different preservation of small and large ammonites (Chapter 5.6.2).

The near-absence of post-mortem drift in shells >100 mm is also indicated by the excellent *in-situ*-preservation of spines in *P. flexuosum*; these were apparently jointed to the shell and would have fallen off during the decay of soft tissues (see Chapter 9.3.3 below).

Heteromorph ammonoids are absent in the Vallecillo sediments. This is unusual, because they are known to exist in many other North American localities of basal Turonian age. For instance, *Allocrioceras larvatum* and *Hamites* sp. are known from the *Watinoceras* zone of the Pueblo area. *A. dentonense*, *A. larvatum*, *Sciponoceras* sp and *Worthoceras* sp. are recorded from the *P. flexuosum* zone of Trans-Pecos Texas, *Puebloites spiralis* is known from the *Vascoceras birchbyi* zone of Colorado, Kansas and New Mexico, and *Baculites yokoyamai* and *Puebloites greenhornensis* from the *Mammites nodosoides* zone of the southern Western Interior Seaway (Kennedy and Cobban 1991). Their absence in Vallecillo may be related to their mode of life. An epibenthonic life strategy of heteromorph ammonoids has been suggested by various authors (e.g. Stinnesbeck, 1986, for *Eubaculites*). Westermann (1996), however, suggested two different options, being aware that heteromorphs often occur in a pseudoplanktonic mode of life with the ammonoids were vertical migrants in the open water, or a bottom feeding strategy in which the animals migrated vertically in and out of dysoxic bottom waters. The absence of heteromorphs at Vallecillo points to a bottom-feeding strategy of heteromorphs, because it can be explained by hostile conditions at the sea floor or by a thick zone of oxygen-depleted bottom waters, which may have excluded an occasional short-term penetration by vertically migrating heteromorphs. Heteromorphs are thus excluded from the Vallecillo area, similar to other benthic organisms.

Phylloceratids and lytoceratids occur mainly in pelagic environments (e.g. Fischer 1967; Fernández-López and Meléndez 1996; Ifrim *et al.* 2004), but were not identified in the pelagic Vallecillo assemblage. Phylloceratids and lytoceratids appear to have been generally rare in low latitudes during the early Turonian (compare e.g. Kennedy *et al.* 1987; Zaborski 1987; Kennedy 1988; Meister 1989; Meister and Abdallah 1996; Courville *et al.* 1998; Lehmann 1998; Villamil and Arango 1998; Gale *et al.* 2005).

The genus *Mammites* has been interpreted as an epibenthonic faunal element, lying on the sediment on its flattened venter (e.g. Hessel 1988, p. 40). However, anoxic bottom conditions of the Vallecillo sea prevented benthic life in Vallecillo (Ifrim *et al.* 2005a and herein). Ammonites are assumed to be slow swimmers and needed hours to migrate up or down within the water column, similar to recent

Nautilus (e.g. Kennedy and Cobban 1976; Jacobs and Chamberlain 1996). They may even have avoided rising in the water column completely (Moriya *et al.* 2003), so that even short-term stays of *Mammites* at the sea-floor seem improbable. An epibenthic mode of life of *Mammites* is not supported from observations in Vallecillo.

9.3.3 Spines of *Pseudaspidoceras flexuosum*

Fourteen of 43 excavated *P. flexuosum* are preserved with long ventrolateral spines. The rate of spined specimens may have been higher, but some specimens are strongly weathered, or spines may have broken off during extraction. Spines of are *P. flexuosum* straight in shells larger than 250 mm, but slightly curved in smaller specimens (Figure 9.4). Obliquely embedded spines were diagenetically compacted (Figure 9.4). The spines are preserved in the same way than the shell which indicates that they were originally of aragonite. No complete spine is preserved uncompacted, it is difficult to give the ratio of spine length to shell diameter; their length is at least half of the whorl diameter. The tip of the spines is rounded (Figure 9.4).

The spines of *P. flexuosum* were jointed to the shell, not rigid extended tubercles. One spine was bent below the shell of specimen UANL-FCT-VCII/95 (Figure 9.4), when the dead ammonite touched the sea floor. Another disarticulated from the laterally embedded specimen UANL-FCT-VC500 (Figure 7.6). Its base is intact (see detail in Figure 7.6) which suggests that the spines were jointed to the shell.

Spines are more abundant in large specimens of *P. flexuosum* (Figure 9.5). This may indicate a sexual dimorphism, with the adult macroconchs wearing spines. The size difference is the only distinguishing factor between dimorphs of most Perisphictina (Page 1996), to which *P. flexuosum* belongs.

Spines have never been documented for *Pseudaspidoceras* previously, but are known to exist in late juvenile growth stages of the late Cenomanian *Euomphaloceras septemseriatum* (Cragin 1893; in Kennedy 1988, pl. 8, figs 4-6, 9), in which they are preserved in grooves of the succeeding whorls. Similar to the genus *Euomphaloceras*, *P. flexuosum* belongs to the Euomphaloceratinae Cooper, 1978. Juvenile and adult *P. flexuosum* from Vallecillo present flanks without grooves. The spines are only present on the living chamber of adult growth stages; no spine was found attached to the phragmocone, and grooves for accommodation of the spines of preceding whorls are missing. This suggests that the spines were connected to the body by soft tissue and fell off as soon as the posterior part of living chamber was sealed it with a septum.

Spines considerably reduced drag during swimming (Jacobs and Chamberlain 1996), so spined *P. flexuosum* were low velocity swimmers. The function of spines in ammonites is hitherto unclear, although the constant recurrence of ribs, tubercles and spines in nearly identical form and combination in distantly related groups indicates that they were highly functional features of the shell (Kennedy and Cobban 1976, p. 26).
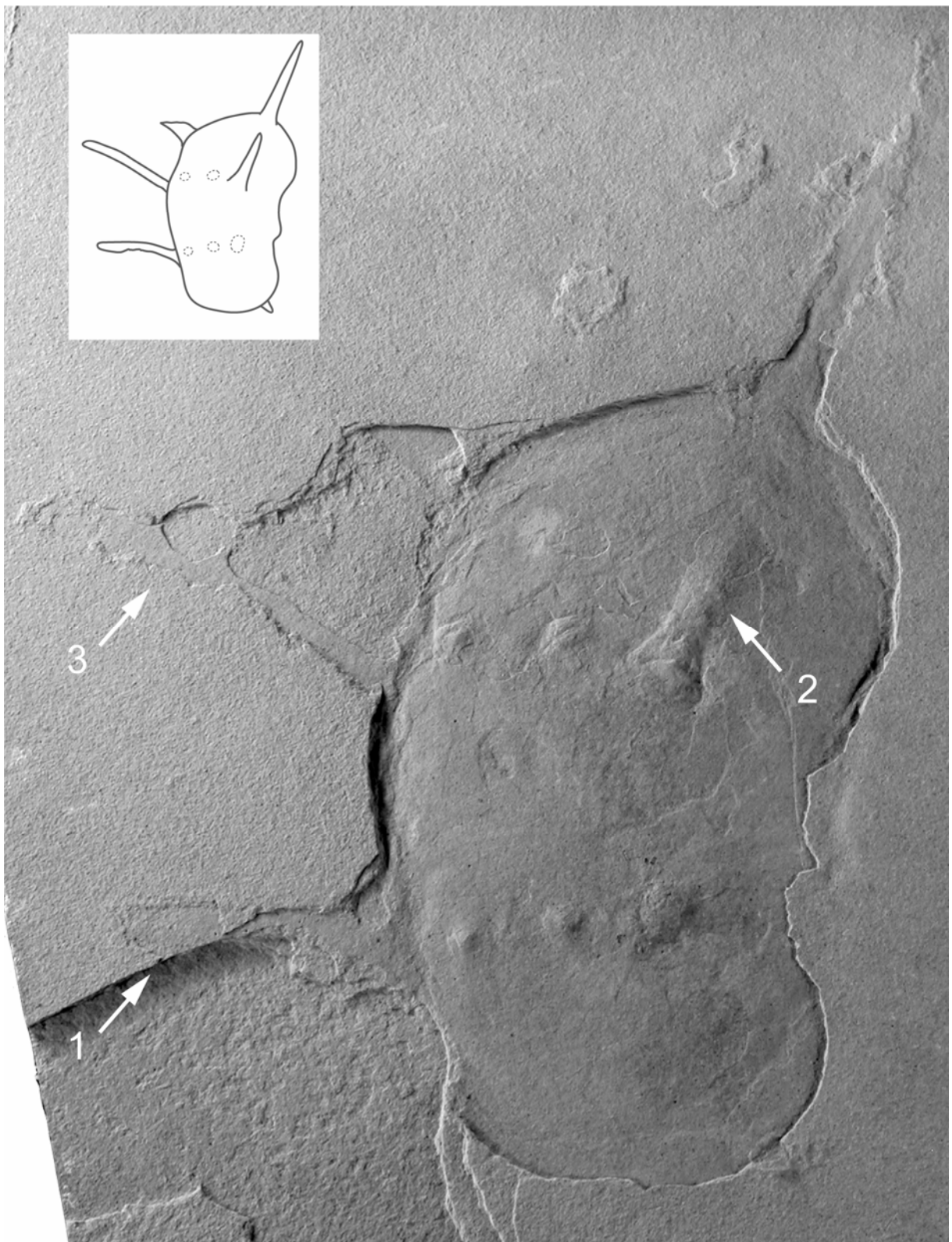
Figure 9.4. Spined specimen of *Pseudaspidoceras flexuosum*. UANL-FCT-VCII/95B. One obliquely embedded spine (1) appears shortened due to compaction. Another spine (2) was folded under the shell when the ammonite touched the sea floor. One spine (3) is slightly curved.

Checa and Martin-Ramos (1989) discussed the function of spines for *Aspidoceras* and *Orthaspidoceras* from Spain. The Jurassic *Aspidoceras* is almost homeomorphous with *Pseudaspidoceras*, but its spines were built at the aperture by secretion from the mantle. These spines were present on ventrolateral and umbilicolateral tubercles of the living chamber and phragmocone of *Aspidoceras*. The hollow, conical, rigidly attached spines were separated from the posterior living chamber by a basal septum, whereas their base was open in the foremost part of the living chamber. Defence against predators was considered an unlikely function by the authors, whereas a sensory function of the spines was considered more probable, based on the fact that the spines were hollow, and each had an aperture in the distal tip (Checa and Martin-Ramos 1989). In the Vallecillo *P. flexuosum*, neither concentrical constructions nor distal apertures are observed, probably as an artefact of preservation. In addition, the spines seem jointed to the shell, instead of rigid extensions.
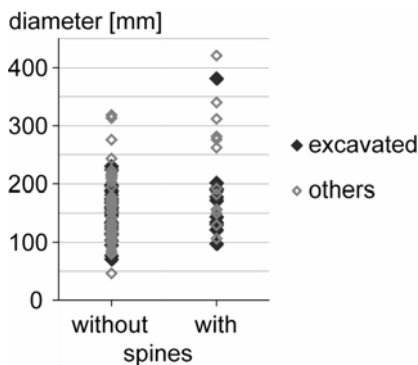
Figure 9.5. Statistical chart of the sizes of spined and unspined *Pseudaspidoceras flexuosum* from Vallecillo. n=117.

Spines may have served as balancing aids when the shells rested on the bottom (Kennedy and Cobban 1976, p. 26). In the case of Vallecillo, however, constant anoxic conditions and a hostile environment at the sea bottom (Ifrim *et al.* 2005a) exclude an epibenthonic mode of life of *P. flexuosum* similar to *Mammites* (see above). Additionally, there are no trace fossils recognized in Vallecillo, neither from ammonites resting on the sea bottom, nor from other organisms.

Strong ornamentation was interpreted by Ward (1981) as an adaptive response of ammonites to increased predation. This view is supported by Cowen *et al.* (1973) who argued that in lateral view, transverse ribbing patterns, and spines in the case of *P. flexuosum*, would break up the smooth outline of the venter viewed from any direction, which would thus camouflage the test.

9.4   THE VALLECILLO FISH ASSEMBLAGE

9.4.1   Statistics of the Vallecillo fishes

The statistical data collection from excavations yielded a total of 942 fish specimens. 96% of them are primary fragments and 4% subcomplete specimens. 73% of the 942 specimens are primary fragments, which are too small to be determined. The rest (209 specimens) is more or less articulated and consists of 79% *Rhynchodercetis*, 6% *Nursallia* cf. *gutturosum*, 6% *Tselfatia formosa*, 4% of a

small, hitherto undescribed teleost discovered during excavation in 2003, 3% *Goulmimichthys roberti*, 1% *Vallecillichthys multivertebratum*, and 1% of an undetermined species referable to the teleost family Pachyrhizodontidae (Figure 9.6).
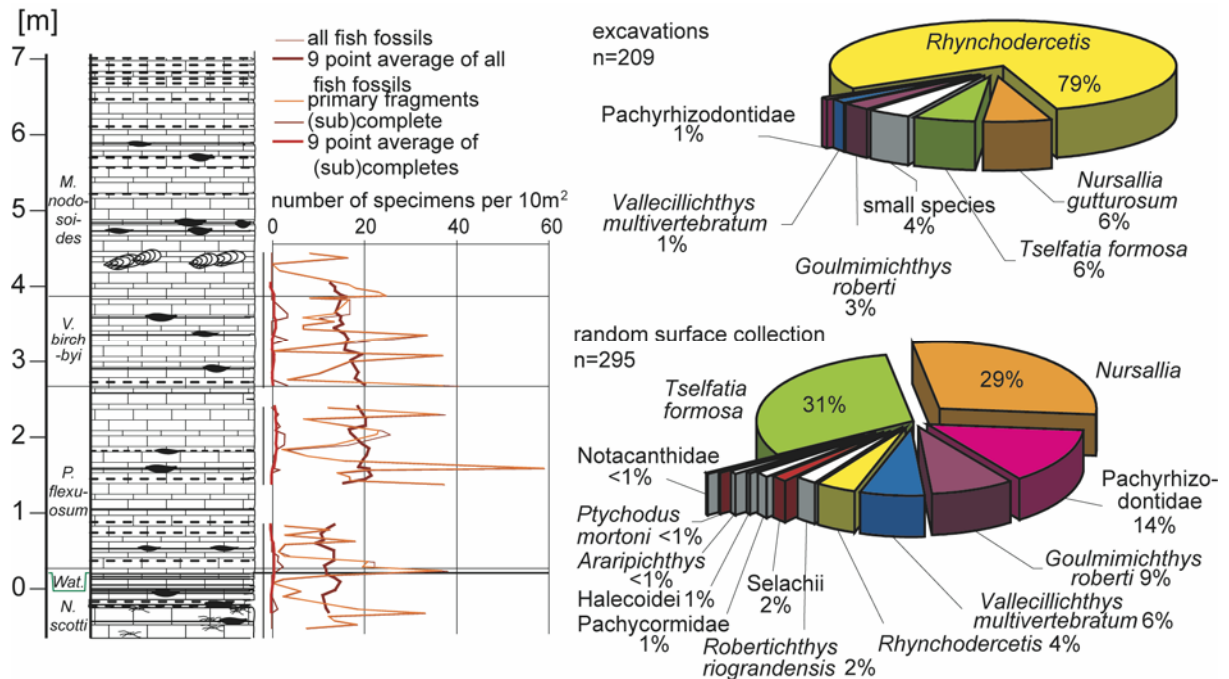
Figure 9.6. Statistical composition of Vallecillo fossil assemblage. Left: distribution of fish fossils over the Vallecillo section. Upper right: determined articulated specimens and primary fragments in the statistical data collection. Lower right: composition of the random surface collection.

Compared to this absolute composition, the random surface collection shows a strongly biased distribution (Figure 9.6). While the relative abundances of *Tselfatia formosa*, *Nursallia* cf. *N. gutturosum*, and *Vallecillichthys multivertebratum* may resemble their distribution in the statistical data collection, the small undescribed taxon is completely neglected in the random surface collection. Sharks, pachycormids, and teleosteids such as *Araripichthys* and *Robertichthys riograndensis* are only known from the random surface survey.

The abundance of *Rhynchodercetis* was clearly underestimated in the random surface survey, and only adult specimens were selectively collected. Large impressive *Tselfatia formosa* specimens were "preferably" collected by quarrymen, while juvenile *Rhynchodercetis* were thrown away. Furthermore, 93% of *Rhynchodercetis* were collected as primary fragments in the statistical data collection, which were never collected in the random surface collection.

9.4.2 Taphonomy of the fish assemblage

Preliminary data on the taphonomic interpretation of the Vallecillo fish assemblage were published by Ifrim *et al.* (2005a; in press). Most fossils of the vertebrate assemblage are primary fragments,

subcomplete and in part disarticulated. Some missing body parts like the tail and other fins, or elements of the skull, can be explained by a failure of mechanically weak articulations due to progressive decay. Scavenging upon carcasses at the sea-floor appears to be uncommon in Vallecillo, because body parts are missing as a whole, without bite marks or traces of violent disruption. They are often found isolated in the sediment (Figure 7.16b-d). Slight dislocation of ribs likely resulted from the disruption of the swim bladder or gas escape from the body cavity, and not from currents or scavengers. Most missing body parts were lost during *post-mortem* drifting.

There is no evidence for scavenger activities at the sea floor. Some carcasses sank to the sea bottom prior to decay with their heads down, and disintegrated there out of the reach of other animals (Figure 7.16). This absence of scavengers and of benthic life, with the exception of inoceramids, is explained by the anoxic conditions at the Vallecillo sea floor (see Chapters 5.1, 5.2.2, 5.6.2, 6.2, and Ifrim *et al.* 2005a; Ifrim *et al.* 2005b). Apparently, carcasses were buried outside the reach of scavengers below the chemocline. The low oxygen zone must have been more than one meter thick. This is concluded from large fishes of more than one meter in length, which disarticulated head-down on the sea floor without any traces of scavenging.

9.4.3 Taphonomy of the three most abundant fish species

Rhynchodercetis sp. (Figure 7.16) is the most abundant taxon of the Vallecillo fish assemblage, with 168 individuals registered in the statistical data collection. The fish was between 60 and 400 mm long (Figure 9.7), with a slender body. The morphology of the species strikingly resembles the recent horn gar *Belone* or the mackerel gar *Scombresox,* which both live close to the water surface. These fishes seize small prey items like small crustaceans as well as small fishes, with their thin, longirostrine jaws and the tiny needle-shaped teeth (Muus and Dahlström 1973). From its overall morphology, *Rhynchodercetis* could have had a life style similar to *Belone* or *Scombresox*. The lack of stomach content, even in the best preserved specimens, indicates a preference for soft bodied prey, such as small mollusc larvae, small, thin shelled crustaceans, or tiny fish with a scarcely mineralized skeleton (Ifrim *et al.* 2005a, in press).

93 % of the *Rhynchodercetis* specimens from Vallecillo are primary fragments, especially isolated skulls or vertebrae. This indicates that this fish was a surface dweller, and the disarticulation prior to embedding resulted from post-mortem drift and gradual disintegration at the water surface as a result of buoyancy and low water pressure, until the internal gases (air from the swim bladder or decay gases) could escape.

Rhynchodercetis occurs throughout the Vallecillo section (Figure 8.4) with an average of 2·0 specimens per 10m^2×5cm, but its abundance varies. It averages two specimens per 10m^2×5cm in the lower and upper excavated Vallecillo column (Figure 9.7). At the 2·03 m level, its frequency abruptly increases to a maximum of 10·7 specimens per 10m^2×5cm. *Rhynchodercetis* is still numerous in the beds above, although the abundance decreases to 8·3 specimens per 10m^2×5cm in the 2·08 m level,

and to 6·6 specimens per 10m²×5cm in the 2·13 m level. This maximum in abundance is thus clearly expressed in the average line. As *Rhynchodercetis* was interpreted to have been a surface-dwelling fish, its maximum in abundance may indicate favourable conditions in the upper water column of the Vallecillo sea, with persisting anoxic conditions at the sea floor.
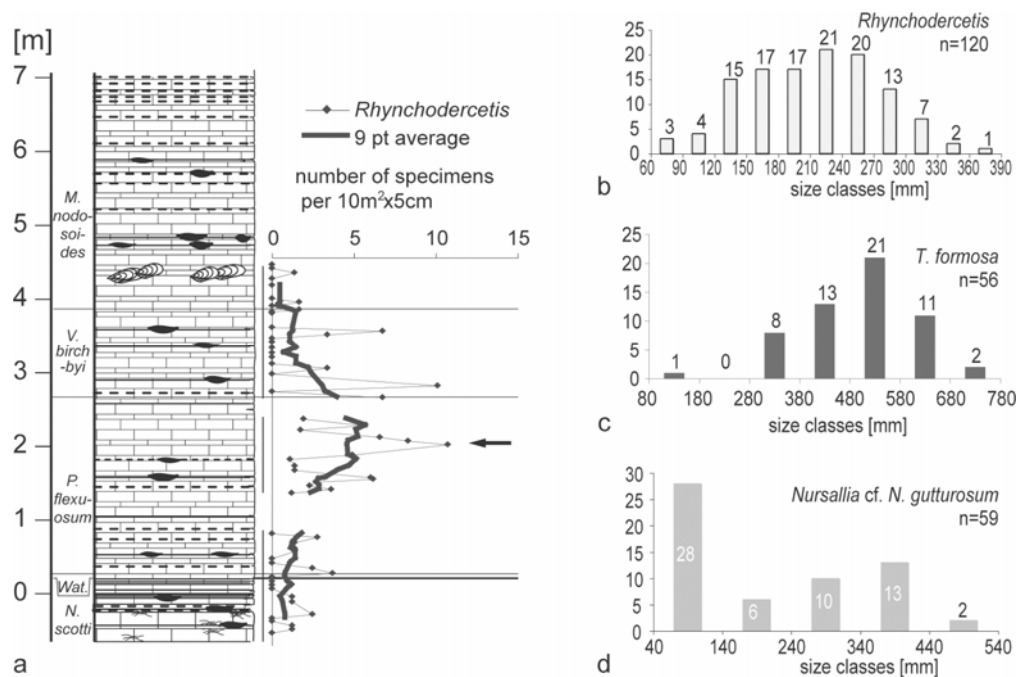
Figure 9.7. a: abundance of *Rhynchodercetis* in the Vallecillo column with a clear maximum at the 2·03 m level. This peak is clearly expressed in both the abundance and the 9-point average curve. b-d: Size distribution of the three most common Vallecillo fishes. b: *Rhynchodercetis*. Data are from the levels with the maximum in abundance. c: *Tselfatia formosa*, with data from the random surface collection. d: *Nursallia gutturosum*. Data are from the random surface collection.

Another abundant fish species in the Vallecillo carbonates is the teleost **Tselfatia formosa** (Figure 7.14). Ninety specimens are recorded in the surface collection database, ranging from 80 to 750 mm in length. With its discoid body and large ventral and dorsal fins, this species is similar to the recent John Dory *Zeus* or the Opah *Lampris*. Both recent fishes are pelagic and preferably swim in open shelf waters (Muus and Dahlström 1973). While *Zeus* has a deep mouth and mainly hunts down small swarm fishes, *Lampris*, with its edentulous jaws, exclusively feeds on squid (Muus and Dahlström 1973). From its body shape and size, *Tselfatia* was likely a pelagic long distance undulatory swimmer similar to *Zeus,* with the ability for rapid acceleration and quick manoeuvring.

With its small edentulous mouth, *Tselfatia formosa* Arambourg, 1954 could have attacked small prey; probably, like *Lampris*, pelagic squid. The stomach content is frequently preserved and consists of a dark, foamy substance without any trace of bone (Figure 7.14).

The high ratio (31 %) of subcomplete specimens from the statistical data collection indicates, that *Tselfatia* inhabited deeper waters, and many individuals died beyond the buoyancy line. They did not drift after death, but sank down to the sea floor immediately.

Nursallia **cf.** *N. gutturosum* (Figures 5.12 and 7.15) is the third common species of the Vallecillo assemblage. The random surface collection yielded 86 specimens, which are between 40 and 500 mm long. There are two size maxima at 40 to 130 and 340 to 430 mm body length (Figure 9.7c), which probably are a consequence of migration at different growth stages. Its small mouth with pycnodont dentition opens rostroventrally. Fishes of this morphotype, such as the recent parrot fishes (Scaridae), are supposed to live in the vicinity of reefs, where they feed on corals, bivalves and echinoderms (Applegate 1992; Brandes 1993a; Nursall 1996). A fossil example for a reef dwelling fish similar to *Nursallia* is *Tepexichthys aranguthyorum* Applegate, 1992 from the Albian of Tepexí de Rodríguez. One specimen of this species preserved "coprolithic masses composed of a white powdery substance … thought to represent smashed coral" (Applegate 1992, p. 176). The sediments at Tepexí de Rodriguez are similar to Vallecillo in grain size and composition, but, according to Applegate (1992), the fossil assemblage in the quarries suggests that they were deposited in a backreef lagoon. *Nursallia* from Vallecillo, apparently inhabited the open sea, hundreds of kilometres away from any coast or reef (e.g. Sohl 1991, Seibertz 1998, Goldhammer and Johnson 2001, and Figure 3.1 herein). In this respect, *Nursallia* resembles the recent Guilthead *Sparus*, a fusiform fish which, like *Nursallia*, has a pycnodont dentition. *Sparus* plunders coastal bivalve banks but also lives in open shelf waters, where it feeds on sea grass, fish and other animals (Brandes 1993b). The Vallecillo *Nursallia* could have preyed on small ammonites, which were certainly abundant, or on soft parts of floating dead ammonites, or dead and living fishes. However, the diet of *Nursallia* remains speculative, because fossilized stomach content is yet unknown (Ifrim *et al.* 2005a, in press).

Nursallia was registered with 13 specimens in the statistical data collection. 6 of these are subcomplete specimens, 3 are articulated. But the 7 primary fragments mostly comprise half a carcass or more, e.g. the thoracal part with head and tail lost; only one fragment of the vertebral column of a very large (>500 mm axial length) *Nursallia* was hitherto recognized. This points to a biased interpretation, with smaller primary fragments probably hidden in the unidentified portion of fish remains. The interpretation of the ratio of subcomplete specimens to primary fragments is therefore avoided for the moment for this species.

The different preservation of *Tselfatia* and *Rhynchodercetis* at Vallecillo likely results from the water depths, in which they preferably lived. The surface dweller *Rhynchodercetis* floated after death, until the carcasses were completely decayed; this fish mostly occurs as isolated fragments (Ifrim *et al.* 2005a, in press). Articulated specimens, or specimens disintegrated in the place of embedding, result from a rupture of the swim bladder shortly after death and subsequent rapid sinking (see e.g. Schäfer 1962; Allison *et al.* 1991). In contrast, a high ratio of *Tselfatia* is complete and articulated. This indicates that this fish dwelled in deeper waters, and the articulated individuals died during a deep dive beyond the buoyancy line and sank down immediately.

The three most common fishes of the Vallecillo assemblage comprise 91% of the determined fish

assemblage of the statistical data collection. They apparently differed in locomotion mode and feeding habits and therefore shared the available food sources without major habitat or food interference.

9.5   FURTHER CONCLUSIONS

Both inoceramids and ammonites depended on oceanic currents for the distribution of their larvae and early juveniles (Kauffman 1975; Landman *et al.* 1996). In consequence, both groups were strongly affected by the Cenomanian-Turonian stagnation and breakdown of the oceanic current system (de Graciansky *et al.* 1984; de Graciansky *et al.* 1986). But they differ in the habitats of their post-metamorphosis growth stages; while ammonites drifted passively in the open water, inoceramids were strictly benthic organisms. Fishes, in contrast, are active swimmers. In consequence, these three fossil groups may have had a different response to the Cenomanian-Turonian OAE 2.

The stratigraphic resolution of the Vallecillo section and the statistical data collection allow to compare the distribution of the three groups during the early Turonian (Figure 9.8). The abundance of fish fossils is stable across the Cenomanian-Turonian boundary and increases slightly in the middle *P. flexuosum* zone. An abundance maximum at the 1·58 m level precedes the maximum abundance of *Rhynchodercetis* at the 2·03 m level. Above this level, the number of findings per $10m^2 \times 5cm$ decreases slowly until the upper end of the excavated section. The permanent occurrence of fishes throughout the Vallecillo section indicates, that the surface waters were constantly oxygenated.

Both ammonites and inoceramids show a slight increase in abundance and diversity above the Cenomanian-Turonian boundary level. This may correspond to a short interval of improved conditions (e.g. oxygenation of the waters below the surface). The recorded assemblages during the lower *P. flexuosum* zone impoverish again; they may indicate specialized low diversity faunas in an unfavourable environment.

Above this level, the abundances of ammonites and inoceramids differ markedly. The abundance of ammonites increases further at the 2·2 m level, which is the abundance maximum of *P. flexuosum*, whereas the abundance of inoceramids remains low. This may indicate another phase of improved conditions such as better oxygenation in the upper water levels in the upper *P. flexuosum* zone, supported by an abundance maximum of the surface dweller *Rhynchodercetis*. *P. flexuosum* has its only occurrence in the Rock Canyon section, the GSSP of the Cenomanian-Turonian boundary, at approximately this level (Figure 8.5), which may correspond to its widest distribution in the Western Interior Seaway during the early Turonian. In Vallecillo, ammonites are more abundant in these layers, but not more diverse. Improved, (fully oxygenated?) conditions at the surface may thus have been a local or regional phenomenon, but without migration of species between the continents. Benthic inoceramids remain rare and could not benefit from these short-term favourable conditions in the upper *P. flexuosum* zone in the same way as the nektic taxa.
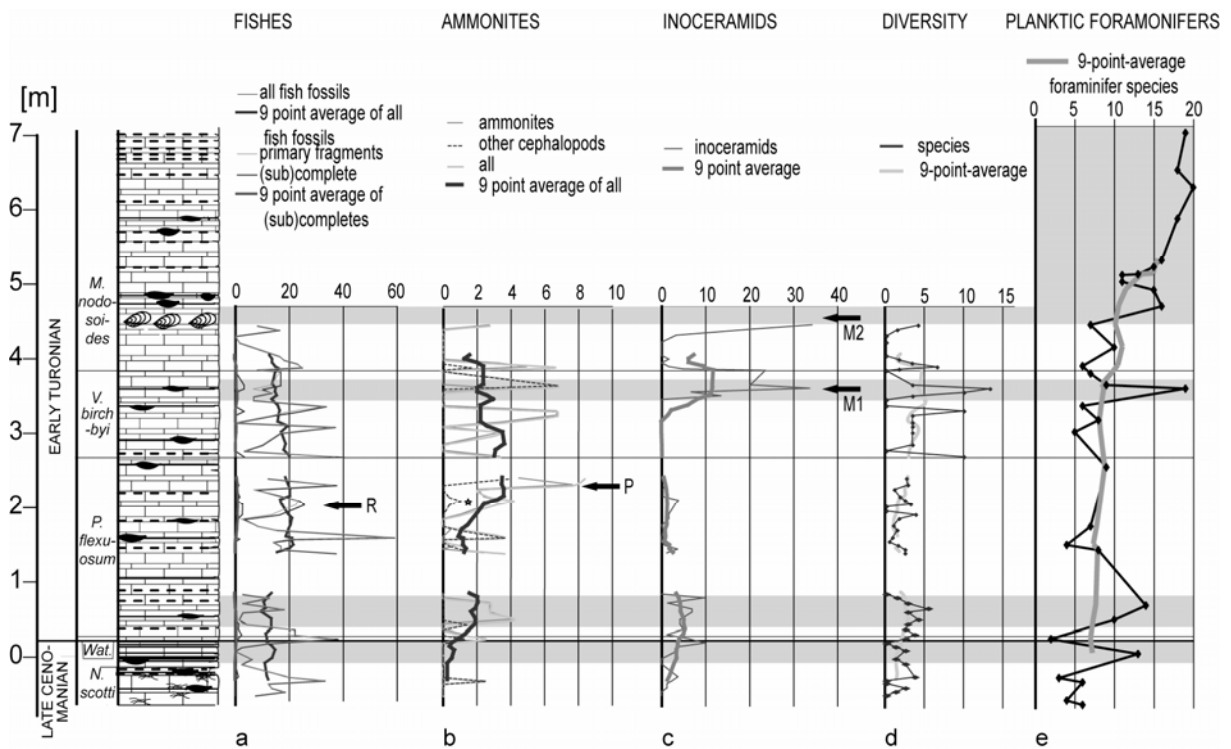
Figure 9.8. Comparison of the abundances and diversity of fossils over the Vallecillo section. a: Abundance of fishes. R: abundance maximum of *Rhynchodercetis*. b: Abundance of ammonites and undetermined cephalopods. The asterisk marks the *Palaeoctopus*. P: maximum abundance of *P. flexuosum*. c: abundance of inoceramids over the Vallecillo section. M1: abundance maximum of *Mytiloides*. M2: flood occurrence of *Mytiloides*. d: diversity of macrofossils over the Vallecillo section. e: diversity of planktic foraminifers. Grey shades indicate levels with >10 planktic foraminifer species recorded.

P. flexuosum becomes scarce above this level, but new ammonite species appear, e.g. *Vascoceras birchbyi*, and the abundance of ammonites remains approximately continuous. In contrast, inoceramids are rare for much of the early Turonian, until the first maximum in abundance in the upper *Vascoceras birchbyi* zone. *Mytiloides kossmati* immigrated into the Vallecillo area in these levels, probably by transportation of larvae by oceanic currents. Its FA coincides with a first increase in diversity, size and abundance of foraminifers. Inoceramids and foraminifers are rare between this level and the base of the flood occurrence of *Mytiloides* in the early *Mammites nodosoides* zone. Foraminifers are increase in size, abundance and diversity from this level on. Unfortunately, statistical data do not yet exist for the uppermost 2·3 section metres for macrofossils.

The distribution of inoceramids from the statistical data collection is apparently independent from that of ammonites. In fact, is resembles the distribution of planktic foraminifers (Figure 9.8). The low diversity and abundance and the small size of latest Cenomanian and early Turonian planktic foraminifers was interpreted to reflect the low oxygenation of the water levels they inhabit (Keller *et*

al. 2001). The diversity was taken here as a measure for the abundance of the foraminiferal assemblage, because it can be best compared to data from other publications.

Planktic foraminifers show four peaks in diversity in the Vallecillo section (Figure 9.8). The first diversity peak at 0·05 m section correlates with the FA of *Mytiloides hattini*. The second peak in diversity of planktic foraminifers parallels the short co-occurrence of the three inoceramid species *I. pictus*, *M. hattini* and *M. puebloensis* (compare Figures 8.3 and 9.8). The abundance maximum of inoceramids at 3·7 m section correlates with the third peak in diversity of planktic foraminifers. The planktic foraminifer *H. helvetica* and the inoceramid *M. kossmati* have their FA in this bed. The base of the flood occurrence at 4·5 m is also paralleled by a diverse foraminifer assemblage. Rocks from levels with foraminifer assemblages low in diversity also contain few inoceramids in mostly monospecific assemblages.

The diversity of planktic foraminifers seems thus closely associated with the abundance and/or diversity of inoceramids. This may be related to the planktonic larval stage of inoceramids (Harries *et al.* 1996). In recent invertebrates, small larval size typically correlates with high adult fecundity, and small larvae must feed on plankton and grow in the plankton for weeks to months before reaching a size that is competent to settle. This may lead to extensive dispersal on currents (Lindquist 2002). Benthic inoceramids were ecologically very tolerant (Harries *et al.* 1996). Their abundance and diversity may have depended on recruitment patterns. Recruitment is the survival of the larval stage and potential establishment in the benthic community. A strong dependence of the composition of benthic invertebrate communities on recruitment patterns, more than on environmental factors, was discussed by Taylor (2003, pp. 31-33). Apparently, the recruitment rate was very low among inoceramids during most of the early Turonian at Vallecillo, although settled inoceramids lived and grew at the Vallecillo sea floor. Sessile inoceramids are interpreted to have harboured symbionts (MacLeod and Hoppe 1992); only symbiosis would have allowed these bivalves to exist in the anoxic habitat of Vallecillo. Their larvae, in contrast, may have lived in the plankton. Recent marine invertebrates either release their symbionts into the environment, and the larvae must acquire them by devouring, such as in the recent hydrothermal vent tube worm *Riftia pachyptila* (Cary *et al.* 1993), or they transmit their symbionts to their offspring (=vertical transmission) such as e.g. the recent *Solemya reidi*. But even in vertical transmission, symbionts are incorporated as a post-metamorphosis event (Cary 1994). Planktotrophic larvae have thus different ecological requirements than their symbiontic parents. The same may have been true for inoceramid larvae. The parallel changes in the diversity of foraminifers and the abundance and/or diversity of inoceramids at Vallecillo (Figure 9.8) supports the presence of long-living planktotrophic larvae of inoceramids, as suggested by Harries *et al.* (1996), and indicates, that the ecology of these larvae was similar to that of planktic foraminifers. In conclusion, planktotrophic inoceramid larvae may have inhabited similar oxygenated water levels as planktic foraminifers, and may have depended on similar ecologic constraints. Combined faunal changes in foraminifers and inoceramids similar to Vallecillo were observed in the Rock Canyon

section, the Cenomanian-Turonian GSSP, and, as far as comparable, at Eastbourne (see Figure 8.5). The abundance of inoceramids in Vallecillo does thus not depend on environmental conditions at the sea floor, but on recruitment.

The dependence of inoceramid larvae on oxygenated water levels provides an explanation for the paradox, why inoceramids, which apparently could exist under the anoxic conditions of the Vallecillo sea, became almost extinct by OAE 2. *Inoceramus pictus* was the only species that survived into the latest Cenomanian (Voigt 1996). The Vallecillo data indicate that the expanded oxygen minimum zone affected the planktotrophic larval stage of inoceramids in a similar way than planktic foraminifers.

The response of ammonites to the changing conditions in the latest Cenomanian to early Turonian differs from that of inoceramids and planktic foraminifers with the exception of the minor peak in abundance above the Cenomanian-Turonian boundary. Ammonites and/or their larvae may either have lived in shallower water levels than foraminifers, or they tolerated lower oxygen levels.

10   THE CENOMANIAN-TURONIAN TRANSITION IN NORTH-EASTERN MEXICO

In the Vallecillo quarries, the upper and lower limit of the Vallecillo Member were not identified with certainty. Another outcrop area was required that allows to study sediments preceding the Vallecillo *Plattenkalk*, in order to explain which conditions led to the change in lithology. Additional fieldwork was hence carried out in a section at Las Mitras, a suburb of Monterrey.

10.1   THE LAS MITRAS SECTION

10.1.1 Introduction

The section named Las Mitras includes the late Cenomanian to early Turonian and is situated at the highest point of Boulevard Rogelio Cantú Gómez at 25°43,39'N and 100°21,20'W (Figure 3.2). This road is reached via highway (*carretera*) 40, which connects the city of Monterrey to Saltillo, by crossing the railway and the Rio Santa Catarina northward at the Colonia del Valle.

The sediments west of Monterrey are folded in the uprising Sierra Madre Oriental, to which they belong. The Las Mitras mountain represents an anticline, shaped by an isoclinal fold with vertical limbs on each side (Gray and Johnson 1995, p. 11). The Las Mitras outcrop is situated on the eastern flanks of the anticline where Cretaceous layers are exposed vertically.

The Indidura Formation and the Vallecillo Member of the Agua Nueva Formation crop out there in a 34 m thick section of vertically exposed layers (Figures 3.4, 10.1). The conformable contact between the Indidura Formation and the underlying Cuesta del Cura Formation is present, estimated 100 m downsection, uphill in the steep eastern slope of the Las Mitras Mountain. The conformable contact to the overlying San Felipe Formation lies downhill and crops out in a road cut, found by following the Boulevard Rogelio Cantú Gomez northwards.

Schistosity is recognized in all sediments. It is weak in limestones and sandy limestones and much stronger in shales. These weather to intersection pencil structures, which are angular, elongated, cm-thick fragments, typical of anchimetamorphous overprint. Their shape is defined by the bedding-cleavage relationship (Durney and Kisch 1994; in Merriman and Peacor 1999).

Inoceramids were found throughout the section, but no determinable specimens could be recovered from the section. An undetermined fragment of a fish jaw was found at 20·10 m section.

10.1.2 The Indidura Formation

Part of the Indidura Formation is exposed in the lower 22·20 m of the Las Mitras section. It consists of bedded, partially laminated, micritic limestone and minor sandy limestone, with intercalated thin (<5 cm) layers of siltstone and shale. The limestones of the Las Mitras section are black when fresh, but weather to bright grey colours. The siltstones and shales are brown through the presence of small

amounts of goethite. Limestones between 0 and 1 m section, at 11 m section, and at 14·5 m section are bioturbated. At 10·0 m and 18·5 m section, sandy limestone layers contain cross bedding. The presence of coarse siliciclastic detritus assigns these layers to the Indidura Formation (Schoenherr 1988; Seibertz 1998, and Chapter 3.2).
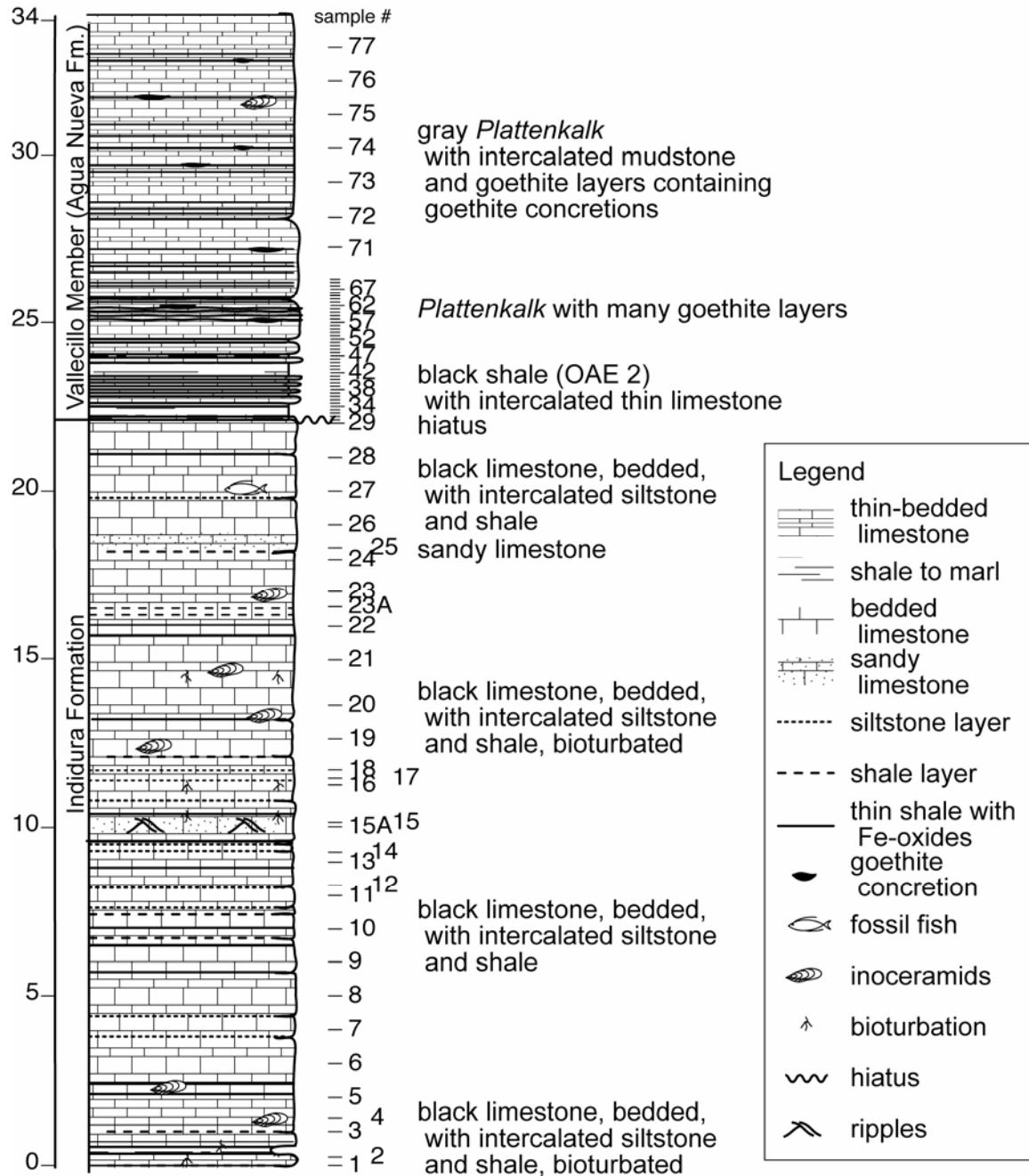
Figure 10.1. The Las Mitras section, with samples and explanation of lithology.

10.1.3 The Vallecillo Member

At 22·20 m section, an abrupt change in lithology is recognized from Indidura limestone towards shale, marking a probable hiatus at the base of the black shale. This unit marks a global marine anoxic

phase during the late Cenomanian, associated with widespread deposition of black shale and organic matter. This conspicuous interruption of carbonate deposition occurs at global scale and linked to OAE 2 (Schlanger *et al.* 1987). The black shale is here regarded base of the Vallecillo Member.

Upsection, a gradual increase of thin limestone beds, intercalated with the shales, is observed. This decrease in black shale and increase in limestone leads to a continuous sequence of thin-bedded, marly, finely laminated *Plattenkalk* above the 24·40 m level. This *Plattenkalk* has a thickness of approximately 9·5 m. Thin layers of Fe-rich mudstones are intercalated with the *Plattenkalks*. Some of them contain layers and concretions of Fe-oxides, mostly goethite. Cubic pseudomorphs in the centre of the concretions indicate oxidation of pyrite. The *Plattenkalk* between 25·0 and 25·5 m section is particularly rich in thin goethite layers. The absence of coarse clastic components assigns this member to the Agua Nueva Formation (Schoenherr 1988; Seibertz 1998, and Chapter 3.2).

The rocks exposed in the Las Mitras section were originally rich in organic matter and are bleached by weathering. This interpretation is supported by the presence of black sediments in fresh road cuts through the upper part of the section.

At present, a precise correlation between the Vallecillo and the Las Mitras sections is unclear. The thick limestone that is intercalated into the upper black shales at 24·5 m section likely corresponds to the basal limestone of the Vallecillo quarries, whereas the interval rich in goethite layers around 25·2 m section may correlate with goethite layers present above the thick mudstone layer near the base of the Vallecillo section.

10.1.4 Microfacies analysis of the Las Mitras rocks

The limestones of the Indidura Formation are wackestones with recrystallized foraminifers, indicating deposition in a pelagic facies. The preferred orientation of bioclasts parallel to the bedding plane supports the millimetric lamination (Figure 10.2a-b). In some beds, a considerable amount of silt is present, which consists of subangular to little rounded quartz and feldspars (Figure 10.2e), indicating a proximal source of terrigenous supply.

The black shales are fine-grained with anchimetamorphous overprint (Figure 10.2c). Foraminifers are below 1 % and thus very rare or absent. Some limestones contain calcispheres, but a few transported ooids with fragmented rims (Figure 10.2f) and mudclasts composed of peloids were identified (Figure 10.2d).

Rare siltstone layers (Figure 10.2e) are intercalated in the lower black shale unit. This points towards a transitional contact between the Indidura- and the Agua Nueva Formation in the Las Mitras section, despite the probable hiatus at the base of the shale unit. Considerable terrigenous (mudclast, siltstone) and coastal (ooids) material was supplied from a near-by coastal environment during black shale deposition.
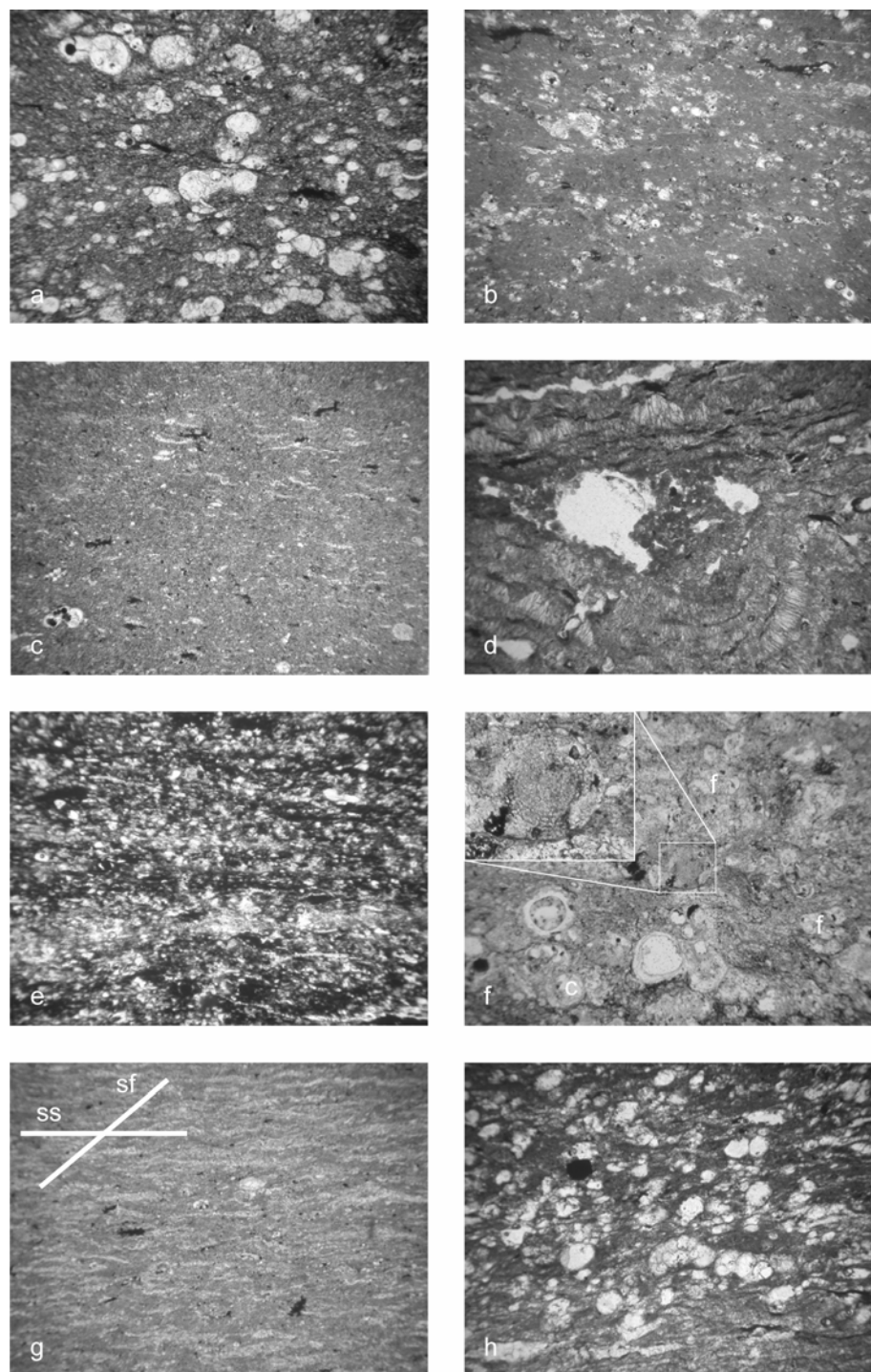
Figure 10.2. Microfacies of the Las Mitras section. a-b: the Indidura Formation. a: wackestone. MT-2. b: wackestone. MT-8. c-f: the black shale unit in the Vallecillo Member. c: mudstone. MT-29. d: mudclast indicating terrigenous influx into the Las Mitras area. MT-30. e: one of the last siltstone layers is intercalated with the black shales. MT-33. f: wackestone with an isolated ooid (zoomed) and badly preserved calcispheres (c) and foraminifers (f). MT-35. g-h: the *Plattenkalks* of the Vallecillo Member. g: marly mudstone, with bedding (ss) and slight schistosity (sf) visible. MT-73. h: marly wackestone with abundant, large-sized foraminifers. MT-76. All are ×25.

The marly limestone of the Vallecillo Member is similar in microstructure to the Vallecillo *Plattenkalks* (Figure 5.3). They are laminated mud- to wackestones, with foraminifers, calcispheres and recrystallized radiolarians.

Clay minerals in the marly *Plattenkalk* are recrystallized with preferred orientation at an angle of about 40° to the layers. This microscopic schistosity is present even in carbonates (Figure 10.2g). Oriented clay minerals show extinction under crossed polars at the same angle. Upsection, mudstone poor in foraminifers is replaced by wackestone with abundant large-sized foraminifers, similar to the Vallecillo section (Figure 10.2h).

10.1.5 X-ray diffractometry

The composition of rocks from the Las Mitras section is variable due to the different lithologies present (Figure 10.3 and Appendix A). The most abundant mineral is calcite (39 wt% to 75 wt%), except in intercalated siltstone (4 wt%). Phyllosilicates are present with contents between 4 wt% and 46 wt%. Further minerals identified are plagioclase (up to 27 wt%), alkali feldspar (up to 8 wt%) and Fe-minerals (up to 2 wt%).

Calcite is of biogenous origin and evenly distributed in limestones and marly *Plattenkalks*. Phyllosilicates and feldspars are more abundant in the lower part of the section and less abundant in the upper part. This contrasts the distribution of quartz, which is almost absent in samples from the lower section, but increases remarkably in relative abundance shortly before the black shale. It thus opposes feldspars and phyllosilicates in behaviour. Fe-minerals are also present in abundances comparable to the Vallecillo section. Their distribution is independent from the other minerals.

Although small amounts of alkali feldspar were detected in the random powder samples almost throughout the section, it was not found in the fraction 2 to 16 μm (see Appendix A). Clay minerals are variable in their distribution in this fraction. IlliteSmectite is the most abundant clay mineral with quantities between 7 wt% and 78 wt%. ChloriteSmectite is less abundant and was detected in amounts of 1 to 73 wt% throughout the section, but forms the major component with a quantity of 93 wt% in a single bed at 25·6 m section. Its distribution over the Las Mitras section is more variable than that of silicic minerals. ChloriteSmectite has a peak abundance in the middle exposed Indidura Formation at 15·0 m section, and another at the transition form the black shale into the *Plattenkalk* at 25·0 m section. However, this clay mineral is almost absent before and after both peaks. This behaviour thus opposes that of IlliteSmectite. Kaolinite was found in minor abundances (up to 13 wt%) in samples from the lower and upper part of the section, but it is absent in the samples between. It roughly correlates with IlliteSmectite, with the exception of the black shales.

Clay minerals from the <2μm glycolated fraction are dominated by illite of the $2M_1$-polytype, with contents between 15 wt% and 98 wt%. Chlorite is present in quantities of up to 85 wt%. An expandable 14Å-phyllosilicate was identified in amounts up to 18 wt% in rocks from the lower part of

the section and in the Vallecillo Member. It replaces chlorite reaching 57 wt% in a single sample at 22·10 m. Kaolinite was not identified in this fraction.

Although the distribution of clay minerals from Las Mitras appears to be similar to Vallecillo at first glance, it cannot be compared to it. Schistosity observed in outcrop and thin section analysis indicates a metamorphous overprint, supported by an average illite crystallinity of 0·33 °Δ2θ. This value indicates that deepest burial was in the low anchizone (Merriman and Peacor 1999) with a maximum burial temperature of approximately 250°C (Merriman and Frey 1999). This interpretation is supported by the presence of the 2M$_1$-illite, which first develops in the anchimetamorphous zone.
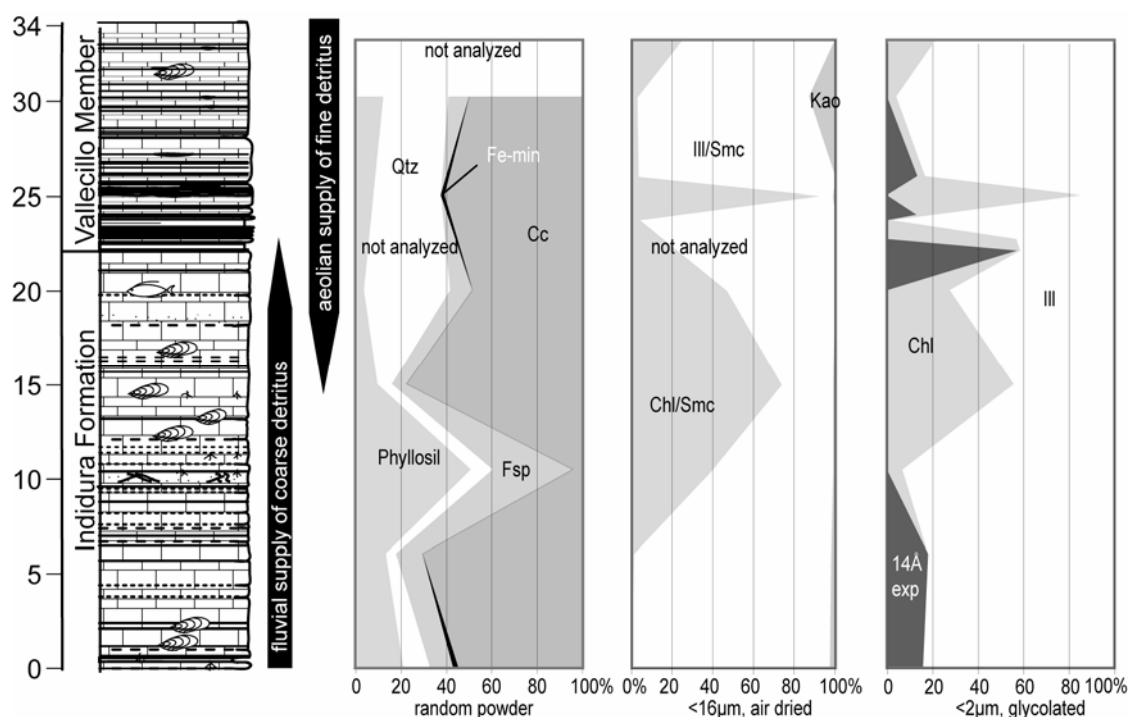
Figure 10.3. Mineralogy of the Las Mitras section, with interpretation of the detrital influx. For abbreviations see Figure 5.5 except 14Åexp: expandable 14Å-clay mineral.

The peaks of the expandable 14Å clay mineral in the <2µm glycolated sample are not reflected in the diffractogram of the 2 to 16µm fraction, whereas the distribution of illite and chlorite is mirrored in both fractions, indicating that these phyllosilicates are recrystallized to large crystals. Expandable 14Å clay minerals may be present to smaller amounts as, e.g., corrensite-chlorite interlayered clay mineral in the early anchizone (Merriman and Peacor 1999), or they may be present as small crystallites in Las Mitras rocks, extant from previous recrystallization phases.

The *Plattenkalk* in Las Mitras is similar in composition to the rocks exposed at Vallecillo. Although the clay minerals are recrystallized and cannot be compared to the Vallecillo *Plattenkalks*, the carbonaceous, silicic and ferrigenous components are similar in distribution. The amounts of calcite are comparable, and quartz is the dominant silicic mineral in the *Plattenkalk*.

In the Las Mitras section, this is different in sediments preceding the black shale. Feldspars and phyllosilicates are the dominant silicic minerals in most of the Indidura sediments, and quartz is present in much smaller quantities. Two metres below the onset of black shale deposition, there is a change in silicic sediment supply, and quartz dominates the detrital component from the 22·0 m level to the upper end of the section. This change does not coincide with the cease in supply of coarse siliciclastic detritus, because the last silt beds are present at 22·4 m section in the basal black shale unit. This points to a gradual change in the supply of detritus, probably from fluvial (coarse siliciclastic) to aeolian (quartz in fine-silt fraction) transport of siliciclastic minerals into the Las Mitras area.

10.1.6 Main and Trace Elements

The distribution of elements over the Las Mitras section is more variable than in the Vallecillo sediments (Chapter 6), and the correlation of elements, visualized by cluster analysis (Figure 10.4a-b) is more difficult to interpret.

Sr and Ca have a common biogenic source, indicated by their excellent correlation. Rb, Zr and Ba are elements of mainly detrital origin and correlate very well. Zn was also included into the detrital group. Pb and Ga correlate well; Pb substitutes K in feldspars, whereas Ga substitutes Al. They may both be included in the feldspars detected by XRD. Pb is present at considerably lower concentrations than in Vallecillo rocks.

Mn is present in Las Mitras at levels slightly above detection limits, indicating low oxygen conditions in the sea water (Jarvis *et al.* 2001). The sample with maximum concentration is the lowest in the column (Appendix B), indicating oxic conditions above the sea floor for this sample only.

The group of chalcophile elements is particularly represented by Fe and Cu in the dendrograms. This is especially clear, when the Fe-rich samples are included in the analysis (Figure 10.4b). Pb element must be included into the elements of biogenic origin by correlation. Pb correlates best with Fe in the Vallecillo samples (Chapter 6.2). However, an XY-plot of Fe and Pb (Figure 10.4c) reveals, that the correlation between Fe and Pb is better than the cluster analysis suggests, and the grouping with biogenic elements is probably a statistical artefact.

Chalcophile elements are generally enriched in the black shale and the Fe-rich layer analyzed (Appendix B). However, their behaviours differ in both lithologies, resulting in a bad correlation. This can be visualized in XY-plots and is particularly reflected by Ni. This element was detected at elevated concentrations, particularly in the black shales (Figure 10.4c and Appendix B). It correlates with Pb, with the exception of the Fe-rich sample from the *Plattenkalk* that distorts the correlation to a behaviour similar to Ti (of predominantly detrital origin) and Y (from phosphates and/or clay minerals). The XY-plot of Ni against Pb can also be interpreted as reflecting two different correlations (Figure 10.4c). Ni seems thus supplied by two different processes in the black shale unit and the Fe-rich mudstones of the Vallecillo Member. A similar pattern is reflected by plotting Fe against As.

Ti and Y oppose Ca and Sr in behaviour, similar to Ni. They are probably of multiple origin in the variable lithology of the Las Mitras section, because they correlate with chalcophile elements in the non-Fe-rich lithologies, but with elements of detrital origin, if the Fe-rich samples are included (Figure 10.4). A similar multiple correlation is shown by the chalcophile As and Cd, and the REE La and Ce. REE may have been enriched originally in phosphates, which were later replaced by another mineral.
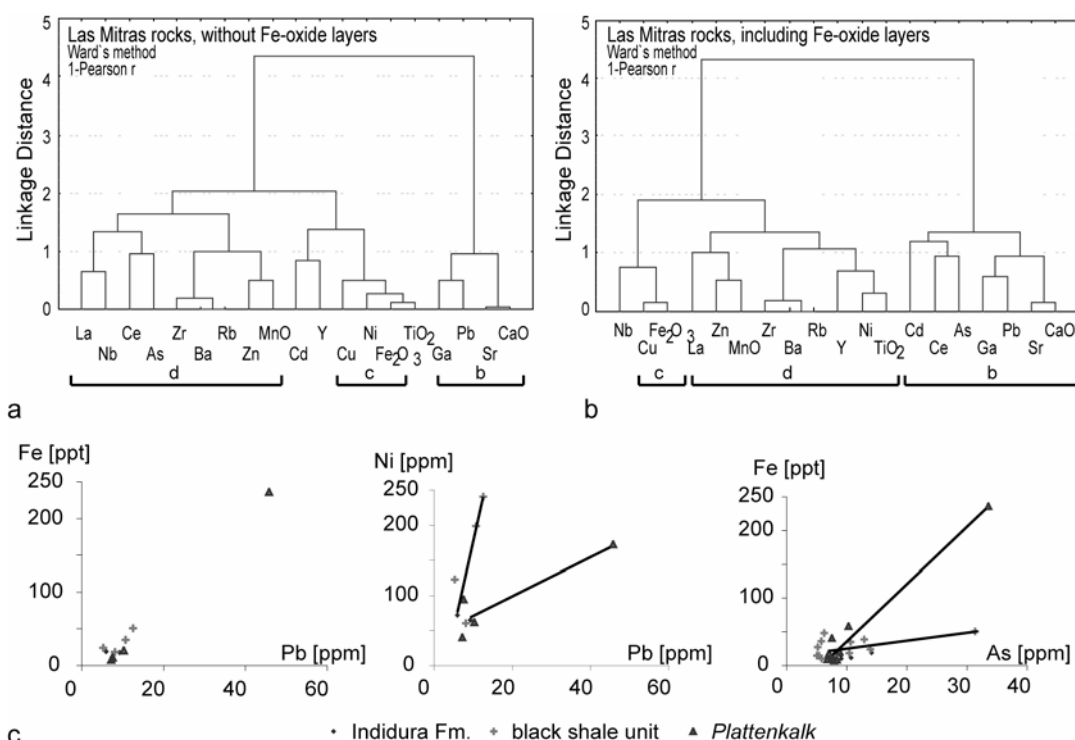
Figure 10.4. a-b: Cluster analysis of main and trace elements from the Las Mitras section. Linkage distance below 1 is a good correlation (d: elements of detrital origin. c: chalcophile elements. b: elements accumulated by biogenic processes). a: only samples with Fe-content below 10% were included. b: Cluster analysis of main and trace elements including the Fe-oxide layers. Chalcophile elements behave different from the elements of detrital or biogenic origin. Some elements are of multiple origin, as they correlate with two different groups in each analysis. c: XY-plots of selected chalcophile elements from Las Mitras rocks. Samples include mudstones rich in Fe-oxides.

Three basic processes of accumulation could be extracted from the data: a biogenic, a detrital origin, and the accumulation of chalcophile elements. The considered elements cannot be grouped as clearly as in the Vallecillo samples. This reflects the different lithologies present in the Las Mitras section, but also the change in supply of detritus, interpreted from the XRD data (Chapter 10.1.5). It is remarkable that the behaviour of some chalcophile elements in the black shale unit differs from their behaviour in the Fe-oxide layers of the *Plattenkalks*.

Low oxygen conditions are indicated by Mn and Ni for most of the section, with the exception of the lowest sample. This contradicts the hypothesis that only the black shale event marks anoxic

conditions (Schlanger and Jenkyns 1976). Apparently, hostile conditions existed above the sea floor before and after this event unit, and that the black shale reflects only the climax of the OAE 2.

10.1.7 Foraminiferal stratigraphy at Las Mitras

Figure 10.5 gives an overview of foraminifers identified from thin sections, whereas their ranges are presented in Figure 10.6. Three biozones were recognized at Las Mitras, indicating late Cenomanian to early Turonian age.

The late Cenomanian *Rotalipora cushmani* biozone was identified throughout the lower 19·2 m section This zone was subdivided into three subzones: the *P. praehelvetica*, *A. multiloculata* and the *Rotalipora* extinction subzone. The *Rotalipora* extinction subzone of the *R. cushmani* zone is expanded in Las Mitras, as compared to the GSSP and other localities (compare Keller and Pardo 2004, and Figure 8.1). This may be an artefact and result from bad preservation of foraminifers from the anchimetamorphous sediments at Las Mitras, in consequence, foraminifers such as the rare *A. multiloculata* may not have been recognized in samples above its registered LA.

The *Whiteinella archaeocretacea* zone reaches from 19·2 m to 21·0 m section and spans the Cenomanian-Turonian boundary (e.g. Keller *et al.* 2001; Keller and Pardo 2004). It was subdivided into tree subzones, starting with the *Globigerinelloides bentonensis* subzone from 19·2 m to 21·0 m section. The LA of *G. bentonensis* defines the base of the subsequent *Dicarinella hagni* subzone at 21·0 m section; this subzonal boundary is well defined at Las Mitras, because *G. bentonensis* is abundant in the sample before its LA. The *Dicarinella hagni* subzone ends at 25·0 m with the *Heterohelix* shift, a faunal turnover in the foraminiferal community which was recognized at global scale. Low oxygen tolerant biserial *Heterohelix* species dominate the assemblage and are indicative of the *Heterohelix moremani* subzone (Keller and Pardo 2004).

The *Heterohelix* shift is weakly expressed and appears delayed in the Las Mitras section, in comparison with the GSSP in Colorado (compare Figures 8.1 and 10.6, and Keller and Pardo 2004). Hedbergellids, whiteinellids and heterohelicids are dwarfed (mostly around 50μm) in the upper *D. hagni* subzone of Las Mitras, so that the *Heterohelix* dominance can be identified only in the large size assemblage of sample 58 at 25·0 m section. Impoverished dwarfed assemblages are also present in several samples above the critical sample. However, few samples show strong dominance of the nominate genus and contain large whiteinellids. In consequence, the record of the *H. moremani* subzonal boundary may be delayed, with an expanded *Dicarinella hagni* subzone is in Las Mitras and a short *H. moremani* subzone in comparison with the GSSP and other localities.
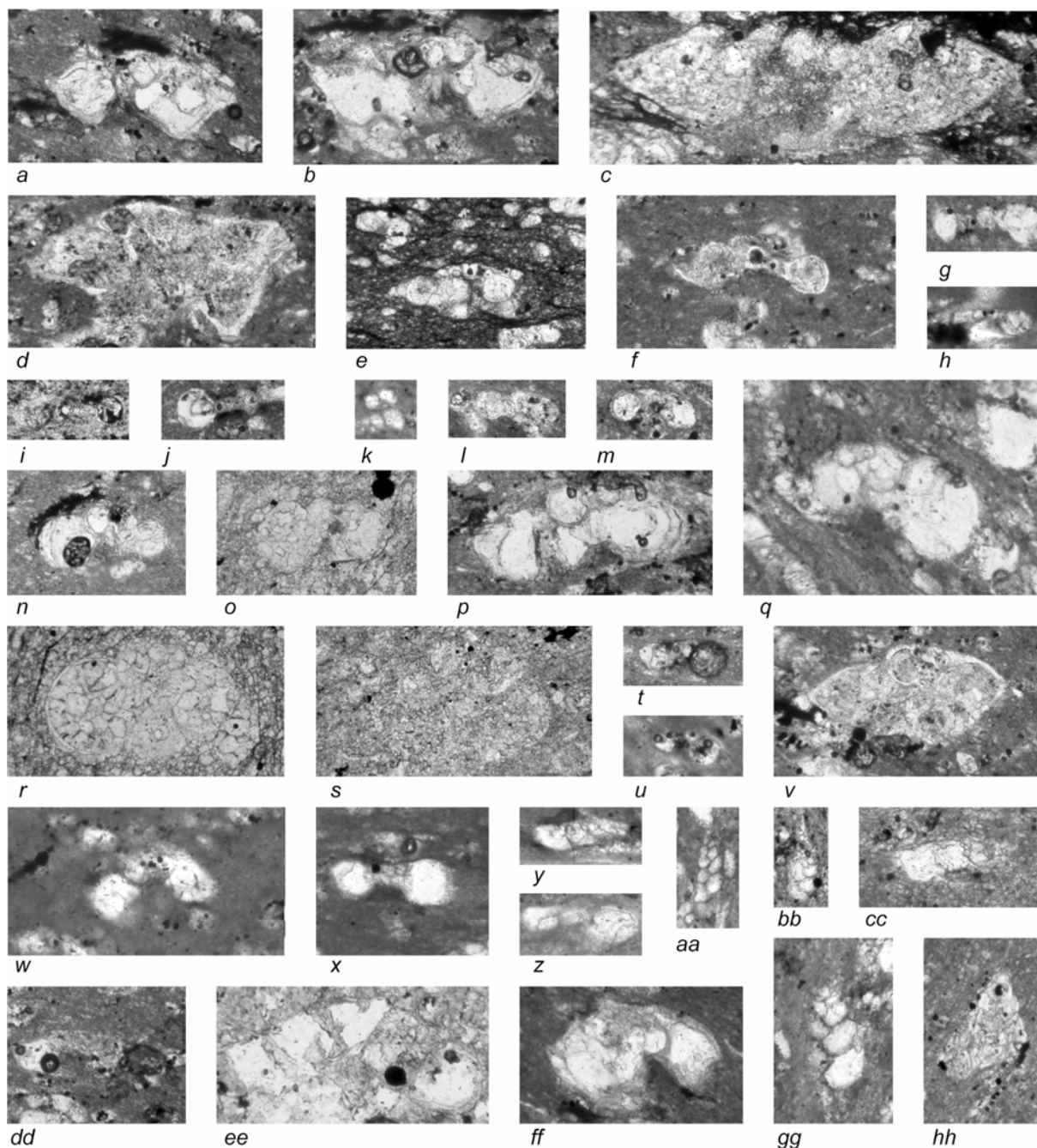
Figure 10.5. Planktic foraminifers identified from thin sections of Las Mitras. a: *Rotalipora cushmani.* **MT-8. b:** *R. greenhornensis.* **MT-8. c:** *R. montsalvensis.* **MT-2. d:** *R. deekei.* **MT-8. e:** *Anaticinella multiloculata.* **MT-2. f:** *Hedbergella delrioensis.* **MT-8. g:** *Hed. planispira.* **MT-25. h:** *Hed. planispira.* **MT-18. i:** *Globigerinelloides ultramicra.* **MT-56. j:** *Gl. bentonensis.* **MT-23A. k:** *Hed. simplex.* **MT-71. l:** *Hed. hoelzli.* **MT-8. m:** *Whiteinella archaeocretacea.* **MT-23A. n:** *W. aprica.* **MT-8. o:** *W. baltica.* **MT-13. p:** *W. archaeocretacea.* **MT-8. q:** *W. paradubia.* **MT-76. r:** *W. brittonensis.* **MT-13. s:** *W. brittonensis.* **MT-21. t:** *Praeglobotruncana aumalensis.* **MT-23A. u:** *P. aumalensis.* **MT-18. v:** *P. inornata.* **MT-8. w:** *P. gibba.* **MT-25. x:** *P. praehelvetica.* **MT-24. y:** *P. stephani.* **MT-24. z:** *Helvetoglobotruncana helvetica.* **MT-74. aa:** *Heterohelix moremani.* **MT-70. bb:** *Het. reussi.* **MT-28. cc:** *H. helvetica.* **MT-71. dd:** *Dicarinella algeriana.* **MT-8. ee:** *D. hagni.* **MT-35. ff:** *D. imbricata.* **MT-24. gg:** *Het. globulosa.* **MT-70. hh:** *Guembelitria cenomana.* **MT-8. All are ×70.**
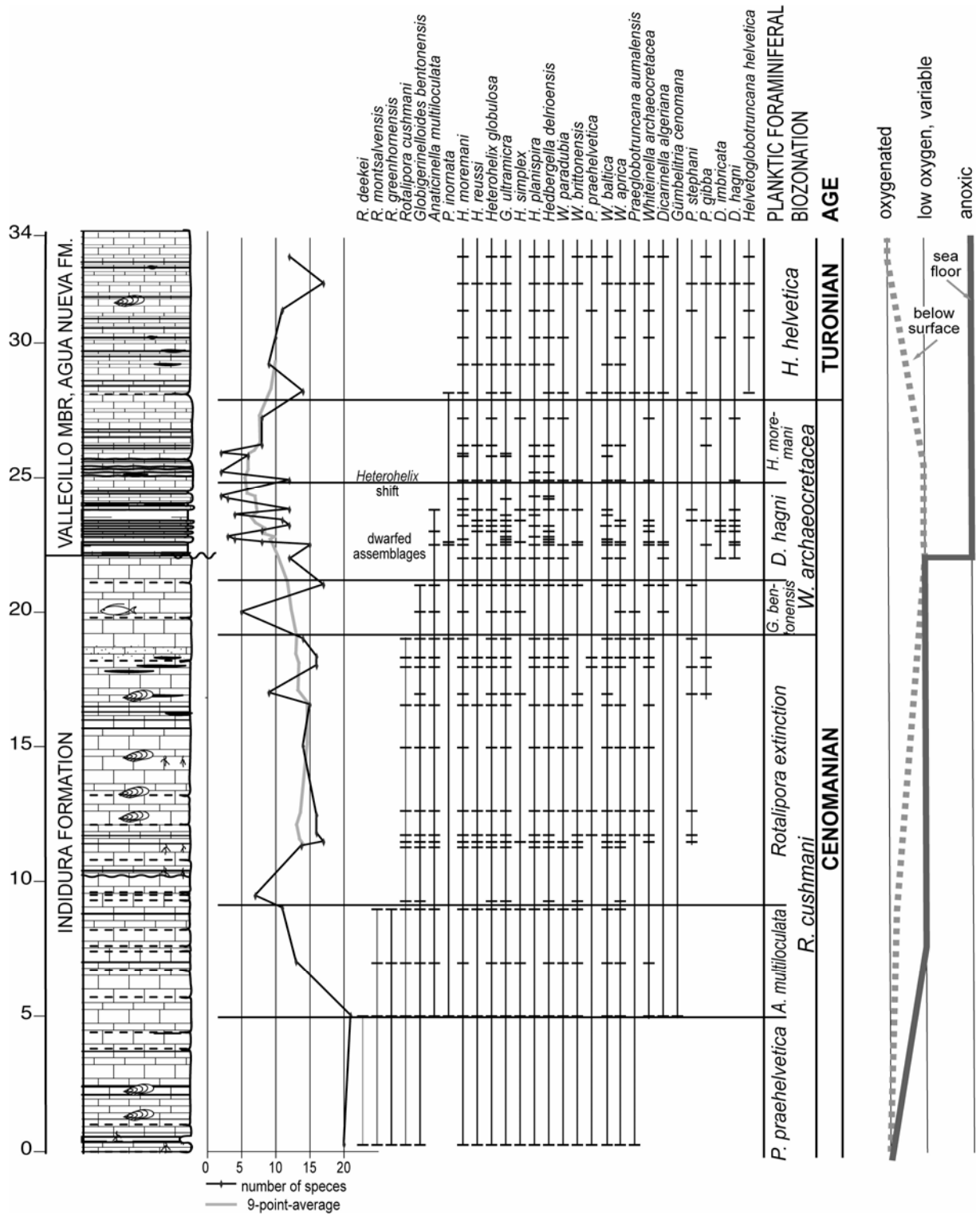
Figure 10.6. Range chart of planktic foraminifers identified from Las Mitras samples, diversity of the planktic foraminiferal assemblages and biostratigraphic subdivision of the Las Mitras section. Oxygen levels at the sea floor are roughly estimated from sedimentological and geochemical analysis, whereas oxygen level below the surface are estimated from the diversity of planktic foraminifers. "below surface" relates to water depths where keeled planktic foraminifers dwelled.

The FA of *H. helvetica* at 28·0 m ends the *Heterohelix moremani* subzone and the *W. archaeocretacea* zone. The FA of this species is generally correlated with the Cenomanian-Turonian boundary as defined by foraminifers (Keller *et al.* 2001). However, the FA of *H. helvetica* is delayed in the western Gulf of Mexico and Western Interior Seaway compared to the boreal Eastbourne section (Keller and Pardo 2004, and Figure 8.5). No transitional forms between *Praeglobotruncana praehelvetica* and the nominate species were identified at Las Mitras or Vallecillo, indicating a general absence of this microfossil in the transition between Western Interior Seaway and the western Tethys. The appearance of *H. helvetica* thus appears to be diachronous, with later immigration into the Gulf of Mexico and Western Interior Seaway, as already pointed out in Chapter 8.6.2.

The early Turonian *Helvetoglobotruncana helvetica* biozone reaches from 21·0 m to the upper end of the Las Mitras section at 34 m section.

10.1.8 Sedimentation rates of Las Mitras

Sedimentation rates calculated for Las Mitras sediments are given in Figure 10.7. The calculation of depositional rates provides an important tool to estimate the reliability of stratigraphic boundaries.
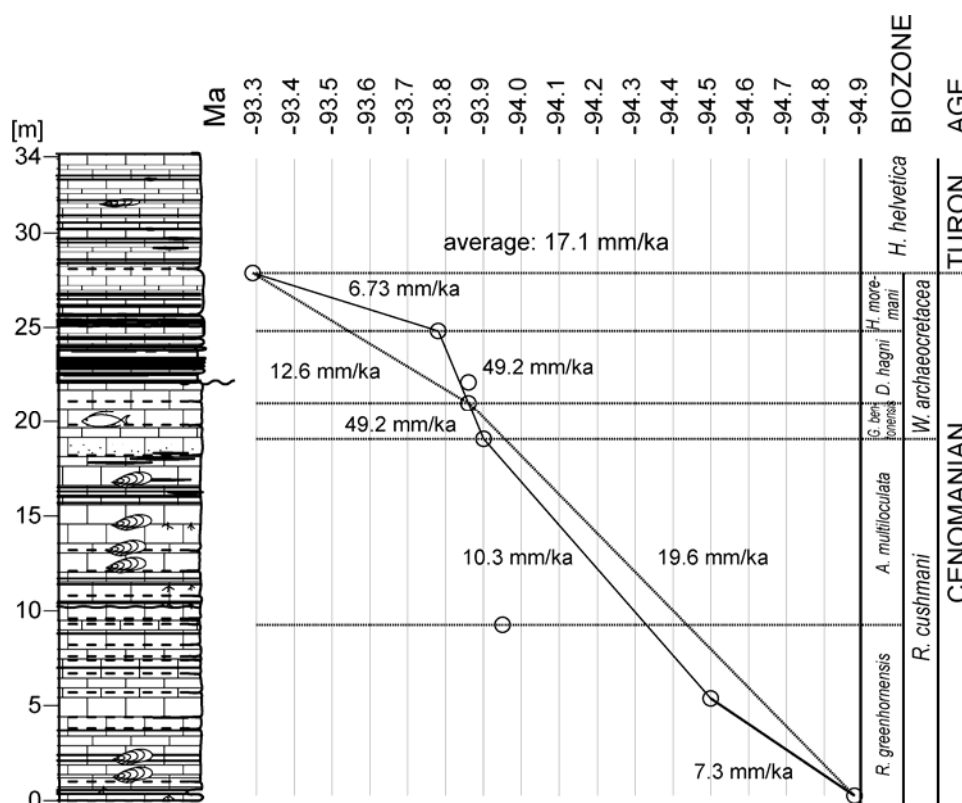
Figure 10.7. Age-depth plot of the Las Mitras section, based on planktic foraminiferal data of Hardenbol *et al.* (1998; *fide* Keller and Pardo 2004) and Keller and Pardo (2004). The thick line includes all biostratigraphic boundaries, the thin line the FA of *P. praehelvetica*, LO of *G. bentonensis* and FA of *H. helvetica*. These are considered the most reliable markers in this section.

The delayed FA of *H. helvetica* compared to the GSSP (Figure 8.5) increases the calculated value of the sedimentation rate, but this stratigraphic datum it is the only marker for the early Turonian and had to be included. Sedimentation rates are thus calculated to 19·6 mm/ka before and 12·6 mm/ka after the LA of *G. bentonensis*. The average sedimentation rate of 17·1 mm/ka is comparable to that of the Vallecillo *Plattenkalk* (Chapter 8.7). All other boundaries defined by planktic foraminifers provide unrealistic sedimentation rates, particularly for the black shale unit. Their boundary levels should therefore be regarded imprecise, although the section is stratigraphically complete.

10.1.9   Stable isotopes

Sediments of the Las Mitras section are anchimetamorphous. The $\delta^{13}C$ and $\delta^{18}O$ values show a correlation (Figure 10.8), which suggests that the pristine isotope values were altered and consequently cannot be used for environmental interpretations. The correlation of $\delta^{13}C$ and $\delta^{18}O$ values differs from the correlation of values from Vallecillo. One end-member of the correlations is similar in both sections and may reflect a primary signal, but it does not provide a realistic signal, as already pointed out in Chapter 8.8.
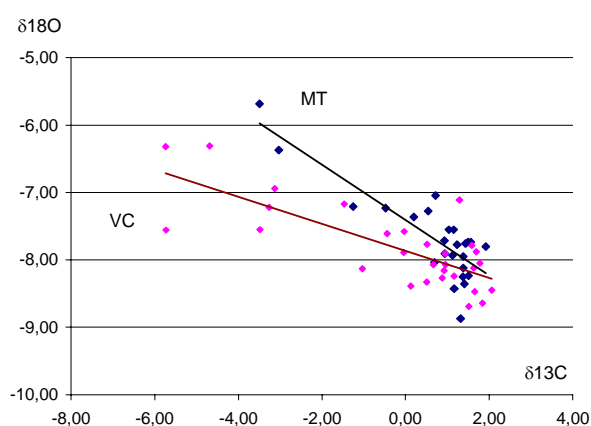
Figure 10.8. Scatter plot of stable isotope data from Las Mitras (MT) and Vallecillo (VC) shows, that $\delta^{13}C$ and $\delta^{18}O$ values correlate for both sections, but in slightly different ways.

The sediments of the Las Mitras section were deposited in an open marine facies. The influx of detritus is too low to consider the influx of meteoric waters, as interpreted at the GSSP of the Cenomanian-Turonian boundary. This section was situated in the epicontinental Western Interior Seaway (Figure 5.6), and fresh water influx from the western or eastern coast is likely there (Keller *et al.* 2004). $\delta^{13}C$-values from the Las Mitras section show a greater variation than $\delta^{18}O$ values. This suggests a late diagenetic overprint, an interpretation supported by the negative correlation of $\delta^{13}C$ and $\delta^{18}O$ values (Figure 10.8).

10.1.10   Discussion of the palaeogeography at Las Mitras

The palaeogeographic situation of Las Mitras was shown to be far from the coast in Figure 3.1, and an open marine facies was concluded from microfacies analysis. This strongly contradicts the presence of siltstone, peloidal mudclasts and fragmented ooids, identified in microfacies analysis. These components indicate the influx from shallow water or coastal matter. Peloidal mudclasts may occur in

the outer shelf environment (Flügel 2004, p. 114), but silt or ooids cannot be transported further than tens of kilometres. There must have been a nearby island or shallow water source area. The palaeogeographic map of Goldhammer and Johnson (2001, and Figure 3.1) is thus incomplete in this aspect.

During the early Cretaceous, several topographic heights existed in the vicinity of the Las Mitras area (Figure 3.1). The Coahuila Block, for instance, a Palaeozoic basement high to the northwest of Monterrey, was covered by carbonates of the Aurora Platform until the Cenomanian. However, this submarine topographic height was mostly blanketed by the calcareous Agua Nueva Formation during the late Cenomanian and Turonian (Goldhammer and Johnson 2001). The Tamaulipas Arch to the southeast of Monterrey, another Palaeozoic basement high (Goldhammer and Johnson 2001), is recognized during the Cenomanian-Turonian by a facies change, but sediments in this region include laminated limestone, limy shale and claystone (Seibertz 1998) and not coarse siliciclastic rocks or ooliths. Both submarine topographic heights were covered with pelagic sediments during the late Cenomanian transgression which indicates a smoothened submarine relief. These topographic heights were not the source areas of the silty or oolithic components.

The palaeogeographic reconstruction of Seibertz (1998) includes the Altiplano Platform in central Mexico, which corresponds to the outcrop area of the Indidura Formation. This author noted the change from the distal facies of the Agua Nueva Formation towards a more proximal facies in the Indidura Formation. However, the topographic height of the Altiplano Platform is interpreted solely from facies change and may not correspond to a Palaeozoic basement high. Islands are included on the Altiplano Platform by this author; they are a probable source for the ooids. However, this palaeogeographic reconstruction of northern Mexico does not yield a source area for the siliciclastic sediments. To the contrary, in this reconstruction, the Altiplano Platform is separated from the Alisitos Magmatic Arch, the only possible source area for siliciclastic sediments in this region, by a deep marine depression. However, this depression was filled with volcaniclastic flysch during the early late Cretaceous (Goldhammer and Johnson 2001, and Figure 3.1), and the reconstruction of Seibertz (1998) is thus incomplete in this aspect. The most probable source for the siltstone is regarded here the Alisitos Arc, with the siltstones representing the most distal sedimentation of clastic sediment eroded there.

The influx of (?fluvially eroded) terrigenous clastic material ceased shortly after (and not with) the onset of black shale deposition. The delay between the change in the silicic mineral composition towards aeolian sediments and the last siltstone layer (Figure 10.3) indicates, that the change in the sedimentary source was gradual. It is explained by a rise in sea level; a first order transgression is known to have occurred during the late Cenomanian and the early Turonian, with the maximum sea-level during the late early Turonian (Haq *et al.* 1987). This transgression may have drowned the source area of the clastic component. This transitional change in sediment source points to a very short lag of

time included in the probable hiatus at the base of the black shale unit, supported by the complete planktic foraminiferal biozonation of the Las Mitras section.

10.2   THE CENOMANIAN-TURONIAN ANOXIC EVENT IN NORTH-EASTERN MEXICO

The Vallecillo Member is present in both the Las Mitras and the Vallecillo sections. These sections are 100 km apart, which shows that the Vallecillo *Plattenkalks* are a regional phenomenon. In the Vallecillo section, with its lower diagenetic influence, the formation of the *Plattenkalk* was studied in detail, whereas sediments preceding the formation of the *Plattenkalk* were studied at Las Mitras.

During the late Cenomanian, normal marine sedimentation prevailed in north-eastern Mexico, indicated by the monotonous limestone-marl alternation of the Agua Nueva Formation in deep basinal areas and the Indidura Formation in more proximal facies. During the late Cenomanian *A. multiloculata* biozone, the waters above the sea floor depleted in oxygen. The successive extinction of deep-dwelling foraminifers indicates further increase of the oxygen minimum zone (Figure 10.6), which culminated in a breakdown of the carbonate factory in a worldwide black shale event, known as OAE 2 (Schlanger and Jenkyns 1976).

The upper water layers were the last to be affected before and the first to be oxygenated after the black shale event. However, anoxic conditions persisted above the sea floor of the ancient shelf (Figure 10.6), expressed by the regional formation of the Vallecillo Member. At the same time, carbonate-producing organisms such as calcispheres, but also the constant record of fishes in the Vallecillo section, indicate permanently oxygenated water at the surface. However, water levels, where keeled foraminifers dwelled, remained hostile, indicated by their absence in the lower *Plattenkalk* unit. The oxygenated zone expanded during the early Turonian, although not constantly. This lead to stepwise changes in the pelagic ecosystem after the late Cenomanian crisis, indicated by several ecoevents during the early Turonian. The results are summarized in Figure 10.9.

Ammonites and inoceramids were strongly affected by the OAE 2 (Westermann 1996; Kennedy *et al.* 2000). Ammonites are absent in the latest Cenomanian at Vallecillo, whereas inoceramids are represented only by *Inoceramus pictus*. Both fossil groups show an increase in diversity and abundance at the Cenomanian-Turonian boundary level, paralleled by a short-term increased diversity of foraminifers. Living conditions remain problematic throughout the *P. flexuosum* zone, indicated by low diversity communities. Another level of short-term favourable intervals is noted by the increased abundances of *Rhynchodercetis* and *P. flexuosum* in the upper *P. flexuosum* zone, but this is only expressed in increased abundance (Chapter 9.5), because the recorded diversity of macrofossils remains low (compare Figures 9.8 and 10.9). This second phase of improved living conditions may have been a regional event, as *P. flexuosum* occurs in the Western Interior Seaway in approximately this level (Figure 8.5). In contrast, inoceramids and foraminifers remain low in diversity and abundance.

A major change is noted in the upper *Vascoceras birchbyi* zone by the coeval appearance of the foraminifer *Helvetoglobotruncana* and the inoceramid *Mytiloides kossmati*. *M. kossmati* reaches a maximum in abundance in the upper *V. birchbyi* zone, paralleled by a peak in diversity of foraminifers. Both decrease in diversity and abundance until another, even more intense maximum in abundance of *M. kossmati* in the early *Mammites nodosoides* zone, which is also paralleled by an increased diversity of foraminifers. Above, plankton proliferated in the water column, shown by further increase in size, abundance and diversity of planktic foraminifers in the uppermost two metres of layers of the Vallecillo section, although the presence of *Plattenkalk* with goethite layers and the absence of benthos apart form inoceramids indicates persistent anoxic conditions at the sea floor. Unfortunately, statistical data for macrofossils do not yet exist for this interval.
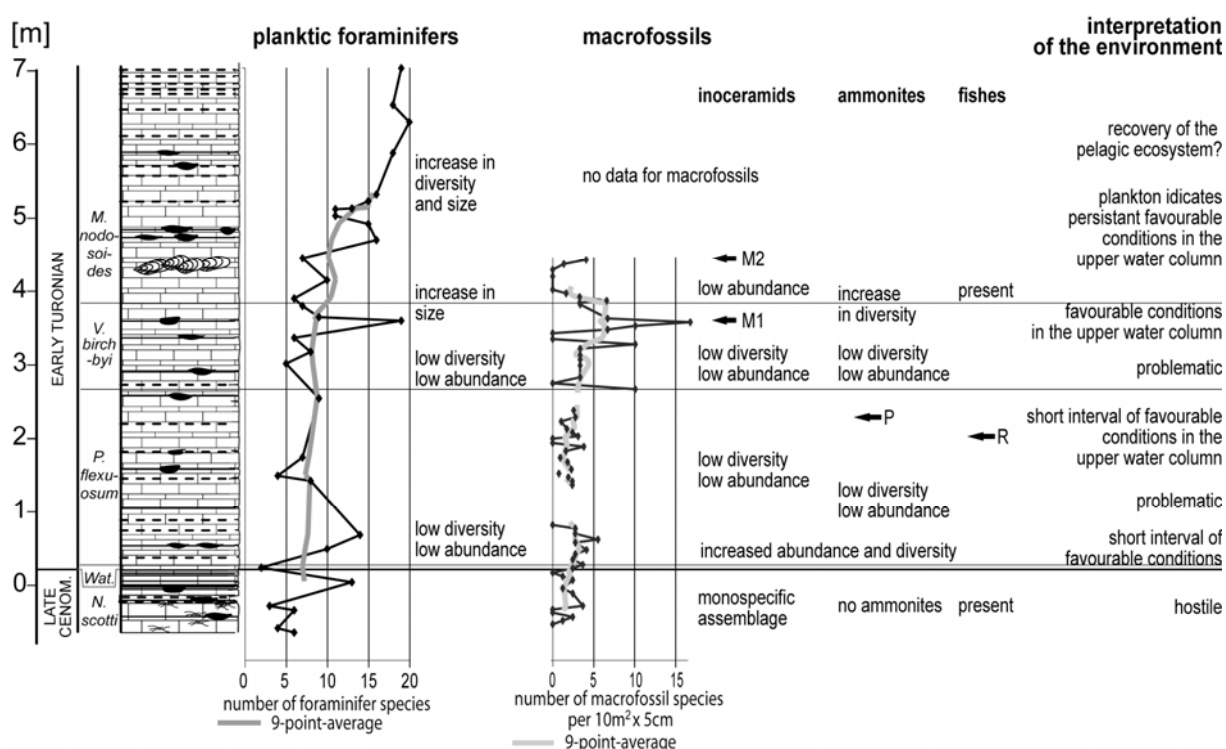
Figure 10.9. Diversity of planktic foraminifers and macrofossils over the Vallecillo section and interpretation of ecoevents during the early Turonian of the Vallecillo section. R: maximum abundance of the fish *Rhynchodercetis*. P: maximum abundance of the ammonite *Pseudaspidoceras flexuosum*. M1 and M2: abundance maxima of the bivalve *Mytiloides kossmati*.

The goethite layers in the Vallecillo *Plattenkalks* of both sections are interpreted to originate from synsedimentary hydrothermal input of sulphides. Jarvis *et al.* (2001) suggested an increased hydrothermal input into the Cenomanian-Turonian oceans, due to high spreading rates at mid-oceanic constructive plate boundaries. The mid-Atlantic Ridge represents a possible source for the synsedimentary ingression of chalcophile elements to Vallecillo. The Caribbean plate, however, is known to be a submarine volcanic hot spot plateau, with a major eruption phase during Cenomanian-

Turonian times (Huber *et al.* 1999). It may thus have been a source for the chalcophile elements. Models of wind and marine circulation patterns for North America indicate that westward currents existed at the Cenomanian-Turonian boundary in the mid-Atlantic and Gulf of Mexico region between the equator and 25°N (Glancy *et al.* 1993). This would exclude the Caribbean plate as a possible source area of hydrothermal deposits. However, these climatic reconstructions do not include the Caribbean plate as a source of significant thermal activity. The effects of major eruptions to air, oceanic currents and marine chemistry in the vicinity of the Caribbean hot spot are not yet studied. The source of these elements may have caused the environmental perturbations in the early Turonian marine assemblages at Vallecillo and Las Mitras.

11   GENESIS OF THE VALLECILLO *PLATTENKALK* AND COMPARISON WITH OTHER *PLATTENKALK* FOSSIL *LAGERSTÄTTEN*

11.1   FORMATION OF THE VALLECILLO *KONSERVAT-LAGERSTÄTTE*

The Vallecillo marly *Plattenkalk* is composed of carbonate of biogenic origin, detrital, very fine-grained material, and Fe-oxides. The sediments formed in the open ocean between two landmasses with arid climate, but far from the coasts. The fossil assemblage at Vallecillo reflects the palaeogeographic position of the locality at the connection of the southern Western Interior Seaway to the western Tethys. No submarine barriers existed in the region such as reefs, island, or other steep submarine topographic heights, which could have inhibited the marine circulation. Even though, the conditions at the Vallecillo sea floor were anoxic and hostile. They were caused by the global anoxic event OAE 2, which excluded benthic life from the Vallecillo area. Only inoceramids existed in this unfavourable environment, but they were rare and low in diversity.

The surface waters of the Vallecillo sea were oxygenated and inhabited by nekton, such as fishes, marine reptiles and ammonites. Planktic organisms, for instance coccolithophorids and foraminifers, provided abundant carbonate. Pellets and coproliths of the living animals, but also carcasses of vertebrates sank to the sea floor and mineralized under the low-oxygen conditions, probably by an early diagenetic precipitation of phosphate. The primary mineralization of fossils was later replaced by sparitic calcite. This two-fold process is indicated by the poikilotopic nature of the crystals that compose bones and soft parts of the Vallecillo vertebrates.

The aragonitic shells of ammonite shells and planktonic organisms were dissolved during early diagenetic dissolution of this metastable mineral. The magnesium released during this dissolution was included into authigenic dolomite; the dissolved calcium carbonate precipitated forming a calcitic matrix. This process lead to alternating limestone-shale lithologies in the Agua Nueva Formation, of which the Vallecillo Member is part, although these alternations are not developed in the Vallecillo Member. Their absence is explained here by the absence of a chemical gradient between sea floor and sediment, resulting from the stagnant, anoxic conditions at the sea floor and sluggish oceanic currents due to OAE2. This interpretation is supported by geochemical analysis.

The Vallecillo *Plattenkalks* were not buried deeply. Late diagenetic processes removed the majority of organic matter from the sediment.

11.2   INTRODUCTION TO OTHER *PLATTENKALK* DEPOSITS

The most famous example for a *Plattenkalk* deposit is the early Tithonian Lithographic Limestone of Solnhofen in Germany. Many other localities became known over the last century, particularly for their well-preserved fossils. Investigation of these fossil *Lagerstätten* showed, that each *Plattenkalk*

has its own depositional model, and it became clear, that *Plattenkalks* form over a wide range of depositional settings. The following chapter presents a choice of depositional models for different *Plattenkalk* localities. It tries to cover the range of depositional settings, although it is far from being complete.

11.2.1 The Solnhofen Lithographic Limestone, Germany (Tithonian)

The Solnhofen Lithographic Limestone is the most celebrated *Plattenkalk Lagerstätte* and known to date early Tithonian (Late Jurassic) in age. It has yielded exceptionally well preserved terrestrial reptiles such as the *Archaeopteryx*, but also pterosaurs and numerous fishes and crustaceans. However, these well preserved fossils are rare.

The Solnhofen limestone is a shallow water carbonate which formed in an epicontinental sea at the northern margin of the Tethys. The Solnhofen waters were shielded from major currents by sponge-algal mounds, which were overgrown by corals on the seaward side and formed a chain of fringing reefs. The *Plattenkalk* is restricted to small basins, separated and underlain by sponge-algal mounds. The variable topography has caused local differences in thickness and in lithology. Thus, in the Solnhofen area the *Plattenkalk* reaches a thickness of 90 m, whereas in the Eichstätt area, 20 km away, only 30 m of thickness are developed. Slumps are recorded within and at the top of the sequence. Several indicators for weak currents exist, such as short drift and re-deposition, roll marks of ammonites, or subparallel orientation of fossils (Barthel *et al.* 1990, p. 91ff).

Most localities in the Solnhofen area show an alternation of two lithologies: the pure, micritic lithographic limestone, the so-called *Flinz*, and the thinner interbeds of argillaceous limestone, called *Fäule*. The *Flinz* beds vary strongly in thickness between 1 cm at the basinal margins and 50 cm within the basins, where the alternation is best developed. Both lithologies are weakly laminated; lamination is enhanced in the lithographic limestone by pressure solution (Hemleben and Swinburne 1991). Benthic foraminifers (Barthel *et al.* 1990, p. 42), but also coccoliths, calcispheres, pellets, coproliths, recrystallized radiolarians, rare ostracods, reefal debris and coccoid cyanobacteria tests are known from these sediments (Barthel *et al.* 1990, p. 46).

Macrofossils are always located on the underside of *Flinz* slabs. Most of Solnhofen fossils represent marine biota, mainly fish, crustaceans and ammonites. Land was not far, as some terrestrial reptiles, insects and plants are preserved in the micritic limestones (Barthel *et al.* 1990, p. 101). The climate on the surrounding landmasses was arid and hot, because types and adaptations of plants (seed fern, conifers) seem to reflect adjustments to water shortage (Barthel *et al.* 1990, p. 72; Park and Fürsich 2001). No substantial runoff supplied the basins from surrounding land masses, causing increased evaporation in the lagoon (Park and Fürsich 2001). The environment at the bottom of the Solnhofen sea was hostile, in part hypersaline, and at times hazardous, shown by mass mortality layers of fishes or crinoids (Barthel *et al.* 1990, p. 90). The hypersaline brines collected at the deepest pools of the lagoon, where the *Plattenkalk* formed, between sponge-algal and coral encrusted mounds that

protruded from the sea floor (Barthel *et al.* 1990, p. 71). Indicators for hypersalinity are osmotic wrinkling of fossil jellyfish, soft part preservation due to slowed decomposition, the early contraction of tendrils in the crinoid *Saccocoma* and the backward bend in the vertebral column of vertebrates. (Barthel *et al.* 1990, pp. 59ff and 90). At the surface, coral reefs grew under normal marine conditions.

Water depths of 50 to 60 m water depth for the Solnhofen basin and 30 m for the Eichstätt basin, calculated from the ancient topography. The stagnant bottom waters apparently caused a hostile environment on the Solnhofen sea bottom, preventing marine organisms to live there. These conditions were lethal to animals washed in, and caused mass mortal events in some cases. Only organisms tolerant to extreme environmental conditions survived for some time, e.g. the horseshoe crab *Mesolimulus*, which left the fossilised body at the end of a trail. This "restricted basin model" is described in detail by Barthel *et al.* (1990, p. 56ff). Whether or not the stagnating brine received sufficient organic input to achieve anoxia is an open question (Hemleben and Swinburne 1991).

11.2.2 The Cerin quarry, France (Kimmeridgian)

These *Plattenkalks* of late Jurassic (Kimmeridgian) age are known from an ancient quarry above the village of Cerin in the southern French Jura mountains, 60 km east of Lyon. Fossils known from Cerin are terrestrial plants (Barale *et al.* 1992), ammonites (Enay *et al.* 1994), limuloids (Gall *et al.* 1996), ophiurids (Bourseau *et al.* 1991), fishes (e.g. Desroches 1971; Desroches 1974; Taverne 1977; Gaudant 1978; Lambers 1988), a pterosaur (Buffetaut *et al.* 1990), a squamate (Evans 1994), and a crocodile (Buffetaut 1979), but also trace fossils such as dinosaur and turtle locomotion tracks (Bernier *et al.* 1984; Gaillard *et al.* 2003).

The depositional facies of Cerin was interpreted to be a lagoon overlying an ancient coral barrier reef. This lagoon was episodically connected to the sea by channels, but frequently emerged (Gaillard *et al.* 1994). Lime mud was supplied both from the sea and from the surrounding emergent land areas. Most marine organisms were transported and/or trapped in the lagoon, where they are associated with very rare autochthonous lagoonal organisms and remains of terrestrial reptiles and plant fragments. Their preservation was enhanced by the presence of the microbial mats. Periods of muddy sedimentation are repeatedly interrupted by peetee structures and mudcracks, and various deformation structures of microbial mats (Bernier *et al.* 1991).

11.2.3 The Tlayúa quarries, Tepexi de Rodríguez, east-central Mexico (Albian)

The Tlayúa Formation is known from an active limestone quarry in the valley of Tlayúa, near Tepexi de Rodríguez, in the Mexican state of Puebla, where approximately 50 m of fish-bearing beds are exposed (Pantoja-Alor 1990). They consist of a honey-coloured to red, platy, laminated limestone, interbedded with mudrock rich in Fe-oxides. Cherts are occasionally intercalated, and a single sandy limestone layer is present. The fine-grained sediment, but also the taphonomy of vertebrate fossils suggest deposition in a shallow lagoon under mostly stagnant conditions. The lagoon was estimated

15×1 km in extend and restricted from the open sea by a reef (Espinosa-Arrubarrena and Applegate 1996).

The fossil assemblage of Tlayúa is a mixture of marine and terrestrial environments. The presence of gymnosperms, an insect and terrestrial reptiles, such as fresh water turtles, lizards and pterosaurs, indicates a close coast (Espinosa-Arrubarrena and Applegate 1996). Marine algae, sponges, fragmented anthozoans, gastropods, ammonites (Cantú-Chapa 1987), annelids, small ostreid bivalves, belemnites (e.g. Seibertz and Buitrón 1987), arthropods, crinoids, echinoids, asteroids, holothurians (e.g. Applegate *et al.* 1996), isopods, decapods (e.g. Feldmann *et al.* 1998; Vega *et al.* 2003), arachnids, numerous fishes, crocodiles, plesiosaurs and a marine turtle are all interpreted to represent allochthonous marine biota. Few tracks or trails are known, but no bioturbation. Autochthonous benthos is restricted to miliolid foraminifers and algal mats (Espinosa-Arrubarrena and Applegate 1996).

The climate at the near-by coast was interpreted to have been hot and arid. Occasional storms and heavy rains may have washed terrestrial biota and much of the Fe-oxides into the Tlayúa lagoon. A barrier reef is supposed to have existed, indicated by the richness of marine and reef biota. They occur only in certain levels in the quarries and are interpreted to have been washed into the hostile Tlayúa lagoon by major storms (Espinosa-Arrubarrena and Applegate 1996).

This model, which is based on mapping, sedimentological evidence and the fossil assemblage, was recently challenged by Kashiyama *et al.* (2004), who concluded that the sediment formed under double-monsoon influences in a tidally influenced, open marine basin with stagnant bottom waters and storm-induced sedimentation. This interpretation is based on statistical microfacies-transition analysis and spectral analysis of depth-series measurements, only.

11.2.4 The Crato Formation, Brazil (Aptian or Albian)

The Crato Formation comprises a series of dark-coloured, calciferous shale laminae, and largely laminated, organic-rich, micritic limestones up to 30 metres in thickness. This unit was deposited under lacustrine conditions in the Araripe Basin in north-eastern Brazil, which formed with the opening of the South Atlantic Ocean during the Aptian-Albian (Martill 1993, p. 16f). The thickness of the Crato Formation reaches up to 30 metres, but it depends largely on the underlying topography. The *Plattenkalks* form three different members in the Crato Formation: the Nova Olinda, Barbalha and Jamacaru members. They are interbedded with clastic deltaic sediments, particularly in the eastern part of the Araripe Basin (Martill 1993, p. 31ff).

Numerous insects are known from the Crato *Plattenkalks*, in addition to fossil spiders, scorpions, ostracods, conchostracans, fishes, possible remains of amphibians and birds. A rich flora of pollen, spores and plant fragments is also present. Detailed overviews on the Crato fossils were given by Martill (1993) and Maisey (1991). More recent findings include pterosaurs with soft part preservation (e.g. Frey *et al.* 2003a;. 2003b) and a crocodile (Salisbury *et al.*). The flora and fauna of the Crato

Formation is interpreted to be allochthonous, with the insects being blown in by wind. Even their larvae may be washed in by rivers, similar to probable freshwater fishes, which occasionally occur in mass mortality events (Martill 1993, p. 51f).

The environment is interpreted as a brackish lake that frequently became hypersaline. This lake was probably thermally and salinity stratified. Evidence for at least occasional high salinity are given by halite pseudomorphs in several layers, but also the general lack of benthic organisms. (Martill 1993, p. 35).

11.2.5 The Haqel and Hjoula *Plattenkalks*, Lebanon (Cenomanian)

The small *Plattenkalk* outcrops of Haqel and Hjoula are Cenomanian fossil *Lagerstätten* that formed in small, steep-sided pull-apart basins, each 100 m across. These basins were filled intermittently with coarse breccia and *Plattenkalk* lithologies and situated on the outer part of the low-relief Lebanese shelf (Hückel 1970). The Haqel *Plattenkalk* unit is 35 m thick. The Hjoula unit is thinner, but its precise thickness is unknown. The *Plattenkalks* are blue-grey in colour when fresh, but weather to white. Only this white, weathered material cleaves easily.

The Haqel *Plattenkalk* contains both laminated and graded beds. The graded beds are composed of a very pure limestone and occur particularly in the outer parts of the basin. Occasionally flat chert layers are present. The Hjoula *Plattenkalk* is similar to the Haqel unit in most respects. However, only laminated beds are known from the Hjoula outcrops, and all beds contain clay. The clay content is mostly around 6 per cent, but some beds are composed of marly lithologies. Pyrite framboids are occasionally present.

Macrofossils are unevenly distributed throughout the units, and usually found in the laminated lithologies. They represent marine biota, commonly fishes and echinoderms, such as holothurian sclerites, crinoids and ophiurids, but also crustaceans (Hemleben and Swinburne 1991), ammonites, nautilids, coleoids, but also badly preserved insects and leaves of terrestrial plants (Hückel 1970). Allochthonous fossils, such as shallow water benthic foraminifers and debris of molluscs and echinoderms, occur particularly at the bases of graded beds.

The Haqel and Hjoula basins were sharp, fault-bounded depressions. After fault movement, the basins began to fill with olistostrome deposits. Quiet water conditions prevailed between these sedimentary phases, and the water column became stratified. The *Plattenkalks* were deposited under these stagnant conditions. Fishes that lived partially or completely in the basin, are exceptionally preserved. Particular fish beds were likely produced by planktic blooms that yielded toxins which poisoned the water and caused mass mortality among fishes (Hemleben and Swinburne 1991).

11.2.6 The Komen Pelagic Limestone, Slovenia (Cenomanian-Turonian)

The Komen Pelagic Limestone is a single unit of black, finely laminated *Plattenkalk* (Hückel 1974a), three to four metres thick. It forms a distinct member within the Repen Formation in western

Slovenia (Jurkovsek *et al.* 1996). During the Cenomanian-Turonian, this region was situated on the outer part of the large Dinaric-Adriatic Platform. This platform submerged with the rising sea level of the late Cenomanian and early Turonian. A pelagic facies developed in its outer parts, in its northern part indicated by the Repen Formation. The intercalated *Plattenkalk* formed during OAE 2 (Jenkyns 1991). The *Plattenkalk* contains calcispheres, recrystallized radiolarians, ammonoids and fishes, such as *Ptychodus* and *Enchodus* (Cavin *et al.* 2000). Although little is known about this fish-bearing deposit, its formation seems similar to that of the Vallecillo *Plattenkalk*. Both are pelagic deposits, caused by stagnant bottom waters during OAE 2.

11.2.7 The *Plattenkalks* of Múzquiz, Mexico (Turonian-Coniacian)

The Múzquiz *Plattenkalks* were recently discovered and described by Stinnesbeck *et al.* (2005). The town of Múzquiz is located in the north-eastern Mexican state of Coahuila. It is the main commercial centre for white and yellow limestone flagstones, which originate from a series of quarries in the remote region to the north-west, approximately 120 km north-west of Múzquiz. The *Plattenkalk* exposed there is about 17 m thick and late Turonian to early Coniacian in age. It consists of micritic, evenly layered, and platy limestone, with internal millimetric bedding, intercalated with fine-layered, fissile calcareous marls.

These sediments contain rich and diverse planktic foraminiferal assemblages which indicate open marine conditions and water depths of at least 50 m. Benthic foraminifers are extremely rare and confined to single specimens and few horizons. Other microfossils include abundant calcispheres.

Inoceramids are abundant. Most of them preserve their thick prismatic shells, whereas the aragonitic layer is always recrystallized. Oysters are rare and were only observed as epizoans, growing on a single plant remain. Heteromorph ammonoids are frequent and in places abundant, and most species are endemic to the Western Interior. The distribution of the non-heteromorph ammonites is significantly more ample than that of the heteromorphs, some species even occur worldwide in low and middle latitudes, but they are rare in the Múzquiz *Plattenkalks*.

Phosphatization of the invertebrate fossils has been recognized in ammonite siphos, but also in crustacean carapaces. Four species of crustaceans are present in the Múzquiz carbonate sequence, which apparently could all swim. The cirriped *Stramentum* is represented by several specimens attached to the shell of an ammonite.

The vertebrate assemblage consists of complete and disarticulated specimens, as well as primary fragments of vertebral columns, fins, single isolated bones, scales *etc.*, randomly distributed in the sediment. Skeletons are embedded laterally, sometimes in dorsoventral position. Most vertebrate fossils are compressed, as a consequence of the compaction of the sediment. Some specimens, however, are preserved in three dimensions. Many skeletons of the Múzquiz *Plattenkalks* are fully articulated, and disarticulated skeletal elements of fishes and other vertebrates appear to be a result of decay during post-mortem floating. Delicate morphological elements (e.g., fin rays, gill rakers and

filaments) of some specimens are obliquely embedded, indicating that the sediment must have been soft. Phosphatization of soft parts such as intestinal contents, myotomes, gill filaments, cycloid scales and fins of fishes, is observed occasionally and indicates that replacement of organic tissues by fluorapatite occurred at a very early diagenetic stage of mineralization, preceding or accompanying microbial decay, and often prior to sediment compaction.

Teleosteans are the most abundant elements of the El Rosario fish fauna and are represented by primary fragments and complete specimens. Isolated teeth of the pycnodont shark *Ptychodus* cf. *P. mortoni* were also found in El Rosario. Marine reptiles were identified in several primary fragments. Among them is an isolated vertebra of a probable varanoid, and sixteen articulated vertebrae referred to the tail of an early mosasaurid, about 3 m in length (Buchy *et al.* 2005). The only known pterosaur specimen is an almost complete and articulated nyctosaurid pterosaur, *Muzquizopteryx coahuilensis* n. gen., n. sp. Frey *et al.* (in press). With a wingspan of about 2 m, it represents the smallest known adult nyctosaurid pterosaur.

Occasional fragments of fossil drift wood are the only evidence of vegetation from the North American continent. During Turonian-Coniacian times, the North American coastline was located at least 200-300 km to the west of El Rosario.

The Muzquiz *Plattenkalk* is similar to the Vallecillo *Plattenkalk* in many aspects. Lamination, fine grained texture, predominance of randomly oriented fossils, and the fossil assemblages themselves indicate sedimentation in an open marine, stenohaline quiet water environment Both localities were deposited on the open shelf, far from the coast. Stagnation and a hostile oxygen-deficient bottom environment are indicated by the millimetric lamination of the sediments and by thin laminae to thick horizons with concretions of goethite, which formed from the oxidation of primary pyrite. Abundant benthic invertebrates are restricted to inoceramids in both localities. In addition, both localities yield fossil assemblages intermediate to the Western Interior and the Tethys. Both deposits formed under similar environmental conditions, but at different ages (Ifrim *et al.* 2005, submitted).

11.3   DISCUSSION OF DEPOSITIONAL MODELS FOR THE FORMATION OF *PLATTENKALKS*

The preceding chapters showed that *Plattenkalks* formed over a wide range of depositional settings, from lacustrine facies (Crato, Brazil, Aptian/Albian) and tidal flats (Cerin, France, Kimmeridgian), to lagoonal environments (Solnhofen, Germany, Tithonian, and Tlayúa, México, Albian), next to drowned platforms (Komen, Slovenia, Cenomanian-Turonian), and on the outer shelf (Haqel and Hjoula, Lebanon, Cenomanian; Vallecillo, Cenomanian-Turonian; Múzquiz, Turonian-Coniacian, both Mexico). Although these facies differ considerably, they all have in common, that the environment at the sedimentary surface was very hostile. Usually, microbial mats are the only identifiable autochthonous organisms. Exceptions are miliolid foraminifers from Tlayúa and Cerin and

inoceramids from Múzquiz and Vallecillo. Apparently, these organisms were able to live under the extreme environmental conditions, lethal to the majority of fossilized organisms.

Fossils are frequently phosphatized in *Plattenkalks* (Hückel 1974b). This preservation supports the hypothesis that the formation of *Plattenkalks* require low-oxygen conditions (compare Prévôt and Lucas 1990). Although the Vallecillo fossils are preserved calcified, they may initially have been phosphatized, with this primary mineralization later replaced (Chapters 5.5 and 6.1).

The most widespread opinion about *Plattenkalks* is that they require a protected environment for their formation, such as a basin with barriers isolating it from the ocean, or a depression in the shelf which sheltered the deposition area from turbulent waters above (Hemleben and Swinburne 1991). This idea is consistent with most depositional models for the *Plattenkalk* deposits described in Chapter 11.2, but the depositional model for the Vallecillo *Plattenkalk* clearly contradicts this hypothesis. No submarine barrier in the Vallecillo region is known or indicated by any geological or palaeontological evidence. The wide geographical occurrence of the Vallecillo Member over 100 km from Vallecillo to Monterrey contradicts the existence of such a barrier and supports the idea that formation took place on the open shelf. Jenkyns (1991) already noticed a link between *Plattenkalk* Formation and OAE 2, although his observations on the Dinaric Platform were never further considered in other depositional models for *Plattenkalks*. However, the *Plattenkalk* of Múzquiz also formed on the open shelf, in a sedimentary and palaeogeographic position similar to Vallecillo. Whether or not this *Plattenkalk* formed during a regional or global anoxic event, remains to be studied.

Plattenkalks reflect an extreme of limestone sedimentation (Hemleben and Swinburne 1991); their formation in deeper seas apparently requires black shale facies. Such a facies is consistent with most depositional models described above. Wetzel (1991) already noted that there exist all intermediate lithologies between very pure *Plattenkalk*, for instance from Solnhofen or Haqel, and black shales. The marly *Plattenkalk* of the Vallecillo Member represents a transitional lithology in this continuum. It seems to be a carbonate equivalent to the black shales formed during OAE 2. This is supported by the fact that a black shales underlie the *Plattenkalk* at Las Mitras. No facies change is visible between these two lithologies, the only difference of the *Plattenkalks* to the black shales is the presence of a carbonate source in the *Plattenkalk*.

The Vallecillo fauna showed that the water masses of the Vallecillo sea were stratified, with oxygenated surface waters and anoxic conditions at the sea floor. A thermal and salinity stratification was interpreted for the Crato lake (Martill 1993, p. 35), but was never considered for marine *Plattenkalks* of deeper environments, even though indicators for such stratifications exist. For instance, the coral reefs around the Solnhofen basin indicate normal marine waters, whereas at the bottom, hypersaline brines existed. This provides evidence, that hostile conditions above the sedimentary surface do not solely include anoxia, they may also have been caused by hypersaline brines. Stratified water masses likely occurred in many of the above described deposits and may be the key to *Plattenkalk* formation in deeper waters.

Exceptions to this generalized model of *Plattenkalk* formation are the *Plattenkalks* that formed in tidal flats (Cerin) or a shallow lagoon (Tlayúa). These environments are too shallow to develop a chemocline or pycnocline, but they include great variations in temperature and salinity. The extreme environment of these deposits is indicated by the scarcity of autochthonous organisms, which are restricted to microbial mats and miliolid foraminifers at both localities.

The *Plattenkalks* at Solnhofen and Vallecillo developed in a hot, arid climate. This is favourable for the generation of phytoplankton in the upper water column and therefore the production of organic matter and carbonate. The high temperatures prevent solution of gas in the sea-water, such as O_2 (important for life in the deeper water column) and CO_2 (low partial pressure of CO_2 supports the biogenic precipitation of carbonates). The high productivity of plankton may have led to eutrophication of the deeper water layers. A hot and arid climate thus likely supported *Plattenkalk* formation.

Plattenkalks do not generally require a restricted basin for their formation. Instead, they require a continuous source of carbonate, and stagnant, hostile, although not necessarily anoxic conditions at the sea floor, so that burrowing organisms are excluded and cannot disturb the fine lamination. Such conditions are occasionally provided by restricted basins, but they may also occur regionally on the open shelves during oceanic anoxic events.

12 SUMMARY

The Vallecillo *Plattenkalks* were deposited during the latest Cenomanian and early Turonian in the outer shelf environment of the western Gulf of Mexico between the southern end of the Western Interior Seaway and the western Tethys. These *Plattenkalks* are characterized by a micritic marly lithology. They form a distinct unit within the Agua Nueva Formation with a regional distribution, and are assigned member of the lower to middle Agua Nueva Formation.

In the Vallecillo quarries, a section of approximately 8 m is exposed. The *Plattenkalks* are composed of marly limestone and mudstone. Calcite is the major mineral in these rocks, minor minerals are quartz, feldspars, clay minerals and Fe-minerals. This petrography was controlled by three different processes: calcite is biogenic in origin, whereas the Fe-minerals were precipitated as sulphides and later oxidized. The detritus was probably supplied by aeolian sedimentation and may have originated from the northern Gulf coast, where an arid climate prevailed by the early Turonian.

Early diagenetic processes in the *Plattenkalk* include the recrystallization of aragonite to calcite. Differential diagenesis did not develop in the Vallecillo Member due to the lack of a chemical gradient in the sediment, pointing to anoxic environments of deposition. This interpretation is supported by the presence of small syngenetic framboids, as well as the low concentrations of Mn and the enrichment of Ni in the rocks. The correlation of chalcophile elements indicates that Fe-minerals were primarily precipitated as sulphides in an anoxic environment and later oxidized.

The fossil assemblage includes ammonites, which are preserved flattened, but with fine details and sometimes even stomach contents. Inoceramids represent the only benthic organisms. The Vallecillo fishes are flattened, only large forms are preserved compressed, but three-dimensional. Rare marine reptiles such as turtles, an aigialosaur and a pliosaur tooth are also known from Vallecillo. The palaeobiogeographical analysis of the fossils indicates that a mixture of Tethyan and Western Interior Seaway endemic species is present at Vallecillo.

Planktic foraminifers, ammonites and inoceramids allow a very detailed biostratigraphic subdivision of the Vallecillo section. The Vallecillo section is biostratigraphically more complete and expanded than the GSSP of the Cenomanian-Turonian boundary near Pueblo, Colorado. The following biozones could be distinguished: Ammonites: the late Cenomanian *Nigericeras scotti* zone, and the Turonian *Watinoceras*, *Pseudaspidoceras flexuosum*, *Vascoceras birchbyi* zones and part of the *Mammites nodosoides* zone; Inoceramids: the late Cenomanian *Inoceramus pictus pictus* and *Mytiloides hattini* zones, and the early Turonian *M. puebloensis* and *M. kossmati* zones; planktic foraminifers: the *Whiteinella archaeocretacea* and the *Helvetoglobotruncana helvetica* zones.

Two reliable stratigraphic markers were identified during the early Turonian, the FA of *Watinoceras* at the beginning of the Turonian, and the FA of *Mammites nodosoides*. Between these two events, the appearances *P. flexuosum* and *Fagesia catinus*, among other stratigraphic index fossils, appear to be diachronous. An average sedimentation rate of 16·8 mm/ka was calculated for the

Vallecillo section, and a compaction rate of about 30% of original thickness.

A series of scientific excavations revealed that fossils are abundant in the Vallecillo rocks. The number of findings averages 29·0 findings per 10m^2×5cm. The absolute composition of the Vallecillo assemblage differs considerably from the composition of the random surface collection. However, this collection is important, because it provides well-preserved fossils, important for anatomical and systematic investigations, and contains rare taxa, uncovered by the excavations. Both types of collections are necessary for the interpretation of the Vallecillo *Konservat-Lagerstätte*.

Inoceramids are rare in the Vallecillo column, with the exception of a minor increase in abundance at the Cenomanian-Turonian boundary level, another at about 3·6 and an abundance event at 4·5 m section. Inoceramids were the only benthic organisms that could persist under the anoxic conditions at the Vallecillo sea floor, supported by the absence of burrowing organisms. The distribution of inoceramids over the Vallecillo section is independent from the substrate they lived on; it seems to reflect improved conditions in the upper water column, because their abundance and diversity parallels that of planktic foraminifers.

Ammonites are well preserved and may not have drifted far after death, despite the scarcity of aptychi in Vallecillo. The preservation of stomach contents, the complete apertures of many living chambers, delicate ornament of the shell and loosely jointed spines support the hypothesis of rapid waterlogging of the phragmocone. Apparently this happened faster for large ammonites than small ones. *P. flexuosum* is preserved with large spines, documented from Vallecillo for the first time. They seem loosely jointed to the living chambers of adult specimens, but their function is unclear. Heteromorph ammonites, known from many early Turonian localities of the Western Interior Seaway, are absent in Vallecillo, probably because of the hostile anoxic conditions in the Vallecillo sea.

The abundance of fish fossils allows the taphonomic interpretation of the three most abundant species in the Vallecillo fossil assemblage, *Rhynchodercetis* sp., *Tselfatia formosa* and *Nursallia* cf. *N. gutturosum*. The different preservation of these three fish species at Vallecillo likely results from the water depths, in which they preferably lived. They also differed in locomotion mode and feeding habits and shared the available food sources without major interference. The taphonomy of the vertebrates supports the interpretation of a very hostile environment at the Vallecillo sea floor.

The statistical distribution of invertebrates over the Vallecillo section differs from the even distribution of the fishes. Both ammonites and inoceramids show a slight increase in abundance above the Cenomanian-Turonian boundary level, indicating a short interval of favourable conditions. Assemblages during the middle *P. flexuosum* zone are low in diversity and specialized. Upsection, abundance maxima of *Rhynchodercetis* and *P. flexuosum* indicate the next phase of improved living conditions at the surface, but the environment at the sea floor remained hostile. Inoceramids were rare during the early Turonian until the *V. birchbyi* zone, when *Mytiloides kossmati* immigrated into the Vallecillo area. This specialized bivalve proliferated despite the hostile conditions at the Vallecillo sea floor, indicated by its dominance in a minor increase in abundance and an abundance event. Both

ecoevents are paralleled by peaks in diversity of foraminifers. The distribution of inoceramids resembles thus more that of foraminifers than ammonites. This is remarkable, because both ammonites and inoceramids may have depended on the distribution of larvae by oceanic currents. Apparently, inoceramid larvae depended on similar water depths and ecologic constraints than planktic foraminifers, whereas ammonite larvae dwelled in different, probably shallower water depths.

The Vallecillo *Plattenkalk* has a regional occurrence. The Las Mitras section in the Las Mitras suburb of Monterrey, 100 km to the south, includes in its lower part sediments preceding *Plattenkalk* formation, such as black shales of latest Cenomanian age. These black shales indicate a conspicuous change in sedimentation, linked to OAE 2, and transist gradually into *Plattenkalk*. The Las Mitras section is biostratigraphically complete from the late Cenomanian *Rotalipora cushmani* to the early Turonian *H. helvetica* foraminiferal zone. The Las Mitras sediments were deposited in an open marine environment, but more proximal than Vallecillo and with a probable island nearby, which may have drowned during the rising sea level of the Cenomanian-Turonian transition. The anchimetamorphous overprint of the Las Mitras section prohibits the comparison of the clay mineralogy to that of Vallecillo. Petrography depended on the same three processes known from Vallecillo, but the distribution is more heterogeneous in the Las Mitras section because of the change in source of the detritus. Most sediments of the Las Mitras section were deposited under low-oxygen conditions, with the exception of the lowest layers investigated.

Deep-water dwelling keeled foraminifers are indicative of distal "blue water" settings in the las Mitras sediments. They were strongly affected by the expansion of the low oxygen zone in the late Cenomanian. The diverse late Cenomanian foraminiferal assemblage is successively replaced by a dwarfed assemblage of low abundance and diversity. After OAE 2, the assemblages remain impoverished until the FA of the keeled *H. helvetica*, similar to the Vallecillo section. The absence of benthic foraminifers at both the Las Mitras and Vallecillo sections is explained by constant anoxic conditions.

The goethite layers in the Vallecillo *Plattenkalks* of both sections originated from synsedimentary, hydrothermal input of sulphides. If climatic models for Cenomanian-Turonian times are correct, the mid-Atlantic Ridge is the next possible source of these elements. However, none of these models includes the Caribbean plate as major source of thermal activity. This submarine hot spot had a major eruption phase during Cenomanian-Turonian times and may have been a source area for the sulphides.

Plattenkalks are known to have formed over a wide range of facies in Earth history. The Vallecillo *Plattenkalk* is the first known to have formed in the open ocean environment, outside restricted basins, and with a wide regional occurrence. Apparently, a global OAE can cause conditions on the open shelf critical for *Plattenkalk* formation. These include the presence of a carbonate source in the upper water column, stagnant conditions in most of the water column and hostile conditions at the sea floor.

REFERENCES

AGASSIZ, J. L. R. 1833-1844. *Recherches sur les poissons fossiles*. Editions Neuchâtel et Soleure, Neuchâtel, 1420 pp.

ALLISON, P. A., SMITH, C., KUKERT, H., DEMING, J. and BENNETT, B. 1991. Deep-water taphonomy of vertebrate carcasses: a whale skeleton in the bathyal Santa Catalina Basin. *Paleobiology*, **17**, 78-89.

ANDERSON, F. M. 1958. Upper Cretaceous of the Pacific Coast. *Geological Society of America Memoir*, **71**, New York, 378 pp.

APPLEGATE, S. P. 1970. The Vertebrate fauna of the Selma Formation of Alabama, Part VIII, Fishes. *Fieldiana Geology*, **3**, 381-433.

——— 1992. A new genus and species of pycnodont from the Cretaceous (Albian) of central Mexico, Tepexi de Rodríguez, Puebla. *Revista Mexicana de Ciencias Geológicas*, **10**, 164-178.

——— P., BUITRÓN-SANCHEZ, B. E. and SOLIS-MARIN, F. A. 1996. Seven new taxa of holothurians (Holothuroidea: Echinodermata) from the Lower Cretaceous (Albian) Tlayua quarries, near Tepexi de Rodriguez, Puebla, Mexico. Sixth North American Paleontological Convention: abstracts of papers, *Special Publications (Paleontological Society)*, **8**, 10.

ARAMBOURG, C. 1943. Note préliminaire sur quelques poissons fossiles nouveaux. *Bulletin de la Société Géologique de France*, **5**, 281-288.

——— 1954. Les poissons crétacés du Jebel Tselfat (Maroc). *Éditions du Service Géologique du Maroc*, Rabat, 208 pp.

ARKHANGUELSKY, A. D. 1916. [The Upper Cretaceous Mollusks of Turkistan. Part 1]. *Trudy geol. kom.*, **152**, 1-57. [in Russian].

ARMSTRONG, H. A. and BRASIER, M. D. 2005. *Microfossils*. Blackwell, Oxford, 296 pp.

ARMSTRONG, R. L. and WARD, P. L. 1993. Late Triassic to earliest Eocene magmatism in the North American cordillera: Implications for the Western Interior Basin. 49-72. *In* KAUFFMAN, E. G. (ed.). Evolution of the Western Interior Basin. *Geological Association of Canada Special Paper*, **39**, 680 pp.

ARTHUR, M. A., JENKYNS, H. C., BRUMSACK, H.-J. and SCHLANGER, S. O. 1988. Stratigraphy, geochemistry, and paleoceanography of organic carbon-rich Cretaceous sequences. 75-119. *In* BEAUDOIN, B. (ed.). *Cretaceous Resources, Events and Rhythms: Background and Plans for Research*. Kluwer Academic Publishing, Digne.

AVANZINI, M. and LUCIANI, V. 1999. *Tselfatia formosa* Arambourg. 1943 (pisces, actinopterygii) dal Cretaceo Superiore del Trentino (Italia settentrionale). *Studi Trentini di Scienze Naturali: Acta Geologica*, **76**, 193-199.

BADILLET, G. and SORNAY, J. 1980. Sur quelques formes du groupe d'*Inoceramus labiatus* décrites par O. Seitz. Impossibilité d'utiliser ce groupe pour une datation stratigraphique du Turonien inférieur du Saumuroi (France). *Comtes Rendus Académie Science Paris, Série D*, **290**, 323-325.

BALUKHOVSKY, A., FLOEGEL, S., HAY, W. W. and MIGDISOV, A. 2004. A paleogeographic map for the Lower Turonian. http://earthref.org/cgi-bin/erda.cgi?n=220.

BARALE, G., PHILIPPE, M. and THÉVENARD, F. 1992. Studies of Mesozoic floras of French Jura; 1 Cerin, 2, Orbagnoux. 45-70. *In* BARALE, G., BROUTIN, J., CHATEAUNEUF, J. J., DEBRIETTE, P., GALTIER, J., LANGIAUX, J., LEMOIGNE, Y., PACAUD, G., PHILIPPE, M., SAMUEL, E. and THEVENARD, F. (eds). *Paleozoic, Mesozoic and Cenozoic floras from the Massif Central and Jura*. **16C**, Organisation Française de Paleobotanique, Informations, Villeneuve d'Asca.

BARDACK, D. and TELLER MARSHALL, S. 1980. *Tselfatia*, a Tethyan Cretaceous teleost; first records from North America and Yugoslavia. *Journal of Paleontology*, **54**, 1075-1083.

BARTHEL, K. W., SWINBURNE, N. H. M. and CONWAY-MORRIS, S. 1990. *Solnhofen, a Study in Mesozoic Palaeontology*. Cambridge University Press, Cambridge, 236 pp.

BE, A. W. H. 1977. An ecological zoogeographic, and taxonomic review of recent planktonic foraminifera. 1-100. In RAMSAY, A. T. S. (ed.). *Oceanic Micropaleontology*. 1-2, Academic Press, New York, 1453 pp.

BENNING, L. G., WILKIN, R. T. and BARNES, H. L. 2000. Reaction pathways in the Fe-S system below 100°C. *Chemical Geology*, **167**, 25-51.

BERNARD, J. M. 1996. Microaerophilic and facultative anaerobic benthic foraminifera: A review of experimental and ultrastructural evidence. *Révue de Paléobiologie*, **15**, 261-275.

BERNIER, P., BARALE, G., BOURSEAU, J. P., BUFFETAUT, E., DEMATHIEU, G. R., GAILLARD, C., GALL, J. C. and WENZ, S. 1984. Découverte de pistes de dinosaurs sauteurs dans les Calcaires lithographiques de Cerin (Kimmeridgien supérieur, Ain, France); implications paléoécologiques. *Geobios, Mémoire Spéciale*, **8**, 177-187, [in French].

——— GAILLARD, C., GALL, J. C., BARALE, G., BOURSEAU, J. P., BUFFETAUT, E. and WENZ, S. 1991. Morphogenetic impact of microbial mats on surface structures of Kimmeridgian micritic limestone (Cerin, France). *Sedimentology*, **38**, 127-136.

BESAIRE, H. 1930. Recherches géologiques à Madagascar. Contributions à l'étude des ressources minérales. *Thèses présentées à la Faculté des Sciences de l'Université de Paris*, Toulouse, 1-172 pp.

BEURLEN, K. 1944. Beiträge zur Stammesgeschichte der Muscheln. *Sitzungsberichte der Bayerischen Akademie der Wissenschaften*, **1-2**, 133-145.

BISHOP, B. A. 1970. Stratigraphy of Sierra de Picachos and Vicinity, Nuevo León, Mexico. *American Association of Petroleum Geologists Bulletin*, **54**, 1245-1270.

BLAKEY, R. C. 2002. *Global Map of the Late Cretaceous*. http://jan.ucc.nau.edu/~rcb7/090Marect.jpg.

BLANCO PIÑON, A. 2003. *Peces fósiles de la Formación Agua Nueva (Turoniano) en el Municipio de Vallecillo, Nuevo León, NE-México*. PhD thesis, Universidad Autónoma de Nuevo León, Linares, 345 pp.

BLANCO, A. and CAVIN, L. 2003. New teleostei from the Agua Nueva Formation (Turonian), Vallecillo (NE Mexico). *Comptes Rendus Paleovol*, **2**, 299-306.

———— STINNESBECK, W., LÓPEZ-OLIVA, J.-G., FREY, E., ADATTE, T. and GONZÁLEZ, A. H. 2001. Vallecillo, Nuevo León: una nueva localidad fosilífera del Cretácico Tardío en el noreste de México. *Revista Mexicana de Ciencias Geológicas*, **18**, 196-199.

BLANCO-PIÑON, A. and ALVARADO-ORTEGA, J. 2005. New dercetid fish (Aulopiformes: Teleostei) from the early Turonian of Vallecillo, NE Mexico. 4th International Meeting on Mesozoic Fishes, Madrid, *Extended Abstracts*, 43-46.

———— FREY, E., STINNESBECK, W. and LÓPEZ-OLIVA, J. G. 2002. Late Cretaceous (Turonian) fish assemblage from Vallecillo, northeastern Mexico. *Neues Jahrbuch für Geologie und Paläontologie, Abhandlungen*, **225**, 39-54.

———— SHIMADA, K. and GONZÁLEZ-BARBA, G. 2005. Lamnoid vertebrae from the Agua Nueva Formation (Upper Cretaceous: lower Turonian), northeastern Mexico. *Revista Mexicana de Ciencias Geológicas*, **22**, 19-23.

BÖSE, E. 1906. Excursions dans les Environs de Saltillo et Monterrey. 10th International Geological Congress, *Excursions du Nord, Livret-Guide*, **29**, 17.

———— 1920. On a new ammonite fauna of the Lower Turonian. *University of Texas Bulletin*, **1856**, 179-257.

BOUANNI, F. 1681. *Ricreatione dell'occhio e della mente nell'osservation delle Chiocciole*. Rome, 16+384 pp.

BOURSEAU, J. P., HESS, H., BERNIER, P., BARALE, G., BUFFETAUT, E., GAILLARD, C., GALL, J. C. and WENZ, S. 1991. Découverte d'ophiures dans les calcaires lithographiques de Cerin (Kimméridgien supérieur, Ain, France); systématique et implications taphonomiques. *Comptes Rendus Académie des Sciences, Série 2*, **312**, 793-799, [in French].

BRAND, U. and VEIZER, J. 1980. Chemical diagenesis of a multicomponent carbonate system. 1, trace elements. *Journal of Sedimentary Petrology*, **5**, 1219-1236.

BRANDES, C. H. 1993a. Meeräschen, Pfeilhechte, Lippfische und Verwandte. 174-159. *In* GRZIMEK, B. (ed.). *Grzimeks Tierleben. Enzyklopädie des Tierreichs*, **5,** Fische **2,** Lurche, Deutscher Taschenbuchverlag, München.

———— 1993b. Die Barschartigen. 73-124. *In* GRZIMEK, B. (ed.). *Grzimeks Tierleben. Enzyklopädie des Tierreichs*, **5,** Fische **2,** Lurche, Deutscher Taschenbuchverlag, München.

BRONGNIART, A. 1822. Sur quelques terrains de Crais hors du Bassin de Paris. 80-101. *In* BRONGNIART, A. (ed.). *Description géologique des environs de Paris*. G. Dufour et E. d'Ocagne, Librairies, Paris, 428 pp.

BRUMSACK, H.-J. 2005. The trace metal content of recent organic carbon-rich sediments: Implications for Cretaceous black shale formation. *Palaeogeography, Palaeoclimatology, Palaeoecology*.

BUCHY, M.-C., SMITH, K. T., FREY, E., STINNESBECK, W., GONZÁLEZ GONZÁLEZ, A. H., IFRIM, C., LÓPEZ-OLIVA, J. G. and PORRAS-MUZQUIZ, H. 2003. Preliminary catalogue of marine squamates (Reptilia) from the Upper Cretaceous of northeastern Mexico. First Mosasaur Meeting, Maastricht, 8-12 May 2004, *Abstract Book*, 17-23.

———— ———— ———— ———— ———— ———— ———— and ———— 2005. Annotated catalogue of marine squamates (Reptilia) from the Upper Cretaceous of northeastern Mexico. *Netherlands Journal of Geosciences*, **84**, 195-205.

BUFFETAUT, E. 1979. *Crocodileimus robustus* et le paléomilieu Kimméridgien de Cerin. *Réunion Annuelle des Sciences de la Terre*, **7**, 92.

———— BERNIER, P., BARALE, G., BOURSEAU, J. P., GAILLARD, C., GALL, J. C. and WENZ, S. 1990. A new pterosaur bone from the Kimmeridgian lithographic limestone of Cerin (France). *Neues Jahrbuch für Geologie und Paläontologie, Monatshefte*, **1990**, 321-328.

BYERLY, G. R. 1991. Igneous activity. 91-108. *In* SALVADOR, A. (ed.). The Gulf of Mexico Basin. *The Geology of America*, **J**, Geological Society of America, 557 pp.

CANTÚ-CHAPA, A. 1987. Las amonitas del Albiano Superior de Tepexi de Rodríguez. *Revista de la Sociedad Mexicana de Paleontología*, **1**, 159-160.

CARON, M. 1985. Cretaceous planktic foraminifera. 17-87. *In* PERCH-NIELSEN, K. (ed.). *Plankton Stratigraphy*. Cambridge University Press, Cambridge, 1032 pp.

CARY, S. C. 1994. Vertical transmission of a chemautotrophic symbiont in the protobranch bivalve *Solemya reidi*. *Molecular Marine Biology and Biotechnology*, **3**, 121-130.

———— WARREN, W., ANDERSON, E. and GIOVANNONI, S. J. 1993. Identification and localitation of bacterial endonymbionts in hydrothermal vent taxa woth species-specific PCR amplification and *in situ* hybridization techniques. *Molecular Marine Biology and Biotechnology*, **2**, 51-62.

CAVIN, L., JURKOVSEK, B. and KOLAR-JURKOVSEK, T. 2000. Stratigraphic succession of the Upper Cretaceous fish assemblages of Kras (Slovenia). *Geologija*, **43**, 165-195.

CHALIFA, Y. 1989. Two new species of longirostrine fishes from the early Cenomanian (late Cretaceous) of Ein-Yabrud, Israel, with comments on the phylogeny of the Dercetidae. *Journal of Vertebrate Paleontology*, **9**, 314-328.

CHAMBERLAIN, J. J. A., WARD, P. D. and WEAVER, J. S. 1981. Post-mortam ascent of *nautilus* shells: implications for cephalopod paleobiogeography. *Paleobiology*, **7**, 494-509.

CHAMLEY, H. 1989. *Clay Sedimentology*. Springer-Verlag, Berlin, 624 pp.

CHANCELLOR, G. R. 1982. Cenomanian-Turonian ammonites from Coahuila, Mexico. *Bulletin of the Geological Institutions of the University of Uppsala*, **9**, 77-129.

———— KENNEDY, W. J. and HANCOCK, J. M. 1994. Turonian ammonite faunas from central Tunisia. *Special Papers in Palaeontology*, **50**, 118 pp.

———— REYMENT, R. A. and TAIT, E. A. 1977. Notes on Lower Turonian ammonites from Loma el Macho, Coahuila, Mexico. *Bulletin of the Geological Institutions of the University of Uppsala*, **12**, 85-101.

CHECA, A. and MARTIN-RAMOS, D. 1989. Growth and function of spines in the Jurassic ammonite *Aspidoceras*. *Palaeontology*, **32**, 645-655.

CHISM, R. E. 1885. The Vallecillo mines (Nuevo Leon), Mex. *Transactions of the Society of Mining Engineers of American Institute of Mining, Metallurgical and Petroleum Engineers, Incorporated (AIME)*, **13**, 351-368.

CHOFFAT, P. 1898. Recueil d'études paléontologiques sur la faune crétacique du Portugal. 2, les ammonites des Couches á *Neolobites Vibraeanus*, du Turonien et du Sénonien. *Section des Travaux Géologiques du Portugal*, **1898**, 41-86.

COBBAN, W. A. 1983. Stratigraphy and paleontology of mid-Cretaceous rocks in Minnesota and contiguous areas. *United States Geological Survey Professional Paper*, **1253**, 1-25.

——— 1984. Mid-Cretaceous ammonite zones, Western Interior, United States. *Bulletin of the Geological Society of Denmark*, **33**, 71-89.

——— 1988. The Upper Cretaceous ammonite *Watinoceras* Warren in the Western Interior of the United States. *United States Geological Survey Bulletin*, **1788**, 1-15.

——— and HOOK, S. C. 1983a. *Pseudaspidoceras pseudonodosoides* (Choffat) - common Upper Cretaceous guide fossil in southwest New Mexico. *New Mexico Bureau of Mines and Mineral Resources, Annual Report*, **1981-1982**, 37-40.

——— and HOOK, S. C. 1983b. Mid-Cretaceous (Turonian) ammonite fauna from Fence Lake area, west-central New Mexico. *Memoir of the New Mexico Bureau of Mines and Mineral Resources*, **41**, 50 pp.

——— and SCOTT, G. R. 1972. Stratigraphy and ammonite fauna of the Graneros Shale and Greenhorn Limestone near Pueblo, Colorado. *United States Geological Survey Special Paper*, **645**, 1-103.

——— HOOK, S. C. and KENNEDY, W. J. 1989. Upper Cretaceous rocks and ammonite faunas of southwestern New Mexico. *Memoir of the New Mexico Bureau of Mines and Mineral Resources*, **45**, 137 pp.

COLLIGNON, M. 1965. *Atlas des Fossiles charactéristiques de Madagascar (Ammonites), XII (Turonien)*. Service Géologique, Tananarive, iv+82 pp.

COOPER, M. R. 1978. Uppermost Cenomanian-basal Turonian ammonites from Salinas, Angola. *Annals of the South African Museum*, **75**, 51-152.

COURVILLE, P. 1992. Les Vascoceratinae et les Pseudotissotiinae (Ammonitina) d'Ashaka (NE Nigeria): relations avec leur environnement biosédimentaire. *Bulletin des Centre de Recherches Exploration-Production Elf-Aquitaine*, **16**, 407-457.

——— LANG, J. and THIERRY, J. 1998. Ammonite faunal exchanges between South Tethyan platforms and South Atlantic during the uppermost Cenomanian-lowermost/middle Turonian in the Benue Through (Nigeria). *Geobios*, **31**, 187-214.

COWEN, R., GERTMAN, R. and WIGGETT, G. 1973. Camouflage patterns in *Nautilus*, and their implications for cephalopod paleobiology. *Lethaia*, **6**, 71-113.

COX, L. R. 1969. Family Inoceramidae Giebel, 1852. N314-N321. *In* MOORE, R. C. (ed.). *Mollusca 6, Bivalvia. Treatise on Invertebrate Palentology*, **Part N, Vol. 1**, Lawrence, Kansas.

CRAGIN, F. W. 1893. A contribution to the invertebrate paleontology of the Texas Cretaceous. *Texas Geological Survey 4th annual Report*, **1892**, 139-246.

DESROCHES, A. 1971. Catalogue des poissons fossiles du gisement de Cerin (Ain); conservés dans les collections du Muséum d'Histoire Naturelle de Lyon (première partie). *Nouvelles Archives du Muséum d'Histoire Naturelle de Lyon*, **9**, 13-108, [in French].

——— 1974. Catalogue des poissons fossiles du gisement de Cerin (Ain) conservés dans les collections du Muséum d'Histoire Naturelle de Lyon. *Nouvelles Archives du Muséum d'Histoire Naturelle de Lyon*, **12**, 13-88, [in French].

DOUVILLE, H. 1912. Evolution et classification des Pulchelliidés. *Bulletin de la Société Géologique de France*, **11**, 285-320.

DUNHAM, R. J. 1962. Classification of carbonate rocks according to depositional texture. 108-121. *In* HAM, W. E. (ed.). Classification of Carbonate Rocks. *American Association of Petroleum Geologists Memoir*, **1**, 279 pp.

DURNEY, D. W. and KISCH, H. J. 1994. A field classification and intensity scale for first-generation cleavages. *Journal of Australian Geology and Geophysics*, **15**, 257-296.

ELDER, W. P. 1991. *Mytiloides hattini* n.sp.: a guide fossil for the base of the Turonian in the Western Interior of North America. *Journal of Paleontology*, **65**, 234-241.

ENAY, R., BERNIER, P., BARALE, G., BOURSEAU, J. P., BUFFETAUT, E., GAILLARD, C., GALL, J. C. and WENZ, S. 1994. Les ammonites des Calcaires Lithographiques de Cerin (Ain, France): Stratigraphie et taphonomie. *Geobios, Special Issue*, **16**, 25-36, [in French].

D'ERASMO, G. 1946. L'ittofauna cretacea dei Dintorni Comeno del Carso Triestino. *Rendiconto della Academia delle Scienze Fisiche e Matematische, Ser. 3*, **2**, 1-136.

ESPINOSA-ARRUBARRENA, L. and APPLEGATE, S. P. 1996. A paleoecological model of the vertebrate bearing beds in the Tlayúa quarries, near Tepexi di Rodríguez, Puebla, México. 539-550. *In* ARRATIA, G. and VIOHL, G. (eds). *Mesozoic Fishes - Systematics and Paleoecology*. Verlag Dr. Friedrich Pfeil, München.

ETTER, W. 1999. Community analysis. 285-360. *In* HARPER, D. A. T. (ed.). *Numerical Palaeobiology*. John Wiley and Sons Ltd, Chichester, x+468.

EVANS, S. E. 1994. A re-evaluation of the Late Jurassic (Kimmeridgian) reptile *Euposaurus* (Reptilia; Lepidoauria) from Cerin, France. *Geobios*, **27**, 621-631.

FELDMANN, R. M., VEGA, F. J., APPLEGATE, S. P. and BISHOP, G. A. 1998. Early Cretaceous arthropods from the Tlayúa Formation at Tepexi de Rodríguez, Puebla, Mexico. *Journal of Paleontology*, **72**, 79-90.

FERNÁNDEZ-LÓPEZ, S. and MELÉNDEZ, G. 1996. Phylloceratina ammonoids in the Iberian Basin during the Middle Jurassic: a model of biogeographical and taphonomic dispersal related to relative sea-level changes. *Palaeogeography, Palaeoclimatology, Palaeoecology*, **120**, 291-302.

FISCHER, A. G. and BOTTJER, D. J. 1995. Oxygen-depleted waters: A lost biotope and its role in ammonite and bivalve evolution. *Neues Jahrbuch für Geologie und Paläontologie, Abhandlungen*, **195**, 133-146.

FISCHER, R. 1967. Zur Ökologie zweier Ammonitenfaunen aus dem Aalenium des Schneibsteins (Berchtesgadener Alpen). *Geologica et Palaeontologica*, **1**, 175-177.

FLÜGEL, E. 2004. *Microfacies of Carbonate Rocks*. Springer, Berlin, 976 pp.

FOLK, R. L. 1974. *Petrology of Sedimentary Rocks*. Hemphill, Austin, 159 pp.

FOREY, P. L., YI, L., PATTERSON, C. and DAVIES, C. E. 2003. Fossil fishes from the Cenomanian (Upper Cretaceous) of Namoura, Lebanon. *Journal of Systematic Palaeontology*, **1**, 227-330.

FREUND, R. and RAAB, M. 1969. Lower Turonian ammonites from Israel. *Special Papers in Palaeontology*, **4**, 1-83.

FREY, E., MARTILL, D. M. and BUCHY, M.-C. 2003a. A new crested ornithocheirid from the Lower Cretaceous of northeastern Brazil and the unusual death of an unusual pterosaur. 55-63. *In* BUFFETAUT, E. and MAZIN, J. M. (eds). *Evolution and palaeobiology of pterosaurs. Geological Society Special Publications*, **217**, Geological Society of London, London, 347 pp.

———— TISCHLINGER, H., BUCHY, M.-C. and MARTILL, D. M. 2003b. New specimens of Pterosauria (Reptilia) with soft parts with implications for pterosaurian anatomy and locomotion. 233-266. *In* BUFFETAUT, E. and MAZIN, J. M. (eds). *Evolution and palaeobiology of pterosaurs. Geological Society Special Publications*, **217**, Geological Society of London, London, 347 pp.

———— BUCHY, M.-C., STINNESBECK, W., GONZÁLEZ GONZÁLEZ, A. H. and DI STEFANO, A. in press. *Muzquizopteryx coahuilensis* n.g., n.sp., first evidence for the presence of nyctosaurid pterosaurs in the Coniacian (Late Cretaceous) of northeastern Mexico (Coahuila). *Oryctos*.

GAILLARD, C., BERNIER, P. and GRUET, Y. 1994. Le lagon d'Aldabra (Seychelles, Océan Indien), un modèle pour le Paléoenvironnement de Cerin (Kimméridgien Supérieur, Jura Meridional, France). *Geobios*, **16**, 331-348.

———— ———— BARALE, G., BOURSEAU, J. P., BUFFETAUT, E., EZQUERRA, R., GALL, J. C., DE LAPPARENT DE BROIN, F., RENOUS, S. and WENZ, S. 2003. A giant Upper Jurassic turtle revealed by its trackways. *Lethaia*, **36**, 315-322.

GALE, A. S., KENNEDY, W. J., VOIGT, S. and WALASZCZYK, I. 2005. Stratigraphy of the Upper Cenomanian-Lower Turonian Chalk succession at Eastbourne, Sussex, UK: ammonites, inoceramid bivalves and stable carbon isotopes. *Cretaceous Research*, **26**, 460-487.

GALL, J. C., BERNIER, P., BARALE, G., BOURSEAU, J. P., BUFFETAUT, E., GAILLARD, C. and WENZ, S. 1996. Découverte de limules dans les calcaires lithographiques de Cerin (Kimmeridgian, France). *Archaeopteryx*, **14**, 75-81,

GAUDANT, J. 1978. Essay de révision taxonomique des "Pholidophorus" (poissons Actinoptérygiens) du Jurassique supérieur de Cerin (Ain). *Nouvelles Archives du Museum d'Hinstoire Naturelle de Lyon*, **16**, 101-121.

GIEBEL, C. G. A. 1852. *Deutschlands Petrefakten. Ein systematisches Verzeichnis aller in Deutschland und den angrenzenden Ländern vorkommenden Petrefacten nebst Angabe der Synonymen und Fundorte*. A. Abel, Leipzig.

GLANCY, T. J., ARTHUR, M. A., BARRON, E. J. and KAUFFMAN, E. G. 1993. A paleoclimate model for the north American Cretaceous (Cenomanian-Turonian) Epicontinental Sea. 219-241. *In* CALDWELL, W. G. E. and KAUFFMAN, E. G. (eds). *Evolution of the Western Interior Basin. Geological Association of Canada Special Paper*, **39**, 680 pp.

GOLDHAMMER, R. K. and JOHNSON, C. A. 2001. Middle Jurassic-Upper Cretaceous paleogeographic evolution and sequence-stratigraphic framework of the northwest Gulf of Mexico rim. *American Association of Petroleum Geologists Memoir*, **75**, 45-81.

———— LEHMANN, P. J., TODD, R. G., WILSON, J. L., WARD, W. C. and JOHNSON, C. R. 1993. Estratigrafía Secuencial y Cicloestratigrafía des Mesozoico de la Sierra Madre Oriental, Noreste de Mexico. *Libreto Guía*, 101 pp.

GÖTTE, M. 1990. *Halotektonische Deformazionsprozesse in Sulfatgesteinen der Minas Viejas-Formation (Ober-Jura) in der Sierra Madre Oriental, Nordost-Mexiko*. PhD thesis, Technische Hochschule, Darmstadt, 268 pp.

DE GRACIANSKY, P. C., DEROO, G., HERBIN, J. P., MONTADERT, L., MÜLLER, C., SCHAAF, A. and SIGAL, J. 1984. Ocean-wide stagnation episode in the late Cretaceous. *Nature*, **308**, 346-349.

———— ———— ———— J. P., JAWUCIN, T., MAGNIEZ, F., MONTADERT, L., MÜLLER, C., PONSOT, C., SCHAAF, A. and SIGAL, J. 1986. Ocean-wide stagnation episode in the late Cretaceous. *Geologische Rundschau*, **75**, 17-41.

GRAY, G. C. and JOHNSON, C. A. 1995. *Structural and Tectonic Evolution of the Sierra Madre Oriental, with Emphasis on the Saltillo-Monterrey Corridor. A Field Guide Book. Annual Convention*, American Association of Petroleum Geologists, Houston, Texas, 17 pp.

GRAY, J. E. 1847. A list of the genera of Recent Mollusca, their synonyms and types. *Proceedings of the Zoological Society London*, **15**, 129-219.

GROSSOUVRE, A. D. 1894. Recherches sur la Craie Supérieure, 2, Paléontologie. Les ammonites de la Craie Supérieure. *Mémoirs pour Servir à l'Explication de la Carte géologique détaillée de la France*, Paris, ii+264 pp.

HALLAM, A. 1992. *Phanerozoic Sea Level Changes*. Columbia University Press, New York, 266 pp.

HAQ, B. U., HARDENBOL, J. and VAIL, P. R. 1987. Chronology of Fluctuating Sea Level Since the Triassic. *Science*, **235**, 1156-1165.

HARDENBOL, J., THIERRY, J., FARLEY, M. B., DE GRACIANSKY, P. C. and VAIL, P. P. 1998. Mesozoic and Cenozoic sequence chronostratigraphic framework of European basins. 3-13, Appendix pp. 763-781. *In* DE GRACIANSKY, P. C., HARDENBOL, J., JACQUIN, T. and VAIL, P. P. (eds). *Mesozoic and Cenozoic Sequence Stratigraphy of European Basins. Society for Sedimentary Geology Special Publication*, **60**, 786 pp.

HARRIES, P. J., KAUFFMAN, E. G., CRAMPTON, J. S., BENGTSON, P., CECH, S., CRAME, J. A., DHONDT, A. V., ERNST, G., HILBRECHT, H., LOPEZ, G., MORTIMORE, R., TRÖGER, K.-A., WALASZCZYK, I. and WOOD, C. J. 1996. Lower Turonian Euramerican Inoceramidae: A morphologic, taxonomic, and biostratigraphic overview. *Mitteilungen aus dem Geologisch - Paläontologischen Museum der Universität Hamburg*, **77**, 641-671.

HAY, W. W., EICHER, D. L. and DINER, R. 1993. Physical oceanography and water masses in the Cretaceous Western Interior Seaway. 297-318. *In* KAUFFMAN, E. G. (ed.). *Evolution of the Western Interior Basin. Geological Association of Canada Special Paper*, **39**, 680 pp.

HEINZ, R. 1930. Zur stratigraphischen Stellung der Sonnenbergschichten bei Walterdorf in Sachsen (west-südwestlich von Zittau). Beiträge zur Kenntnis der oberkretazischen Inoceramen IX. *Jahresbericht des Niedersächsischen Geologischen Vereins zu Hannover*, **23**, 23-29.

——— 1933. Inoceramen von Madagaskar und ihre Bedeutung für die Kreide-Stratigraphie - Beiträge zur Kenntnis der Inoceramen XII. *Zeitschrift der Deutschen Geologischen Gesellschaft*, **85**, 241-259.

——— 1935. Unterkreide-Inoceramen von der Kapverden-Insel Maio - Beiträge zur Kenntnis der Inoceramen XVIII. *Neues Jahrbuch für Geologie, Abhandlungen*, **73**, 302-311.

HEMLEBEN, C. and SWINBURNE, N. H. M. 1991. Cyclical deposition of the plattenkalk facies. 572-591. *In* EINSELE, G., RICKEN, W. and SEILACHER, A. (eds). *Cycles and Events in Stratigraphy*. Springer-Verlag, Berlin, 955 pp.

HENDERSON, J. 1908. New species of Cretaceous invertebrates from northern Colorado. *Proceedings of the US National Museum*, **34**, 259-264.

HESSEL, M. H. R. 1988. Lower Turonian inoceramids from Sergipe, Brazil: Systematics, stratigraphy, and palaeoecology. *Fossils and Strata*, **22**, 1-49.

HUBER, B. T., LECKIE, R. M., NORRIS, R. D., BRALOWER, T. J. and COBABE, E. 1999. Foraminiferal assemblage and stable isotopic change across the Cenomanian-Turonian boundary in the subtropical North Atlantic. *Journal of Foraminiferal Research*, **29**, 329-417.

HÜCKEL, U. 1970. Die Fischschiefer von Haqel und Hjoula in der Oberkreide des Libanon. *Neues Jahrbuch für Geologie und Paläontologie, Abhandlungen*, **135**, 113-149, [in German].

——— 1974a. Fossil-Diagenese, Nr. 5: Vergleich des Mineralbestandes der Plattenkalke Solnhofens und des Libanon mit anderen Kalken. *Neues Jahrbuch für Geologie und Paläontologie, Abhandlungen*, **145**, 153-182, [in German].

——— 1974b. Fossil-Diagenese, Nr. 7: Geochemischer Vergleich der Plattenkalke Solnhofens und des Libanon mit anderen Kalken. *Neues Jahrbuch für Geologie und Paläontologie, Abhandlungen*, **145**, 279-305, [in German].

HUERTA-DIAZ, M. A. and MORSE, J. W. 1992. Pyritization of trace metals in anoxic marine sediments. *Geochimica et Cosmochimica Acta*, **56**, 2681-2702.

HUMPHREY, W. E. 1949. Geology of the Sierra de los Muertos area, Mexico (with description of Aptian Cephalopods from the La Peña Formation). *Geological Society of America Bulletin*, **60**, 89-176.

HYATT, A. 1889. *Genesis of the Arietidae. Smithsonian Contributions to Knowledge*, **673**, Washington, DC, xi+238 pp.

——— 1900. Cephalopoda. 502-604. *In* ZITTEL, K. A. (ed.). *Textbook of Palaeontology*. Macmillan, London & New York, viii+306.

——— 1903. *Pseudoceratites of the Cretaceous. Monograph of the US Geological Survey*, **44**, Government Printing Office, Washington, 351 pp.

ICE, R. G. and MCNULTY, C. L. 1980. Foraminifera and calcispheres from the Cuesta del Cura and lower Agua Nueva Formations (Cretaceous) and east-central Mexico. *Transactions of the Gulf Coast Association of Geological Societies*, **30**, 403-425.

IFRIM, C. and STINNESBECK, W. submitted. Early Turonian (late Cretaceous) ammonites from Vallecillo, north-eastern Mexico: taxonomy, biostratigraphy and palaeobiogeographic significance. *Cretaceous Research*.

——— ——— and FREY, E. 2005. *Upper Cretaceous (Cenomanian-Turonian and Turonian-Coniacian) open marine Plattenkalk-deposits in NE Mexico*. 4th International Symposium on Lithographic Limestone and *Plattenkalk*, Eichstätt, Germany, 12-18 Sept. 2005, *Zitteliana*, **B26**, 15-16.

——— ——— and ——— submitted. Upper Cretaceous (Cenomanian-Turonian and Turonian-Coniacian) open marine *plattenkalk* deposits in NE Mexico. *Erlanger Earth Sciences Conference Series*.

——— ——— and LOPEZ-OLIVA, J. G. 2004. Maastrichtian Cephalopods from the Méndez Formation at Cerralvo, Northeastern Mexico. *Palaeontology*, **47**, 1575-1627.

——— FREY, E., STINNESBECK, W., BUCHY, M.-C., GONZÁLEZ GONZÁLEZ, A. H. and LÓPEZ OLIVA, J. G. 2005. Fish assemblage in Lower Turonian carbonates at Vallecillo, N.L., México. *Paleos Antiguo*, **1**, 43-51.

——— ——— ——— ——— ——— ——— and ——— in press. Composition and taphonomy of the early Turonian fish assemblage at Vallecillo, N.L., Mexico. *Semana de Paleontología 1995-2004, Special Publication*. INAH Coahuila, Saltillo.

——— Stinnesbeck, W., FREY, E., BUCHY, M.-C., SMITH, K. T., LÓPEZ OLIVA, J. G. and GONZÁLEZ GONZÁLEZ, A. H. 2005b. Fossils assemblage in early Turonian carbonates at Vallecillo, N.L., Mexico. *Terra Nostra*, **2005**, 60.

IMLAY, R. W. 1936. Geology of the western part of the Sierra de Parras. *Geological Society of America Bulletin*, **47**, 1091-1152.

JACOBS, D. K. and CHAMBERLAIN, J. A. 1996. Buoyancy and hydrodynamics in ammonoids. 169-224. *In* DAVIS, R. A. (ed.). Ammonoid Paleobiology. *Topics in Paleobiology*, **13**, Plenum Press, New York, London.

JARVIS, I., MURPHY, A. M. and GALE, A. S. 2001. Geochemistry of pelagic and hemipelagic carbonates: criteria for identifying systems tracts and sea-level change. *Journal of the Geological Society of London*, **158**, 685-696.

JENKYNS, H. C. 1991. Impact of Cretaceous sea level rise and anoxic events on the Mesozoic carbonate platform of Yugoslavia. *American Association of Petroleum Geologists Bulletin*, **75**, 1007-1017.

JOHNSON, S. C., LUCAS, S. G. and FRIEDMAN, V. 2002. Stratigraphic range and biostratigraphic utility of the Cretaceous shark genus *Ptychodus. Geological Society of America 2002 Annual Meeting - Anonymous Abstracts with Programs*, **34**, 424.

JURKOVSEK, B., KOLAR-JURKOVSEK, T. and CAVIN, L. 2001. *Fishes in the Late Cretaceous fossil assemblages of Kras (Slovenia).* 3rd International Meeting on Mesozoic Fishes. Systematics, Paleoenvironments and Biodiversity, Serpiano-Monte San Giorgio, 26-31 August 2001, 44-45.

——— TOMAN, M., OGORELEC, B., SRIBAR, L., DROBNE, K., POLJAK, M. and SRIBAR, L. 1996. *Geological map of the Southern Part of the Trieste-Komen Plateau - Cretaceous and Paleogene carbonate rocks 1 : 50 000.* Institute of Geology, Geotechnics and Geophysics, Ljubljana, 143 pp, [Slovenian and English].

KARRENBERG, H. 1935. Ammonitenfaunen aus der Nordspanischen Oberkreide. *Palaeontographica*, **82**, 125-161.

KASHIYAMA, Y., FASTOVSKY, D. E., RUTHERFORD, S., KING, J. and MONTELLANO, M. 2004. Genesis of a locality of exceptional fossil preservation: paleoenvironments of Tepexi de Rodríguez (mid-Cretaceous, Puebla, Mexico). *Cretaceous Research*, **25**, 153-177.

KAUFFMAN, E. G. 1975. Dispersal and biostratigraphic potential of Cretaceous benthonic bivalvia in the Western Interior. 163-194. *Geological Association of Canada Special Paper*, **13**.

——— 1978. Benthic environments and paleoecology of the Posidonienschiefer (Toarcian). *Neues Jahrbuch für Geologie und Paläontologie, Abhandlungen*, **157**, 18-36.

——— and CALDWELL, W. G. E. 1993. The Western Interior Basin in space and time. 1-30. *In* KAUFFMAN, E. G. (ed.). Evolution of the Western Interior Basin. *Geological Association of Canada Special Paper*, **39**, 680 pp.

——— HATTIN, D. E. and POWELL, J. D. 1977. Stratigraphic, paleontologic, and paleoenvironmental analysis of the Upper Cretaceous rocks of Cimarron County, northwestern Oklahoma. *Geological Society of America Memoir*, **149**, 150 pp.

KELLER, G. and PARDO, A. 2004. Age and paleoenvironment of the Cenomanian-Turonian global stratotype section and point ant Pueblo, Colorado. *Marine Micropaleontology*, **51**, 95-128.

——— BERNER, Z., ADATTE, T. and STUEBEN, D. 2004. Cenomanian-Turonian and δ^{13}C, and δ^{18}O, sea level and salinity variations at Pueblo, Colorado. *Palaeogeography, Palaeoclimatology, Palaeoecology*, **211**, 19-43.

——— HAN, Q., ADATTE, T. and BURNS, S. J. 2001. Palaeoenvironment of the Cenomanian-Turonian transition at Eastbourne, England. *Cretaceous Research*, **22**, 391-422.

KELLY, W. A. 1936. Geology of the mountains bordering the valleys of Acatita and Las Delicias. *Geological Society of America Bulletin*, **47**, 1009-1038.

KENNEDY, W. J. 1988. Late Cenomanian and Turonian ammonite faunas from north-east and central Texas. *Special Papers in Palaeontology*, **39**, 1-131.

——— 1994. Lower Turonian Ammonites from Gard (France). *Palaeopelagos Special Publication*, **1**, 255-275.

——— and COBBAN, W. A. 1976. Aspects of ammonite biology, biogeography, and biostratigraphy. *Special Papers in Palaeontology*, **17**, 1-94.

——— and ——— 1991. Stratigraphy and interregional correlations of the Cenomanian-Turonian transition in the Western Interior of the United States near Pueblo, Colorado; a potential boundary stratotype for the base of the Turonian stage. *Newsletters on Stratigraphy*, **24**, 1-33.

——— ——— ELDER, W. P. and KIRKLAND, J. I. 1999. Lower Turonian (Upper Cretaceous) *Watinoceras devonense* Zone ammonite fauna in Colorado, USA. *Cretaceous Research*, **20**, 629-639.

——— WALASZCZYK, I. and COBBAN, W. A. 2000. Pueblo, Colorado, USA, candidate global boundary stratotype section and point for the base of the Turonian stage of the Cretaceous, and for the base of the middle Turonian substage, with a revision of the Inoceramidae (Bivalvia). *Acta Geologica Polonica*, **50**, 295-334.

——— WRIGHT, C. W. and HANCOCK, J. M. 1987. Basal Turonian ammonites from west Texas. *Palaeontology*, **30**, 27-74.

KEUPP, H. 2000. Ammoniten: Paläobiologische Erfolgsspiralen. *Species*, **6**, Thorbecke, Stuttgart, 165 pp.

KIRKLAND, J. I. 1991. Lithostratigraphic and biostratigraphic framework for the Mancos Shale (Late Cenomanian to Middle Turonian) at Black Mesa, northeastern Arizona. 85-111. *Geological Society of America Special Paper*, **260**.

KISCH, H. J. 1990. Calibration of the anchizone: a critical comparison of illite 'crystallinity' scales used for definition. *Journal of Metamorphic Geology*, **8**, 31-46.

KLINGER, H. C., KAUFFMAN, E. G. and KENNEDY, W. J. 1980. Upper Cretaceous ammonites and inoceramids from the off-shore Alphard Group of South Africa. *Annals of the South African Museum*, **82**, 293-320.

KNAUER, G. A. and MARTIN, J. H. 1982. Trace elements and primary production: Problems, effects and solutions. 825-840. *In* GOLDBERG, E. D. (ed.). *Trace metals in sea water. NATO Conference Series*, **9**, Plenum Press, New York.

KOCH, K. E. and NICOLAUS, H. J. 1969. Zur Geologie des Ostpindos-Flyschbeckens und seiner Umrandung. *Eidikai Meletai epi tes Geologias tes Ellados*, **9**, 1-190.

KOSSMAT, F. 1897. Untersuchungen über die Südindische Kreideformation. Zweiter Theil. *Beiträge zur Paläontologie Österreich-Ungarns und des Orient*, **11**, 1-46 (108-153).

KRAMAR, U. 1997. Advances in energy-dispersive X-ray fluorescence. *Journal of Geochemical Exploration*, **58**, 73-80.

KRUMM, S. 1992. Illitkristallinität als Indikator schwacher Metamorphose. Methodische Untersuchungen, regionale Anwendungen und Vergleiche mit anderen Parametern. *Erlanger Geologische Abhandlungen*, **120**, 1-75.

KÜBLER, B. 1987. Cristallinité de l'illite, méthodes normalisées de préparations, méthodes normalisées de mesures. *Cahiers Institut Géologie de Neuchâtel Série A*, **DX**, 1-56.

LAMBERS, P. 1988. *Orthocormus teyleri* nov. sp., the first pachycormid (Pisces, Actinopterygii) from the Kimmeridge lithographic limestone at Cerin (Ain), France; with remarks on the genus *Orthocormus* Weitzel. *Proceedings of the Koninklijke Akademie van Wetenschappen, Series B*, **91**, 369-391.

LANDMAN, N. H., TANABE, K. and SHIGETA, Y. 1996. Ammonoid embryonic development. 343-405. *In* DAVIS, R. A. (ed.). Ammonoid Paleobiology. *Topics in Geobiology*, **13**, Plenum, New York, London.

LAUBE, G. C. and BRUDER, G. 1887. Ammoniten der böhmischen Kreide. *Palaeontographica*, **33**, 217-267.

LAUVERJAT, J. and BERTHOU, P. Y. 1974. Le Cénomano-Turonien de l'embouchure du Rio Montego, Beira Litoral, Portugal. *Comunicações dos Serviços Geológicos de Portugal*, **57**, 263-301.

LECKIE, R. M., YURETICH, R., WEST, L. O. L., FINKELSTEIN, D. and SCHMIDT, M. G. 1998. Paleoceanography of the southwestern Interior Sea during the time of the Cenomanian-Turonian boundary (late Cretaceous). 101-126. *In* DEAN, W. E. and ARTHUR, M. A. (eds). *Concepts in Sedimentology and Paleontology*. **6**, Society of Economic Paleontologists and Mineralogists.

LEHMANN, J. 1998. Systematic palaeontology of the ammonites of the Cenomanian-Lower Turonian (Upper Cretaceous) of northern Westphalia, north Germany. *Tübinger Geowissenschaftliche Arbeiten*, **37**, 1-57.

LEONHARDT 1897. Die Fauna der Kreideformation in Oberschlesien. *Palaeontographica*, **44**, 11-70.

LEWAN, M. D. and MAYNARD, J. B. 1982. Factors controlling enrichment of vanadium and nickel in bitumen of organic sedimentary rocks. *Geochimica et Cosmochimica Acta*, **46**, 2547-2560.

LINDQUIST, N. 2002. Chemical defense of early life stages of benthic marine invertebrates. *Journal of Chemical Ecology*, 28, 1987-2000

LINNÉ, C. 1758. *Systema Naturae per tria regna naturae, etc.*, **1**, Laurentii Salvii, Stockholm, ii+824 pp.

LUGER, P. and GRÖSCHKE, M. 1989. Late Cretaceous ammonites from the Wadi Qena area in the Egyptian eastern desert. *Palaeontology*, **32**, 355-407.

LYONS, T. W. 1997. Sulfur isotopic trends and pathways of iron sulfide formation in upper Holocene sediments of the anoxic Black Sea. *Geochimica et Cosmochimica Acta*, **61**, 367-382.

MACLEOD, K. G. and HOPPE, K. A. 1992. Evidence that inoceramid bivalves were benthic and harbored chemosynthetic symbionts. *Geology*, **20**, 117-120.

MAEDA, H. and SEILACHER, A. 1996. Ammonoid taphonomy. 543-578. *In* DAVIS, R. A. (ed.). Ammonoid Paleobiology. *Topics in Geobiology*, **13**, Plenum, New York, London.

MAGARITZ, M. 1975. Sparitization of pelleted limestone: a case study of carbon and oxygen isotopic composition. *Journal of Sedimentary Petrology*, **45**, 599-603.

MAISEY, J. G. 1991. *Santana fossils: An Illustrated Atlas. Tropical Fish Hobbyist Publications*, New Jersey, 459 pp.

——— and MOODY, J. M. 2001. A review of the problematic extinct teleost fish *Araripichthys*, with a description of a new species from the Lower Cretaceous of Venezuela. *American Museum Novitates*, **3324**.

MANTELL, G. A. 1822. *The fossils of the South Downs, or illustrations of the Geology of Sussex.* Lupton Relfe, London, xvi+327 pp.

MARTILL, D. M. 1993. *Fossils of the Santana and Crato Formations, Brazil. Field Guides to Fossils*, **5**, Palaeontological Association, London.

MATSUMOTO, T. 1959a. Upper Cretaceous Ammonites of California, Part I: Introduction and Baculitidae. *Memoirs of the Faculty of Science, Kyushu University, Series D, Geology*, **8**, 91-171.

——— 1959b. Upper Cretaceous Ammonites of California, Part II. *Memoirs of the Faculty of Science, Kyushu University, Series D, Geology, Sp. Vol.* **1**, 1-172.

MEISTER, C. 1989. Les ammonites du Crétacé supérieur d'Ashaka (Nigéria). Analyse taxonomique, ontogénétique, biostratigraphique et évolutive. *Bulletin des Centres de Recherches Exploration-Production Elf-Aquitaine*, **13**, suppl.

——— and ABDALLAH, H. 1996. Les ammonites du Cénomanien supérieur et du Turonien inférieur de la région de Gafsa-Chotts, Tunisie du centre-sud. [Upper Cenomanian-Lower Turonian ammonites of the Gafsa-Chott area, southern part of Central Tunisia]. *Geobios*, **29**, 3-49.

MERRIMAN, R. J. and FREY, M. 1999. Patterns of very low-grade metamorphism in metapelitic rocks. 61-107. *In* FREY, M. and ROBINSON, D. (eds). *Low-grade Metamorphism*. Blackwell Science, Oxford, 313+x.

——— and PEACOR, D. R. 1999. Very low-grade metapelites: mineralogy, microfabrics and measuring reaction progress. 10-60. *In* ROBINSON, D. (ed.). *Low-grade Metamorphism*. Blackwell Science, Oxford, 313+x.

MITCHELL, S. F., BALL, J. D., CROWLEY, S. F., MARSHALL, J. D., PAUL, C. R. C., VELTKAMP, C. J. and SAMIR, A. 1997. Isotope data from Cretaceous chalks and foraminiferal environmental or diagenetic signals? *Geology*, **25**, 691-694.

MOORE, D. M. and REYNOLDS, R. C. 1997. *X-Ray Diffraction and the Identification and Analysis of Clay Minerals*. Oxford University Press, New York, 378 pp.

MORÁN-ZENTENO, D. 1994. Geology of the Mexican Republic. *Studies in Geology*, **39**, American Association of Petrologists and Geologists, 150 pp.

MORIYA, K., NISHI, H., KAWAHATA, H., TANABE, K. and TAKAYANAGI, Y. 2003. Demersal habitat of Late Cretaceous ammonoids: Evidence from oxygen isotopes for the Campanian (Late Cretaceous) northwestern Pacific thermal structure. *Geology*, **31**, 167-170.

MORROW 1935. Cephalopods from the Upper Cretaceous of Kansas. *Journal of Paleontology*, **9**, 463-473.

MUIR, J. M. 1934. Limestone reservoir rocks in the Mexican oil fields. 377-398. *Problems of Petroleum Geology*. **1934**, American Association of Petroleum Geologists.

MUIR, J. M. 1936. *Geology of the Tampíco region Mexico*. American Association of Petroleum Geologists, Tulsa, 280 pp.

MUNNECKE, A. and SAMTLEBEN, C. 1996. The formation of micritic limestones and the development of limestone-marl alternations in the Silurian of Gotland. *Facies*, **34**, 159-176.

——— WESTPHAL, H., ELRICK, M. and REIJMER, J. J. G. 2001. The mineralogical composition of precursor sediments of calcareous rhythmites: a new approach. *International Journal of Earth Sciences*, **90**, 795-812.

——— ——— REIJMER, J. J. G. and SAMTLEBEN, C. 1997. Microspar development during early marine burial diagenesis: a comparison of Pliocene carbonates from the Bahamas with Silurian limestones from Gotland (Sweden). *Sedimentology*, **44**, 977-990.

MUUS, B. J. and DAHLSTRÖM, P. 1973. *BLV Bestimmungsbuch Meeresfische der Ostsee, der Nordsee, des Atlantiks*. BLV Verlagsgesellschaft, München, 244 pp.

NEWELL, N. D. 1965. Classification of the Bivalvia. *American Museum Novitates*, **2206**, 1-25.

NIEBUHR, B., BALDSCHUHN, R., ERNST, G., WALASZCZYK, I., WEISS, W. and WOOD, C. J. 1999. The Upper cretaceous succession (Cenomanian - Santonian) of the Staffhorst Shaft, Lower Saxony, northern Germany: integrated biostratigraphic, lithostratigraphic and downhole geophysical log data. *Acta Geologica Polonica*, **49**, 175-213.

NORRA, S. 2001. Umweltgeochemische Signale urbaner Systeme. *Karlsruher Mineralogische und Geochemische Hefte*, **18**, 1-296.

NURSALL, J. R. 1996. Distribution and ecology of pycnodont fishes. 115-144. *In* VIOHL, G. (ed.). *Mesozoic fishes - Systematics and paleoecology*. Verlag Friedrich Pfeil, München.

OBRADOVICH, J. D. 1993. A Cretaceous time scale. 379-396. *In* KAUFFMAN, E. G. (ed.). Evolution of the Western Interior Basin. *Geological Association of Canada Special Paper*, **39**, 680 pp.

PADILLA Y SANCHEZ, R. 1982. *Geologic evolution of the Sierra Madre Oriental between Linares, Concepción del Oro, Saltillo, and Monterrey, Mexico*. PhD thesis, University of Texas, Austin, 217 pp.

PAGE, K. N. 1996. Mesozoic ammonoids in space and time. 755-794. *In* DAVIS, R. A. (ed.). Ammonoid Paleobiology. *Topics in Geobiology*, **13**, Plenum, New York, London.

PANTOJA-ALOR, J. 1990. Geología y paleoambiente de la cantera Tlayúa. Tepexi de Rodríguez, estado de Puebla. *Revista Mexicana de Ciencias Geológicas*, **9**, 156-169.

PARK, M.-H. and FÜRSICH, F. T. 2001. Solnhofen. *International Journal of Earth Sciences (Geologische Rundschau)*, **90**, 847-854.

PAUL, C. R. C., LAMOLDA, M. A., MITCHELL, S. F., VAZIRI, M. R., GOROSTIDI, A. and MARSHALL, J. D. 1999. The Cenomanian-Turonian boundary at Eastbourne (Sussex, UK): a proposed European reference section. *Palaeogeography, Palaeoclimatology, Palaeoecology*, **150**, 83-121.

PERVINQUIERE, L. 1907. Études de paléontologie tunisienne 1: Céphalopodes des terrains sécondaires. *Carte Géologique de Tunisie*, De Rudeval, Paris, v+438 pp.

PETRASCHECK, W. 1902. Die Ammoniten der sächsischen Kreideformation. *Beiträge zur Paläontologie und Geologie Österreich-Ungarns*, **14**, 131-162.

PETSCHICK, R. 2001. MacDiff 4.2.5. *http://servermac.geologie.uni-frankfurt.de/Staff/Homepages/Petschick/RainerE.html#MacDiff*.

POLLASTRO, R. M. 1985. Mineralogical and morphological evidence for the formation of illite at the expense of illite/smectite. *Clay and Clay Minerals*, **33**, 265-274.

POWELL, J. D. 1963. Cenomanian-Turonian (Cretaceous) ammonites from Trans-Pecos Texas and northeastern Chihuahua, Mexico. *Journal of Paleontology*, **37**, 09-323.

PRÉVÔT, L. and LUCAS, J. 1990. Phosphate. 256-257. *In* BRIGGS, D. E. G. and CROWTHER, P. R. (eds). *Palaeobiology*. Blackwell scientific Publications, Oxford, 583 pp.

REESIDE, J. B. 1923. A new fauna from the Colorado Group of Southern Montana. *United States Geological Survey Professional Paper*, **132**, 25-33.

RENZ, O. 1982. *The Cretaceous Ammonites of Venezuela*. Birkhäuser Verlag, Basel, 132 pp.

REYMENT, R. A. 1954. Some new Upper Cretaceous ammonites from Nigeria. *Colonial Geology and Mineral Ressources, London*, **4**, 248-270.

ROBASZYNSKI, F. and CARON, M. 1979. Atlas de foraminifères planctoniques du Crétacé moyen (Mer Boréale et Téthys). *Cahiers de Micropaléontologie*, **1979**, 1-185; 182, 181-181.

——— CARON, M., DUPUIS, C., AMEDRO, F., GONZALES DONOSO, J.-M., LINARES, D., HARDENBOL, J., GARTNER, S., CALANDRA, F. and DELOFFRE, R. 1990. A tentative integrated stratigraphy in the Turonian of Central Tunisia: Formations, zones and sequential stratigraphy in the Kalaat Senan area. *Bulletin du Centre des Recherches et Exploration Production de Elf-Aquitaine*, **14**, 213-384.

ROMAN, F. 1938. *Les ammonites jurassiques et crétacées. Essai de généra*. Masson, Paris, 554 pp.

SALISBURY, S., FREY, E., MARTILL, D. M. and BUCHY, M.-C. 2003. *A new crocodilian from the Lower Cretaceous Crato Formation of north-eastern Brazil*. 63rd annual meeting, Society of Vertebrate Paleontology, Minnesota, *Journal of Vertebrate Paleontology*, **23 (3, suppl.)**, 92.

SAWLOWICZ, Z. 2000. Framboids; from their origin to application. *Prace Mineralogiczne*, **88**, 1-80.

SCHÄFER, W. 1962. *Ecology and palecology of marine environments*. University of Chicago Press, Chicago.

SCHLANGER, S. O. and JENKYNS, H. C. 1976. Cretaceous oceanic anoxia events: causes and consequences. *Geologie en Mijnbouw*, **55**, 179-184.

SCHLANGER, S. O., JENKYNS, H. C. and PREMOLI SLIVA, I. 1981. Volcanism and vertical tectonics in the Pacific Basin related to global Cretaceous transgressions. *Earth and Planetary Science Letters*, **52**, 435-449.

——— ARTHUR, M. A., JENKYNS, H. C. and SCHOLLE, P. A. 1987. The Cenomanian-Turonian anoxic event: I. Stratigraphy and distribution of organic-rich beds and the marine ¹³C excursion. *Geological Society of London, Special Publication*, **26**, 371-399.

SCHLOTHEIM, E. T. 1813. Beiträge zur Naturgeschichte der Versteinerungen in geognistischer Hinsicht. *Leonhard's Taschenbuch für Mineralogie*, **5**, 93.

SCHLÜTER, C. 1871. Cephalopoden der oberen deutschen Kreide. *Palaeontographica*, **21**, 1-24, plates 1-8 (1871)**; 21**, 25-120, plates 9-35 (1872); **24**, 1-144 (121-264)+x, plates 36-55 (1876).

SCHOENHERR, P. 1988. *Litho- und Microbiostratigraphie der Mittel- und Oberkreide Nordmexikos (Alb bis Campan)*. PhD thesis, Hannover, 178 pp.

SCHRAG, D. P., DePAOLO, D. J. and RICHTER, F. M. 1995. Reconstructing past sea surface temperatures: correcting for diagenesis of bulk marine carbon. *Geochimica et Cosmochimica Acta*, **59**, 2265-2278.

SEELING, J. and BENGTSON, P. 2002. Palaeobiogeography of the upper Cenomanian-lower Turonian macroinvertebrates of the Sergipe Basin, northeastern Brazil. *Schriftenreihe der Erdwissenschaftlichen Kommissionen der Österreichischen Akademie der Wissenschaften*, **15**, 151-168.

SEIBERTZ, E. 1985. Paleogeography of the San Felipe Formation (mid-Cretaceous, NE Mexico) and facial effects upon the inoceramids of the Turonian/Coniacian transition. *Zentralblatt für Geologie und Paläontologie*, **9/10**, 1171-1181.

——— 1998. Evolution of the mid-Cretaceous in northern Mexico under paleoceanographic aspects. *Revista Mexicana de Ciencias Geológicas*, **15**, 87-90.

——— and BUITRÓN, B. 1987. Paleontología y estratigrafía de los *Neohibolites* del Albiano de Tepexi de Rodríguez. *Revista de la Sociedad Mexicana de Paleontología*, **1**, 285-299.

SEILACHER, A. 1982. Ammonite shells as habitats in the Posidonia Shales of Holzmaden - floats or benthic islands? *Neues Jahrbuch für Geologie und Paläontologie, Monatshefte*, **1982**, 98-114.

SEITZ, O. 1935. Die Variabilität des *Inoceramus labiatus* v. Schloth. *Jahrbuch der Preußischen Geologischen Landesanstalt*, **55**, 429-474.

SHIMADA, K. 1996. Selachians from the Fort Hays limestone member of the Niobrara Chalk (Upper Cretaceous), Ellis County, Kansas. *Transactions of the Kansas Academy of Science*, **99**, 1-15.

DA SILVA SANTOS, R. 1985. *Araripichthys castilhoi*, novo genero e especie de Teleostei da Formaçao Santana, Chapada do Araripe, Brazil. 133-139. *In* MACHADO BRITO, I. (ed.). Cletanea de trabalhos paleontologicos. *Serie Geologia, Seçao Paleontologia e Estratigrafia*, **27**.

SOHL, N. F., MARTINEZ, R. E., SALMERÓN-UREÑA, P. and SOTO-JARAMILLO, F. 1991. Upper Cretaceous. 205-215. *In* SALVADOR, A. (ed.). The Gulf of Mexico Basin. *The Geology of North America*, **J**, Geological Society of America, Boulder, Colorado, 557 pp.

SORNAY, J. 1980. Inocérames (Bivalvia) du Turonien Inférieur de Colombie (Amérique du Sud). *Annales de Paléontologie (Invertebrés)*, **67**, 135-144.

SOTO-JARAMILLO, F. 1981. Zonificación microfaunistica del Cañon de la Borrega, Tamaulipas. *Revista del Instituto mexicano de Petróleo*, **8**, 7-23.

SOWERBY, J. 1826-1829. *The Mineral Conchology of Great Britain*. **6**, B. Meredith, London, 235 pp.

——— 1841-46. *The Mineral Conchology of Great Britain*. **7**, B. Meredith, London.

SPATH, L. F. 1922. On the Senonian ammonite fauna of Pondoland. *Transactions of the Royal Society of South Africa*, **10**, 113-148.

STELCK, C. R., MOORE, W. E. and PEMBERTON, S. G. 2002. Early Turonian (Late Cretaceous) age of the Tuskoola sandstone Pine River area, northeastern British Columbia. *Canadian Journal of Earth Sciences*, **39**, 1783-1793.

STINNESBECK, W. 1986. Zu den faunistischen und palökologischen Verhältnissen in der Quiriquina Formation (Maastrichtium) Zentral-Chiles. *Palaeontographica*, **A194**, 99-237.

——— IFRIM, C., SCHMIDT, H., RINDFLEISCH, A., BUCHY, M.-C., FREY, E., GONZÁLEZ GONZÁLEZ, A. H., VEGA-VERA, F. J., PORRAS-MUZQUIZ, H., CAVIN, L., KELLER, G. and SMITH, K. T. 2005. A new lithographic limestone deposit in the Upper Cretaceous Austin Group at El Rosario, county of Muzquiz, Coahuila, northeastern Mexico. *Revista Mexicana de Ciencias Geológicas*, **22**, 401-418.

STOLICZKA, F. 1863-1866. Ammonitidae, with revision of the Nautilidae. (1), 41-56, pls 26-31 (1863); (1862-1865), 1857-1106, pls 1832-1854 (1864); (1866-1869), 1107-1154, pls 1855-1880 (1865); (1810-1813), 1155-1216, pls 1881-1894 (1866). *In* STOLICZKA, F. (ed.). The fossil cephalopoda of the Cretaceous rocks of southern India. *Memoirs of the Geological Survey of India, Palaeontologia indica (series 3)*, **1**.

TAVERNE, L. 1977. Ostéologie et position systématique du genre *Thrissops* Agassiz, 1833 (sensu stricto) (Jurassique supérieur de l'Europe occidentale) au sein de Téléostéens primitifs. *Geobios*, **10**, 5-33, [in French].

TAYLOR, P. D. and WILSON, M. A. 2003. Palaeoecology and evoltion of marine hard substrate comunities. *Earth-Science Reviews*, **62**, 1-103.

THOMAS, P. and PERON, A. 1889-1893. *Description des mollusques fossiles des Terrains Crétacées de la région sud des Haut-Plateaux de la Tunisie recueillis en 1885 et 1886 par M. Phillippe Thomas. Exploration Scientifique de la Tunisie*, Masson, Paris, xii+405 pp.

TRÖGER, K.-A. 1967. Zur Paläontologie, Biostratigraphie und faziellen Ausbildung der unteren Oberkreide (Cenoman bis Turon), Teil I, Paläontologie und Biostratigraphie der Inoceramen des Cenomans bis Turons Mitteleuropas [in German]. *Abhandlungen des Staatlichen Museums für Mineralogie und Geologie zu Dresden*, **12**, 12-207.

TSIKOS, H., JENKYNS, H. C., WALSWORTH-BELL, B., PETRIZZO, M. R., FORSTER, A., ERBA, E., PREMOLI SLIVA, I., BAAS, M. and SINNIGHE DAMSTÉ, J. S. 2004. Carbon-isotope stratigraphy recorded by the Cenomanian-Turonian Oceanic Anoxic Event; correlation and implications based on three key localities. *Journal of the Geological Society of London*, **161**, 711-719.

TUCKER, M. E. 1991. *Sedimentary Petrology*. Blackwell Science, Oxford, 260 pp.

———. 1996. *Methoden der Sedimentologie*. Ferdinand Enke Verlag, Stuttgart, 366 pp.

VEGA, F. J., GARCÍA-BARRERA, P., COUTIÑO, M., NYBORG, T., CIFUENTES.RUIZ, P., GONZÁLEZ RODRIGUEZ, K., MARTENS, A., DELGADO, C. R. and CARBOT, G. 2003. Early Cretaceous Arthropods from plattenkalk facies in Mexico. *Contributions to Zoology*, **72**, 187-189.

VEGA, F. J., GARCÍA-BARRERA, P., COUTIÑO, M., NYBORG, T., CIFUENTES.RUIZ, P., GONZÁLEZ RODRIGUEZ, K., MARTENS, A., DELGADO, C. R. and CARBOT, G. 2003. Early Cretaceous Arthropods from plattenkalk facies in Mexico. *Contributions to Zoology*, **72**, 187-189.

VILLAMIL, T. and ARANGO, C. 1998. Integrated stratigraphy of latest Cenomanian and early Turonian facies of Colombia. 129-159. *In* PINDELL, J. L. and DRAKE, C. L. (eds). Paleogeographic Evolution and Non-Glacial Eustasy, Northern South America. *Society of Economic Paleontologists and Mineralogists Special Publication*, **58**.

VOIGT, S. 1996. Paläobiogeographie oberkretazischer Inoceramen und Rudisten- Ozeanographische und klimatologische Konsequenzen einer neuen Paläogeographie. *Münchner Geowissenschaftliche Abhandlungen*, **31, Reihe A**, 101.

WALASZCZYK, I. 1992. Turonian through Santonian deposits of the Central Polish Uplands; their facies development, inoceramid paleontology and stratigraphy. *Acta Geologica Polonica*, **42**, 1-122.

WANI, R., KASE, T., SHIGETA, Y. and DE OCAMPO, R. 2005. New look at ammonoid taphonomy, based on field experiments with modern chambered nautilus. *Geology*, **33**, 849-852.

WARD, P. D. 1981. Shell sculpture as a defensive adaptation in ammonoids. *Paleobiology*, **7**, 96-100.

WARREN, P. S. 1930. New species of fossils from Smoky River and Dunvegan Formations, Alberta. *Report of the Research Council of Alberta*, **21**, 57-68.

WEST, O. L. 1993. *Do foraminifera in sulfide-rich environments harbor symbiotic chemautotrophic bacteria?* 4th East Coast Conference on Protozoa, *Abstracts with Programme*, 9.

WESTERMANN, G. E. G. 1996. Ammonoid life and habitat. 607-707. *In* DAVIS, R. A. (ed.). *Ammonoid Paleobiology. Topics in Geobiology*, **13**, Plenum, New York, London.

WETZEL, A. 1991. Stratification in Black Shales: Depositional models and timing - an overview. 508-523. *In* EINSELE, G., RICKEN, W. and SEILACHER, A. (eds). *Cycles and Events in Stratigraphy.* Springer-Verlag, Berlin, 955 pp.

WHITE, I. C. 1913. Petroleum fields of northeastern Mexico between the Tameso and Tuxpan Rivers. *Geological Society of America Bulletin*, **24**, 253-274.

WILKIN, R. T., ARTHUR, M. A. and DEAN, W. E. 1997. History of water-column anoxia in the Black Sea indicated by pyrite framboid size distributions. *Earth and Planetary Science Letters*, **148**, 517-525.

——— BARNES, H. L. and BRANTLEY, S. L. 1996. The size and distribution of framboidal pyrite in modern sediments: An indicator of redox conditions. *Geochimica et Cosmochimica Acta*, **60**, 3897-3912.

WILSON, M. V. and CHALIFA, Y. 1989. Fossil marine actinopterygian fishes from the Kasapau Formation (Upper Cretaceous: Turonian) near Watino, Alberta. *Canadian Journal of Earth Sciences*, **26**, 2604-2620.

WINDLEY, B. F. 1995. *The evolving continents*. Wiley, New York,, 526 pp.

WRIGHT, C. W. 1952. A classification of the Cretaceous ammonites. *Journal of Paleontology*, **26**, 213-222.

——— and KENNEDY, W. J. 1981. The ammonoidea of the Plenus Marls and the Middle Chalk. *Monograph of the Palaeontographical Society*, **134**, 148 pp.

——— CALLOMAN, J. H. and HOWARTH, M. K. 1996. *Cretaceous Ammonoidea. Treatise of Invertebrate Paleontology*, **Part L, Mollusca 4**, University of Kansas & Geological Society of America, xx+362 pp.

ZABORSKI, P. M. P. 1987. Lower Turonian (Cretaceous) ammonites from south-east Nigeria. *Bulletin of the British Museum of Natural History (Geology)*, **41**, 31-66.

——— 1995. The Upper Cretaceous ammonite *Pseudaspidoceras* Hyatt, 1903, in north-eastern Nigeria. *Bulletin of the British Museum of Natural History (Geology)*, **51**, 53-72.

——— 1996. The Upper Cretaceous ammonite *Vascoceras* Choffat, 1898 in north-eastern Nigeria. *Bulletin of the British Museum of Natural History (Geology)*, **52**, 61-89.

ZITTEL, K. A. 1884. Cephalopoda. (Abteilung 2, Lieferung 3), 329-522. *Handbuch der Paläontologie*. **1**, R. Oldenburg, München, Leipzig, 893 pp.

——— 1895. *Grundzüge der Paläontologie*. Oldenburg, viii+971 pp.

APPENDIX A: RESULTS OF THE XRD ANALYSIS

Sample	Phyllo-silicates	Gypsum	Goethite	Hematite	Quartz	Alkali-feldspar	Plagioclase	Calcite	Dolomite	Pyrite
°2θ	± 19,8	11,6	21,20	24,1	26,7	27.5	<<27.9	29,4	30,8	56,3
VC1+2	117	0	19	0	592	0	0	1159	0	0
VC1-13	12	0	0	0	872	0	0	3577	0	0
VC1-24	27	0	72	21	401	0	0	2781	13	16
VC1-33	17	0	0	0	1215	0	0	3077	0	0
VC1-43	103	0	0	25	6564	0	22	93	0	0
VC1-54	20	0	39	0	941	0	0	2513	0	0
VC1-66	18	0	10	0	431	0	0	3141	0	0
VC1-74	46	0	38	0	1343	0	0	3578	0	0
VC1-90	14	0	0	0	896	0	0	3302	0	0
VC1-99	21	0	0	0	607	0	0	2284	0	0
VC1-114	13	0	0	0	770	0	21	2924	0	0
VC2-37	26	0	0	0	454	0	38	4634	0	0
VC2-47	16	0	0	0	499	0	0	3622	0	0
VC2-63	31	0	0	0	590	0	42	3783	0	0
MT-1	47	0	20	21	905	0	143	2303	0	0
MT-9	32	0	9	0	326	0	243	3059	0	0
MT-15	170	0	0	0	1009	73	621	248	0	0
MT-21	23	0	0	0	467	0	145	3351	0	0
MT-26	10	0	0	0	4368	0	67	3103	0	0
MT-57	22	0	0	0	2614	0	0	3522	0	0
MT-74	15	0	0	9	1176	0	149	1690	0	0

Table A2. Peak intensities [cps] of random powder samples.
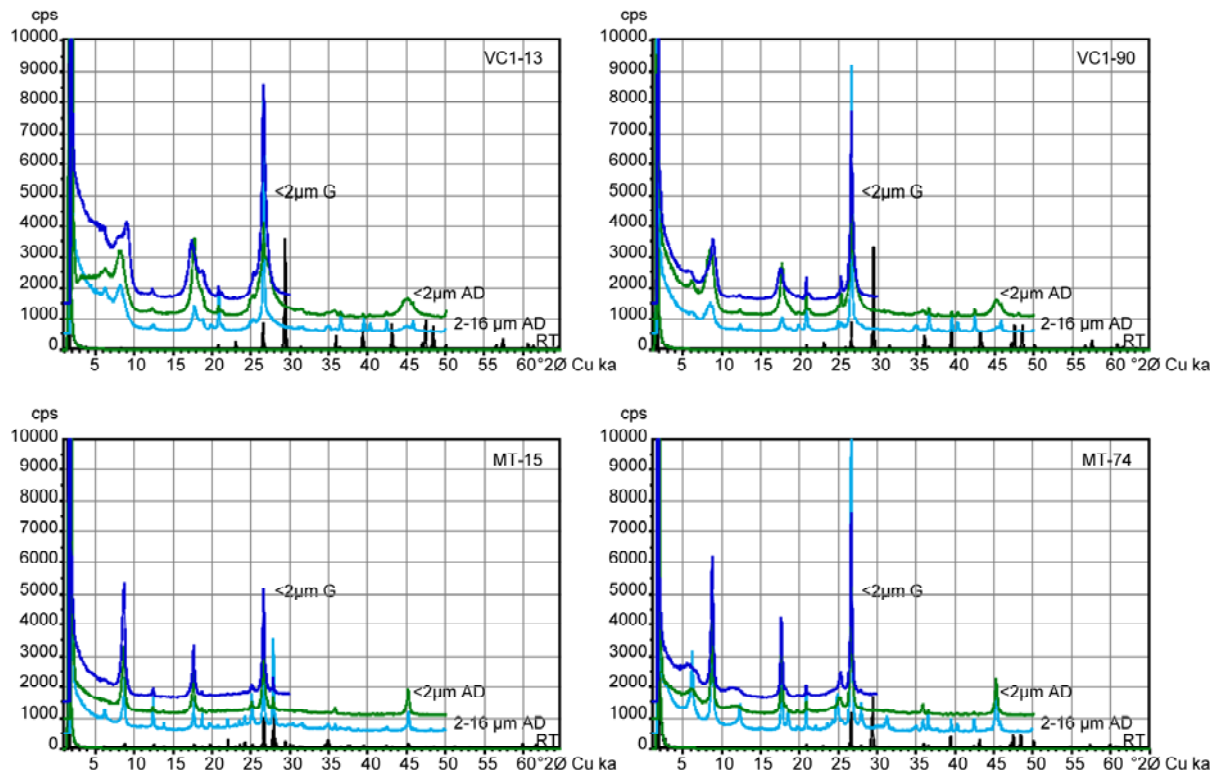
Figure J. Unfiltered diffractograms of selected samples.

Sample	Chl/Smc001	Ill/Smc001	Kao001+Chl002	Ill002	Chl003	Qtz	Kao002	Chl004	Qtz101/Ill003	Kfs	Plg
°2θ	6	8,8	12,3	17,7	18,3	20,85	24,9	25,1	26,64	27,5	27,9
VC1+2	67	707	252	539	119	620	255	107	3338	198	0
VC1-13	391	917	166	749	315	1284	159	218	7147	256	0
VC1-24	208	516	141	452	132	1107	122	148	5961	161	90
VC1-33	188	1278	178	850	125	1858	202	153	10478	0	180
VC1-43	249	299	103	167	102	3094	87	95	13502	0	51
VC1-54	153	275	0	668	0	1296	59	132	7152	278	0
VC1-66	122	606	57	561	84	936	62	296	5269	149	116
VC1-74	252	165	238	267	116	776	244	209	3907	100	80
VC1-90	131	657	173	443	82	1555	182	191	8473	0	878
VC1-99	262	176	47	209	97	1155	54	115	6373	127	0
VC1-114	0	69	39	42	0	1367	73	75	5903	96	137
VC2-37	177	338	133	368	81	908	132	234	4735	0	255
VC2-47	0	212	155	182	0	1456	181	119	6835	0	200
VC2-54	125	237	163	181	58	1713	143	154	8582	0	376
VC2-63	257	205	55	246	103	734	44	155	3853	125	157
MT-1	1116	7980	351	6565	247	587	343	115	12114	0	445
MT-15	269	1491	996	936	464	92	0	972	2064	0	2751
MT-21	1004	1231	3383	631	1332	618	0	3047	4325	0	837
MT-26	406	265	230	128	147	2401	0	399	12657	0	271
MT-44	109	1222	50	698	125	178	0	250	2151	0	68
MT-57	429	70	894	44	437	1637	0	1059	8798	0	0
MT-67	476	3426	148	2258	99	366	0	211	5359	0	70
MT-74	2013	4082	730	2466	530	1154	1013	190	9709	0	726
MT-77	367	3321	1104	1792	475	679	0	911	6223	0	323
MT-9	739	4001	78	4091	0	267	72	71	5940	0	602

Table A3. Peak intensities [cps] of decarbonated samples, fraction 2…16μm.

Sample	Smc001	Chl001	Ill001	IS001+Smc002	Kao001+Chl002	Ill002	Chl003	Qtz	Kao002	Chl004	Qtz101+Ill003
°2θ	5,2	6,2	8,8	9…10	12,3	17,7	18,3	20,85	24,9	25,1	26,64
VC1+2	0	114	3152	150	240	1341	95	239	191	134	3110
VC1-13	228	390	1856	1691	205	1556	653	354	115	527	6435
VC1-24	307	301	548	957	127	1021	376	278	153	291	4899
VC1-33	0	76	853	181	503	498	111	1194	182	260	7278
VC1-43	0	1181	1112	0	142	528	448	1495	0	316	9462
VC1-54	266	0	447	0	66	302	74	1195	0	213	5499
VC1-66	0	53	0	431	40	311	67	390	0	215	2844
VC1-90	0	214	1629	0	90	891	182	689	102	592	5871
VC1-99	473	468	0	514	80	564	277	259	0	235	3048
VC2-37	612	0	1687	0	133	1015	149	417	111	496	4848
VC2-47	81	0	473	0	85	267	0	579	72	242	3063
VC2-54	515	59	600	0	112	311	64	728	111	321	4383
VC2-63	364	0	0	262	49	240	68	317	55	168	2352
MT-1	874	170	4779	0	53	3420	104	254	74	123	11620
MT-9	1624	0	7327	0	0	4266	0	135	0	0	11891
MT-15	0	73	3452	0	249	1670	126	28	0	268	3319
MT-21	0	658	2029	0	2559	921	1093	216	0	2730	2716
MT-26	0	64	179	0	68	204	117	451	0	337	2295
MT-30	2629	0	1902	0	72	1436	0	244	0	321	5939
MT-36	0	157	496	0	657	367	346	119	0	1072	1296
MT-44	0	160	1965	0	43	903	50	202	0	248	2516
MT-47	419	0	2665	0	169	1573	103	93	0	307	4181
MT-57	0	290	105	0	593	53	268	258	0	622	1259
MT-67	589	279	3703	0	121	1902	80	319	0	245	6069
MT-74	0	375	4208	0	177	2518	240	323	0	648	5765
MT-77	0	118	1795	0	488	1447	274	161	0	625	3893

Table A4. Peak intensities [cps] of decarbonated samples, fraction <2μm.

APPENDIX B: RESULTS OF THE EDX ANALYSIS

	CaO [%]	TiO2 [%]	MnO [%]	Fe2O3 [%]	Ni [ppm]	Cu [ppm]	Zn [ppm]	As [ppm]	Br [ppm]	Rb [ppm]	Sr [ppm]
detection limit	<0.1	<0.02	<0.02	<0.02	<20	<7	<5	<5	<3	<2	<2
VC1-006	26,22	0,24	0,03	1,63	32	41	12	7	27	48	627
VC1-010	26,29	0,28	0,03	1,54	84	45	34	11	8	50	664
VC1-013	33,53	0,14	0,02	1,52	47	32	15	13	27	31	440
VC1-018	25,72	0,30	0,02	2,25	74	53	47	18	15	61	611
VC1-024	25,72	0,23	<0.02	20,85	262	184	332	173	27	23	341
VC1-029	32,30	0,08	<0.02	0,56	110	177	60	6	4	17	421
VC1-034	25,67	0,16	0,06	0,97	139	46	186	9	7	37	390
VC1-037	6,53	0,29	0,02	1,25	85	44	260	10	5	56	186
VC1-044	3,55	0,32	<0.02	29,47	343	211	1192	287	<3	99	107
VC1-045	23,59	0,11	0,02	0,94	30	17	72	7	<3	29	532
VC1-050	21,89	0,12	<0.02	0,95	29	17	48	8	<3	29	475
VC1-056	33,81	0,15	0,05	2,50	164	33	192	28	5	25	486
VC1-060	24,60	0,12	0,03	1,12	103	145	37	17	7	30	542
VC1-069	35,63	0,10	0,03	0,65	45	31	42	10	25	25	662
VC1-076	32,65	0,09	<0.02	0,52	44	37	105	7	4	22	439
VC1-078	27,73	0,07	<0.02	0,64	85	169	53	<5	3	19	593
VC1-082	32,32	0,14	0,02	1,35	41	41	112	12	<3	24	577
VC1-086A	33,52	0,13	0,02	1,10	50	28	173	10	<3	30	662
VC1-088	33,85	0,08	0,02	0,64	44	31	72	7	<3	16	710
VC1-094	31,72	0,13	0,02	1,25	44	35	148	7	<3	28	755
VC1-100	9,01	0,98	<0.02	22,73	313	176	1619	97	4	85	129
VC1-101	27,16	0,10	0,02	0,75	98	171	167	<5	<3	28	545
VC1-106	34,57	0,07	0,02	0,62	33	7	49	5	5	16	679
VC1-112	29,15	0,08	<0.02	0,60	24	14	77	<5	9	23	655
VC2-034	29,65	0,14	0,02	1,01	42	50	458	10	<3	29	879
VC2-037	36,51	0,28	0,04	3,12	98	53	364	29	19	25	769
VC2-041	27,29	0,08	<0.02	1,84	37	37	144	17	22	23	774
VC2-046	33,04	0,22	0,03	1,17	52	46	1192	10	<3	42	672
VC2-049	38,65	0,26	0,03	4,14	96	67	348	41	<3	23	392
VC2-053	32,88	0,09	0,02	0,68	51	24	116	8	<3	22	710
VC2-056	36,35	0,10	0,03	2,18	64	35	150	13	<3	14	729
VC2-060A	33,70	0,08	<0.02	0,73	33	34	148	7	<3	16	887
VC2-063	30,51	0,12	<0.02	0,91	41	19	245	6	<3	27	727
VC2-065	31,86	0,13	0,02	1,63	53	27	212	18	4	23	745
VC2-066	29,01	0,09	<0.02	0,71	37	24	134	7	<3	22	703
MT-02	37,99	0,07	0,15	1,61	76	15	67	<5	<3	10	785
MT-08	34,00	0,11	0,06	2,11	51	31	86	9	<3	23	822
MT-15	2,02	0,26	<0.02	2,02	<20	14	118	<5	<3	109	190
MT-21	38,43	0,07	0,04	2,31	52	21	90	5	<3	16	833
MT-22	36,86	0,06	0,05	1,97	44	27	99	<5	<3	14	799
MT-23	35,59	0,12	0,04	1,61	131	232	216	11	4	28	870
MT-23A	32,60	0,09	0,03	1,46	49	59	77	8	<3	22	788
MT-24	32,76	0,11	0,04	2,59	65	36	149	<5	<3	21	886
MT-25	28,66	0,06	0,03	1,45	57	38	96	9	<3	18	758
MT-26	22,45	0,07	0,03	2,75	72	17	154	14	<3	8	536
MT-27	38,85	0,07	0,04	0,87	51	<7	54	<5	<3	22	1119
MT-28	12,53	0,30	0,02	2,45	59	39	250	11	<3	38	328
MT-29	16,18	0,10	0,02	1,60	56	37	43	8	<3	15	385
MT-30	36,51	0,19	<0.02	1,28	72	44	60	6	6	22	569
MT-31	0,98	0,56	<0.02	3,23	122	109	138	14	<3	92	80
MT-32	0,94	0,77	<0.02	4,84	197	230	211	11	4	123	115
MT-33	1,33	1,16	<0.02	7,10	239	137	318	32	<3	111	146
MT-34	26,81	0,07	0,07	1,92	114	151	40	6	<3	11	478
MT-36	29,33	0,24	0,08	5,00	130	64	74	6	<3	16	528
MT-38A	8,75	1,07	0,04	6,68	163	168	176	6	<3	73	267
MT-41	13,36	0,26	0,04	3,76	86	54	42	5	<3	37	208
MT-44	6,32	0,65	0,02	5,38	111	108	66	13	<3	68	157
MT-47	35,97	0,24	0,06	1,91	68	56	44	5	<3	33	827
MT-49	15,56	0,81	0,04	8,16	121	194	112	10	<3	45	274
MT-52	10,62	1,16	0,02	5,60	101	250	129	8	<3	88	318
MT-58	11,49	0,38	<0.02	33,54	171	629	161	34	5	9	1045
MT-67	13,22	0,36	<0.02	2,74	61	42	168	9	3	64	343
MT-71	26,15	0,18	0,02	1,36	93	172	151	8	5	31	469
MT-72	8,75	0,34	<0.02	2,34	39	18	166	7	<3	133	289
MT-73	19,94	0,07	<0.02	0,78	23	22	173	8	<3	17	500
MT-74	25,26	0,16	<0.02	1,21	42	19	77	8	<3	34	545
MT-75	25,32	0,13	<0.02	0,94	39	27	340	<5	<3	27	513
MT-76	37,27	0,06	0,03	1,13	45	17	69	7	<3	13	739
MT-77	33,48	0,14	<0.02	0,96	32	33	539	8	<3	33	855

(continued)

sample	Y [ppm]	Zr [ppm]	Nb [ppm]	Mo [ppm]	Ag [ppm]	Cd [ppm]	Sn [ppm]	Ba [ppm]	La [ppm]	Ce [ppm]	Pb [ppm]	Ga [ppm]
limit	<3	<5	<2	<5	<1	<1	<2	<10	<10	<10	<5	<5
VC1-006	15	58	6	5	<1	<1	<2	244	23	28	28	6
VC1-010	13	57	4	<5	<1	<1	3	298	<10	12	38	8
VC1-013	14	46	<2	5	2	1	4	175	<10	37	20	6
VC1-018	19	86	4	6	<1	<1	3	311	27	47	34	6
VC1-024	4	36	<2	39	<1	<1	<2	235	20	28	123	9
VC1-029	15	26	<2	<5	<1	2	<2	106	17	28	12	12
VC1-034	12	49	<2	<5	1	<1	3	222	14	23	17	<5
VC1-037	7	54	<2	6	3	2	<2	328	18	38	10	7
VC1-044	8	175	<2	52	2	<1	4	595	11	9	201	24
VC1-045	13	39	2	<5	<1	<1	<2	192	23	36	20	7
VC1-050	13	36	4	<5	1	<1	<2	194	13	23	20	<5
VC1-056	18	75	<2	5	<1	<1	<2	205	16	25	16	<5
VC1-060	11	39	<2	<5	2	<1	<2	182	21	25	19	8
VC1-069	14	39	2	<5	<1	<1	3	242	15	19	9	<5
VC1-076	10	31	3	<5	1	<1	2	164	16	29	13	<5
VC1-078	10	27	<2	<5	<1	<1	<2	118	12	10	11	11
VC1-082	12	42	<2	<5	1	<1	3	149	19	29	6	<5
VC1-086A	16	52	3	<5	<1	<1	<2	155	<10	6	12	<5
VC1-088	9	27	<2	<5	1	1	<2	114	15	12	5	<5
VC1-094	10	45	<2	<5	<1	3	<2	162	<10	31	21	7
VC1-100	13	305	7	53	<1	<1	<2	571	11	<5	145	26
VC1-101	7	40	<2	<5	3	1	<2	292	14	15	13	9
VC1-106	9	24	<2	<5	<1	<1	<2	116	22	33	6	<5
VC1-112	7	33	<2	<5	2	<1	<2	333	10	11	7	<5
VC2-034	11	48	3	<5	3	4	<2	186	12	22	6	6
VC2-037	15	59	<2	9	2	2	3	286	<10	32	19	6
VC2-041	12	37	<2	<5	1	1	<2	182	18	44	26	<5
VC2-046	12	63	<2	<5	2	20	3	228	<10	14	12	12
VC2-049	8	61	4	<5	1	2	<2	169	<10	10	39	<5
VC2-053	8	37	<2	<5	<1	<1	<2	169	<10	24	5	<5
VC2-056	8	37	3	5	2	<1	<2	164	23	44	10	6
VC2-060A	8	33	<2	<5	2	<1	<2	155	<10	12	<5	6
VC2-063	9	44	<2	<5	1	4	<2	238	<10	19	<5	<5
VC2-065	10	40	<2	<5	2	<1	<2	220	13	<5	15	<5
VC2-066	9	31	<2	<5	3	<1	<2	177	<10	13	<5	<5
MT-02	8	27	<2	<5	<1	<1	<2	106	10	34	<5	6
MT-08	9	41	<2	<5	1	<1	<2	154	17	36	<5	<5
MT-15	9	204	<2	<5	<1	2	<2	736	<10	23	<5	23
MT-21	10	30	2	<5	<1	1	<2	114	<10	18	<5	<5
MT-22	8	31	<2	<5	<1	<1	<2	110	14	27	<5	<5
MT-23	6	36	<2	6	1	5	2	179	15	<5	<5	7
MT-23A	16	43	<2	<5	<1	2	<2	162	33	47	<5	<5
MT-24	10	54	4	<5	2	1	<2	143	14	32	9	9
MT-25	7	44	<2	<5	1	<1	<2	135	13	<5	<5	<5
MT-26	9	25	<2	<5	1	2	<2	62	<10	<5	6	5
MT-27	16	50	2	<5	<1	<1	<2	153	26	31	<5	7
MT-28	13	64	3	7	2	2	<2	255	<10	30	8	9
MT-29	15	36	3	<5	2	<1	2	122	15	33	<5	<5
MT-30	15	32	4	<5	2	<1	<2	165	21	25	<5	6
MT-31	23	93	5	<5	1	<1	<2	692	<10	25	5	12
MT-32	7	97	7	<5	<1	1	4	839	<10	10	11	19
MT-33	21	94	6	8	1	<1	2	889	20	33	13	24
MT-34	13	19	<2	<5	1	1	2	103	20	8	<5	11
MT-36	13	24	<2	<5	<1	<1	<2	181	<10	23	<5	<5
MT-38A	13	77	7	<5	1	1	<2	545	<10	38	<5	17
MT-41	14	39	<2	<5	<1	<1	<2	282	21	20	<5	10
MT-44	25	66	4	5	3	<1	<2	520	22	33	<5	10
MT-47	24	31	<2	<5	1	<1	<2	257	12	50	<5	9
MT-49	21	61	4	<5	1	2	2	326	<10	24	<5	8
MT-52	22	84	4	<5	<1	1	<2	623	13	16	<5	7
MT-58	17	38	<2	20	2	<1	<2	79	32	57	46	<5
MT-67	16	85	6	8	2	2	<2	408	<10	44	10	11
MT-71	9	44	<2	<5	1	<1	2	202	27	39	8	6
MT-72	19	190	7	5	<1	<1	4	972	45	77	<5	25
MT-73	11	29	<2	<5	<1	4	<2	142	<10	28	<5	<5
MT-74	11	50	<2	<5	<1	<1	<2	246	14	34	<5	<5
MT-75	11	34	3	5	1	4	2	187	10	<5	7	5
MT-76	10	36	<2	<5	1	<1	<2	104	11	27	<5	<5
MT-77	11	58	2	<5	2	10	<2	231	12	27	<5	<5

Table B1. Element quantification from EDX analysis.

139

APPENDIX C: TAXONOMIC DESCRIPTIONS OF THE VALLECILLO INOCERAMIDS AND AMMONITES

Vallecillo inoceramids and ammonites described here are housed in the collection of the Facultad de Ciencias de la Tierra of the Universidad Autónoma de Nuevo León in Linares, Nuevo León. Registration is UANL-FCT-VC (VC for Vallecillo). Other collections mentioned are BMNH: British Museum (Natural History), London; KU: Kansas University Museum of Invertebrate Palaeontology; MNHP: Muséum National d'Histoire Naturelle, Paris; SP: Sorbonne Collections, Paris (parts of the collection may have been transferred to the MNHP, see Chancellor et al., 1994, p. 18); USNM: U.S. National Museum, Washington, D.C.; UTA: University of Texas at Austin collections, housed in the Texas Memorial Museum, Austin, Texas.

Other abbreviations. All dimensions are given in mm. The use of morphologic terms for inoceramids is explained in Figure B. The abbreviations used for ammonites are: D: whorl diameter, WB: whorl breadth, WH whorl height, U: umbilical diameter. Dimensions in brackets are relative to D. L: lateral lobe. Ribs were counted from the given diameter downwards.
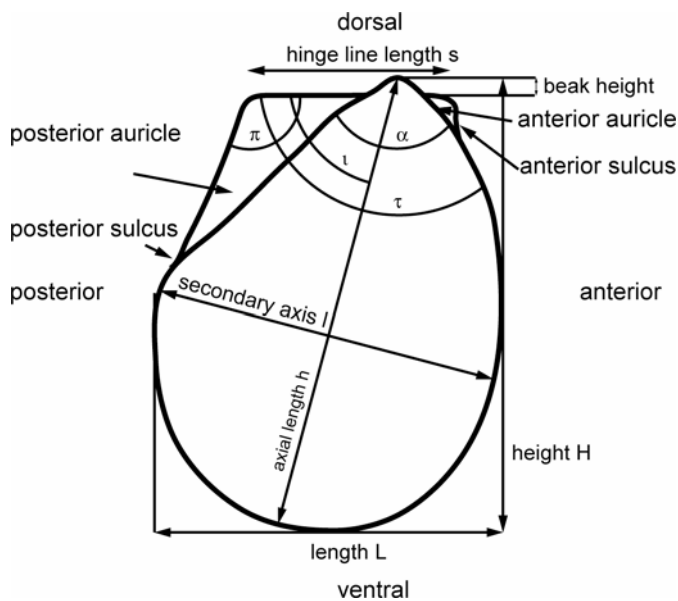
Figure K. Morphologic terms are based on Walaszczyk (1992), Harries *et al.* (1996) and Walaszczyk and Cobban (in Kennedy *et al.* 2000). τ
g   α: apical angle; π: posterodorsal angle; ι: inclination; RV: right valve; LV: left valve.

Systematics. The taxonomy of *Mytiloides* follows the view of Walaszczyk and Cobban (in Kennedy *et al.* 2000). Higher taxonomy follows the Treatise of Invertebrate Paleontology to family level (Cox 1969).Systematic nomenclature of ammonites follows the *Treatise of Invertebrate Paleontology* (Wright *et al.* 1996) to subgenus level.

Synonymies. The synonymy includes only the original description, some synonyms, and all references used for determination. More complete synonymy lists are indicated where possible.

Class BIVALVIA Linné, 1758 (Bouanni, 1681)

Subclass PTERIOMORPHA Beurlen, 1944

Order PTERIOIDA Newell, 1965

Suborder PTERIINA Newell, 1965

Superfamily PTERIACEA Gray, 1847

Family INOCERAMIDAE Giebel, 1852

Genus *Inoceramus* Sowerby, 1814

Type species. *Inoceramus cuvierii* Sowerby by subsequent designation of Cox (1969, p. N315). The genus is discussed by Kauffman *et al.* (1977) and Klinger *et al.* (1980).

Inoceramus pictus Sowerby, 1829

Type. The holotype is BMNH 43272 by original designation of Sowerby, 1829, p.215, pl. 604, fig. 1. It comes from the Lower Chalk near Guildford, England. A plastoholotype of *Inoceramus pictus pictus*, USNM 169393, was re-figured by Kauffman and Powell (in Kauffman *et al.* 1977, pl. 1, fig. 1).

Inoceramus pictus pictus Sowerby, 1829
Figure 7.10a-b

1829   *Inoceramus pictus* Sowerby, p. 215, pl. 604, fig. 1
1967   *Inoceramus pictus pictus* Sowerby; Tröger, p. 35, pl. 3, figs. 1-6
1977   *Inoceramus pictus pictus* Sowerby, Kauffman and Powell, in Kauffman, p. 55, pl 1, fig. 1
2000   *Inoceramus pictus pictus* Sowerby; Walaszczyk and Cobban, in Kennedy *et al.*, pl. 4, figs 1-6

Type. As for species.

Material. Fourteen specimens.

Description. The medium to large sized disc has a rounded oval outline and a short, straight to slightly rounded hinge line. The anterior margin is moderately long and slightly convex, and transists into a widely rounded ventral margin and a slightly convex posterior margin which is straight or concave at the posterior auricle. The growth axis is straight. The posterior auricle is moderately sized, but poorly separated from the disc. Juvenile growth stages are covered with evenly spaced microrugae. At later growth stages irregular rugae with rounded edges are added. The microrugae vanish at the transition to the adult growth stage. Both types of rugae are persistent towards the anterior and posterior margins but seem to affiliate, although this might be an effect of compression of the shell within the sediment.

Dimensions.

	L	H	L/H	l	h	l/h	s	s/h	τ	α	π	ι	
UANL-FCT VC530	70·3	72·1	0·98	68·7	78·1	0·88	37·7	0·48	120°	95°	120°	60°	RV
UANL-FCT VC522	90·5	97·0	0·93	84·2	114·0	0·74	66·2	0·58	110°	85°	115°	55°	LV
UANL-FCT VC521	95·0	116·0	0·82	100·5	120·8	0·83	57·8	0·48	120°	-	110°	70°	RV

Discussion. Tröger (1967) differentiates the subspecies of *Inoceramus pictus* through ontogenetic development of several shell features and measures (e.g. l/h or ι) during ontogeny. Our material resembles strongly the types described by Tröger (1967) and Kauffman and Powell (in Kauffman *et al.* 1977) with respect to ornamentation and measurement relationships.

Occurrence. Inoceramus pictus pictus is common in the uppermost Cenomanian of the Western Interior, the northern Gulf coast, and Western Europe (Kauffman *et al.* 1977).

Genus *Mytiloides* Brongniart, 1822

Type species. Ostracites labiatus Schlotheim (1813, p. 93). The genus is described by Walaszczyk (1992). A recent re-definition of the genus was rendered by Harries *et al.* (1996).

Mytiloides hattini Elder, 1991

Figure 7.10c

<div style="margin-left:2em">

1991   *Mytiloides hattini* Elder, p. 235, figs 3.1-3.9 (with full synonymy)

2000   *Mytiloides hattini* Elder, Walaszczyk and Cobban, in Kennedy *et al.* 2000, p. 320, pl. 4, figs 7-13; pl. 4, figs 1-10 (with additional synonymy)

</div>

Type. The holotype is KU 82132 by original designation of Elder (1991, fig. 3.13), from the upper part of the Hartland Shale Member of the Greenhorn Limestone, Hodgeman County, Kansas.

Material. Eight specimens.

Description The small to medium-sized disc with subquadrate outline. The anterior margin is moderately long and convex, and transists into a rounded ventral margin and into a straight to slightly convex posterior margin. The growth axis is straight or slightly convex anteriorly. The posterior auricle is small and poorly separated from the disc. The beak projects slightly over the hinge line. The ornament is composed of regularly to sub-regularly spaced microrugae.

Dimensions.	L	H	L/H	l	h	l/h	s	s/h	τ	α	π	λ	
UANL-FCT VC934	49	65	0·75	50	66	0·76	27	0·41	115	95	115	70	RV
UANL-FCT VCI/269	57	67	0·85	58	71	0·82	44	0·62	105	90	115	55	LV

Discussion. Mytiloides hattini is smaller than the other *Mytiloides* species described herein. The ornament consists only of regularly to subregularly spaced microrugae.

Occurrence. Latest Cenomanian *Neocardioceras juddii* to early Turonian *Vascoceras birchbyi* zone of the Western Interior Seaway, Texas, northern Mexico, southern England, Germany, Portugal and Kazakhstan (Walaszczyk and Cobban, in Kennedy *et al.* 2000).

Mytiloides puebloensis Walaszczyk and Cobban, 2000

Figures 5.10a-b, 7.10d

<div style="margin-left:2em">

p.1987   *Mytiloides columbianus* (Heinz); Kennedy *et al.*, text-fig. 9a-b (*non* 9c)

2000   *Mytiloides puebloensis* Walaszczyk and Cobban, in Kennedy *et al.* 2000, p. 321, pl. 6, figs 1-11; pl. 7, figs 2-3, 5-8, 12-15, pl. 8, figs 1-11, 13; pl. 10, figs 1, 4, 6-8 (with full synonymy)

</div>

Type. The holotype is USNM 507315 from the *Watinoceras devonense* zone of the lowermost Turonian.

Material. Seven specimens.

Description The small to medium-sized disc has a subquadrate outline and relatively short, straight hinge line. The anterior margin is moderately long and slightly convex, and transists into a narrowly rounded ventral margin and into a straight to slightly convex posterior margin. The growth axis is straight or slightly convex anteriorly. The posterior auricle is small and poorly separated from the disc. The beak projects slightly over the hinge line. Rugae are regularly spaced in the juvenile growth stage, with rounded edges, and covered with regular microrugae. Both types of rugae weaken towards the anterior and posterior margins. Microrugae weaken during the adult growth stage, whereas rugae become irregular and asymmetrical with steeper ventral slopes.

Dimensions.	L	H	L/H	l	h	l/h	s	s/h	τ	α	π	λ	
UANL-FCT VC182	73	82	0·89	67	90	0·74	33	0·37	135	118	136	53	
UANL-FCT VC025	80	98	0·82	105	115	0·91		0·00			115		
UANL-FCT VC531	45·7	58·5	0·78	45·0	61·8	0·73	27·8	0·45	95°	80°	130°	55°	LV
UANL-FCT VC554	91·3	90·8	1·01	67·5	109·5	0·62	41·3	0·38	100°	80°	130°	50°	LV

Discussion. Mytiloides puebloensis is similar in outline to *M. kossmati* and *M. goppelnensis*, but possesses a different type of ornament with microrugae during the juvenile growth stages and rugae that weaken and become irregular during the adult growth stage. *Mytiloides kossmati* is very regularly ornamented throughout ontogeny with double ridged rugae, whereas *M. goppelnensis* is similar to *M. kossmati*, but its ornament consists of raised single rugae.

Occurrence. Lowermost Turonian of Colorado, where it co-occurs with *M. goppelnensis* and *M. kossmati*. Other records are from Texas, Portugal, Spain, and Kazakhstan (Walaszczyk and Cobban, in Kennedy *et al.* 2000).

<div align="center">

Mytiloides goppelnensis Badillet and Sornay, 1980

Figure 7.11a

</div>

1935	*Inoceramus labiatus* var. *opalensis* Böse; Seitz, p. 457, pl. 39, fig.1
1977	*Mytiloides opalensis* (Böse); Kauffman, pl. 6,fig. 10
1980	*Inoceramus goppelnensis* nom. nov., Badillet and Sornay, p. 324
1991	*Mytiloides* sp., Kennedy and Cobban, p.17, text-fig. 11d-e
1991	*Mytiloides opalensis* (*sensu* Kauffman); Elder, text-fig. 4.3-4.5
p.1992	*Mytiloides kossmati* (Heinz), Walaszczyk, p. 10, pl. 1, figs 1-8 (*non* fig. 9)
2000	*Mytiloides goppelnensis* Badillet and Sornay; Walaszczyk and Cobban, in Kennedy *et al.*, p. 323, pl. 7, figs 9-11; pl. 8, figs 12, 14; pl. 9, figs 1-3; pl.10, figs 2, 5, 9-10, 12; pl. 11, figs 2, 5, 7, 10; p. 12, fig. 6; pl. 13, fig. 6 (with full synonymy)

Type. The holotype is No. 78 of Seitz (1935, pl. 39, fig.4, text-figs 14c, 15) by original designation. It comes from Goppeln near Dresden, Germany.

Material. Four specimens.

Description. The inequilateral shell is subquadrate to elongated oval in outline. The disc is poorly separated from the posterior auricle. The beaks projects slightly over the hinge line, which is straight and short to moderately long. The long anterior margin is slightly convex and passes into a rounded ventral margin and then into a weakly convex, almost straight posterior margin. The juvenile ornament consists of variably spaced, single rugae that weaken towards the margins.

Dimensions. UANL-FCT VC595. L: 89; H: 88; L/H: 1·01; l: 70; h: 92; l/h: 0·76; s: 44; s/h: 0·48; τ: 105°; α: 90°; π: 130°; λ: 65°.

Discussion. Mytiloides goppelnensis is very similar to *M. kossmati*, but displays single rugae instead of regular double-ridged rugae. *Mytiloides puebloensis* is similar in outline but possesses a different type of ornament.

Occurrence. Lower Turonian of Pueblo, Colorado. Other records are from England, Spain, France, Germany, Poland, Russia, and Japan (Walaszczyk and Cobban, in Kennedy *et al.* 2000).

<div align="center">

Mytiloides kossmati (Heinz, 1930)

Figure 7.11b-c

</div>

1930	*Inoceramus naumanni* Yok. var. *kossmati*; Heinz, in Besaire, p. 94, 121
1933	*Striatoceramus kossmati* Heinz, p. 247, pl. 18, fig. 4
1935	*Orpheoceramus columbianus* Heinz, p. 304
1980	*Inoceramus Mytiloides modeliaensis*, Sornay, p. 136, pl. 1, figs1, 3-4; pl. 2, figs 1, 3-4
1991	*Mytiloides columbianus* (Heinz); Elder, figs 4.2, 4.9
non 1992	*Mytiloides kossmati* (Heinz), Walaszczyk, p. 10, pl. 1, figs 1-8 (= *M. goppelnensis*)
2000	*Mytiloides kossmati* (Heinz), Walaszczyk and Cobban, in Kennedy *et al.*, p. 323, pl. 9, figs 4-9 (with additional synonymy)

Type. The left valve of the specimen from Anontsy, Madagascar, illustrated by Heinz (1933, pl. 18, fig. 4) is the holotype by original designation. It was re-figured by Walaszczyk and Cobban (in Kennedy *et al.* 2000, pl. 9, figs 4-5).

Material. Fourteen specimens.

Description. The outline of the shell is subrectangular to obliquely ovate. The growth axis is weakly inclined. The anterior margin is straight to convex, the ventral margin is rounded. and passes into an almost straight posterior margin. The hinge line is short and straight. The posterior auricle is small, subtriangular, and almost continuous with the disc. The ornament is composed of rounded, evenly spaced rugae which are crossed obliquely by concentric, rounded, asymmetrical, subevenly spaced microrugae.

Dimensions.

	L	H	L/H	l	h	l/h	s	s/h	τ	α	π	λ	
UANL-FCT VC580	54·5	66·0	0·83	48	69	0·70	26	0·38	100		135	55	RV
UANL-FCT VC552	71·3	83·0	0·86	63·3	90·5	0·70	29·0	0·32	100		140	60	RV
UANL-FCT VC245	58·0	58·8	0·99	44·5	62·3	0·71	24·5	0·39	110	90	135	55	LV
UANL-FCT VC525	92·5	94·5	0·98	75·3	111·8	0·67	38·5	0·34	105	85	135	50	LV

Discussion. Compared to other *Mytiloides* species *M. kossmati* displays a very regular ornamentation throughout ontogeny. It is similar to *M. goppelnensis* with respect to ornamentation and shell outline, but this species does not have double ridged rugae.

Occurrence. The species is known from the Lower Turonian of Pueblo, Colorado, and the U.S. Western Interior, Colombia, England, France, Germany, Spain, Poland, Czech Republic, Ukraine, Kazakhstan, Japan, and Madagascar (Walaszczyk and Cobban, in Kennedy *et al.* 2000).

Order AMMONOIDEA Zittel, 1884

Suborder AMMONITINA Hyatt, 1889

Superfamily DESMOCERATACEAE Zittel, 1895

Family MUNIERICERATIDAE Wright, 1952

Genus *Tragodesmoceras* Spath, 1922

Type species. Desmoceras clypealoides Leonhardt, 1897, by original designation of Spath (1922, p. 127).

Tragodesmoceras bassi Morrow, 193

Figure 7.7a

1935   *Tragodesmoceras bassi* Morrow, p. 468, pl. 52, fig. 1a-c; pl. 53, figs. 3-5; text-fig. 1, 3

1972   *Tragodesmoceras bassi* Morrow; Cobban and Scott, p. 58, pl. 38, figs. 2-3, 5-13; pl. 39

Type. The holotype is the original of Morrow (1935, pl. 52, fig. 1; pl. 53, fig. 3; text-fig. 3) by original designation. It comes from the Jetmore Member of the Greenhorn Formation, Lincoln County, Kansas.

Material. One specimen.

Description. The imprint is almost flat but preserves convergent flanks. Ribs are sigmoidal and bend forward ventrolaterally. 23 primary ribs and approximately 36 secondary ribs are present on the last whorl. The body chamber is partly preserved. Ornamentation of the living chamber consists of ribs which are weak and undulose, as compared to the phragmocone. The suture is intensely incised with a deep lateral lobe.

Dimensions. D: 196; WH: 84 (0·43); U: 43 (0·22).

Discussion. In contrast to material housed in other collections, the Vallecillo specimen is ornamented to a large diameter, possibly indicating a juvenile stage (Cobban and Scott 1972, p. 58). Density and type of ribs match the specimens illustrated by Cobban and Scott (1972, pl. 38, figs 2-3, 5-13). Other North American species of this rare genus are *Tragodesmoceras ashlandicum*, *T. carlilense* and *T. socorroense* described from the Western Interior Seaway and the Pacific Coast (e.g. Anderson 1958; Matsumoto 1959b; Cobban 1983; Cobban and Hook 1983b), but these are characterised by stouter ornamentation and a higher number of secondary ribs.

Occurrence. T. bassi is an early Turonian species previously recorded from Kansas and Colorado.

Superfamily: ACANTHOCERATACEAE de Grossouvre, 1894

Family: ACANTHOCERATIDAE de Grossouvre, 1894

Subfamily: ACANTHOCERATINAE de Grossouvre, 1894

Genus *Quitmaniceras* Powell, 1963

Type species. Quitmaniceras reaseri Powell, 1963 (p. 313, pl. 32, figs. 5 and 13; text-fig. 3*h, j*) by original designation.

Quitmaniceras reaseri Powell, 1963

Figure 7.5d-e

1923	*Pseudotissotia* (*Choffaticeras*) sp.? Reeside, p. 30, pl. 12, figs. 3-6	
1963	*Quitmaniceras reaseri* Powell, p. 313, pl. 32, figs. 5, 13; text-figs. 3h, j	
1963	*Quitmaniceras brandi* Powell, p. 314, pl. 32, figs. 6, 8, 11-12, 14-16; text-figs. 3i, p-q	
1982	*Metoicoceras*? sp., Chancellor, 1982, p. 83, figs. 5-6	
1987	*Quitmaniceras reaseri* Powell, Kennedy et al., p. 30, pl. 1, figs. 1-38; text-figs. 2a-c (with additional synonymy)	
1989	*Quitmaniceras reaseri* Powell; Cobban et al., p. 34, fig 75ee-hh	
1991	*Quitmaniceras reaseri* Powell, Kennedy and Cobban, fig. 6a-n, s-u	
1999	*Quitmaniceras reaseri* Powell, Kennedy et al., p. 636, figs. 3a, 4b-d, h-i, k-m, p-t, z-b'	

Type. The holotype is no. 36225 in the collection of the Texas Memorial Museum at Austin, Texas, by original designation of Powell (1963, pl. 32, figs 5, 13). It comes from the early Turonian Ojinaga Formation, Chihuahua, Mexico.

Material. Four specimens.

Description. The shell is moderately evolute. Umbilical bullae give rise to irregularly spaced primary ribs which are straight and rectiradiate. They terminate in ventrolateral bullae. Prorsiradiate ribs are present on the outer ventrolateral flank. Secondary ribs are also intercalated irregularly on the outer flanks. The suture is not visible.

Dimensions. UANL-FCT-VC585: D: 67 mm, WH: 27 mm (0·40), U: 21 mm (0·31). UANL-FCT-VC583: D: 74 mm, WH: 29 mm (0·39), U: 18 mm (0·24).

Discussion. Irregular ornament on the moderately evolute shell make this species easily distinguishable from all other taxa.

Occurrence. Basal Turonian of Chihuahua (Powell 1963), Colorado, Texas, New Mexico and Montana (Kennedy *et al.* 1999).

Genus *Watinoceras* Warren, 1930

Type species. Watinoceras reesidei Warren, 1930 (p. 67, pl. 3, fig. 2; pl. 4, figs. 9-12) by original designation. The genus was revised by Cobban (1988).

Watinoceras coloradoense (Henderson 1908)

Figure 7.5a-c

1902	*Schlönbachia gracilima* Kossmat, Petrascheck, p. 153, pl. 9, figs. 3a-b
1908	*Acanthoceras coloradoense* Henderson, p. 259, pl. 13, figs. 10-11
1916	*Acanthoceras amudariense* Arkhanguelsky var. *horridum* Arkhanguelsky, p. 49, pl. 8, figs. 8-10, 14-15
1972	*Watinoceras coloradoense* (Henderson), Cobban and Scott, p. 76, pl. 27, pl. 3, figs. 11-19; pl. 28, figs. 1-3, 5-9; text-figs. 36-37
1978	*Watinoceras* (*Watinoceras*) *coloradoense* (Henderson), Cooper, p. 123 (*pars*), text-fig 31 only, *non* figs. 18c-d, 19e-f, 32-33

1981	*Watinoceras coloradoense coloradoense* (Henderson), Wright and Kennedy, p. 53, text-figs. 18c-f (with additional synonymy)
1988	*Watinoceras coloradoense* (Henderson), Cobban, p. 7, pl. 2, pl. 3, figs. 4-5; text-fig 4 (with additional synonymy)
1988	*Watinoceras coloradoense* (Henderson), Kennedy, p. 52, pl. 7, figs. 1-2, 5, 7-11; pl. 14, fig. 6 (with additional synonymy)
1994	*Watinoceras coloradoense* (Henderson), Chancellor et al., p. 24, pl. 2, figs. 2-3
2002	*Watinoceras coloradoense* (Henderson), Stelck et al., p. 1791, text-fig 5a, i-l

Type. The holotype is USNM 30877 from the Greenhorn limestone near Lyons, Colorado, by original designation by Henderson, 1908, pl. 13, figs. 10-11, re-figured by 1, text-fig. 18e-f.

Material. 3 specimens.

Description. Moderately evolute with fairly wide umbilicus (U/D between 0·30 and 0·38). In the small specimens UANL-FCT-VC563 and UANL-FCT-VC555, 10-12 straight, rectiradiate ribs are present on the last whorl. Most ribs initiate with a round to bullate tubercle on the umbilical shoulder. A second row of sharp ventrolateral tubercles is located on the ribs near the ventrolateral shoulder, a third outer row of well defined tubercles near the venter. With increasing diameter, bullate to curved ribs replace the inner ventrolateral tubercles, whereas the outer ventrolateral tubercles become clavate. The venter and suture lines are not visible.

Dimensions. UANL-FCT-VC563. D: 57; WH: 23 (0·40); U: 19 (0·33). UANL-FCT-VC555. D: 60; WH: 24 (0·40); U: 18 (0·30). UANL-FCT-VC542. D: 119; WH: 42 (0·35); U: 45 (0·38).

Discussion. Our small hypotypes (Fig. 6B-C) match the specimen illustrated by Cobban (1988, pl. 2, fig. 10). Our large specimen (Fig. 6A) resembles the holotype which was re-figured by Wright et al. (1981, text-fig. 18e-f), although ribs of this specimen are projected slightly more forward on the flanks, and inner ventrolateral tubercles are more clavate.

Occurrence. Basal Turonian throughout the US and Canadian Western Interior Seaway. Other records are from British Columbia, northern Alaska, arctic Canada, Brazil, Germany, Uzbekistan, and Turkistan (see Kennedy 1988; Chancellor *et al.* 1994; Stelck *et al.* 2002).

<div align="center">

Subfamily: EUOMPHALOCERATINAE Cooper, 1978

Genus *Pseudaspidoceras* Hyatt, 1903
</div>

Type species. Ammonites footeanus Stoliczka (1864, p. 101, pl. 52, figs. 1-2) by original designation of Hyatt, 1903, p. 106.

<div align="center">

Pseudaspidoceras pseudonodosoides (Choffat, 1898)

Figure 5.7
</div>

1898	*Acanthoceras* (?) *pseudonodosoides* Choffat, p. 65, pl. 16, figs. 5-8; pl. 22, figs. 32-33
1989	*Pseudaspidoceras pseudonodosoides* (Choffat), Cobban et al., p. 40, figs. 41, 81-83 (with additional synonymy)
1995	*Pseudaspidoceras pseudonodosoides* (Choffat), Zaborski, p. 57, figs. 2-5, 8, 14 (with additional synonymy)

Type. The lectotype is the original of Choffat, 1898, pl. 16, fig. 5, by subsequent designation of Cobban et al. (1989, p. 40).

Material. 34 specimens.

Description. Coiling is evolute to very evolute, with a moderately sized umbilicus (U/D between 0·28 and 0·38, increasing with diameter). The umbilical and ventrolateral shoulders are narrowly rounded. 11-15 rounded umbilical tubercles are present per whorl. Strong undulose, straight ribs initiate on these tubercles, cross the flanks rectiradiately, and terminate in strong, slightly bullate outer ventrolateral tubercles. These extend towards the venter while bending slightly forward. They disappear before crossing the venter. The suture is rather simple.

Dimensions.	D	WH	U
UANL-FCT-VC585	67	27 (0·40)	21 (0·31)
UANL-FCT-VC507	135	49 (0·36)	44 (0·33)
UANL-FCT-VC110	151	60 (0·40)	42 (0·28)
UANL-FCT-VC065	168	74 (0·44)	54 (0·32)
UANL-FCT-VC543	188	69 (0·37)	64 (0·34)
UANL-FCT-VC104	208	75 (0·36)	77 (0·37)
UANL-FCT-VC513	210	75 (0·36)	72 (0·34)
UANL-FCT-VC544	213	73 (0·34)	80 (0·38)
UANL-FCT-VC540	268	98 (0·37)	91 (0·34)

Discussion. Kamerunoceras develops similar ornamentation when adult. *P. pseudonodosoides* can be distinguished from this genus by different juvenile growth stages. Juvenile *Pseudaspidoceras* are characterized by ventrolateral and umbilical rows of tubercles, whereas juvenile *Kamerunoceras* are ornamented with conspicious single ribs without tubercles. *P. pseudonodosoides* differs from *P. flexuosum*, described below, in stouter ornamentation and straight instead of flexuous ribs. The Vallecillo specimens are larger than specimens known, for example, from New Mexico or Nigeria, but their diameters correspond to material described from Israel (Freund and Raab 1969). Also unusual for the genus, ribs of the Vallecillo material become stronger and denser near the aperture of large specimens. These differences in size and form of the species may be controlled by environmental factors (Zaborski 1995).

Occurrence. Records of *P. pseudonodosoides* are from the latest Cenomanian of the southern Western Interior (e.g. Cobban *et al.* 1989), Brazil (Seeling and Bengtson 2002), Nigeria (Meister 1989; Courville 1992; Zaborski 1995), Israel (Freund and Raab 1969) and northern Spain (Karrenberg 1935). An early Turonian record is known to exist from Portugal (Lauverjat and Berthou 1974).

<div align="center">

Pseudaspidoceras flexuosum Powell, 1963

Figures 5.8, 5.11, 5.16, 7.6, 7.12

</div>

1902	*Mammites footeanus* Stoliczka spec.; Petrascheck, p. 144, pl. 9, fig. 1
1920	*Pseudaspidoceras* aff. *pedroanum* White; Böse, p. 209, pl. 13, fig. 1; pl. 15, fig. 1
1963	*Pseudaspidoceras flexuosum* Powell, p. 318, pl. 32, figs. 1, 9; text-fig. 2*c*
1972	*Ampakabites collignoni* Cobban and Scott, p. 81, pl. 29, figs. 1-3; text-figs. 39-40
1977	*Pseudaspidoceras* aff. *pedroanum* White; Chancellor, p. 91, figs. 8-10
1987	*Pseudaspidoceras flexuosum* Powell; Kennedy *et al*, p. 34, pl. 2, figs. 1-4, 8-13, 16-17; text- figs. 3a-c, 5, 6c-d, 7a-c (with additional synonymy)
1989	*Pseudaspidoceras barberi* Meister, p. 8, pl. 1, fig. 2; pl. 2, figs. 2, 5; text-fig. 4
1989	*Pseudaspidoceras flexuosum* Powell; Cobban et al., p. 41, fig. 91l
1990	*Pseudaspidoceras flexuosum* Powell; Robaszynski et al., p. 264, pl. 17, fig. 1; pl. 18
1992	*Pseudaspidoceras barberi* Meister; Courville, pl. 2, fig. 2
1994	*Pseudaspidoceras flexuosum* Powell; Chancellor et al., p. 30, fig. 11h-j
1995	*Pseudaspidoceras flexuosum* Powell; Zaborski, p. 63, figs. 11-13, 17-18, 20-21 (with additional synonymy)
2002	*Pseudaspidoceras flexuosum* Powell; Seeling & Bengtson, p. 155

Type. The holotype, by original designation of Powell, 1963 (p. 318, pl. 32, figs. 1, 9; text-fig. 2*c*), is UTA 30842. It comes from the Ojinaga Formation at Kelsey Crossing in Hudspeth County, Texas.

Material. 120 specimens.

Description. Very evolute. Obliquely embedded specimens indicate that the whorl section is subquadrate to subrounded. The umbilical wall is steep with a rounded shoulder. The flanks are flattened, broad, subparallel, and they pass into the flattened to widely rounded venter in a wide arch. Sharp umbilical tubercles give rise to moderately to very weak single ribs. These are prorsiradiate on the umbilical wall, but flex back before mid-flank and become rectiradiate. The venter is smooth with the exception of a widely arched striation, but an additional row of clavate tubercles is present on both sides of the sipho in some specimens. Other specimens

display pairs of spines extending from ventrolateral tubercles on the living chambers. The suture is partially visible on some larger specimens and characterised by moderately incised elements. Specimen UANL-FCT-VC500 is preserved with the aptychus in front of the aperture (Figure 7.6).

Dimensions.	D	WB	WH	U
UANL-FCT-VC834	78	-	36 (0·46)	23 (0·29)
UANL-FCT-VC565	104	-	35 (0·34)	33 (0·32)
UANL-FCT-VC63	120	-	46 (0·38)	32 (0·27)
UANL-FCT-VC557	131	-	59 (0·45)	32 (0·24)
UANL-FCT-VC858	140	-	50 (0·36)	43 (0·31)
UANL-FCT-VC836	148	-	56 (0·38)	48 (0·32)
UANL-FCT-VC549	160	-	63 (0·39)	39 (0·24)
UANL-FCT-VC517	168	-	68 (0·40)	53 (0·32)
UANL-FCT-VC511	180	-	70 (0·39)	63 (0·35)
UANL-FCT-VC24	207	-	79 (0·38)	71 (0·34)
UANL-FCT-VC835	212	(56)	62 (0·29)	79 (0·37)
UANL-FCT-VC512	220	80	83 (0·38)	83 (0·38)
UANL-FCT-VC500	275	-	103 (0·37)	90 (0·33)
UANL-FCT-VC501	310	-	125 (0·40)	103 (0·33)
UANL-FCT-VC109	339	-	108 (0·32)	137 (0·40)

Discussion. The species differs from *P. pseudonodosoides* by its finer ornamentation and flexuous ribs. It is distinguished from *M. nodosoides* by evolute coiling, type of ribbing and tuberculation, suture line, and the absence or other type of ventral ornamentation.

Occurrence. Lower Turonian of western Texas (Powell 1963; Kennedy *et al.* 1987), northern (Böse 1920) and north-western Mexico (Chancellor *et al.* 1977), Colorado (Cobban and Scott 1972), Tunisia (Robaszynski *et al.* 1990; 1994), Germany (Petrascheck 1902), Nigeria (Courville 1992; Zaborski 1995), Brazil (Seeling and Bengtson 2002), and Madagascar (Collignon 1965).

Subfamily: MAMMITINAE Hyatt, 1900

Genus *Mammites* Laube and Bruder, 1887

Type species. Ammonites nodosoides Schlüter, 1871 (p. 19, pl. 8, figs. 1-4) by monotypy. The genus is discussed by Wright and Kennedy (1981).

Mammites nodosoides (Schlüter 1871)

Figure 7.4

1871　*Ammonites nodosoides* Schlüter, p. 19, pl. 8, figs. 1-4

1981　*Mammites nodosoides* Schlüter; Wright and Kennedy, p. 75, pl. 17, fig. 3; pl. 19, fig. 3; pl. 20, fig. 4; pl. 22, fig. 4; pl. 23, figs. ?1, 2-3; pl. 24, figs. 2-3; text-figs. 19b, 23-24 (with full synonymy)

1990　*Mammites nodosoides* Schlüter; Robaszynski *et al.*, p. 265, pl. 19, figs2-4

1994　*Mammites nodosoides* Schlüter; Kennedy, p. 260, pl. 1, figs. 7-11; pl. 2, figs. 3-5 (with additional synonymy)

Type. The lectotype, by subsequent designation of Wright and Kennedy (1981, p. 76), is the original of Schlüter (1871). It comes from Mecholup, Czech Republic, and is housed in the Museum für Naturkunde, Berlin. It was refigured by Wright and Kennedy (1981, text-fig. 23).

Material. Eight lateral imprints.

Description. Juvenile growth stages are moderately involute. The umbilical walls bend narrowly into widely rounded to flat flanks. Seven to eleven rounded to slightly bullate tubercles are present near the umbilicus, their number increasing with diameter. Flattened, single or paired ribs are connected to these tubercles with eleven to seventeen rounded inner ventrolateral tubercles. The suture line displays a narrow L.

Dimensions.	D	WH	U
UANL-FCT-VC202	74	32 (0·43)	19 (0·26)
UANL-FCT-VC506	97	38 (0·39)	26 (0·27)
UANL-FCT-VCIII/61	117	50 (0·43)	32 (0·27)
UANL-FCT-VCIII/59	132	55 (0·42)	33 (0·25)
UANL-FCT-VCIII/76	134	47 (0·35)	39 (0·29)
UANL-FCT-VC185	136	53 (0·39)	34 (0·25)
UANL-FCT-VC505	143	55 (0·38)	42 (0·29)

Discussion. The species is separated from *Pseudaspidoceras* through more involute coiling, the absence of umbilical bullae or tubercles when adult, and the more intensely incised suture line with a narrower L.

Occurrence. This species is widely distributed and was recorded from the early Turonian (*Mammites nodosoides* zone) of Tunisia, Algeria, Morocco, Nigeria, Brazil, Colombia, Peru, Venezuela, Mexico, the US Western Interior, England, north-western and south-eastern France, Spain, Germany, the Czech Republic, Romania, Madagascar, Lebanon, Israel, and Turkistan (see Chancellor *et al.* 1994).

Family: VASCOCERATIDAE Douvillé, 1912

Subfamily: VASCOCERATINAE Douvillé, 1912

Genus *Vascoceras* Choffat, 1898

Type species. Vascoceras gamai Choffat, 1898, p. 54, pl. 7, figs. 1-4; pl. 8, fig. 1; pl. 10, fig. 2; pl. 21, figs. 1 and 5, by the subsequent designation of Roman, 1938, p. 452. Genus discussed by Wright and Kennedy (1981, p. 86), Kennedy et al. (1987, p. 44) and Zaborski (1996).

Vascoceras birchbyi Cobban and Scott, 1972

Figure 7.3b-c

1972   *Vascoceras* (*Greenhornoceras*) *birchbyi* Cobban and Scott, p. 85, pl. 22, pl. 23, figs. 1-13; pl. 24, figs. 1-12; pl. 25; pl. 26; figs. 5-8, 11-12; pl. 27, figs. 1-6; text-figs. 43-47

1989   *Vascoceras birchbyi* Cobban and Scott, Cobban et al., p. 48, figs. 71g, 88a, 89a-l (with full synonymy)

Type. The holotype is USNM 164022 from the middle Bridge Creek Member of the Greenhorn Limestone of south-eastern Colorado by original designation of Cobban and Scott (1972, p. 85, pl. 22).

Material. Five specimens.

Description. Coiling is moderately evolute. The whorl is widest at the umbilical flank where 8-10 strong umbilical bullae give rise to straight, single or paired rectiradiate ribs which are slightly projected forward towards the venter. They smoothen on the outer flanks in larger specimens (approx. 100 mm). The suture is barely visible in specimen UANL-FCT-VC 968; auxiliary elements correspond to sutures given by Cobban and Scott (1972).

Dimensions. UANL-FCT-VC968. D. 104; WH: 42 (0·40); U: 28 (0·27). UANL-FCT-VC38. D. ?120; WH: ?57 (0·47); U: 19 (0·16). UANL-FCT-VCV/54. D. 88; WH: 43 (0·49); U: 15 (0·17).

Discussion. Our material matches well with the paratypes presented by Cobban and Scott (1972) regarding shell ratios and ornamentation. The Vallecillo specimens resemble *Fagesia superstes*, but the number of umbilical tubercles is higher in *F. superstes*, and more ribs are rising from them. In addition, the incisions of the suture line of this species are more complex.

Occurrence. This early Turonian species was recorded in many localities in eastern Colorado, central and south-western Kansas, north-eastern and south-western New Mexico (see Cobban *et al.* 1989). This is the first record outside the US Western Interior Seaway.

cf. *Vascoceras* sp.

Figure 7.8a-b

Material. Five imprints.

Description. Our material indicates an involute, cadicone and strongly inflated ammonite with smooth whorls that sunk subvertically to obliquely into the sediments.

Dimensions.	D	WB	WH	WB/WH	U
UANL-FCT-VCIII/72	115	103 (0·90)	55 (0·53)	1·87	7 (0·06)
UANL-FCT-VC574	140	117	63 (0·45)	1·86	14 (0·10)
UANL-FCT-VC840	150	127 (0·83)	66 (0·44)	1·92	13 (0·09)

Discussion. Our material corresponds to shells with a WB much larger than WH. All specimens are embedded with the living chamber downwards; consequently no suture line is visible.

The following early Turonian ammonite species develop cadicone growth stages similar to the Vallecillo specimens: *Vascoceras globosum* (of which *V. proprium* Reyment, 1954, according to Zaborski, 1996, is a subspecies) was described in detail by Kennedy (1987) and Zaborski (1996). Records for this species include north-eastern Mexico (Böse 1920; Powell 1963; Chancellor *et al.* 1977; Chancellor 1982). *V. hartti* also occurs in north-eastern Mexico and was described in detail by Zaborski (1996). *Vascoceras durandi* (Thomas and Peron 1889-1893) shows a smooth adult growth stage at smaller diameters, but WB/WH is smaller, and U/D (0,30 to 0,54) is much larger than in the Vallecillo specimens. This species is only known from the Tethyan region (see Chancellor *et al.* 1994). *Vascoceras birchbyi* Cobban and Scott, 1972 (described above) is not cadicone when adult.

The rare *Fagesia peroni* Pervinquière, 1907 develops a cadicone and smooth adult growth stage, but at considerably smaller diameter (between 50 and 80 mm, see Kennedy 1994). *Fagesia catinus* (Mantell, 1922), described below, develops diameters similar to our specimens, but is not as cadicone in the smooth adult growth stage.

Diameters and shell outline of the Vallecillo specimens correspond to that of large, cadicone *Vascoceras*, but no additional diagnostic features are present. Assignation to this genus is uncertain.

Genus *Fagesia* Pervinquière, 1907

Type species. Olcostephanus superstes Kossmat, 1897, p. 26 (133), pl. 6 (17), fig. 1, by original designation of Pervinquière, 1907, p. 322.

Fagesia catinus (Mantell 1822)

Figures 7.2b-c, 7.3a

1822	*Ammonites catinus* Mantell, p. 198, pl. 22, fig. 10 (*non* fig. 5 = *Ammonites navicularis* Mantell)
1981	*Fagesia catinus* (Mantell); Wright and Kennedy, p. 88, pl. 26, fig. 2; text-figs. 31-36 (with full synonymy)
1982	*Fagesia haarmanni* Böse; Chancellor, p. 106, figs. 43-48 (with full synonymy)
1987	*Fagesia catinus* (Mantell); Kennedy et al., p. 51, pl. 7, figs. 1-3; pl. 8, figs. 1-4, 6-9; text-figs. 2j-k, m-n, 10 (with additional synonymy)
1994	*Fagesia catinus* (Mantell); Kennedy, p. 260, pl. 7, figs. 6-8

Type. The holotype, by monotypy, is BMNH C3379, which is the original of Mantell (1822, pl. 22, fig. 10) from the Lower Turonian Middle Chalk near Lewes, Sussex. It was refigured by Wright and Kennedy, 1981, text-fig. 31.

Material. Four specimens.

Description. Coiling is moderately to very evolute. Strong crushing of the shell during early diagenesis indicates a depressed whorl section. At diameters of about 100 mm, 11 large, smooth umbilical tubercles are present per whorl. All specimens correspond to juvenile macroconchs.

Dimensions. UANL-FCT-VC572. D: (110); WH: 46 (0·42); U: 42 (0·38). UANL-FCT-VC838. D: (120); WH: 31(0·26); U: 52 (0·43). UANL-FCT-VC250. D: 140; WH: 46 (0·33); U: 52 (0·37).

Discussion. Low U/D values are the result of flattened and crushed whorls. *Fagesia catinus* is separated from *F. superstes* by fewer and weaker umbilical tubercles which are situated higher on the flank.

Occurrence. Early Turonian, with records from France (Kennedy 1994), England (e.g. Mantell 1822; Wright and Kennedy 1981), Venezuela (Renz 1982), northern Mexico (Böse 1920), Texas (Kennedy *et al.* 1987), California (Matsumoto 1959a), New Mexico (*fide* Kennedy, 1994), and Montana (Reeside 1923).

Fagesia superstes (Kossmat 1897)

Figure 7.2a

<div style="margin-left:2em">

1897   *Olcostephanus superstes* Kossmat, p. 26 (133), pl. 6 (17), fig.1

1907   *Fagesia superstes* var. *turoniensis* Pervinquière, p. 323, pl. 20, figs. 1a-c, 2a-c

1907   *Fagesia superstes* var. *spheroidalis* Pervinquière, p. 324, pl. 20, figs. 3a-b, 4a; text-fig. 122

1983b   *Fagesia superstes* (Kossmat); Cobban and Hook, p. 16, pl. 3, figs1-2; pl.13, figs. 6-11; text-fig. 12 (with full synonymy)

1990   *Fagesia superstes* (Kossmat); Robaszynski et al., p. 266, pl. 20, fig. 1a-b; pl. 21, fig. 2a-b

1994   *Fagesia superstes* (Kossmat); Chancellor et al., p. 56, pl. 13, figs. 1-2; pl. 15, figs. 4-9; pl. 32, fig. 4 (with additional synonymy)

</div>

Type. Olcostephanus superstes Kossmat, 1897, p. 26 (133), pl. 6 (17), fig.1, by original designation.

Material. Two specimens.

Description. Coiling is moderately evolute. 12 umbilical tubercles are present per whorl which give rise to two slightly prorsiradiate ribs. 3-4 ribs are intercalated between these tubercles. The maximum whorl breadth is reached near the umbilicus.

Dimensions. UANL-FCT-VC021. D: 85 mm; WH: 27 mm (0·32), U: 29.5 mm (0·35). UANL-FCT-VC499. D. 97; WH: 50 (0·52); U: 16 (0·16).

Discussion. Umbilical tubercles of *F. catinus* are thicker, less densely arranged (7-11 per whorl), and situated higher on the flank. Ornamentation of *F. superstes* resembles that of *Vascoceras birchbyi* at comparable diameters, but this latter species is characterised by fewer umbilical bullae, with fewer ribs arising from these bullae.

Occurrence. Early to middle Turonian of Tunisia (Pervinquière 1907; Robaszynski *et al.* 1990), ?Egypt (Luger and Gröschke 1989), southern India (Kossmat 1897), New Mexico (Cobban and Hook 1983b), Mexico (Chancellor *et al.* 1994), and ?Venezuela (Renz 1982)

incertae familiae

Figure 5.9a-b

Material. Eleven specimens.

Description. Smooth, involute shells with a small, flat umbilicus (U is between 0·09 and 0·14). Traces of the septum are present in UANL-FCT-VC576 and 848 (Figure 5.9b); it is little folded. Some shells are crushed, their dimensions are likely distorted.

Dimensions. UANL-FCT-VC576. D: 85; WH: 37 (0·44); U: 9 (0.11). UANL-FCT-VC848. D: 86; WH: 44 (0·51); U: 8 (0·09). UANL-FCT-VC575. D: 91; WH: 43 (0·47); U: 12 (0·13). UANL-FCT-VC601. D: 98; WH: 49 (0·50); U: 14 (0·14).

Discussion. The following early Turonian ammonite taxa develop involute and smooth growth stages at comparable diameters: *Vascoceras*, *Fagesia*, *Thomasites*, *Choffaticeras*, *Wrightoceras*, and *Hoplitoides*. Diagnostic features such as whorl section, juvenile growth stages or suture lines are not preserved in our material. In consequence, a precise assignation to a genus or even species is impossible.